T H E U N I V E R S I T Y O F M I C H I G A N

COLLEGE OF ENGINEERING
Department of Mechanical Engineering

Final Report

A STUDY OF THE ROLE OF CUTTING FLUIDS

L. V. Colwell
J. C. Mazur
L. J. Quackenbush

ORA Project 04100

under contract with:

THE SUN OIL COMPANY
RESEARCH AND DEVELOPMENT DIVISION
MARCUS HOOK, PENNSYLVANIA

administered through:

OFFICE OF RESEARCH ADMINISTRATION ANN ARBOR

August 1962

TABLE OF CONTENTS

TABLE OF CONTENTS (Concluded)

LIST OF TABLES

LIST OF TABLES (Continued)

LIST OF TABLES (Concluded)

LIST OF FIGURES

LIST OF FIGURES (Continued)

LIST OF FIGURES (Continued)

LIST OF FIGURES (Continued)

LIST OF FIGURES (Continued)

LIST OF FIGURES (Concluded)

ABSTRACT

Progress is reported in a study of the behavior of cutting fluids in the three major zones in metal cutting; the chip-tool interface, the shear zone and the wedge between the machined work surface and the flank of the cutting tool. Nine plain and blended oils and trichlorethylene were studied in two noncutting bench tests and six different machining operations. Friction, wear, surface finish, power requirements, size control and cutting forces were analyzed.

Considerable information was developed on the relative influence of size of cut, relief angles, tool surface roughness, modulus of elasticity of the work material, chemical reactions, and film strength of lubricants. Surface finish and size control emerge as the most important objectives toward which the design of cutting fluids should be aimed. The optimum compromise often results in increasing the power required to cut.

SECTION I

INTRODUCTION

This study was undertaken to develop new information on the role of cutting fluids as lubricants in metal cutting operations. Considerable information already existed on behavior and mechanisms in the general area of boundary lubrication. On the other hand, there was very little information on the relationship of such information to metal cutting beyond the impression that metal cutting somehow required extreme pressure lubrication.

A laboratory program was set up to obtain information on all three of the major zones in metal cutting where cutting fluids might assert themselves. These zones are the shear zone, the chip-tool interface and the contact area between the freshly cut work surface and the tool flank following the cutting edge. Both ferrous and nonferrous work materials were included to help sort out the influence of chemical reactions from other mechanisms. Magnesium and leaded brass were studied because they have little tendency toward tool loading. Stainless steel was studied because of its strong tendency toward built-up-edge formation on the one hand and its relative chemical inertness on the other.

Six different machining operations; turning, milling, reaming, tapping, broaching, and planing were included so as to provide information on the relative influence of size of cut, continuous versus interrupted cuts, and different tool geometry. Reaming involves light cuts only, but a reamer is restricted to small rake angles which increase the tendency to form built-up edges which in turn destroy size control and finish. In addition, machine reamers have margins or lands which correspond to zero relief angle thus permitting rubbing between the reamer and the wall of the hole.

Taps have very small relief angles so that rubbing is possible as in reaming. On the other hand, tapping is a thick-chip operation so that difficulty from built-up edges is greater compared with the rubbing tendency. Broaching involves very thin cuts and unusually small relief angles but large total forces so that elastic distortion of the work material can influence lubrication. Broaching, tapping, and reaming are similar in that all three need effective lubrication between the tool and the freshly cut work surface.

Lubrication between the work surface and the tool is not necessary in turning and milling where the relief angle can be relatively large. Therefore, these operations were selected to study lubrication in the chip-tool interface: milling for interrupted cuts and turning for continuous cuts.

Planing was selected for study of the ability of cutting fluids to influence the cutting process by direct action on the shear zone between the chip and the work material. This operation made it possible to prestress the work material to any level in both tension and compression and thereby determine whether cutting fluids could weaken the metal and make it easier to cut.

In addition to cutting operations, orthodox friction and wear studies were carried out on all combinations of fluids and work materials to develop information for possible correlation with cutting behavior.

Briefly the results are the following:

a. Reaming, Tapping, and Broaching:

1. Very significant differences were observed between the ten fluids.

2. At some conditions, additives appeared to inhibit beneficial properties of base oils.

3. A given oil may be superior for one type of metal but inferior for another.

4. Chemical reactions are potent factors in the behavior of cutting fluids.

5. Lubrication between the tool and the workpiece in these operations is a dominant consideration.

6. The relative behavior of fluids is very sensitive to small differences in tool geometry. For example, one fluid might require twice as much torque as a second fluid when reaming a particular metal with reamer No. 1. Reamer No. 2 may cause the torque requirements for the second fluid to increase nearly 40 times while the requirements for the first fluid are increased less than five times, a condition which would reverse the relative ratings of the two fluids as far as this parameter is concerned.

b. Turning and Milling:

1. Both turning and milling demonstrate that it is possible to achieve a significant amount of lubrication between the chip and the cutting tool.

2. Turning data indicate further that fluids may differ by as much as three to one in the thrust force required to start a cut. This could explain differences in tendency toward chatter in intermittent cuts like form-turning in automatic screw machines.

3. Milling data indicate further that roughness of the tool rake face plays an important role in lubrication. A moderately rough tool may require 25% less total power than an exceptionally smooth tool.

4. Milling data indicate also that the effectiveness of a cutting fluid is very sensitive to the size of cut.

c. Planing:

1. Reduction in total power from the use of cutting fluids ranged beyond 30%.

2. None of the reduction in energy requirements could be attributed to direct action on the shear zone.

3. All of the energy reduction was demonstrated to be the result of lubrication between the chip and the tool.

d. Friction and Wear Studies:

1. Substantial differences between the fluids as to coefficients of friction and rates of wear were observed.

2. Some high wear can be attributed to chemical reactions; other high wear rates were associated with high coefficients of friction.

3. The presence of additives gave distinctive data.

Considered together the study has demonstrated that both chemical activity and film strength of cutting fluids exert identifiable influence on metal cutting. Further, it has emphasized the uniqueness of different operations as to lubrication requirements. Differences between fluids as large as ten to one have been demonstrated and a preponderant need for lubrication between the cutting tool and the freshly cut work surface has been confirmed.

Complete interpretation of the results of this study requires further analysis of correlations between quantitative properties of the fluids and data obtained from cutting. Therefore, this report will document the metal-cutting data and present an analysis of the relationships of such data to the fundamental mechanisms and characteristics of the metal-cutting process.

SECTION II

THE CUTTING-FLUID PROBLEM

The central theme of this discussion is that the behavior of cutting fluids may be more complex than many people realize. Considerable effort has been expended in search of a single test that will predict the effectiveness of a fluid for all types of metal-cutting operations. The fact that such a test has not been found in all these years can be attributed partly to lack of knowledge of what to look for and partly to inadequate appreciation of the broad range of conditions to be found in metal cutting. Therefore, the objective of this section of the report will be to review metal cutting from the viewpoint of a mechanical engineer.

Before proceeding to the details of metal-cutting phenomena, it is well to review what the user would like a cutting fluid to do for him. He is not concerned with the ultimate sources of all good that might be derived from them so it is necessary in some instances to translate his objectives into fundamental functions and properties.

FUNCTIONS OF CUTTING FLUIDS

The qualities which consumers desire in cutting fluids can be classified into either of two categories depending upon whether they are directly related to the metal-cutting function. These are:

1. Cutting Qualities: The ability to:

    a. Increase tool life
    b. Increase production rate
    c. Improve surface finish
    d. Assist in controlling size
    e. Aid in breaking up chips.

2. Noncutting Qualities:

    a. Noncorrosive to machine elements
    b. Nontoxic
    c. Low cost
    d. High stability

The list of noncutting qualities is by no means complete, but these qualities are not the primary concern of this discussion since they have no objective relationship to the cutting process. The fact that a cutting fluid

may be noncorrosive and nontoxic may tend to inhibit the achievement of desirable cutting properties, but the problem of incompatible qualities is discussed in later sections.

The cutting or functional qualities as described by the user of cutting fluids appear at first to be discrete and quite simple, but they are actually very complex, interdependent and difficult to assess. Probably the most varied assessments are made of tool life and of surface finish. From the practical viewpoint, a cutting tool is wornout and has reached the end of its useful life either when it will no longer cut or when the machined parts no longer meet specifications. The first property is expressed in the well-known Taylor formula and has been the basis for a great many cutting-fluid evaluations. Many of the ratings based on the results of this type of test have failed to stand up in practice. Where this has happened it must be due to failure to meet product specifications prior to complete tool breakdown.

Inspection for size usually is made during or soon after a machining operation and the techniques for doing so are well developed so that this criterion of tool failure could have been used to provide significant information on the actual performance of cutting fluids in industrial plants. The analysis of such information would be useful not only to the manufacturer but also its publication would provide useful guides for the research efforts of cutting-fluid suppliers.

Inspection for surface finish has undergone considerable development in recent years and surface roughness specifications are quite common. However, surface finish itself is a complex of properties whose relationship to manufacturing processes and the functional qualities of the product are not yet fully understood. Inspection of surface finish is frequently visual and inexact. Furthermore, it has been established that finish is very sensitive to cutting conditions in many operations. Often it is the first quality to fail to meet specifications. If finish specifications and requirements themselves were better understood, it is probable that tool failure based on this criterion would be even more common.

The objective qualities which the user would like in cutting fluids do not provide an explicit set of specifications for the supplier, but one can readily conclude from them that cooling and lubrication are desirable. However, the relative importance of these two properties and the conditions at which they must remain effective are seldom stated. Therefore, it is desirable to take a close look at what goes on when metal is cut with particular reference to forces, pressures, temperature, quantity of heat, and rubbing velocities.

WHAT HAPPENS IN METAL CUTTING

Figure 2.1 shows the general features which prevail in cutting most metals

which tend to form continuous chips. The rake angle of the cutting tool may vary from large positive values as in twist drills to large negative values where the tool is a grain of a grinding wheel. The chip is always thicker than the layer of metal being removed. Consequently, the velocity of the chip across the tool face is less than the velocity of the tool relative to the workpiece.

Severe frictional rubbing takes place in Zone-A at the chip-tool interface. This always gives rise to some smearing of the work material on the tool face and at the most severe conditions a large built-up edge will be formed at the nose of the tool. Frictional rubbing also occurs in Zone-B between the cut surface and either the built-up edge or the tool flank. Rubbing of the built-up edge on the cut surface usually produces a badly torn surface and very poor finish. Rubbing between the flank of the tool and the cut surface may cause some deterioration of the surface particularly at low cutting speeds; it also has a great influence on the character and magnitude of the residual stresses produced by the cutting process.

WORK AND HEAT

The power and energy requirements for cutting are well known. For most metals it is reasonable to assume that the amount of work required to cut a cubic inch of the metal into chips is a constant regardless of the cutting speed and type of cut. Significant exceptions to this assumption will be noted as the need arises. It will be useful to make a few calculations of forces, temperatures, and pressures for a typical operation as illustrated in Fig. 2.1.

Let us assume that a mild steel is being cut with a zero-rake-angle cutting tool. Approximately 26,000 foot-pounds of energy will be required to cut a cubic inch of this material into chips. Substantially, all of this energy will appear as heat. If it is assumed that all of the heat is retained in the chips and the specific heat is 0.1, the temperature will be approximately 1200°F above room temperature. Part of this energy is converted into heat in the shear zone at the junction of the chip with the workpiece, another part is used to overcome friction between the chip and the tool, and an undetermined third part is used up between the flank of the tool and the cut surface.

Obviously, the <u>average</u> temperature of the chip cannot rise above the calculated value. In practice however, the <u>maximum</u> temperature can be either above or below this value. At low cutting speeds the maximum temperature will be in the shear zone and significant amounts of heat will flow from the chip into both the workpiece and the cutting tool. Increasing the cutting speed decreases the amount of heat flowing into the workpiece and increases the temperature between the chip and the face of the cutting tool. Thus, it is possible for heat to be flowing from the chip into the tool at low

cutting speeds and to be flowing from the chip-tool interface into the chip at high speeds.

Experimental data show that the shear angle for the assumed cutting conditions would be about 25°. Applying the conditions established by Merchant,[1] the rubbing velocity between the chip and tool would be 0.423 times the cutting speed and the frictional forces between the chip and the tool would be 0.84 times the force in the direction of cutting so that the friction energy would be:

$$E_f = 0.423 \times 0.84\ E_t = 0.355\ E_t$$

where E_t is the total energy required to cut the metal. In other words, approximately one third of the total work required to cut the metal is needed to overcome friction between the chip and the tool. From another viewpoint, the total cutting energy and therefore the total heat generated could be reduced by more than half through perfect lubrication between the chip and tool face. Reducing friction as a means of reducing heat and temperature is thereby demonstrated to be a worthwhile objective. However, the problem of heat and temperature is by no means simple, as will be shown later.

FORCES AND PRESSURE

Let us assume that the cut illustrated in Fig. 2.1 is 0.010 inch thick. At this condition the force in the cutting direction is 3,120 pounds for each inch of cutting edge. Similarly, the friction force acting in the vertical direction would be 2,620 pounds. The cutting component creates normal pressure between the chip and the tool face while the friction component is the result of shear stress in the same region. Thus, the averages of normal pressure and shear stress would be 312,000 psi and 262,000 psi, respectively, if the area of contact between the tool and chip were equal to that of the cut. As a lubricating condition, the pressure would still be high even if the area of contact were ten times that of the cut.

There is a pronounced shortage of published information on the relationship of tool contact area to area to cut. This is unfortunate since such data would at least bracket the ranges of pressure at which lubrication is desired. Takeyama and Usui[2] have thrown some light on this problem by experiments in which the available contact area was limited. By this means he succeeded in reducing the friction force below that required by conventional practice with a full-width tool face. The implications of this approach are explored in the next section of this report.

TEMPERATURE AND WEAR

It was pointed out in the sample calculation for mild steel that the temperature rise of the chips would be about 1200°F if all the heat from cutting remained in the chips. It was suggested further that the maximum temperature between the chip and the tool might be even higher at high cutting speeds; a condition which is closely related to tool wear.

Figure 2.2 shows, for a range of work materials, a plot of average cutting temperatures measured at the same speed versus the cutting speed (V_{60}) for a one-hour tool life. A temperature range of a little more than two to one at the same speed is accompanied by a permissible speed range of nearly five to one for the same tool life or as much as ten million to one on tool life at the same cutting speed. The conclusion is that tool life is hypersensitive to temperature, a condition that points to both lubrication and cooling as worthwhile functions of cutting fluids.

The higher temperatures in Fig. 2.2 were produced by titanium alloys in spite of relatively low coefficients of friction. Similarly, hard steels produce high temperatures at low friction. Thus the potential for improving temperature-dependent tool life by lubrication appears to decrease as the problem becomes more acute. This suggests the use of coolants for high-strength materials and lubricants for low-strength, high-friction materials.

Tool wear does not appear to be due solely to temperature level, however. The most obvious other cause is the familiar "abrasive wear," but there are other causes as well. It has been demonstrated recently that thermal conductivity, specific heat, melting points, and chemical reaction rates all are significant influences on tool wear. Trigger and Chao[3] have suggested diffusion as an important mechanism of wear.

Industrial practice varies over a wide range of conditions so that both crater wear and flank wear are practical problems. The former is likely to be dominant with heavy cuts at moderate speed while the latter is more general in occurrence.

TOOL LIFE

Thus far the discussion has been focussed on heat generation, friction, pressure, and temperature. These are factors which contribute to tool wear and they are very important because they represent the conditions at which cutting fluids must operate if they are to be effective in reducing the rate of wear. However, reduced tool wear is only an intermediate objective; the final goal is increased tool life, which has a variable dependency on tool wear.

For example, a carbide turning tool with 0.015 inch of flank wear will continue to cut very satisfactorily. The same would be true of a high-speed steel tool on the same operation. On the other hand, a high-speed steel form-turning tool with only 0.004 inch flank wear would be completely worn-out for many applications despite the fact that there may be no perceptible change in chip formation; it will still cut metal very readily but not satisfactorily. In other words, useful tool life is often only a small fraction of the time during which a tool can still cut.

Surface finish can be very sensitive to small amounts of tool wear, particularly in relatively thin-chip operations such as reaming, form-turning, gear shaving, broaching, and even some gear cutting. However, it appears to be substantially a lubrication problem in the region between the flank of a tool and the cut surface.

Similarly, the tool flank enters into the problem where tool life is determined by loss of size control. Studies carried out in this research have demonstrated that feeding forces can increase trememdously with otherwise negligible tool wear. This can result in more or less change in size of the machined part depending upon the rigidity of the machine. Here also is a complicated lubrication problem; one which affects not only size control but also the residual stresses which result from the cutting operation.

BASIS FOR APPROACH

In summarizing the significant characteristics of metal cutting, from the viewpoint of cutting-fluid application, one might conclude:

(1) Cutting temperature can be very high as the strength of the work material increases and the thermal-diffusivity decreases.

(2) Both high temperature and extremely high pressures can occur in Zone-A at the chip-tool interface.

(3) Temperature may be high in Zone-B between the flank of the tool and the cut surface.

(4) The pressure in Zone-B between the flank of the tool and the cut surface may vary over a broad range depending upon the type of machining operation.

It will make a useful approach to oversimplify the cutting-fluid problem by characterizing all cutting fluids as either coolants or lubricants. Further, all machining operations to which cutting fluids are to be applied should similarly be classified as requiring either cooling or lubrication. Obviously, situations will arise which require a compromise with these different functions. The basis for classifying the machining operations could be substan-

tially as follows:

(1) Heavy cuts in continuous cutting operations on high-strength materials can be considered one extreme for which there is little hope of doing any good by any other means than cooling.

(2) The other extreme would be characterized by thin chips, interrupted cuts, low-strength and low-modulus work materials.

With this classification in mind, let us proceed to examine the results of this laboratory study which was restricted to the problem of lubrication.

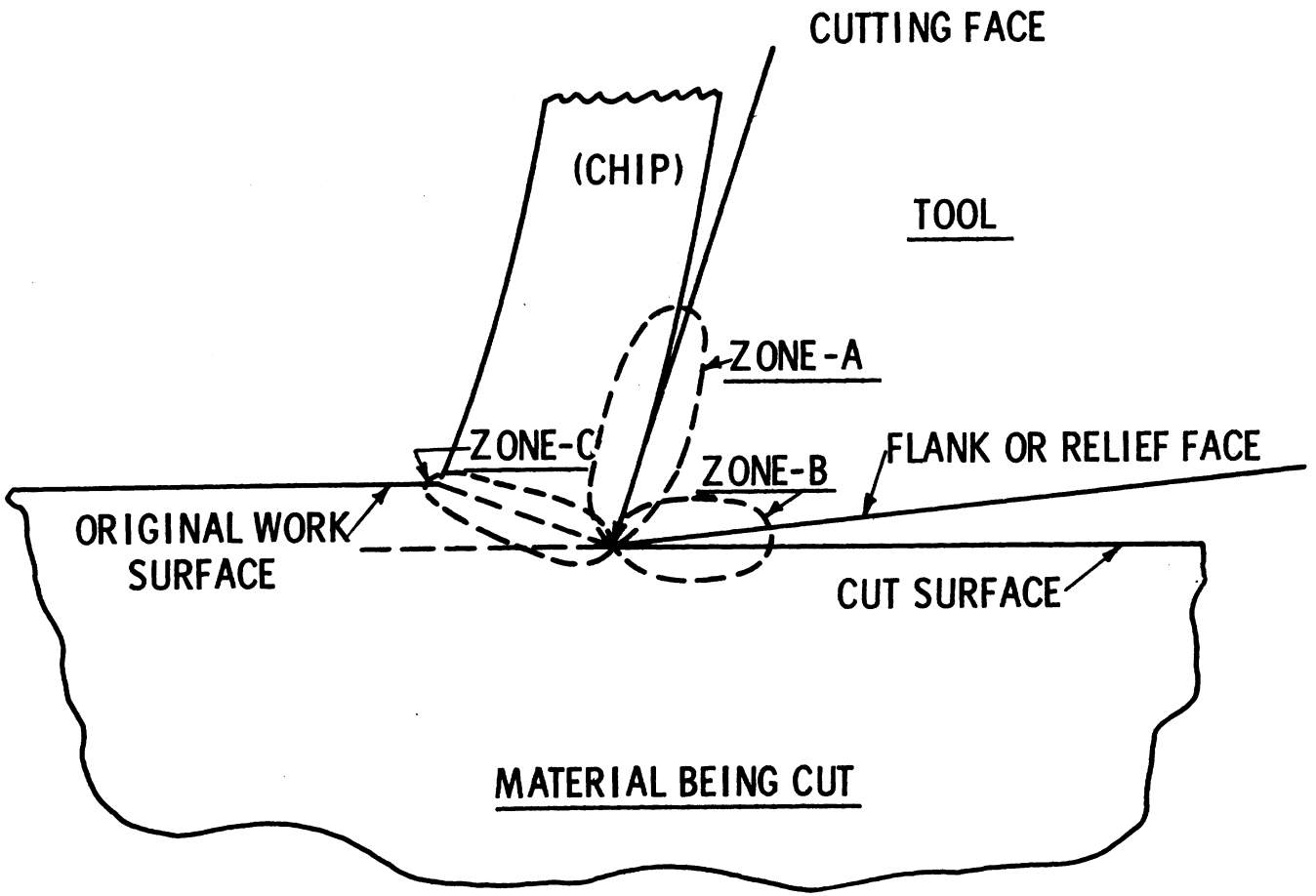

Fig. 2.1. Illustration of the two most important zones of cutting tools related to cutting-fluid action. Zone-A is a high-pressure area characterized by almost continuous seizure. Zone-B involves lower pressure where boundary lubrication is possible. Zone-C is commonly referred to as the shear zone wherein ductile metals are deformed in the process of forming a chip.

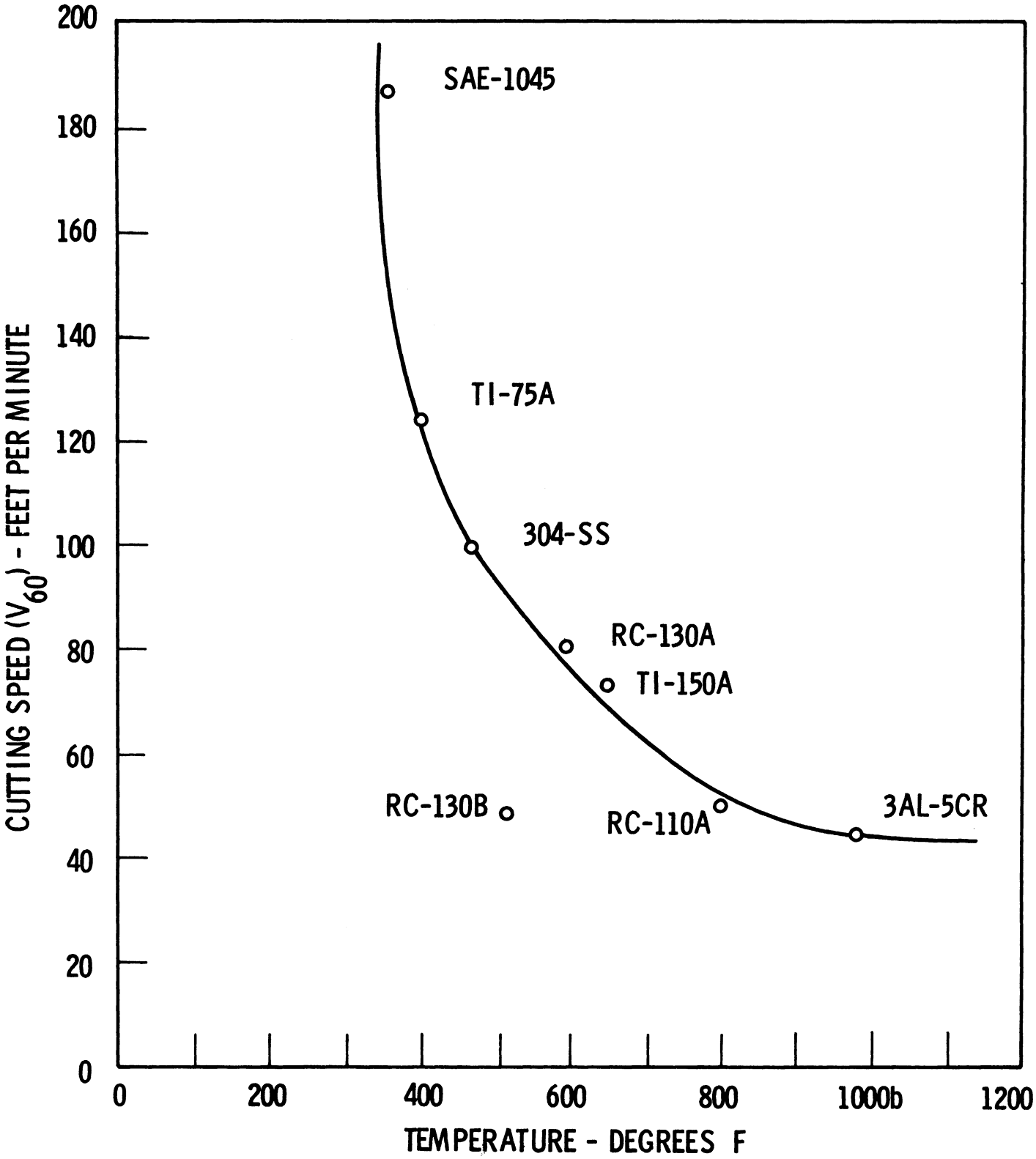

Fig. 2.2. Cutting temperatures measured at the same cutting speed for a range of materials correlate well with the cutting speed required to give a 60-minute tool life. The measured temperature for RC-130B probably is less than the actual temperature because of pulsating motion accompanying chip segmentation.

SECTION III

LABORATORY STUDIES INVOLVING THE CHIP-TOOL INTERFACE

Two studies were devoted to investigations of lubrication in the chip-tool interface. Turning and milling were selected for this purpose because the relief angles could be made relatively large, thus at least minimizing the problem of rubbing between the tool and the freshly cut work surface. Consequently, such differences as were observed in the major data could be attributed primarily to differences in the effectiveness of the ten test lubricating fluids.

TURNING WITH LIMITED-CONTACT TOOLS

A series of orthogonal turning tests was made with ten different cutting fluids. The work materials are referred to in the report by name but the cutting fluids are designated by Nos. 1 through 10 and are identified by these numbers in all charts and tables. Properties of the work materials and identification of the cutting fluids appear in the appendix to this report.

The turning tests were carred out on 1-inch-diameter bar stock of the work materials. The bars were mounted in a lathe and drilled with a 7/8-inch-diameter drill so as to convert the work materials to the form of a 1-inch-diameter tube with a 1/16-inch-wall thickness. Test cuts were made with the high-speed steel single-point tool mounted in a two-component force dynamometer, which made it possible to measure both the cutting and feeding components of force while cutting on the end of the tube. The cutting edge was oriented parallel to the end of the tube and was fed longitudinally to the axis of rotation. The cutting tool was basically a conventional tool having a 40° rake angle modified by a zero rake flat 0.010 inch wide parallel to and immediately adjacent to the cutting edge. Before a test was made, the end of the tube was carefully squared up so that the entire end face would be perpendicular to the axis of rotation. Next, the longitudinal feed was engaged with the cutting tool a few thousandths of an inch from the end of the tube and the cutting forces were recorded continuously for a few revolutions and the feed then disengaged. The end of the tube was then again carefully squared up and the test repeated. This procedure was followed until four such tests were completed with each combination of conditions.

Typical chart records for all of the test conditions are reproduced in Figs. 3.1 through 3.8. Figure 3.1 shows a complete chart record of a single test for dry cutting of copper. The first third of the record represents that time interval during which the size of cut increases from zero to the equilibrium value determined by the feed rate. The middle portion of the

chart represents the equilibrium conditions which persisted for about two revolutions of the workpiece, after which time the feed was disengaged so that the last third of the chart record represents the change in cutting forces as the size of cut once more decreases. The information on cutting force is most significant in the first third of the record, the time interval during which the size of cut increased from zero to the value of the feed rate at 0.030 ipr. Chart records for these intervals are reproduced for all seven work materials and all ten cutting fluids in Figs. 3.2 through 3.8.

Figure 3.8 illustrates those features of the cutting-force information which are most important. Results are shown for all ten fluids applied to cutting of No. 18-8 stainless steel. The results for Fluid No. 3 demonstrate all of the significant characteristics which this type of test reveals. It will be noted, for example, that the horizontal, or feeding component of force, increases to over 50 pounds before the vertical, or cutting component of force, begins to rise. This means that there is considerable rubbing between the end of the tube and the cutting tool before the formation of a chip actually begins. At the beginning of chip formation, the vertical force rises very rapidly and the feeding force relaxes to about 40 pounds for a short period of time before increasing still further. The rubbing interval represents nearly 45° of rotation of the workpiece so that the full size cut is not achieved until at least another full revolution has taken place. It will be noted that the initial rubbing force varied considerably between the ten fluids. It was as low as 16 pounds for Fluid No. 10 and ranged up to 54 pounds for Fluid No. 3.

It will be noted that the horizontal, or feeding force, achieves its maximum level long before the cutting component reaches its maximum. This is due to the existence of the narrow flat adjacent to the cutting edge. Actually, there are four discreet phases involved in this type of test. The first phase has already been described as that interval during which the feeding force builds up to an appreciable value before cutting actually begins. The second phase includes the beginning of cutting during which the underside of the chip is in contact with only part of the narrow flat. Consequently, during this interval the cutting tool is behaving as any ordinary zero-rake tool. As the thickness of the cut increases, both the cutting and feeding components of force continue to increase, but the feeding force reaches a maximum long before the full thickness of cut has been achieved. During this interval the chip contacts more and more of the narrow flat until finally contact is made not only on the tops of all of the roughness marks but in the low points and valleys as well. In other words, a point of saturation is reached beyond which there is no further rubbing surface available and the feeding, or frictional component, of the cutting force cannot increase further. The end of the second phase is indicated by the leveling off of the horizontal cutting component, or feeding force.

The third phase, which may be relatively short, is characterized by further increases in the cutting component of force while the feeding component remains substantially constant. During this interval the chip is in contact only with the narrow flat. As the cut continues to get thicker, the vertical force will continue to increase and the shear angle will also increase. Eventually, the vertical force increases to the point where the contact conditions between the chip and the narrow flat become unstable and the chip then begins rubbing on the 40° rake face as well. This marks the end of the third phase. During the fourth, or last, phase the thickness of cut increases further until equilibrium is reached and both cutting forces remain substantially constant. During the fourth phase the horizontal, or feeding force, may actually decrease as is evident in the records for Fluids Nos. 6 and 9 in Fig. 3.8. The amount of reduction in the feeding force during this phase is a measure of the degree of lubrication achieved in the interface between the underside of the chip and the 40° rake face of the cutting tool. Thus, at least, three values relevant to the question of lubrication can be obtained from each of these records. Such values have been summarized for all of the test conditions in Tables 3.1, 3.2, and 3.3.

Maximum values of the vertical, or cutting force, component are summarized in Table 3.1. This is called the power, or energy, component since it is responsible for well over 99% of all of the energy required to perform the cut. It will be noted in Table 3.1 that the cutting force for dry cutting is not always the highest. For example, the force for dry cutting of aluminum was 120 pounds while the cutting with Fluid No. 9 increased the force to 145 pounds. This means that the power requirements were increased about 20% through the use of the fluid. It does not mean, however, that the fluid failed to lubricate. Instead, it means that a substantial built-up edge was formed during dry cutting and the built-up edge effectively increases the rake angle, thus resulting in a reduction in total power requirements. On the other hand, the existence of the built-up edge invariably results in serious deterioration of the surface finish and loss of size control. Thus, a net increase in cutting force can signify improvement in surface finish and size control. On the other hand, very effective lubrication can result not only in improvement of surface finish and size control but also a reduction in the total cutting force, or power requirements. This is exemplified in the maximum forces for Fluids Nos. 1 and 3 on aluminum. Similar characteristics will be noted for other materials represented in the table, notably brass and steel.

The feeding force at maximum size of cut is also significant. Values of this force for all of the cutting conditions are summarized in Table 3.2. The values recorded in this table represent the average during sustained cutting. It will be noted from the chart records that some of the fluids achieved somewhat lower values in the earlier stages of cutting, but the steady-state value is characterized by some smear or build-up on the tool face which results in somewhat higher friction for continuous cuts than would be experienced in intermittent or interrupted cuts. It will be noted that

Fluid No. 6 is particularly effective in reducing the feeding force for the plain carbon steels and for copper.

Table 3.3 contains values of the feeding force required to start cutting. This is the rubbing force which builds up during the first phase of the test. This could be one of the most significant characteristics revealed by this particular study. This force could be important because of its possible relation to the problem of chatter in machining operations. For example, the high force of 54 pounds which built up on stainless steel with Fluid No. 3 indicates that an interference of approximately 0.004 inch developed before cutting began. The chart records indicate that cutting also stops and the tool is pushed out of the work when the feeding force drops to this value upon disengaging the feeding mechanism. This property has considerable significance in such operations as plunge forming in automatic screw machines, for example.

A feeding force of 50 pounds required to start a cut in the test program is the equivalent of 800 pounds per inch of cutting edge. Thus, for example, a 1-inch wide form tool in an automatic screw machine would have to build up a radial load of 800 pounds on the bar stock before cutting could begin. If the rate of rise on the cam resulted in a feed rate of 0.0005 ipr, then the bar stock would rub on the flank of the tool for as many as 8 to 10 revolutions before cutting would begin rather suddenly. As a result of this sudden increase in the cutting component of force, a chatter vibration could be triggered. The consequences might be even worse near the end of the cut as the cam approaches the dwell position because the tool would stop cutting with almost equal suddenness.

Summary analysis of the turning data indicates conclusively that lubrication between the chip and the cutting tool is possible. Further, it indicates that such lubrication has two objectives: the first is the removal or prevention of a built-up edge; and secondly, the reduction of friction resulting from the rubbing of the underside of the chip across the face of the tool. For example, in aluminum, Fluid No. 9 was effective in removing the built-up edge. On the other hand, it is a poor lubricant so that the net result of applying Fluid No. 9 to aluminum was a 20% increase in power requirements. At the other extreme, Fluid No. 1 not only removed the built-up edge but lubricated the interface well enough to reduce the friction substantially, resulting in an over-all power reduction of about 10%. This represents a far greater percentage reduction in the frictional froce and coefficient friction. Finally, this study has also revealed a possible area of incompatibility so far as lubrication is concerned. This involves the relatively high feeding force required to start cutting in the case of some of the cutting fluids. This leads to the tentative conclusion that lubrication achieved through the formation of low-strength chemical reaction products may be more desirable than that derived from higher film strength. Chatter in metal-cutting operations is not fully understood, but it is theoretically possible that high

film strength of a lubricant could aggravate this problem, particularly in intermittent cuts of variable thickness.

MILLING WITH LIMITED-CONTACT TOOLS

A series of studies was carried out with a milling operation because it involves an interrupted cut in which a fluid need sustain lubrication between the chip and the cutting tool for only a short period of time before the fluid can again be renewed. As in the case of turning and other single-point tool operations, most milling cutters can have a relatively large relief angle so that lubrication between the flank of the cutting tool and the freshly cut machined surface is not a prime necessity. Exceptions arise in the case of gear and spline hobbing and similar operations where the relief angle must be small in the interest of tool economy.

All of the tests in this series were carried out on annealed AISI 1020 steel. It was necessary to change the carbon content from 1018 to 1020 because of the size of the specimen required for this operation. The tests were made with a special milling dynamometer illustrated in Fig. 3.9. In this device a pendulum provides the energy source and rotates a single-tooth milling cutter into the workpiece which has been adjusted previously for any desired depth of cut and feed rate or cut thickness. The number of foot pounds of energy required to perform the cut are read directly from a calibrated dial.

All ten of the test fluids in the program were studied in cutting the AISI 1020 steel. The investigation was limited to one work material since it required over 15,000 individual tests to evolve the necessary information for just this one material. Studies with a limited-contact flat of the same type used in the turning tests yielded new information on the mechanisms involved in frictional rubbing between the chip and the cutting tool. The data obtained from this investigation are summarized in Figs. 3.10 through 3.17.

Typical data for the limited-contact tool are shown for dry cutting and for Fluid No. 1 in Fig. 3.10. The energy required to cut each individual chip is shown plotted against the corresponding feed in inch per tooth for a constant depth of cut of 0.050 inch and a constant width of cut of 0.200 inch. It will be noted that although the energy per chip increases throughout the range of increasing feed, the rate of increase is different in each of three distinct regions. Although the feed rate is as high as 0.012 ipt, the actual maximum thickness of cut never exceeds 0.0023 inch. Thus, this is essentially a thin-chip operation over the entire range. Contact between the chip and the cutting tool is limited to the 0.010-inch wide flat throughout the entire range.

In the region of light feeds, the rubbing contact between the chip and the cutting tool is confined to the ridges of the grinder marks so that as

the size of cut increases through increased feed, contact is distributed over more and more of these ridges. Each of these ridges behaves as an individual limited-contact area so far as frictional rubbing is concerned. Consequently, the frictional energy will remain substantially constant for a feed interval from 0.0025 to 0.0035 inch for example. This results in a relatively slow increase in the total energy required to cut one chip even though the thickness of the cut has been increased. This condition corresponds to the plateau of the feeding force as observed in the turning study. Consequently, the individual data points in the region of light feeds did not progress in a continuous straight line but demonstrated discreet groupings analogous to quantum jumps. This behavior characteristic was confirmed statistically from a very large number of tests. Thus, it is reasonably certain that contact between the chip and the tool is confined to the ridges of the grinder marks in this light feed interval. In Fig. 3.10 that interval is from 0.001 to 0.006 inch for Fluid No. 1, whereas it ends at a feed of 0.003 inch with dry cutting.

At the upper end of the first interval, the chip is large enough so that all of the available ridges on the limited-contact flat are brought into rubbing contact with the underside of the chip. At larger feeds, as in the second interval, the cutting component of force continues to increase, thus causing the underside of the chip gradually to extrude down into the valleys between the ridges of the tool marks so that frictional energy is increased disproportionately due to shear flow of the underside of the chip. This process continues with its disproportionately high rate of increase in frictional energy until the entire available surface of the limited-contact flat has been saturated just as in the case of turning. Consequently, the third interval corresponds exactly to the plateau of the feeding force charts obtained for the turning operation.

The limited-contact area of the milling cutter is saturated only near the end of the cut where the thickness of the chip achieves its maximum. Consequently, the upper interval of the data lines shown in Fig. 3.10 still represent some lubrication because saturation is not in effect during the entire cut. In other words, the energy values represent an integral of the energy requirements for cut thicknesses ranging from zero to the maximum in each case. Therefore, even though saturation may be in effect for the last 30% to 40% of the cut, the lubrication which took place in the earlier stages will be reflected in a lower total energy indication.

Similar data plots for all ten fluids at identical test conditions are shown in Figs. 3.10 through 3.14. Particular note should be taken of the second interval in each case since the width of the interval, the level of feed rate at which it occurs, and the rate of increase of energy within the interval as represented by the slope of the line all reflect properties of the fluids as lubricants. Note the substantial difference between Fluids Nos. 1 and 2 in Fig. 3.10, for example. Fluid No. 2 must be characterized

as a poorer lubricant than Fluid No. 1. Note also the family resemblance between Fluids Nos. 2 and 8 on the one hand and Fluids Nos. 1 and 3 on the other. One can also see the effect of the additive which is present in Fluids Nos. 2 and 3.

Significant energy values for all ten fluids and dry cutting in this series of tests are summarized in Tables 3.4 and 3.5. The actual energy values in foot pounds per chip are recorded in Table 3.4 for all ten fluids and dry cutting at each of four different feed rates representing the entire range. The corresponding total energy requirements for each of the ten fluids are represented as percentages of that required for dry cutting at the corresponding conditions in Table 3.5. This table indicates that the use of the cutting fluid can decrease the energy requirements by more than 50% at intermediate feed rates. Appreciably less energy is saved at extremely light cuts and at the heavy cuts, with all of the lubricants being least effective at the heaviest cuts at the third interval where saturation of the tool surface is achieved before the end of each cut. The energy requirements are higher at the very light cuts for two reasons: first, because of the existence of some rubbing on the flank of the tool; and secondly, because the unit pressures are always higher immediately adjacent to the cutting edge. Therefore, a degree of saturation always occurs in this region and it tends to become dominant for very thin cuts.

The friction mechanisms and lubrication characteristics demonstrated by all ten fluids, as illustrated in Figs. 3.10 through 3.14, were found to be valid also for both shallower and deeper cuts. An illustration of this is given in Fig. 3.15 for dry cutting and the most effective and least effective cutting fluids from the previous series. Data from the relatively shallow depths of cut of 0.025 inch are plotted at the left in the figure and those for a deeper cut of 0.100 inch are illustrated at the right in the figure. It will be noted that the energy requirements tend to converge upon a common value at feed rates beyond the test range. They would never quite intersect because the energy value is an integral involving some cutting conditions at which lubrication was effective. However, the relative importance of early lubrication decreases in significance as the size of cut increases and lubrication becomes increasingly difficult. One might conclude also from this figure that the relative ratings given different cutting fluids depends very strongly on the size and severity of the cut.

A third series of tests was carried out for the purpose of evaluating the relative significance or potency of the available contact area versus the degree of lubrication which can take place. For this purpose tools were prepared with limited-contact flats of only 0.005 inch or, in other words, only half as much as that available for rubbing contact in the first two series of tests. Typical results are illustrated in Fig. 3.16, where the energy per chip is plotted for a range of feed rates for dry cutting with the narrow flat and for cutting with Fluid No. 6, the most effective fluid, with the wider flat. The lines for dry cutting with the two heavier depths

represent only the third interval of the energy curves whereas those for the two shallower depths include the third interval and part of the second interval. It is significant that at the high feed rates of 0.008 to 0.010 ipt, dry cutting with the narrow flat requires less energy than cutting with the best lubricant and with a flat twice as large. In other words, effective lubrication drops off very rapidly at higher pressures. Typical comparative data are summarized in Table 3.6.

A fourth series of tests was carried out to investigate the role of tool roughness in relation to the problem of lubrication. Typical results of this study are summarized in Fig. 3.17. Zero-rake angle tools with no flats were prepared at two different levels of surface roughness--three micro-inches and about thirty micro-inches. It is interesting to note that the smoother tool surface requires up to 20% more energy than the rougher tool. This is due in part to the fact that there is a larger area of contact with the smooth tool than with the rough tool for the same normal force acting between the chip and the tool surface. It could also be due in part to larger reservoirs of lubricant on the rough tool in those regions of size of cut where the contact surface has not yet become saturated.

It is also significant that the energy line in Fig. 3.17 demonstrates the same three intervals peculiar to the earlier data obtained with the limited-contact tools. This is due to the fact that the chips do curl away from the rake face of the tool, thus effectively limiting the available contact area. Therefore, the three intervals have the same significance and the same meaning as with the limited-contact tools even though the theoretically available contact area is unlimited. The results for the two different levels of tool roughness simply confirm the existence of the mechanisms which have been attributed to the results of the previous series.

MILLING WITH CONVENTIONAL TOOLS

An exhaustive investigation was carried out for all ten fluids in milling AISI 1020 steel with conventional tools having a 30° rake angle and no limited-contact flat. The results for wide ranges of both feed rate and depth of cut are plotted in Figs. 3.18 through 3.28. The energy requirements are represented by straight lines on double logarithmic coordinates. There is considerable information of this type in the technical literature and the results usually are represented through exponential equations of the type which have been summarized in Table 3.7. This table also includes typical values of the energy requirements for both dry cutting and each of the ten fluids for a single size of cut. In addition, the percentage reduction in energy over dry cutting is given for each of the fluids.

It will be noted in Table 3.7 that the energy reduction due to the use of cutting fluids ranges from as little as 4% for Fluid No. 10 to a maximum of 20% for Fluid No. 6. These are substantially less than the more than 50%

reduction recorded in Table 3.5 from the series of tests with limited-contact flats. On the other hand, they are not much lower than the values shown in Table 3.5 for the heaviest cuts in the third interval of the energy curves. Thus, it would appear that all of the lines in Figs. 3.18 through 3.28 represent behavior characteristic of the third interval of the energy lines of the type contained in Figures 3.10 through 3.14. In other words, cutting with tools with high-rake angles involves a high degree of saturation in the contact area between the chip and the tool face. It has been known for years that the coefficient of friction increases considerably with increases in rake angle. It has not been known why this was true. Professor M. C. Shaw has suggested that it might be related to the degree of constraint peculiar to the two different values of rake angle. In other words, he was suggesting that small rake angles make the chip act harder and therefore result in a lower coefficient of friction by virtue of the greater apparent hardness. The results of this particular investigation do not support this suggestion but instead point to a predominance of saturation as the cause. This is also consistent with the observation that the coefficients of friction are invariably greater than unity with large rake angles whereas they may be as low as .35 to .4 with zero-rake angle for the same metal pair.

Summary analysis of the milling investigation brings out several important points. First, it is evident, as in the case of turning, that lubrication between the chip and the cutting tool is possible. Second, the degree of lubrication between the chip and the cutting tool is substantially less with large rake angles than with small rake angles. Third, saturation of the contact area between the chip and the cutting tool is the dominant mechanism limiting the degree of lubrication. Fourth, the friction between chip and the cutting tool is indeed a function of the area of contact, but the area of contact can be substantially less than the projected area. Fifth, the actual contact area between the chip and the cutting tool is less for greater surface roughness at the same level of normal force.

TABLE 3.1

MAXIMUM CUTTING FORCE IN TURNING

(Pounds)

Fluid No.	Work Material						
	Aluminum	Magnesium	Brass	Copper	1042 Steel	1018 Steel	Stainless Steel
1	105	50	160	170	340	290	400
2	140	56	170	172	360	325	410
3	110	52	160	180	330	270	385
4	130	53	160	160	350	300	400
5	120	55	160	160	320	290	400
6	115	50	150	160	300	380	400
7	125	54	140	195	360	315	400
8	140	54	160	185	380	330	390
9	145	54	165	150	330	300	425
10	115	55	160	170	365	320	390
Dry	120	56	140	215	340	320	390

TABLE 3.2

FEEDING FORCE AT MAXIMUM CUT IN TURNING

(Pounds)

No.	Work Material						
	Aluminum	Magnesium	Brass	Copper	1042 Steel	1018 Steel	Stainless Steel
1	-1	11	-14	4	16	16	65
2	-4	12	-11	4	25	40	72
3	-6	13	-16	4	24	14	65
4	-4	12	-14	4	28	32	68
5	-7	12	-11	5	28	30	68
6	-7	11	-14	2	14	2	56
7	-1	13	-10	8	30	42	72
8	-4	12	-10	6	26	42	80
9	1	11	-14	-11	20	16	56
10	3	14	-14	7	30	44	70
Dry	6	15	-13	18	30	40	68

TABLE 3.3

FEEDING FORCE REQUIRED TO START CUTTING

(Pounds)

Fluid No.	Work Material						
	Aluminum	Magnesium	Brass	Copper	1042 Steel	1018 Steel	Stainless Steel
1	6	4	6	13	12	7	28
2	8	6	14	8	12	19	30
3	8	6	14	8	10	16	54
4	6	6	9	8	19	18	50
5	7	7	6	10	15	14	40
6	9	5	12	10	11	17	46
7	8	7	7	7	14	18	36
8	8	5	8	6	12	11	27
9	6	4	8	8	16	20	32
10	10	8	8	7	12	12	16
Dry	4	10	7	8	12	14	12

TABLE 3.4

MILLING ENERGY AT DIFFERENT FEEDS

(Foot-Pounds per Chip)

Feed (in./tooth)	Fluid Number										
	Dry	1	2	3	4	5	6	7	8	9	10
.001	.95	.61	.72	.63	.63	.56	.55	.71	.80	.60	.58
.005	4.35	1.95	2.15	1.90	2.00	1.90	1.85	2.28	2.30	2.20	2.85
.006	4.75	2.20	2.70	2.12	2.30	2.20	2.12	2.60	3.15	2.55	3.65
.012	6.70	5.00	5.40	4.95	5.45	5.00	4.85	5.50	5.90	6.50	5.80

TABLE 3.5

MILLING ENERGY AS PERCENT OF DRY CUTTING

Feed (in./tooth)	Fluid Number									
	1	2	3	4	5	6	7	8	9	10
.001	64	76	66	66	59	58	75	84	63	61
.005	45	50	44	46	44	43	52	53	50	66
.006	46	57	45	48	46	45	55	66	54	77
.012	75	81	74	81	75	72	82	88	85	87

TABLE 3.6

EFFECT OF FLAT WIDTH ON ENERGY REQUIREMENTS

(Foot-Pounds at 0.012 Inch per Tooth)

Depth of Cut (inch)	Fluid Number					
	Dry		No. 6		No. 10	
	.005 Flat	.010 Flat	.005	.010	.005	.010
.025	2.65	3.50	2.30	2.75	2.45	3.45
.050	4.25	6.30	4.00	4.90	4.10	5.40
.075	5.70	8.10	5.10	6.50	5.50	6.90
.100	6.90	9.70	6.30	8.10	6.80	8.30

TABLE 3.7

SUMMARY OF ENERGY REQUIREMENTS FOR 30-DEGREE TOOL

Fluid No.	Energy/Chip (ft/lb) w = .200, f = .010, d = .100	Percent Reduction Over Dry Cutting	Energy Equation* $E = K\ wf^a\ d^b$
Dry	5.5	0	$E = 3445\ wf^{.68}\ d^{.73}$
1	4.7	8	$E = 3250\ wf^{.68}\ d^{.77}$
2	4.85	12	$E = 3480\ wf^{.68}\ d^{.79}$
3	5.20	8	$E = 3625\ wf^{.68}\ d^{.73}$
4	4.55	9	$E = 3575\ wf^{.68}\ d^{.83}$
5	4.50	14	$E = 3350\ wf^{.68}\ d^{.81}$
6	4.25	20	$E = 3530\ wf^{.68}\ d^{.86}$
7	4.70	10	$E = 2750\ wf^{.68}\ d^{.71}$
8	4.90	10	$E = 2790\ wf^{.68}\ d^{.69}$
9	4.50	14	$E = 3740\ wf^{.68}\ d^{.85}$
10	4.90	4	$E = 3725\ wf^{.68}\ d^{.82}$

*E = energy per chip in foot-pounds
w = width of cut in inches
f = feed in inches per tooth
d = depth of cut in inches

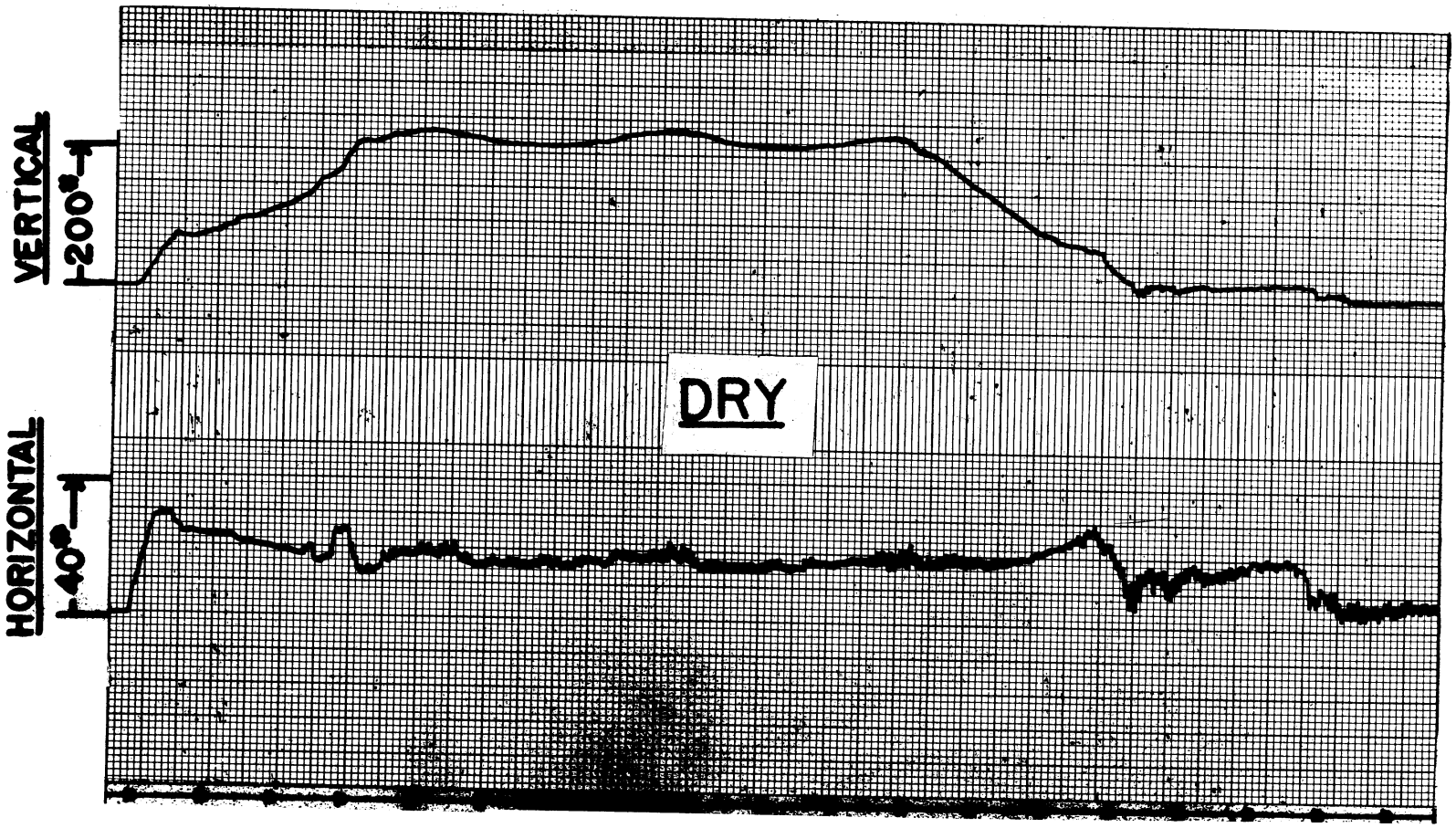

Fig. 3.1. Cutting force chart for complete turning cut on copper with no cutting fluid. Cutting is on the end of a one-inch-diameter tube having a wall thickness of 1/16 inch. Feed rate: 0.030 ipr. Spindle speed: 18 rpm.

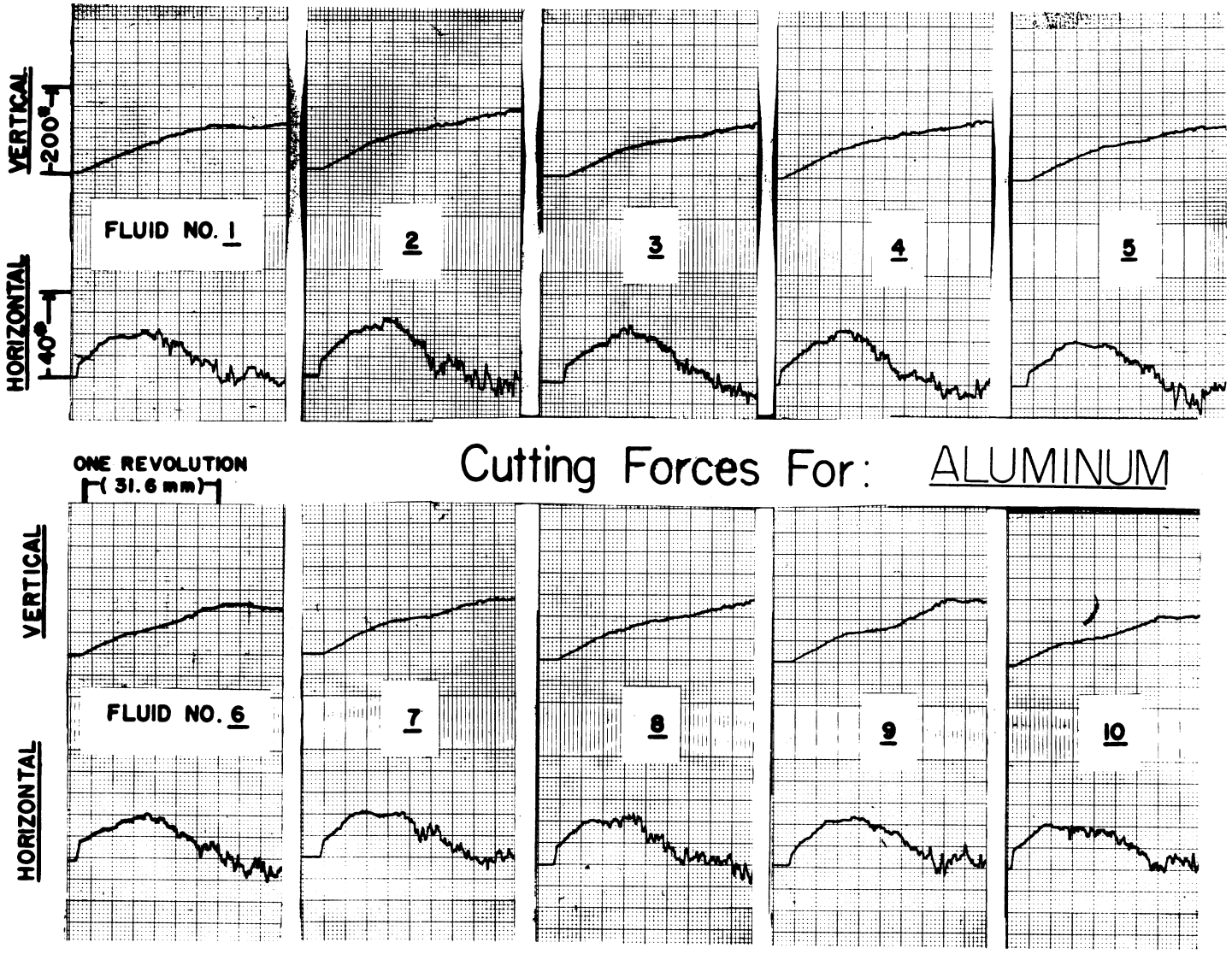

Fig. 3.2. Cutting forces for each of ten different cutting fluids. Cutting conditions same as in Fig. 3.1.

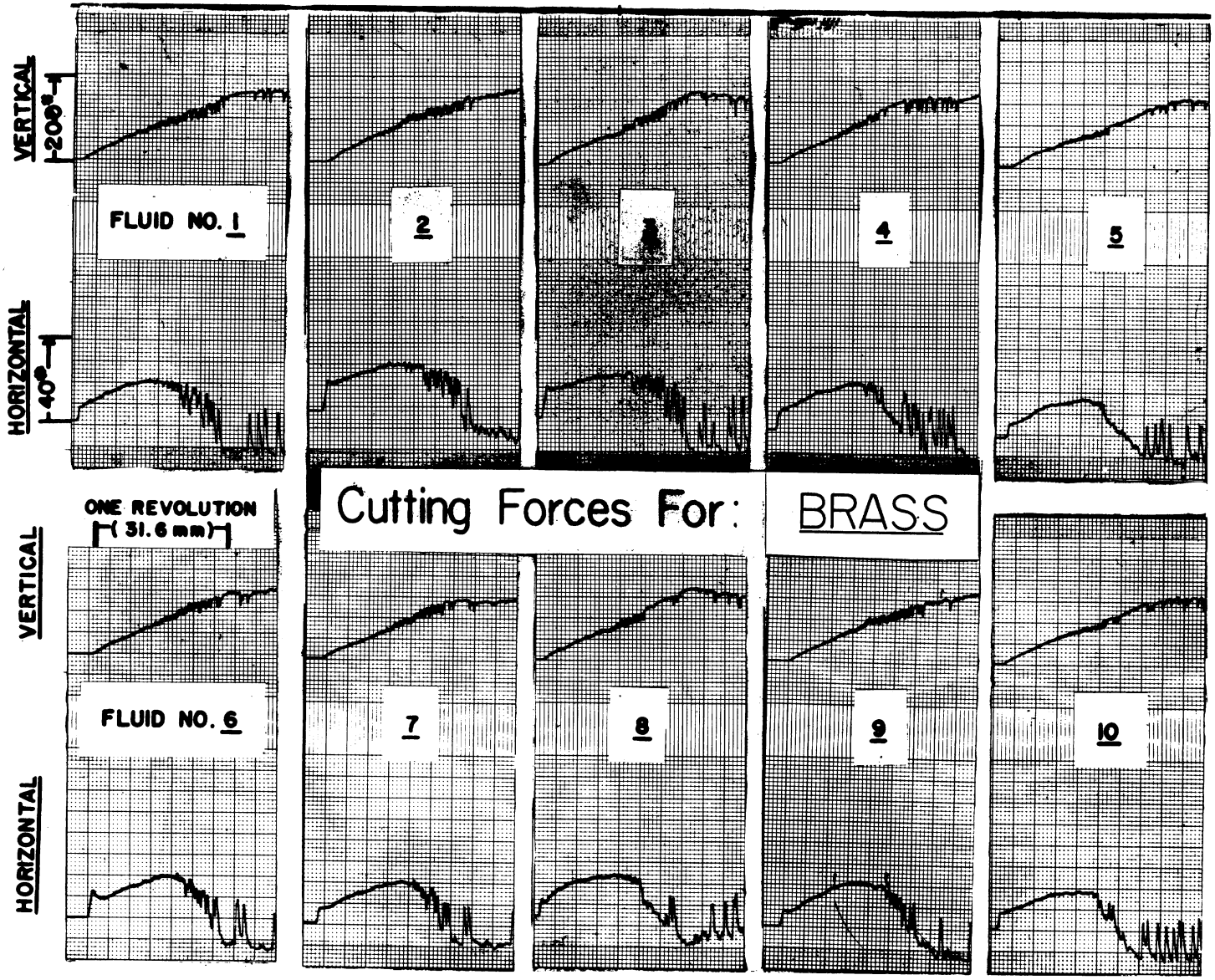

Fig. 3.3. Cutting forces for each of ten different cutting fluids. Cutting conditions same as in Fig. 3.1.

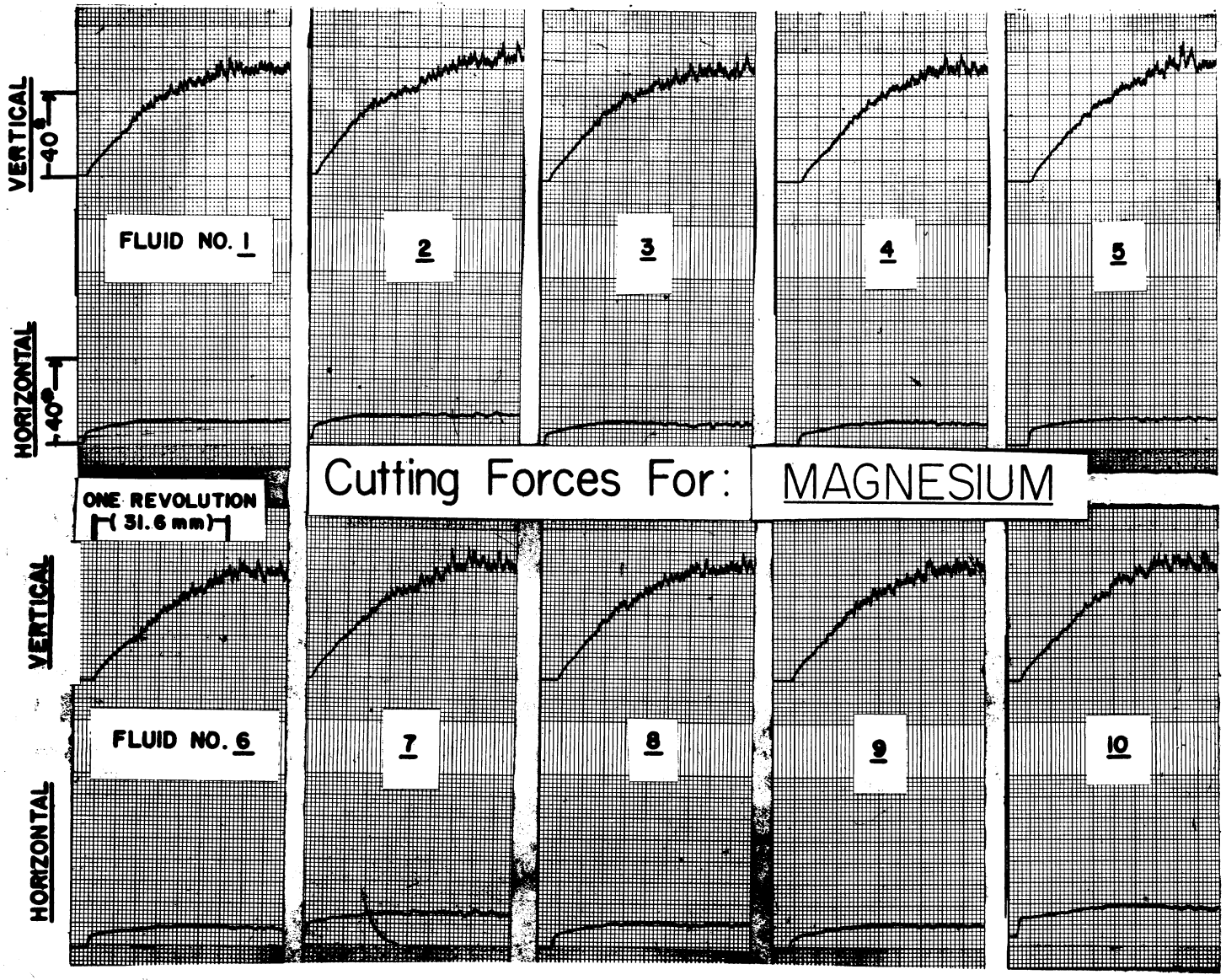

Fig. 3.4. Cutting forces for each of ten different cutting fluids. Cutting conditions same as in Fig. 3.1.

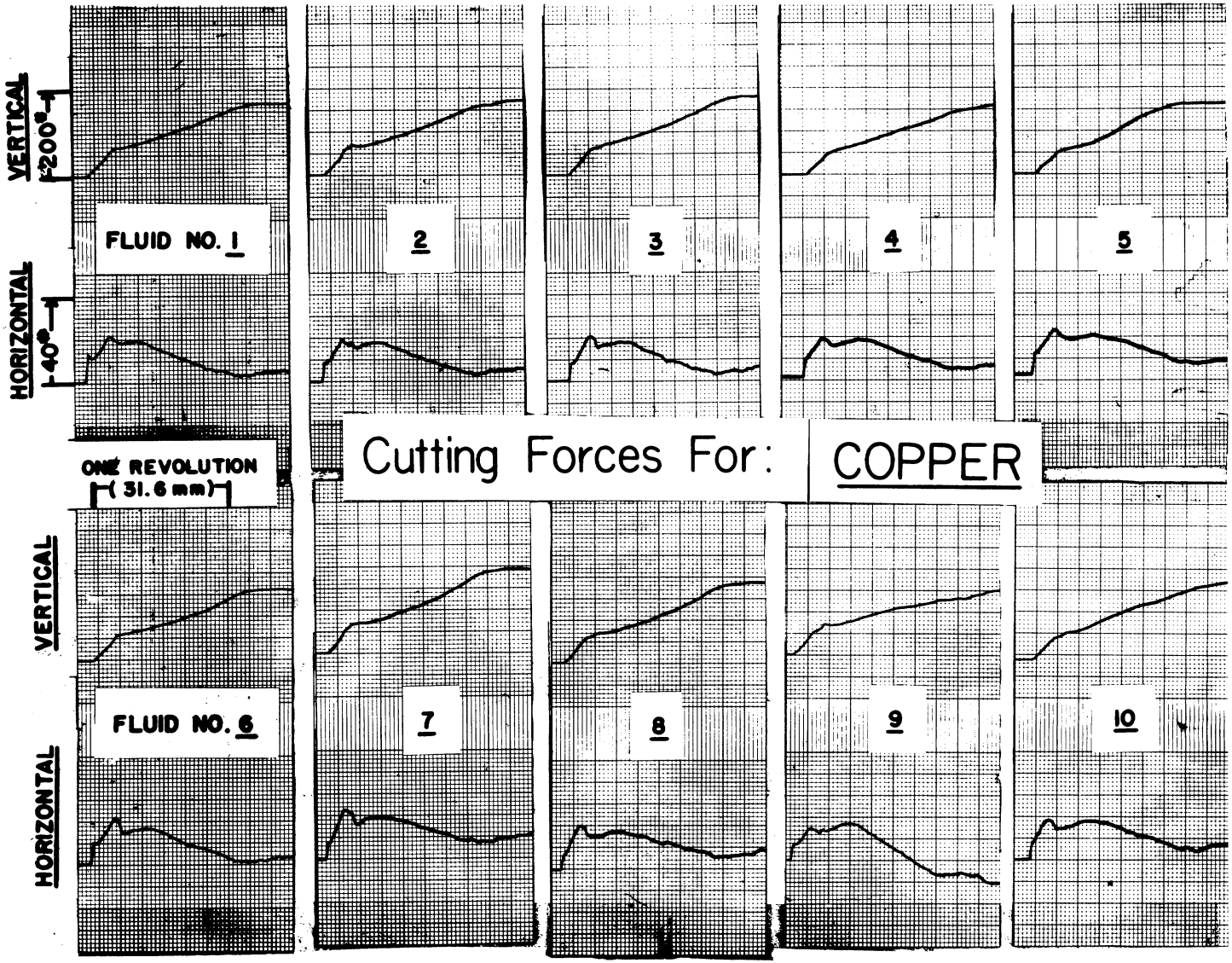

Fig. 3.5. Cutting forces for each of ten different cutting fluids. Cutting conditions same as in Fig. 3.1.

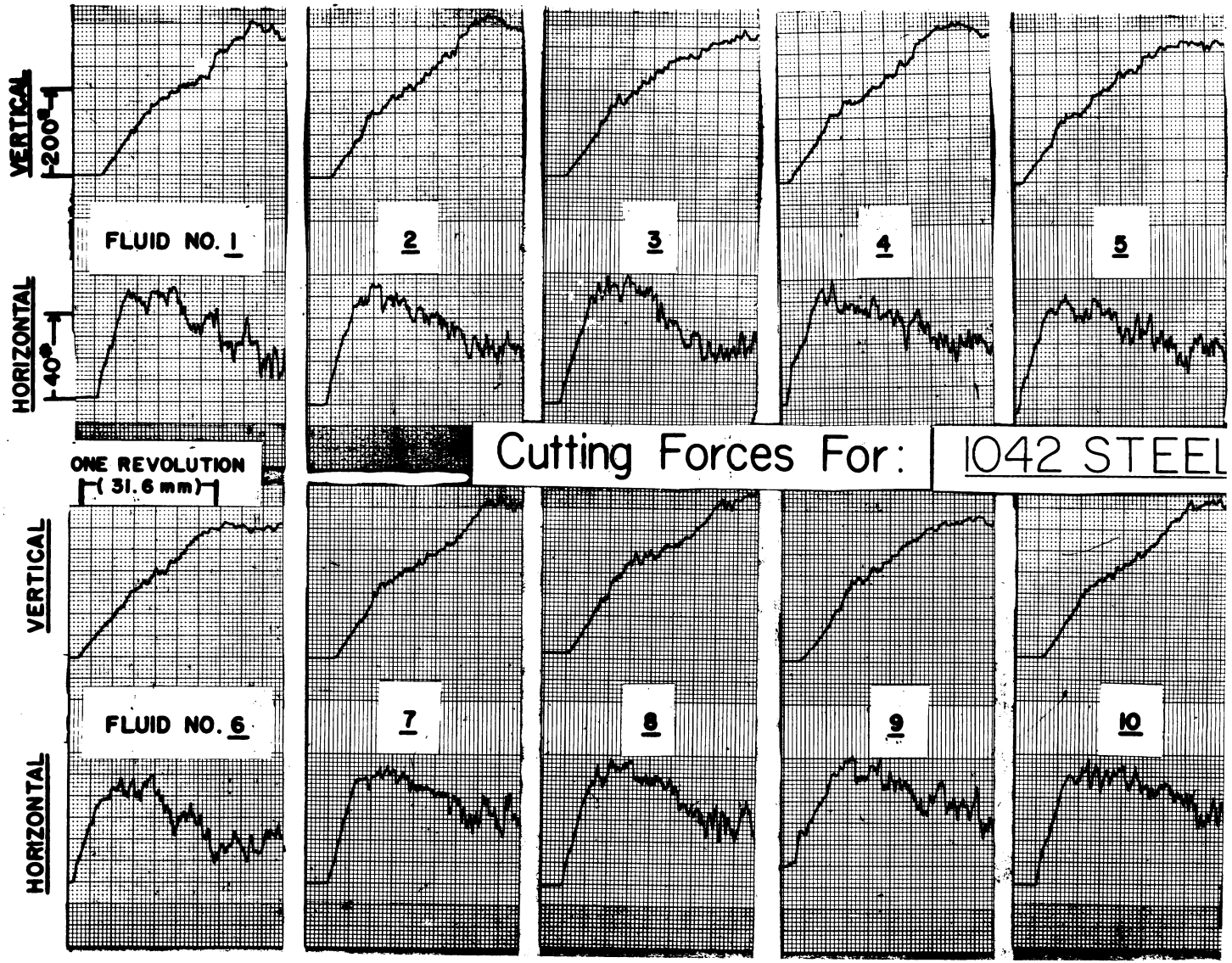

Fig. 3.6. Cutting forces for each of ten different cutting fluids. Cutting conditions same as in Fig. 3.1.

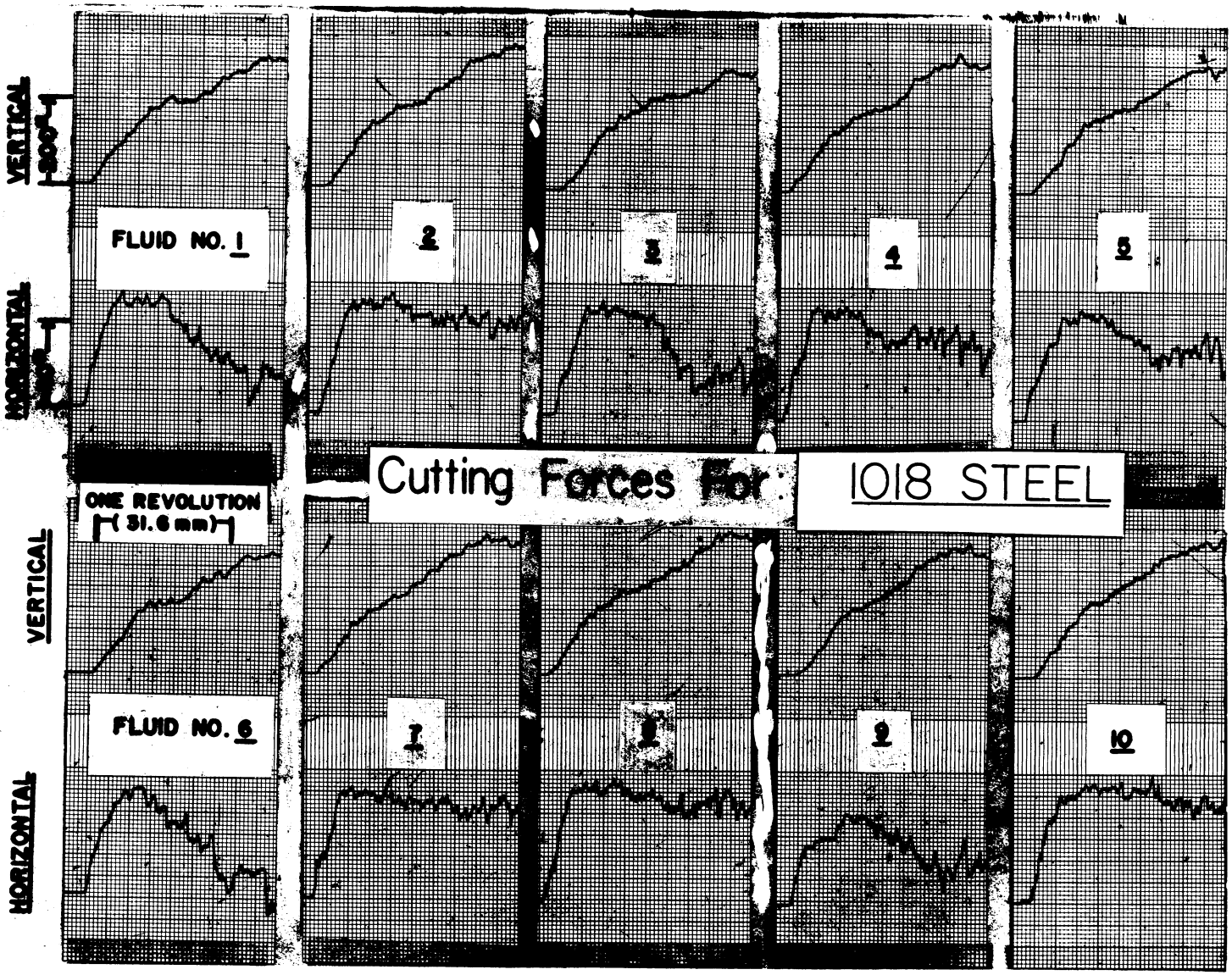

Fig. 3.7. Cutting forces for each of ten different cutting fluids. Cutting conditions same as in Fig. 3.1.

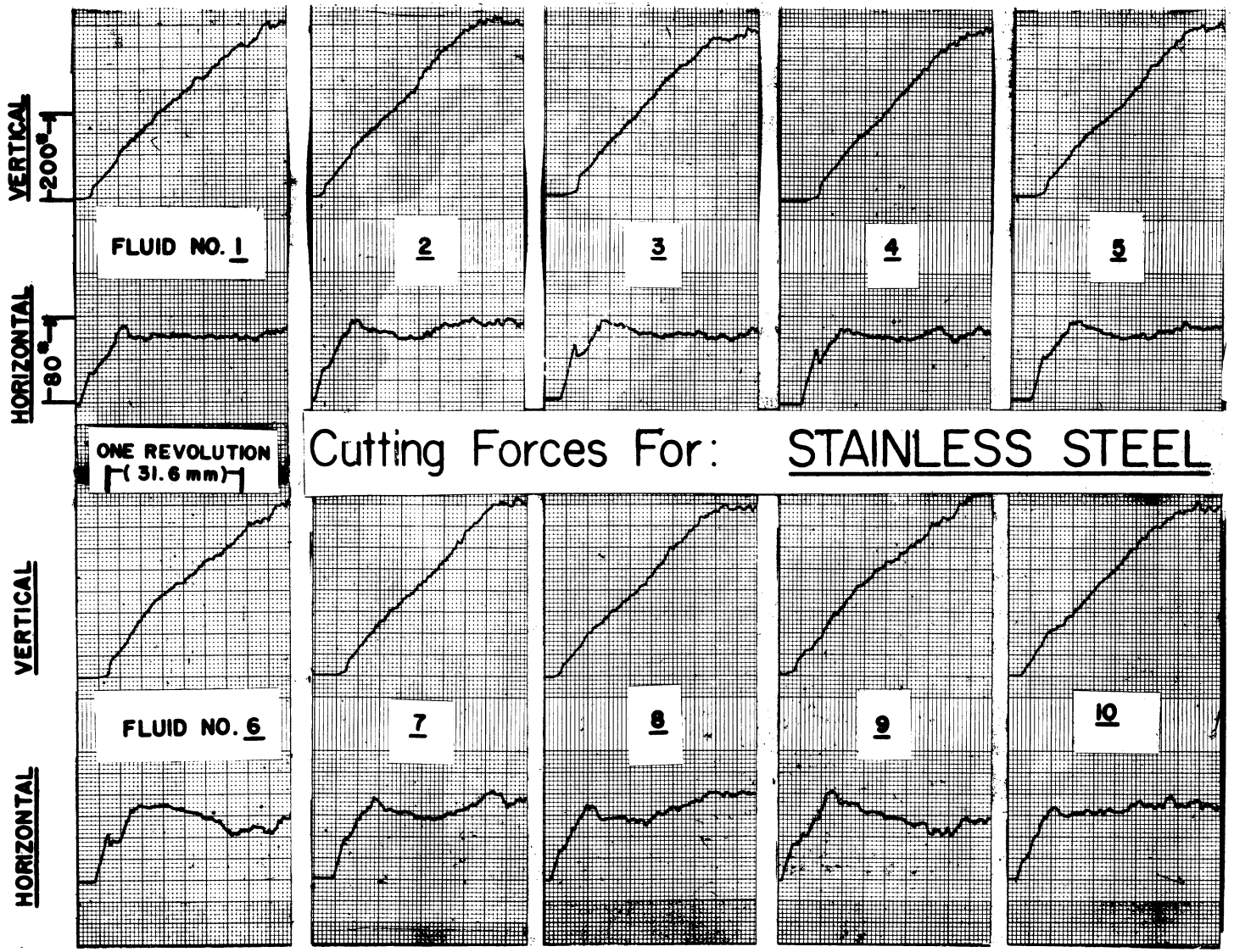

Fig. 3.8. Cutting forces for each of ten different cutting fluids. Cutting conditions same as in Fig. 3.1.

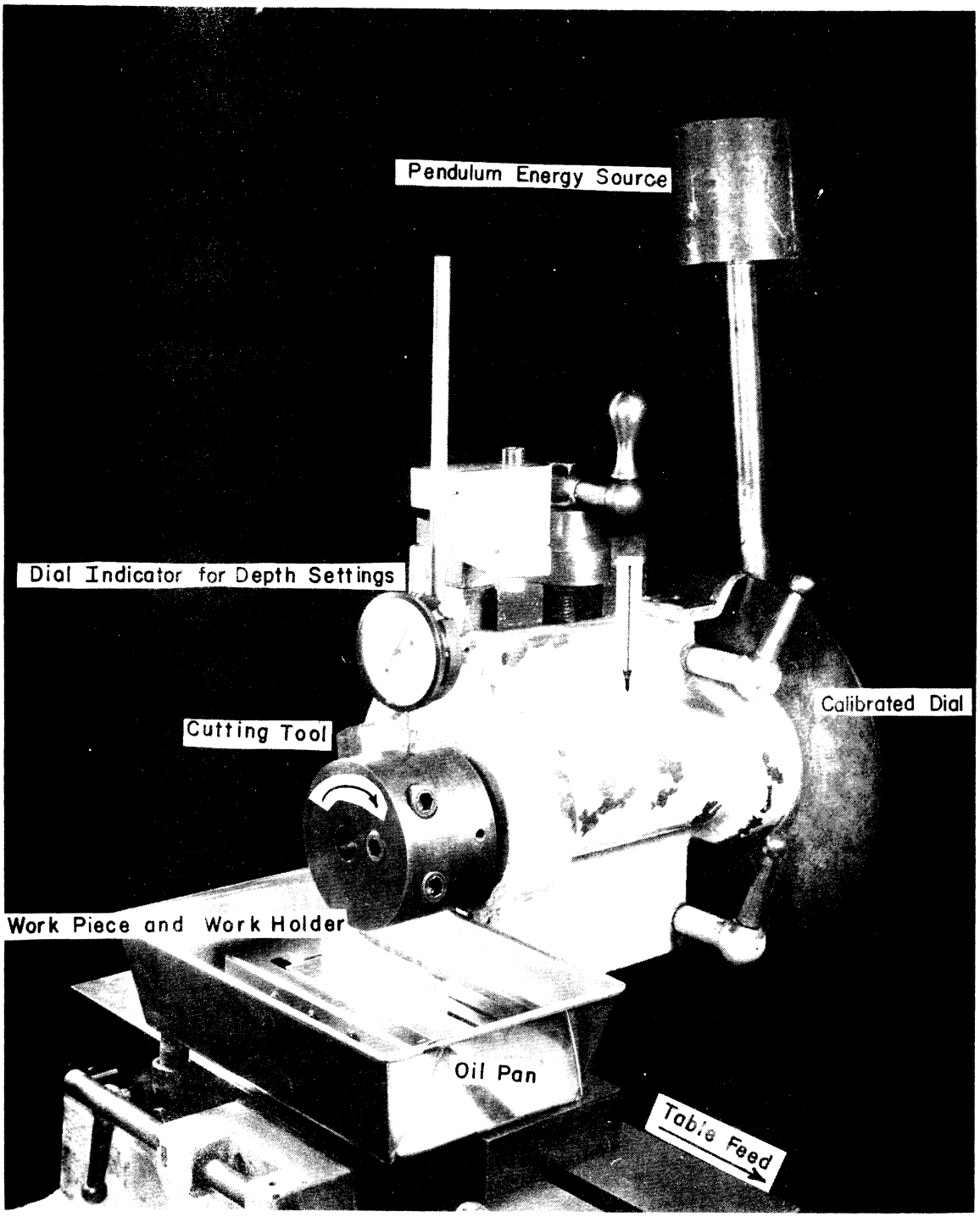

Fig. 3.9. [illegible] drilling dynamometer. The amount of over-travel of the pendulum [illegible] reading of the amount of energy required to cut a single [illegible]

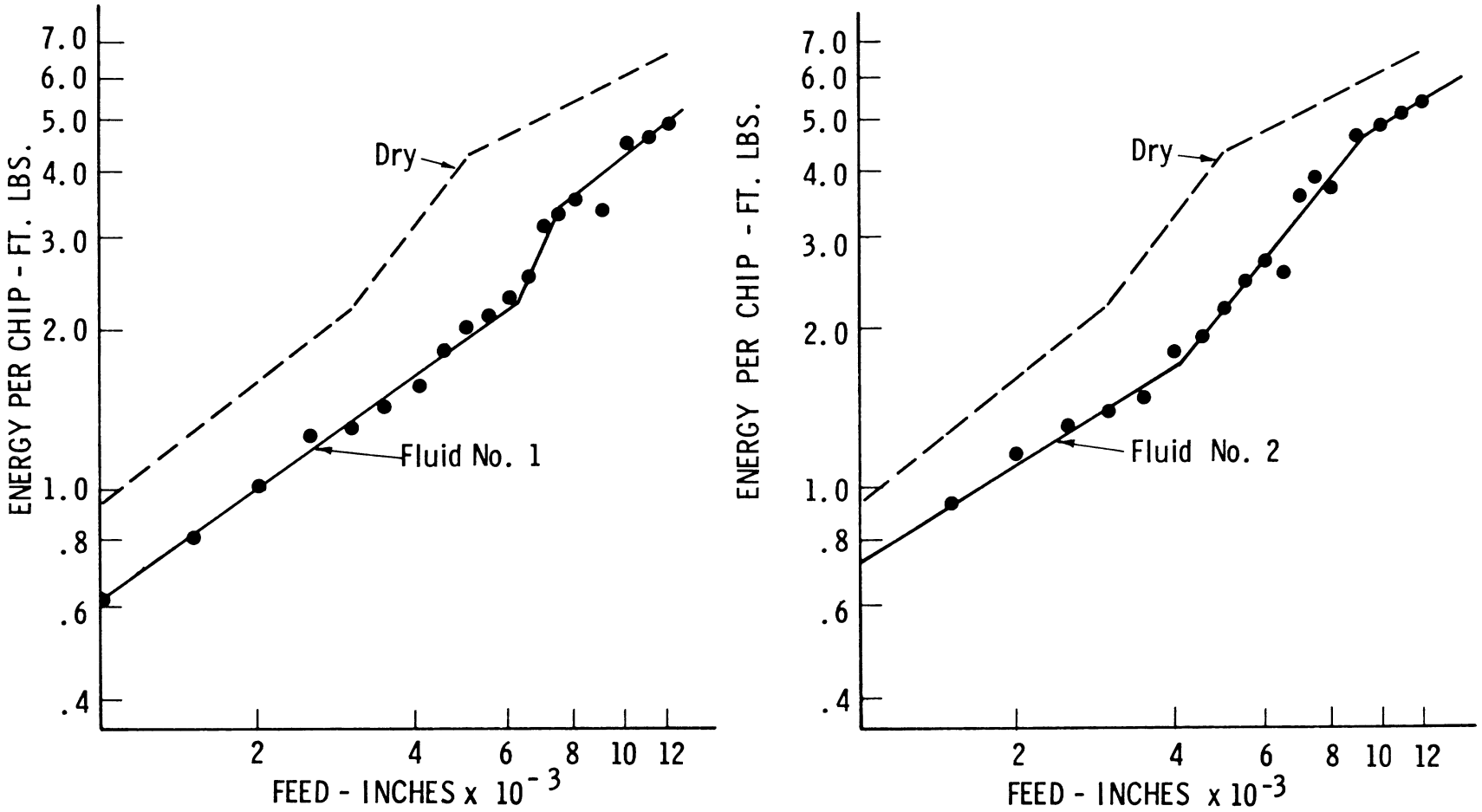

Fig. 3.10. Energy per chip as determined by the Pendulum Milling Dynamometer for each of ten different cutting fluids on annealed AISI 1020 steel. Width of cut = 0.200 inch. Depth of cut = 0.050 inch. Cutting tool: M-2 high-speed steel ground with 10° primary relief, 20° secondary relief, 30° degree secondary rake, and a 0.010 inch wide by 0° flat.

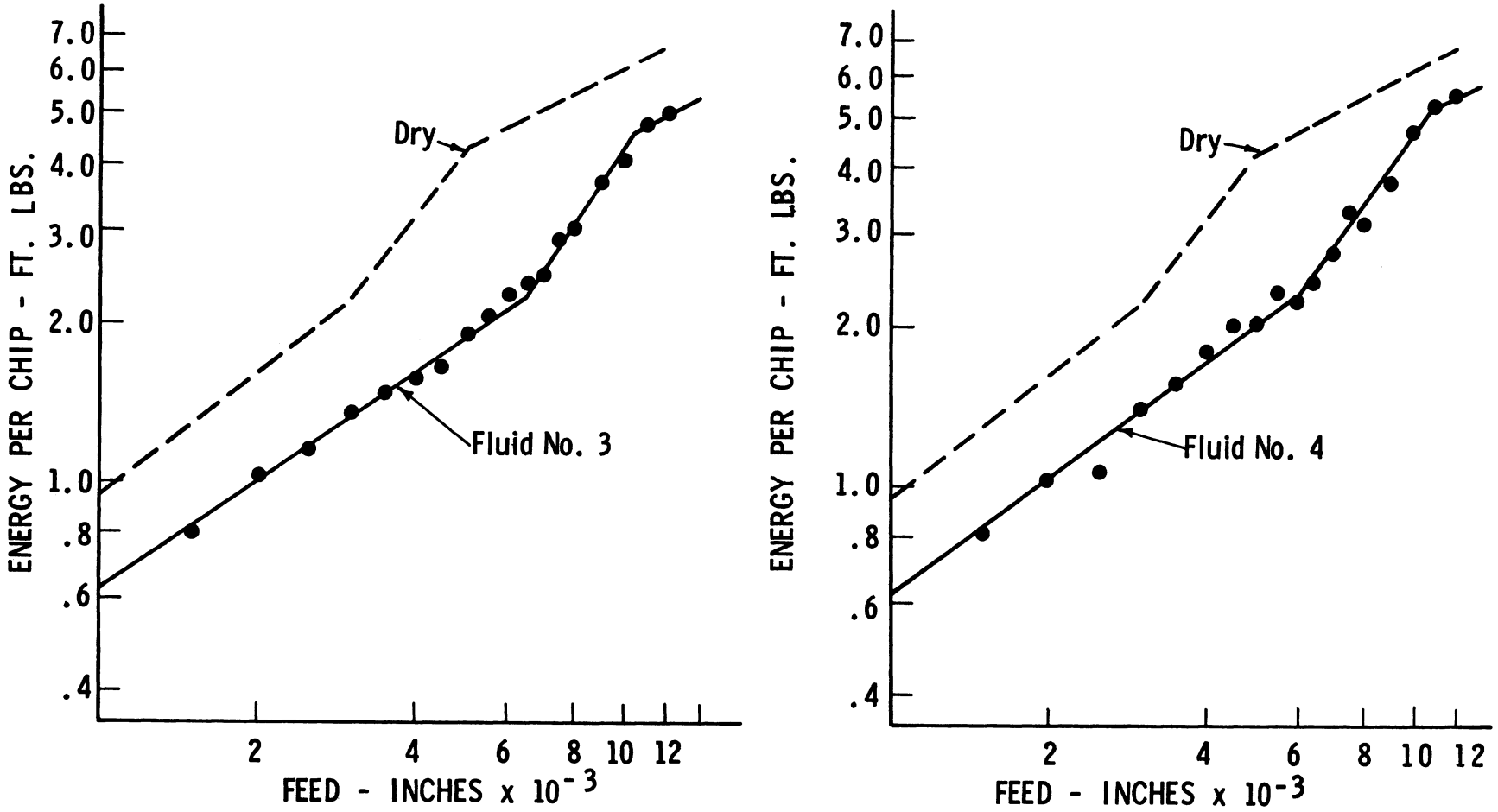

Fig. 3.11. Energy per chip as determined by the Pendulum Milling Dynamometer for each of ten different cutting fluids on annealed AISI 1020 steel. Cutting conditions same as Fig. 3.10.

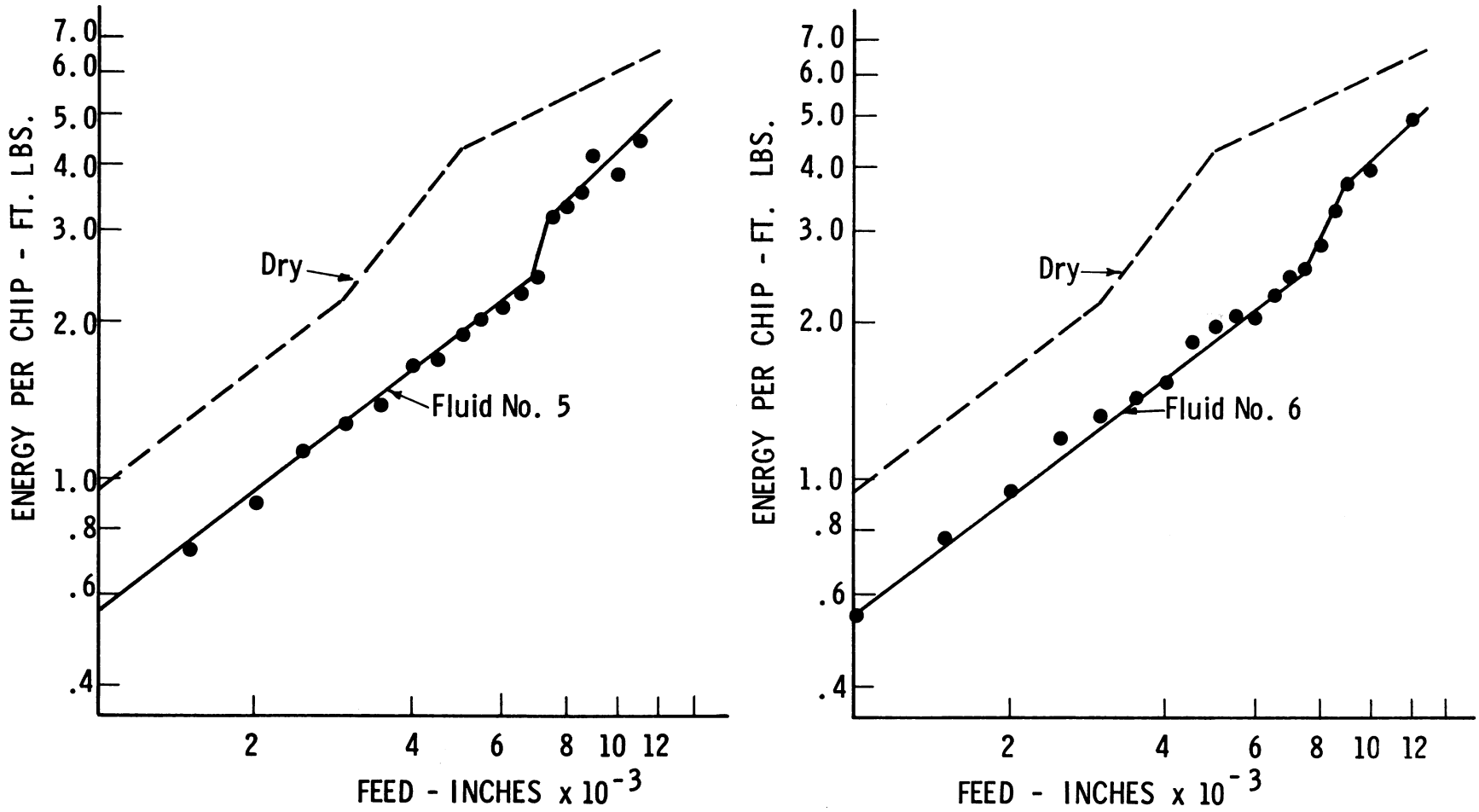

Fig. 3.12. Energy per chip as determined by the Pendulum Milling Dynamometer for each of ten different cutting fluids on annealed AISI 1020 steel. Cutting conditions same as Fig. 3.10.

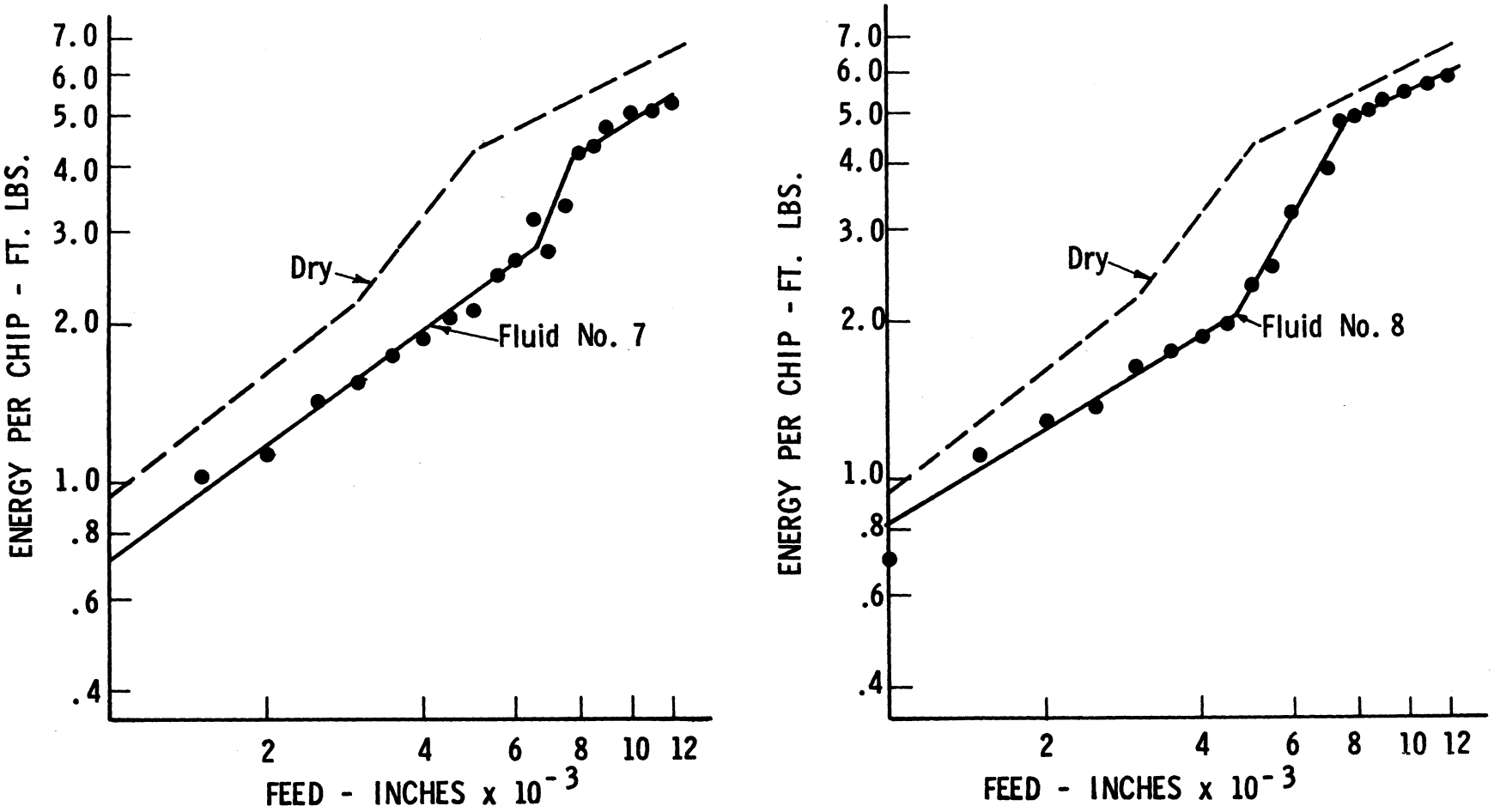

Fig. 3.13. Energy per chip as determined by the Pendulum Milling Dynamometer for each of ten different cutting fluids on annealed AISI 1020 steel. Cutting conditions same as Fig. 3.10.

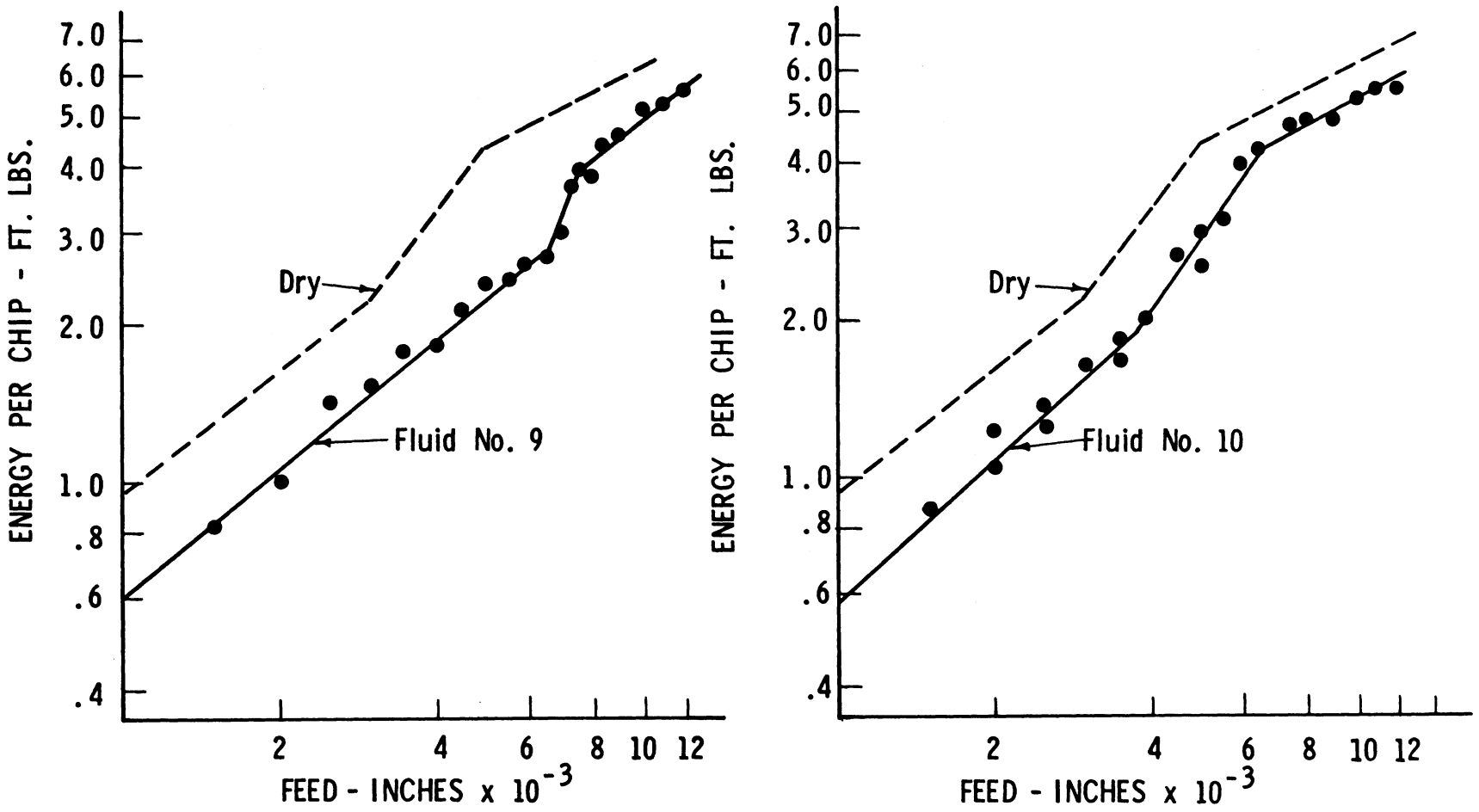

Fig. 3.14. Energy per chip as determined by the Pendulum Milling Dynamometer for each of ten different cutting fluids on annealed AISI 1020 steel. Cutting conditions same as Fig. 3.10.

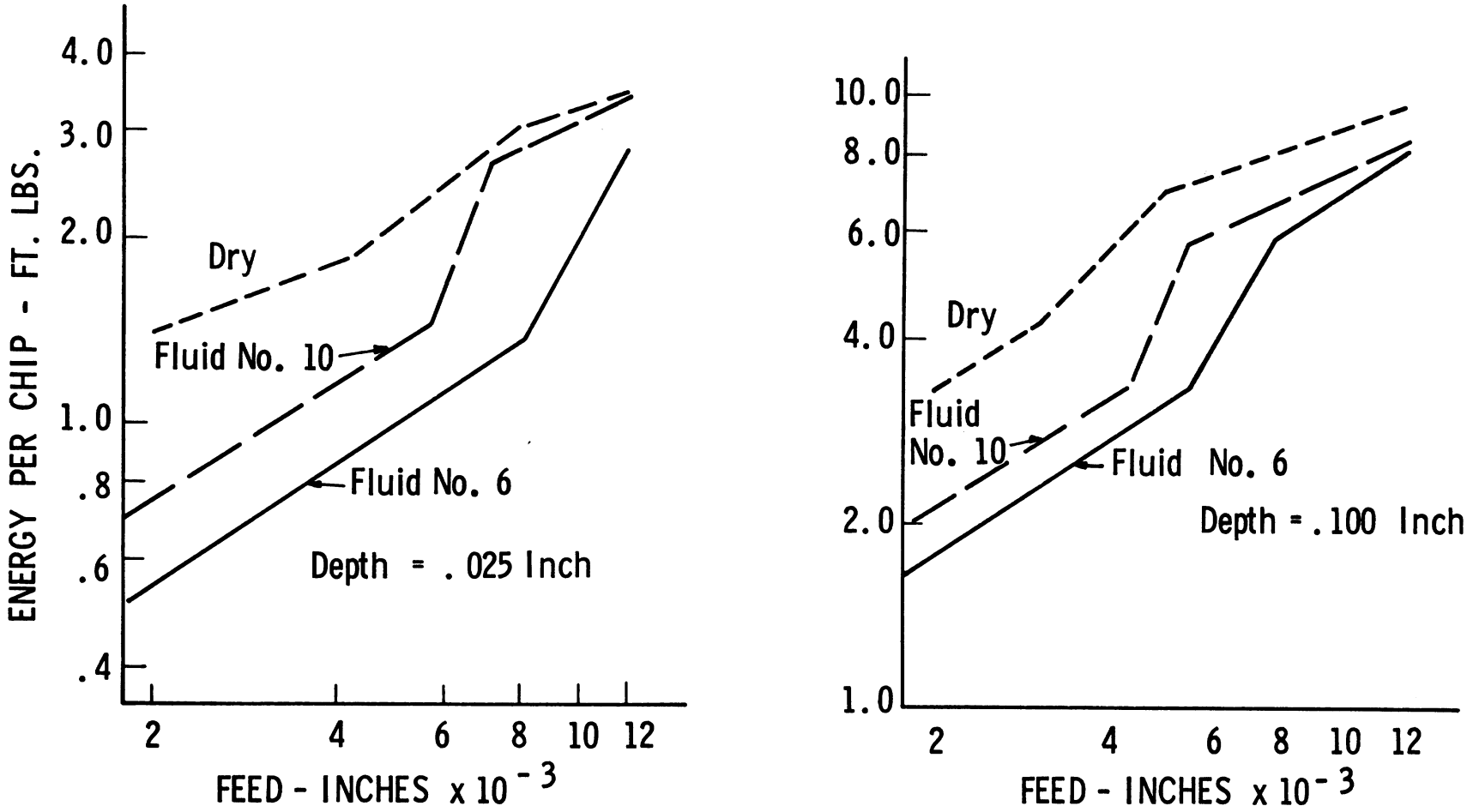

Fig. 3.15. Shows dependency of fluid rating on size of cut; beneficial effects of fluids tend to disappear at large feed rates. Cutting conditions same as Fig. 3.10 except as indicated.

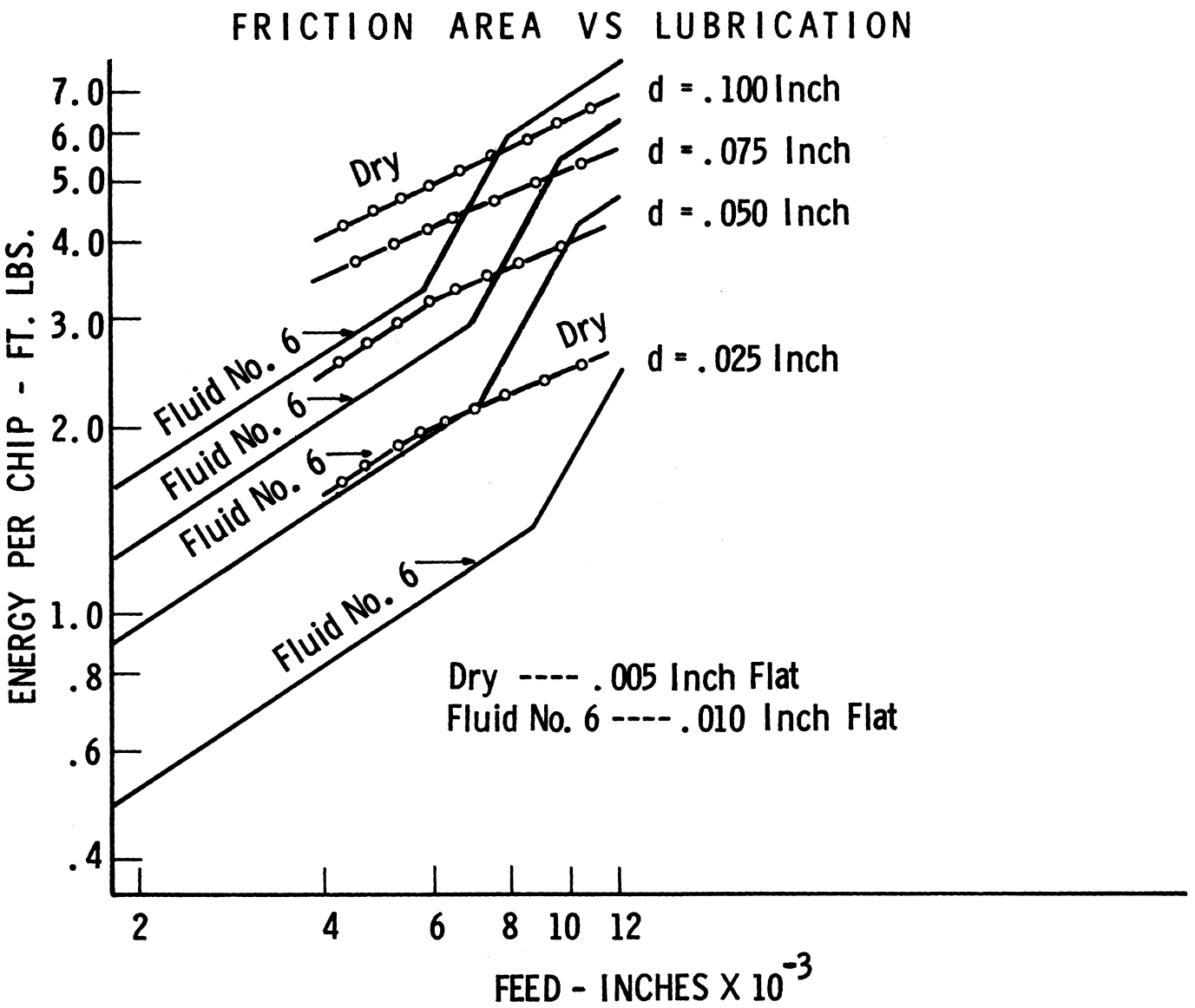

Fig. 3.16. Shows the relative potency of lubrication and friction area. The best lubricant with twice as much available friction area requires more energy than dry cutting at high feed rates. Cutting conditions same as for Fig. 3.10 except as indicated.

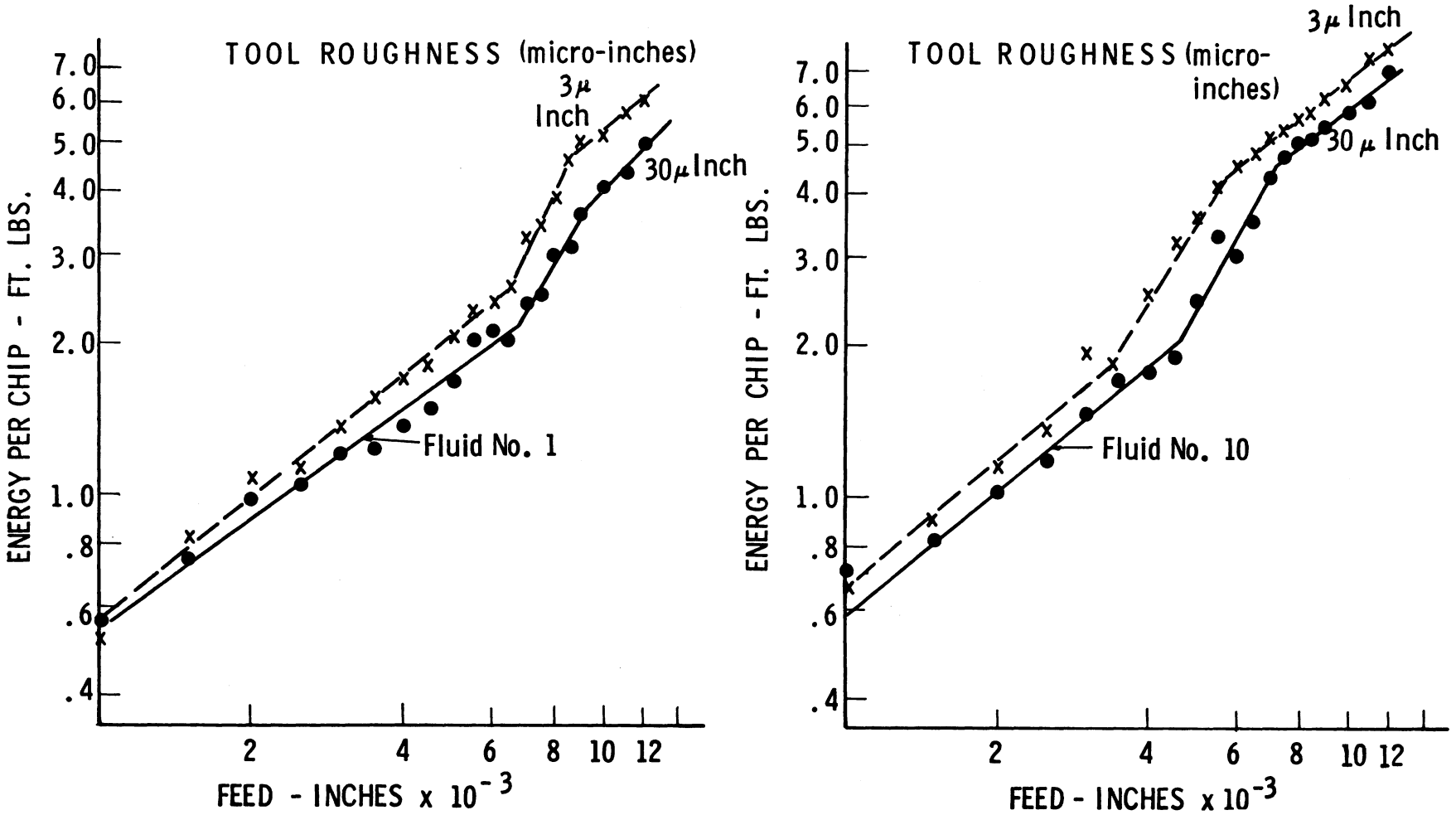

Fig. 3.17. Energy requirements are lower for rougher tools because each roughness peak acts as a limited contact area. Cutting conditions same as for Fig. 3.10 except that the tool rake angle was 0°.

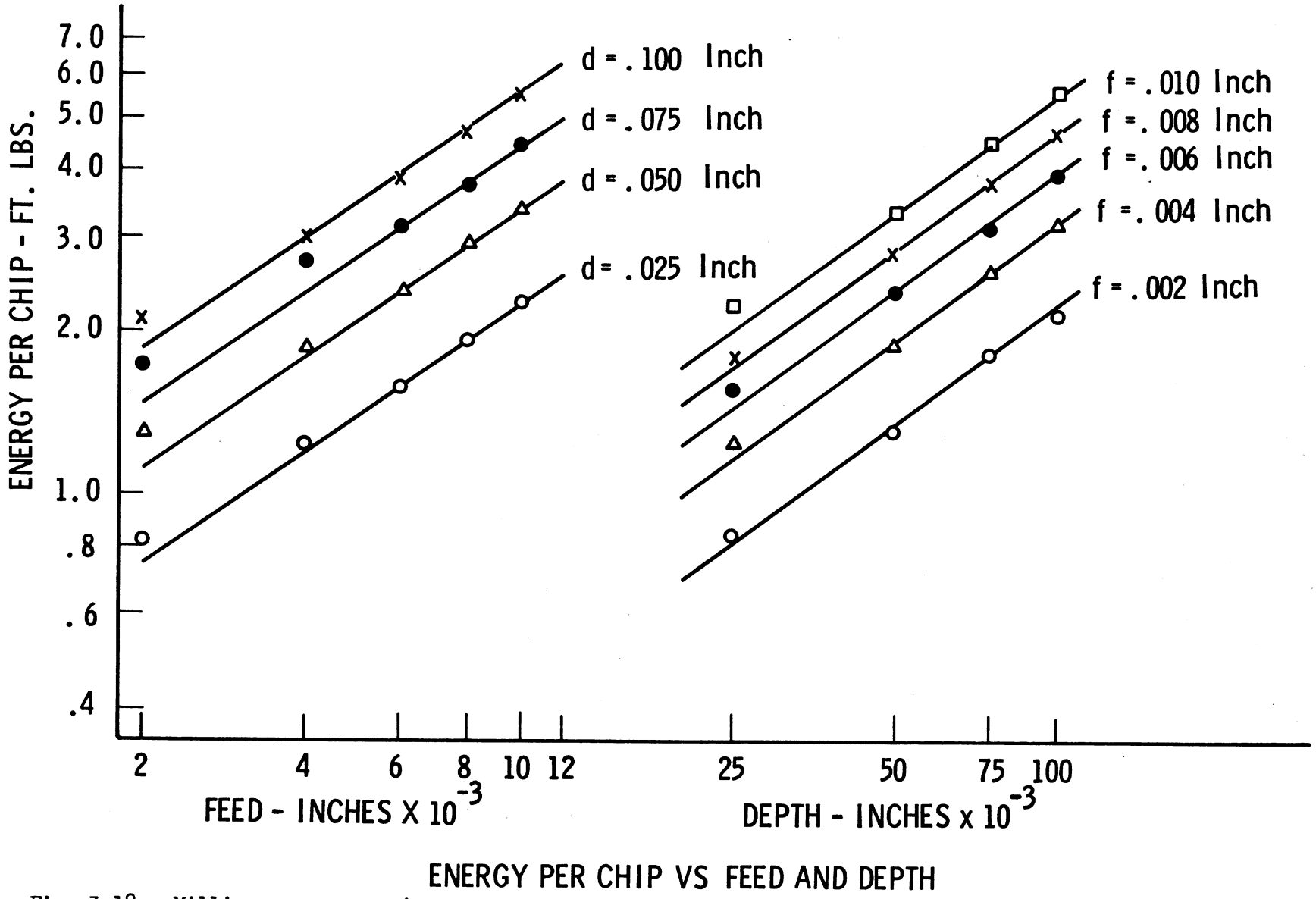

ENERGY PER CHIP VS FEED AND DEPTH

Fig. 3.18. Milling energy requirements for ranges of both feed rate and depth of cut for ten different cutting fluids and dry cutting with a conventional 30° rake-angle tool. Relief angles and width of cut same as for Fig. 3.10.

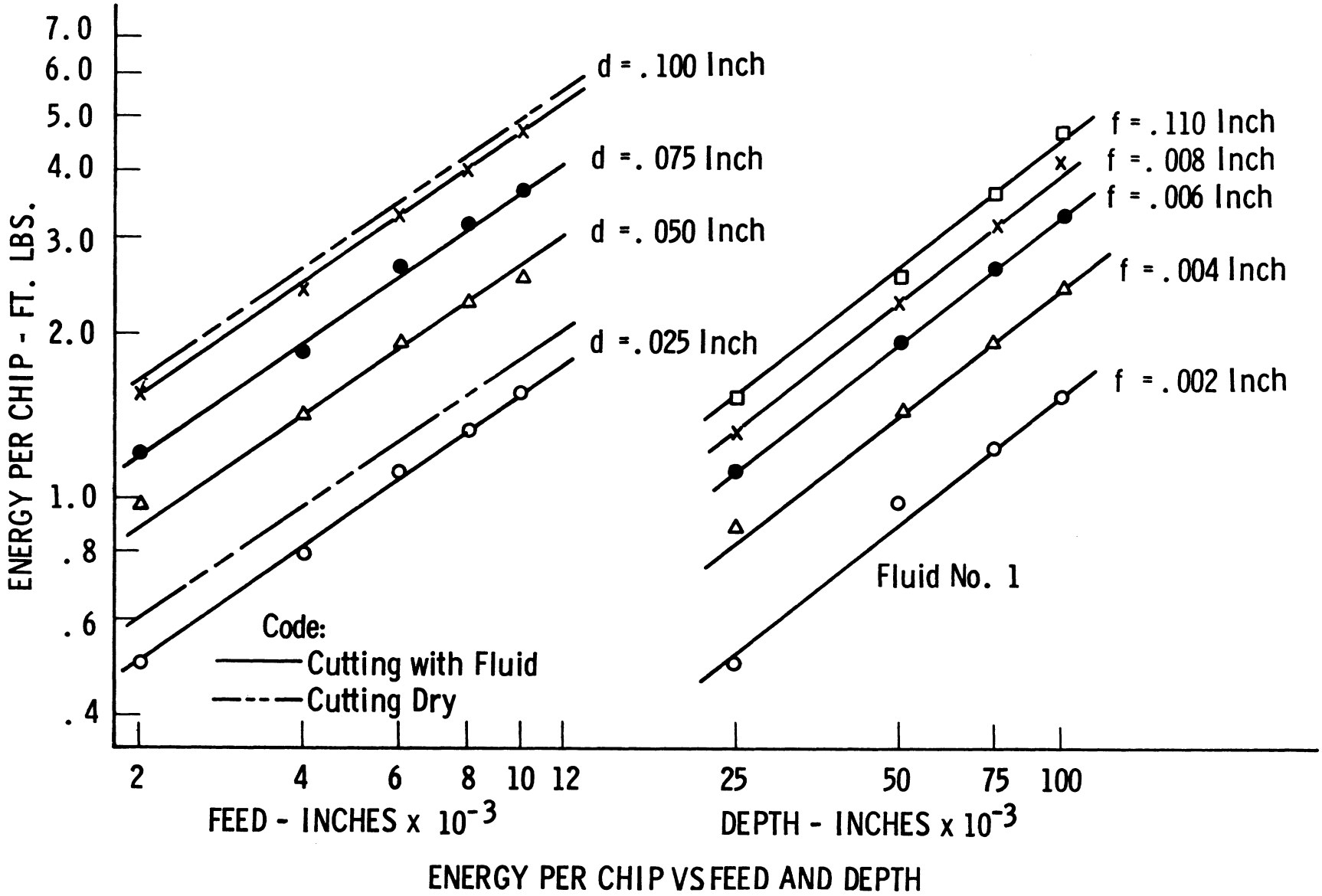

Fig. 3.19. Milling energy requirements for ranges of both feed rate and depth of cut for ten different cutting fluids and dry cutting with a conventional 30° rake-angle tool. Relief angles and width of cut same as for Fig. 3.10.

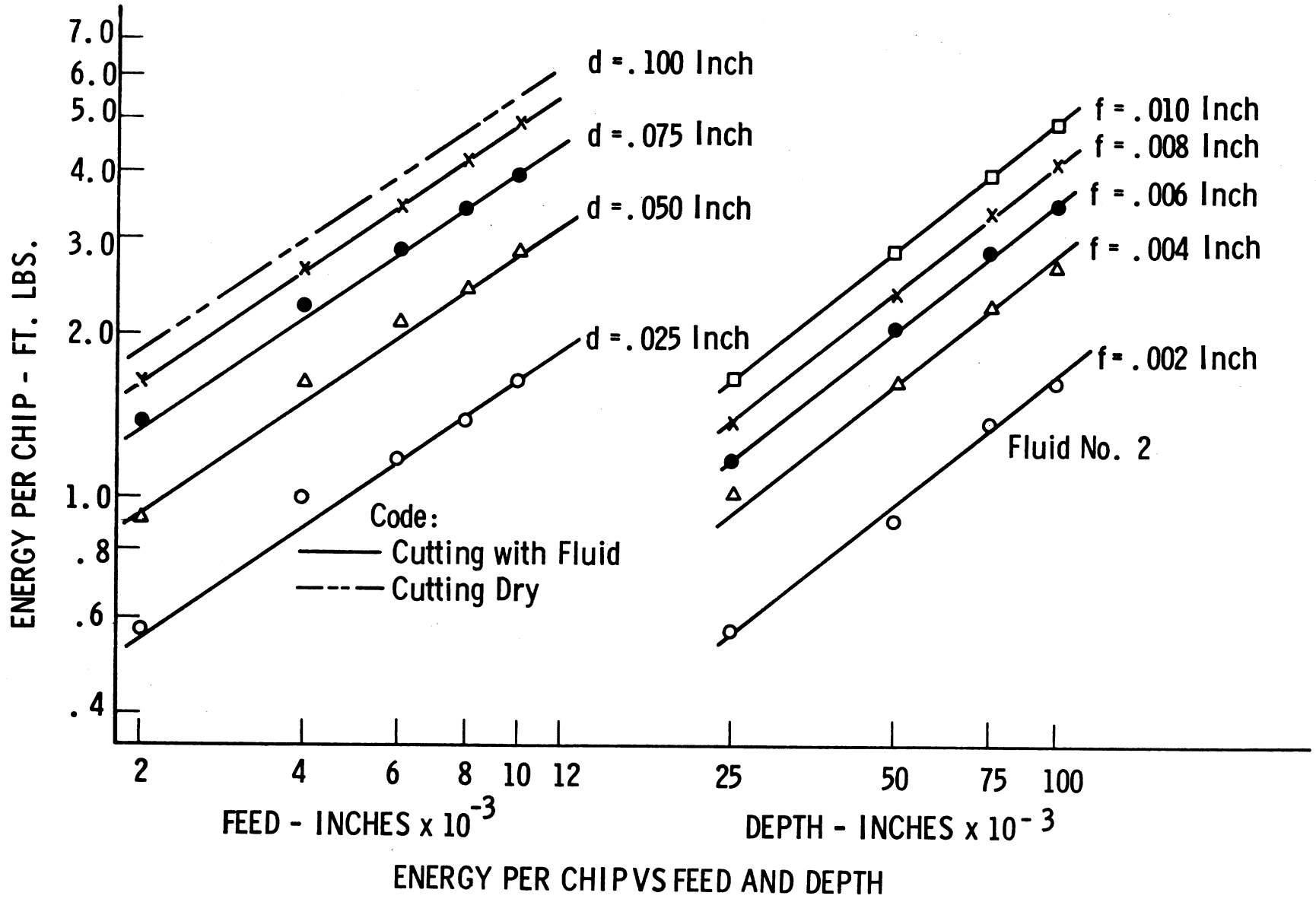

Fig. 3.20. Milling energy requirements for ranges of both feed rate and depth of cut for ten different cutting fluids and dry cutting with a conventional 30° rake-angle tool. Relief angles and width of cut same as for Fig. 3.10.

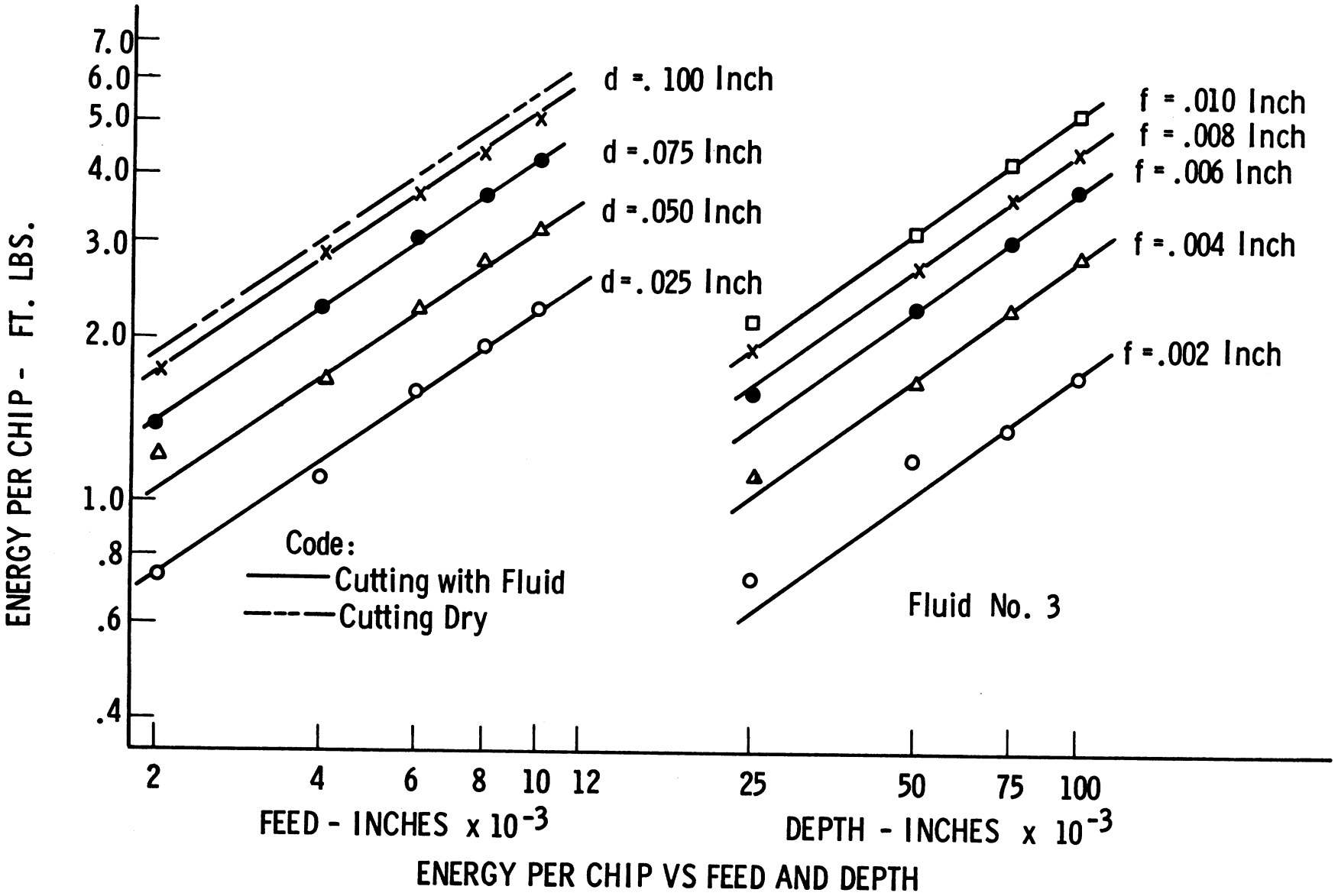

Fig. 3.21. Milling energy requirements for ranges of both feed rate and depth of cut for ten different cutting fluids and dry cutting with a conventional 30° rake-angle tool. Relief angles and width of cut same as for Fig. 3.10.

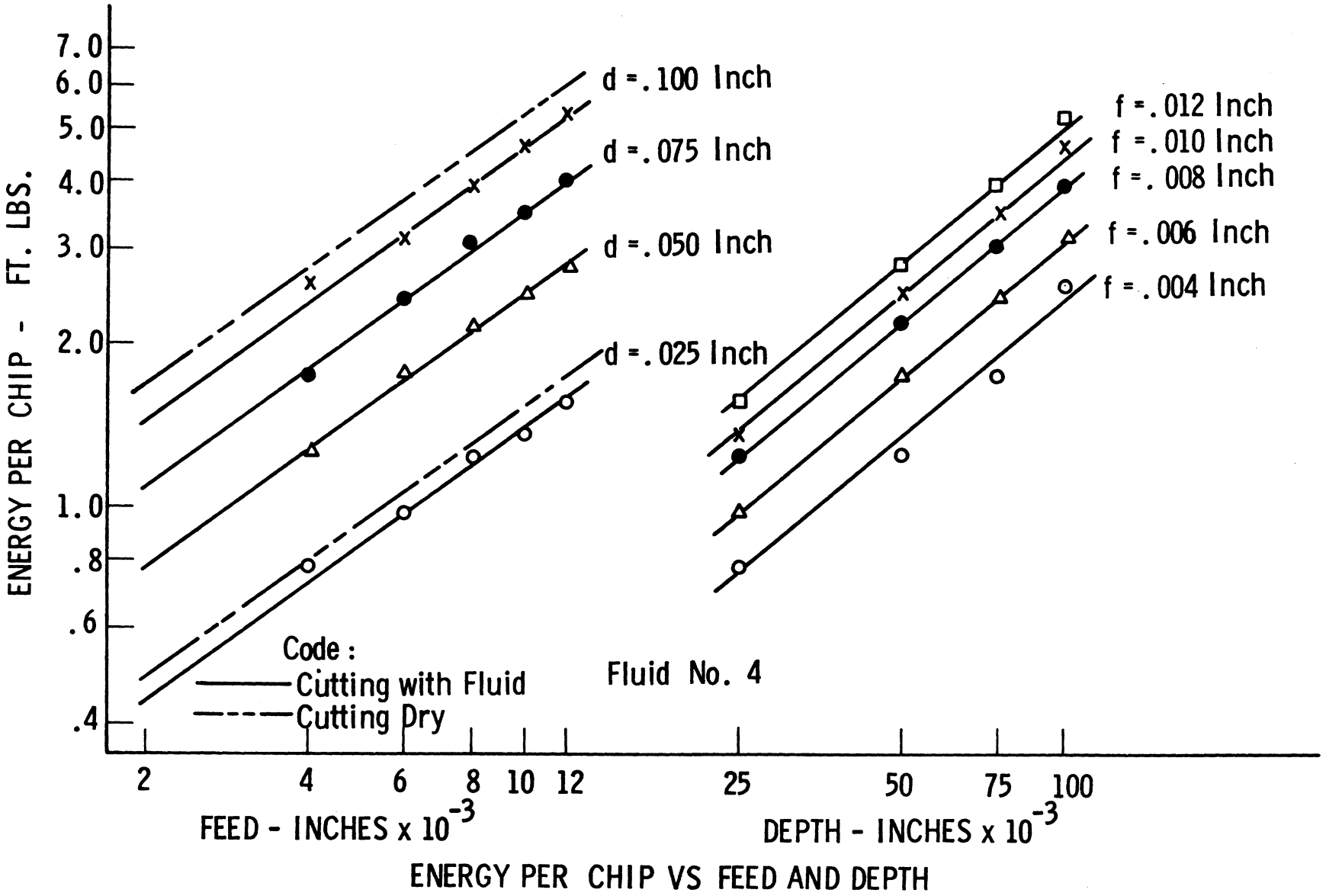

Fig. 3.22. Milling energy requirements for ranges of both feed rate and depth of cut for ten different cutting fluids and dry cutting with a conventional 30° rake-angle tool. Relief angles and width of cut same as for Fig. 3.10.

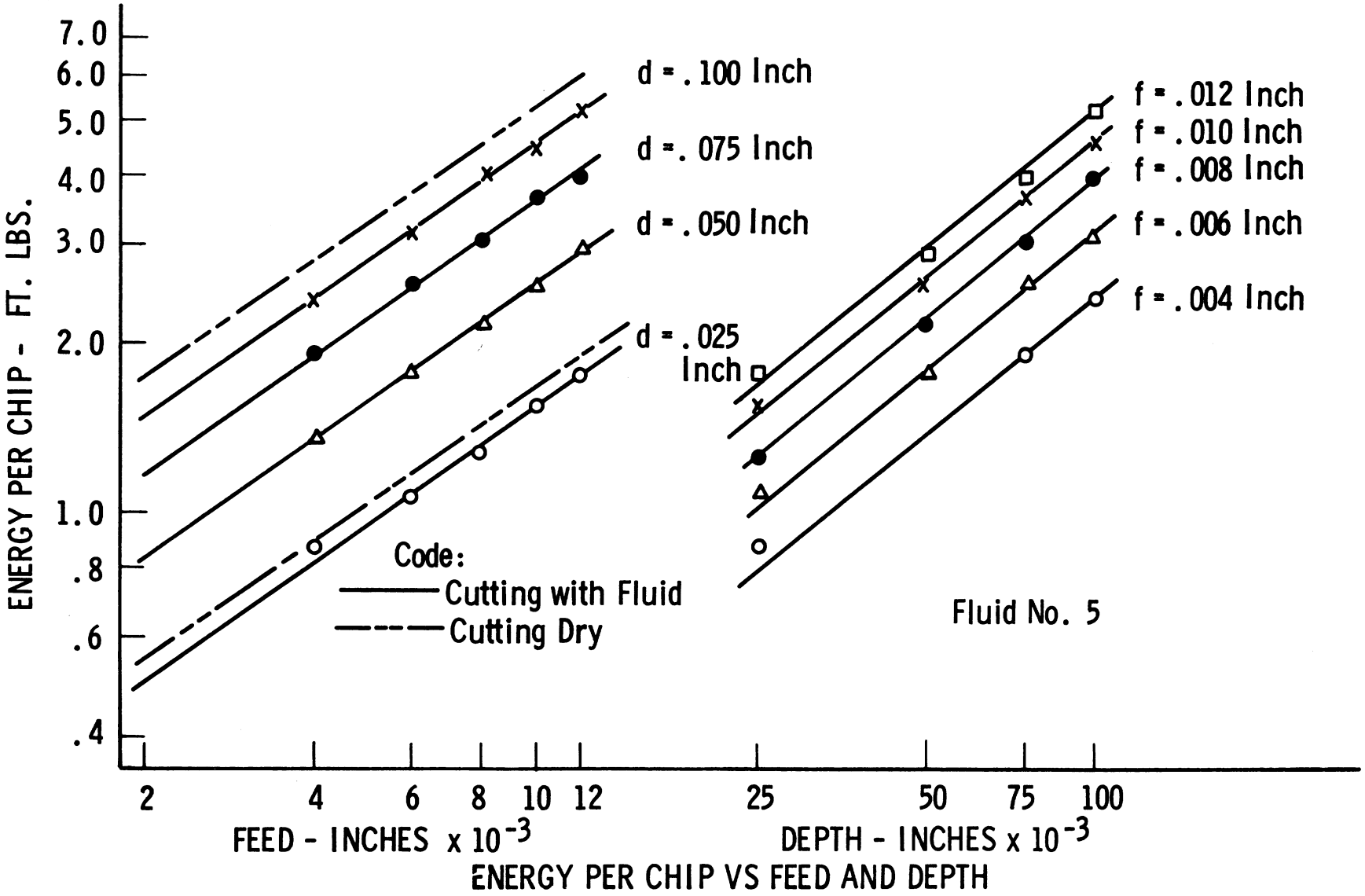

Fig. 3.23. Milling energy requirements for ranges of both feed rate and depth of cut for ten different cutting fluids and dry cutting with a conventional 30° rake-angle tool. Relief angles and width of cut same as for Fig. 3.10.

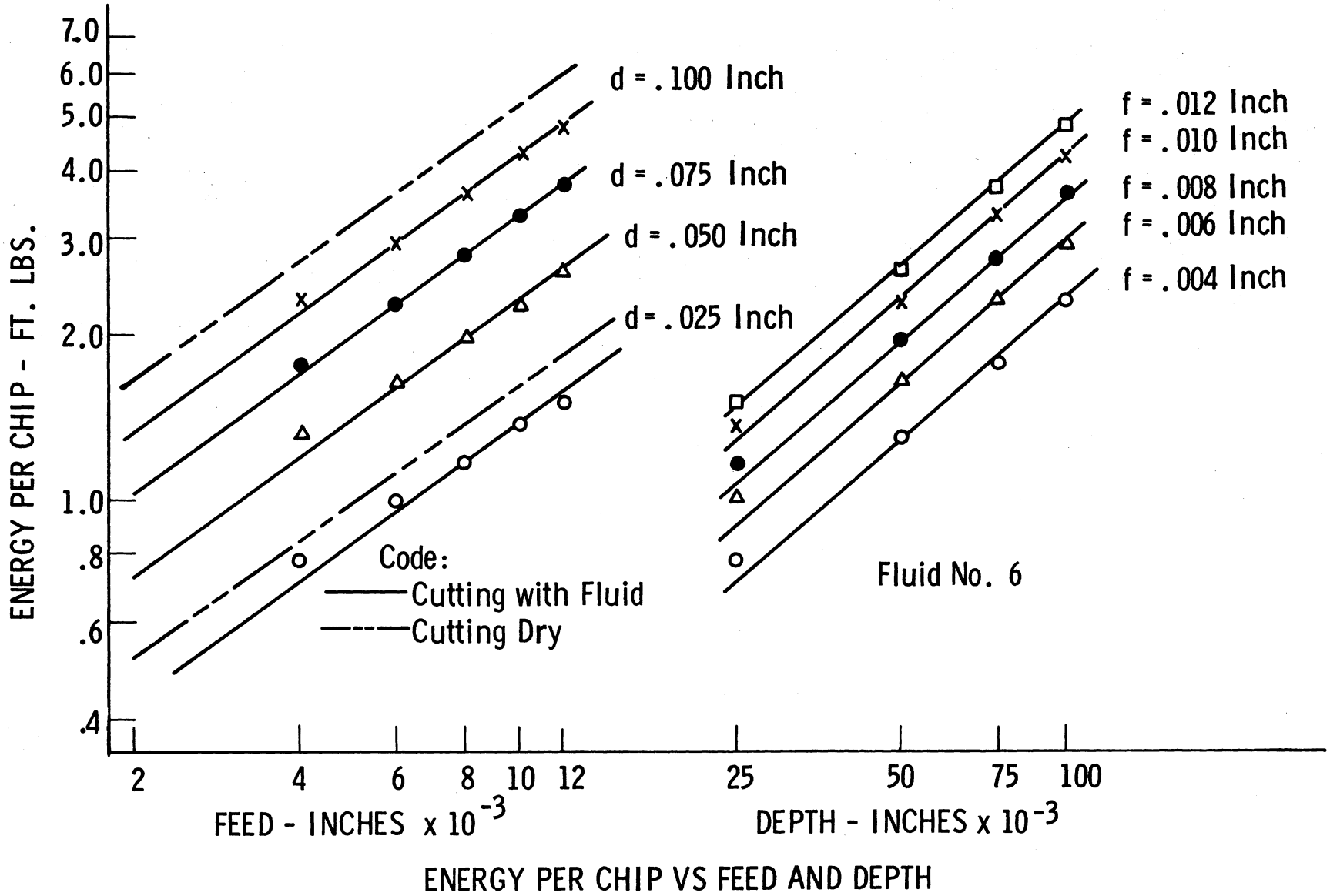

Fig. 3.24. Milling energy requirements for ranges of both feed rate and depth of cut for ten different cutting fluids and dry cutting with a conventional 30° rake-angle tool. Relief angles and width of cut same as for Fig. 3.10.

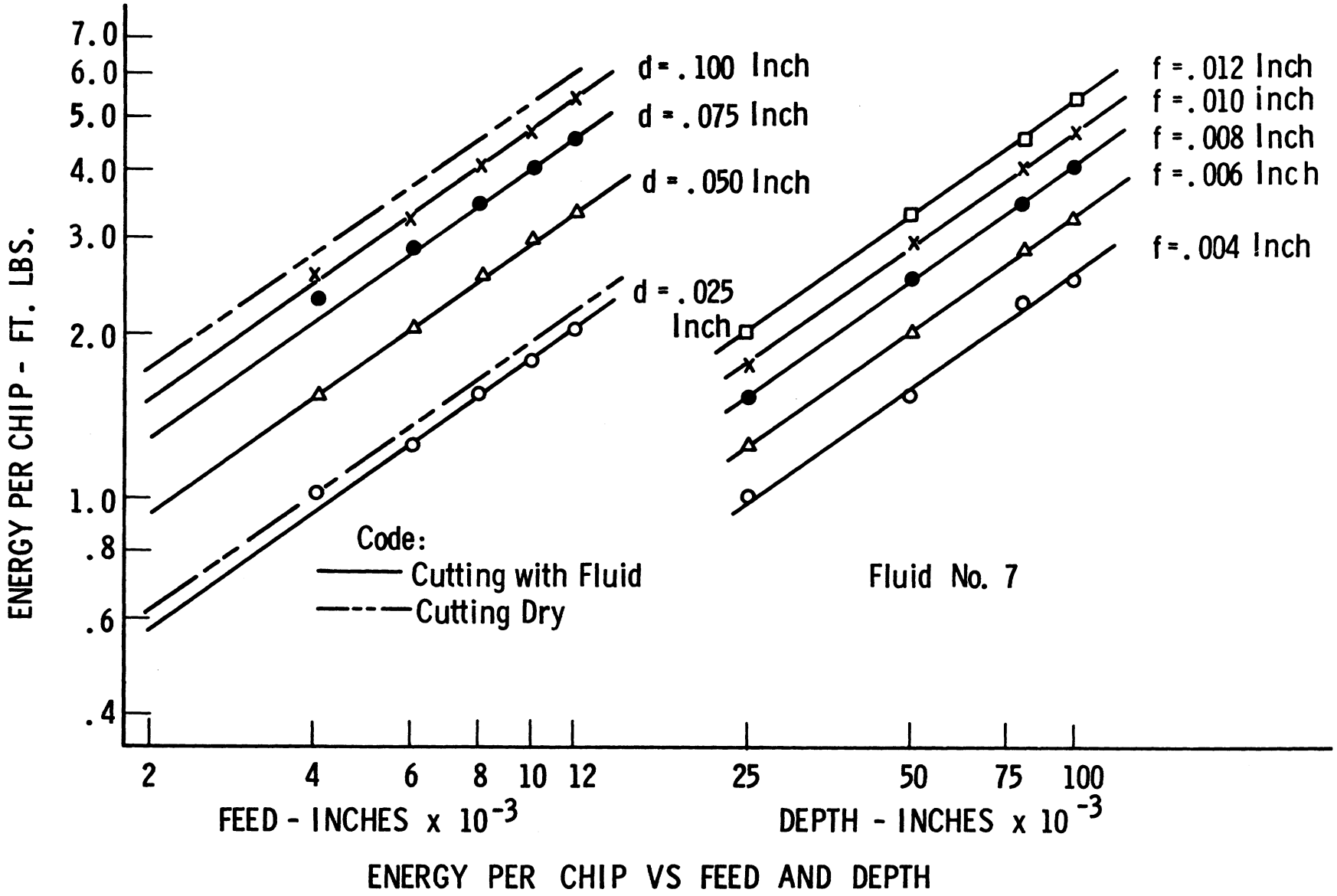

Fig. 3.25. Milling energy requirements for ranges of both feed rate and depth of cut for ten different cutting fluids and dry cutting with a conventional 30° rake-angle tool. Relief angles and width of cut same as for Fig. 3.10.

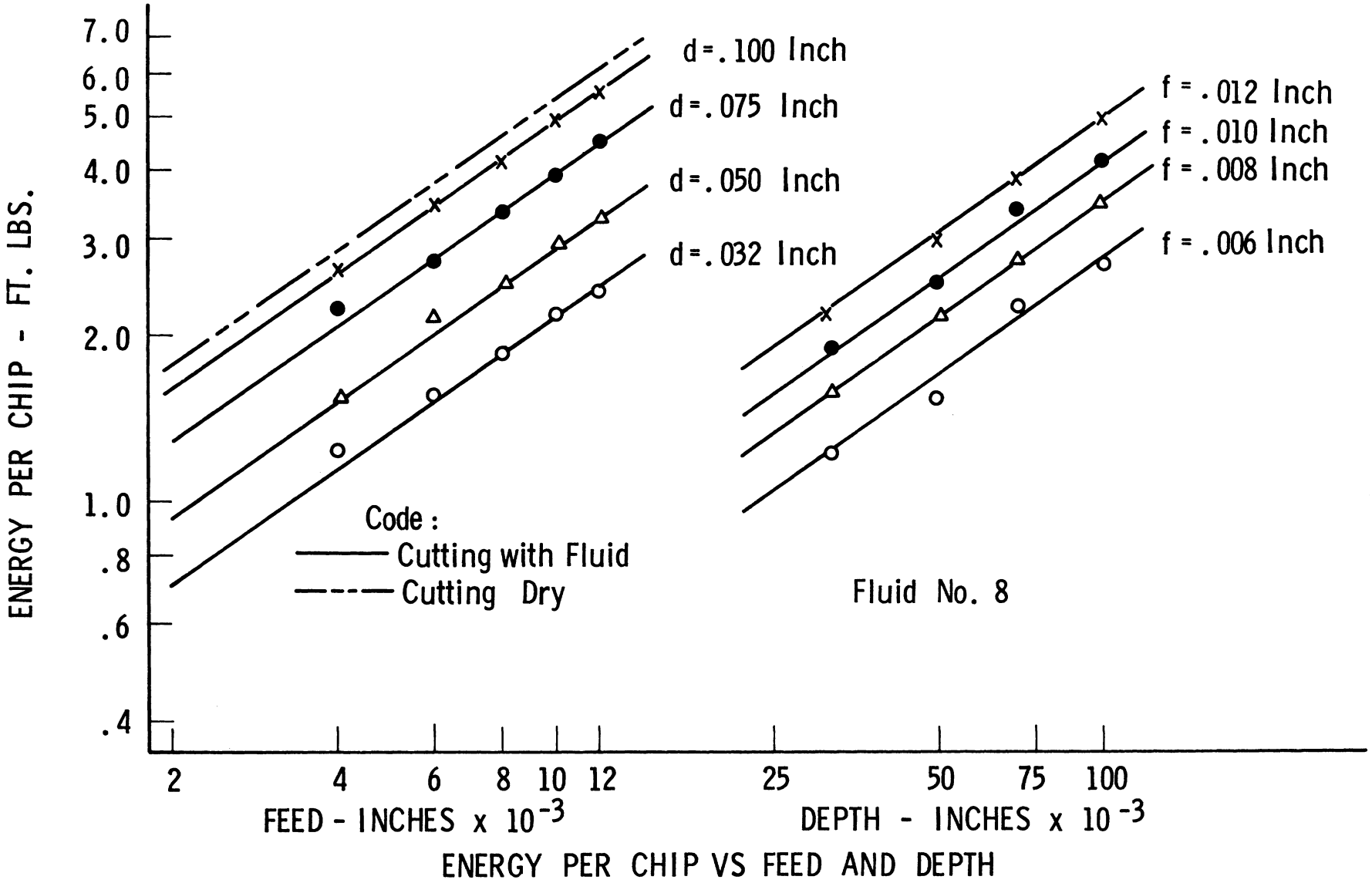

Fig. 3.26. Milling energy requirements for ranges of both feed rate and depth of cut for ten different cutting fluids and dry cutting with a conventional 30° rake-angle tool. Relief angles and width of cut same as for Fig. 3.10.

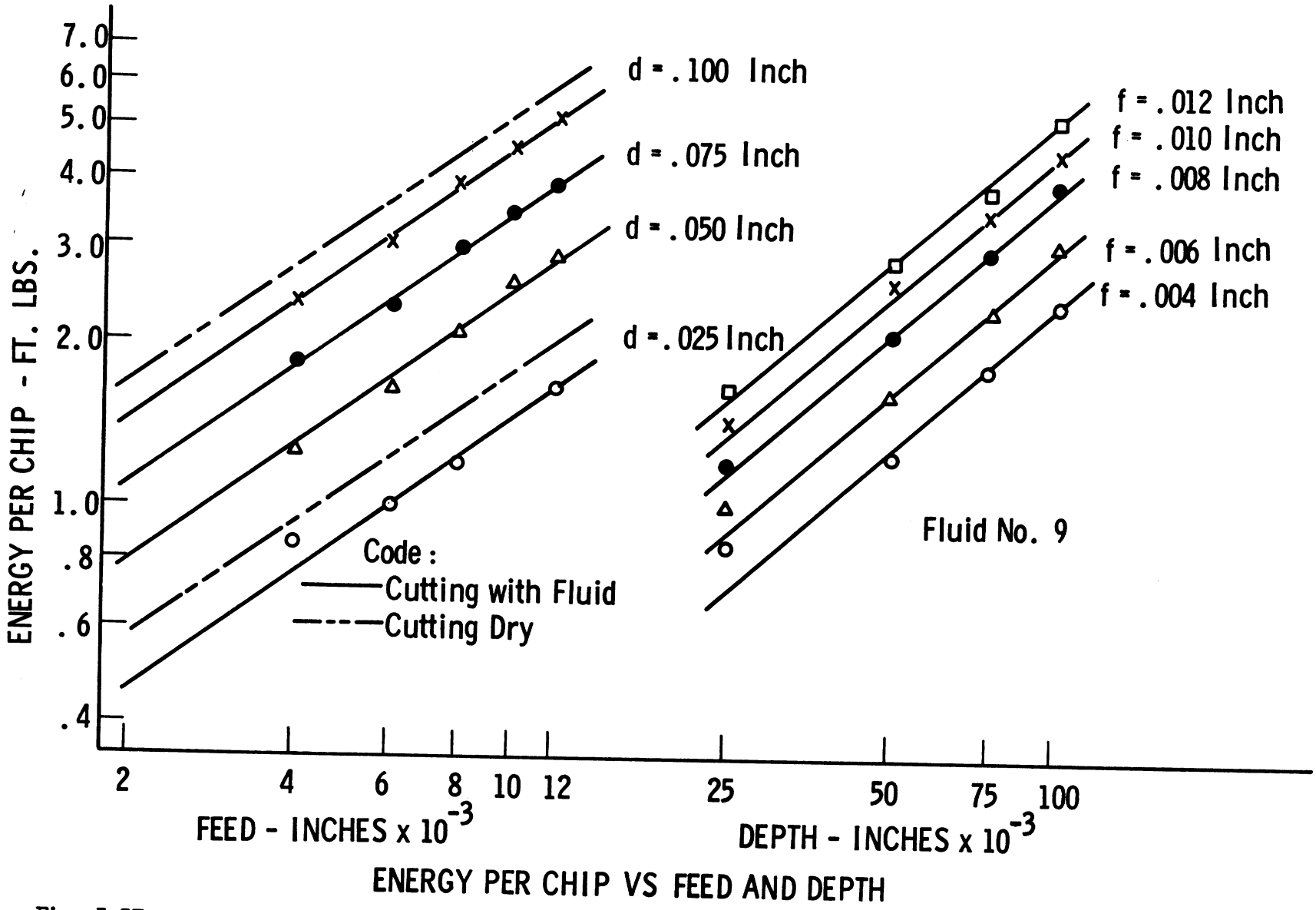

Fig. 3.27. Milling energy requirements for ranges of both feed rate and depth of cut for ten different cutting fluids and dry cutting with a conventional 30° rake-angle tool. Relief angles and width of cut same as for Fig. 3.10.

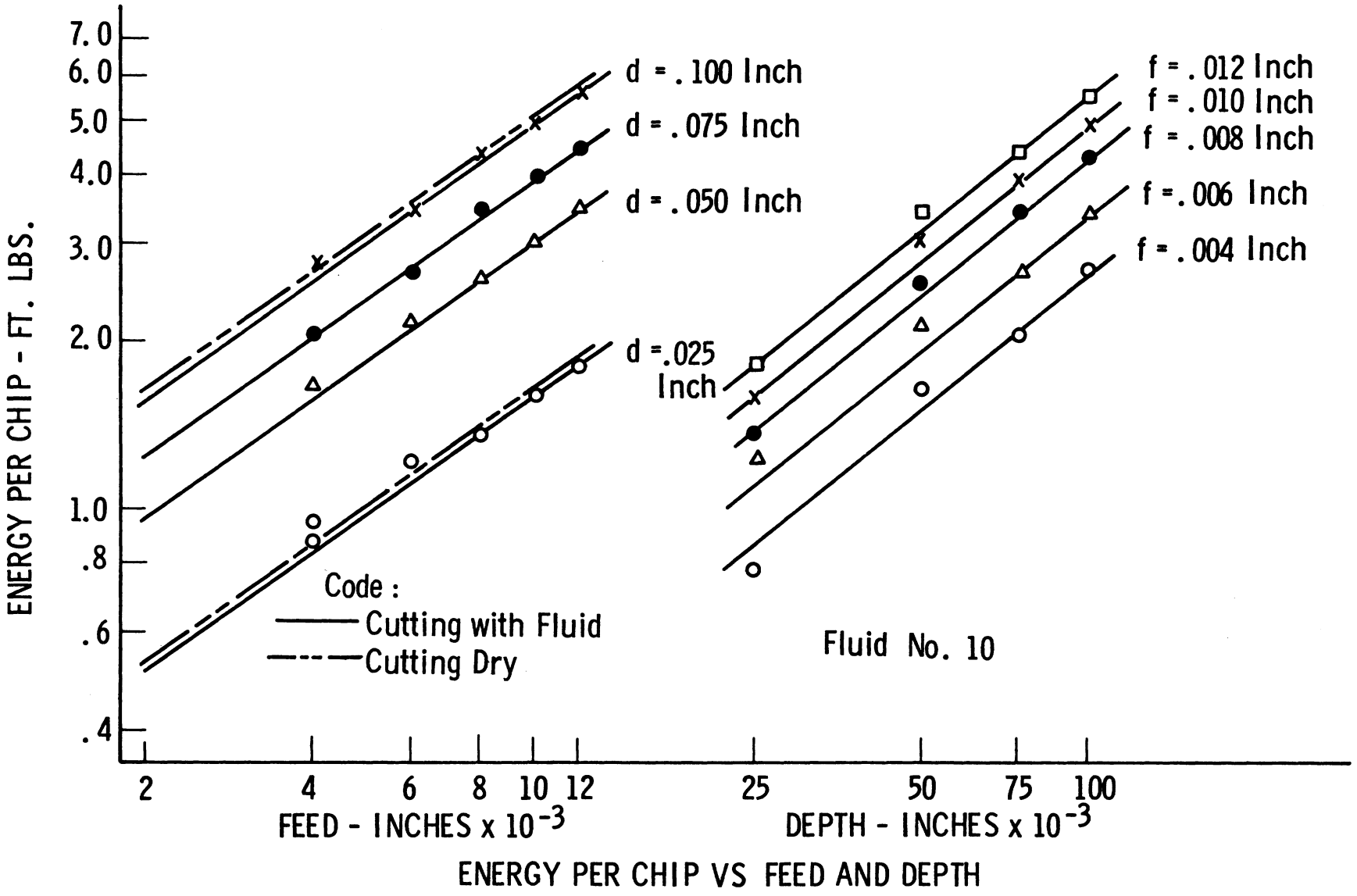

Fig. 3.28. Milling energy requirements for ranges of both feed rate and depth of cut for ten different cutting fluids and dry cutting with a conventional 30° rake-angle tool. Relief angles and width of cut same as for Fig. 3.10.

SECTION IV

LABORATORY STUDIES INVOLVING THE TOOL FLANK

Reaming, tapping, and hole broaching were selected for this particular study because they represent a group of machining operations which by their very nature or purpose imply that rubbing between the tool and the work is an inherent part of the cutting process. By comparison with other metal-cutting operations, this group is unique in that each operation uses a multiple-tooth, fixed-diameter type of tool and the final size of the hole or thread is a direct function of the tool and the behavior in the cutting zone. There is no convenient adjustment for size short of regrinding or replacing a given tool.

Machine reamers and taps are rotary-type cutters that are designed to do the cutting at or near the end of the tool. The main body of the tool establishes the listed diameter of the cutter and guides the tool in the hole made by the leading cutting edges as they advance in a helical path into the work. Thus, there is a noncutting relative motion between the body of the tool and the hole surface, leading to potential rubbing. A hole broach, on the other hand, is composed of a series of circular cutting edges, each at a progressively larger diameter. The broach is pushed or pulled through the workpiece and each tooth cuts around the full circumference for entire length of hole. As a rule, for better size control, the last three or four teeth of a broach are dwell teeth, or teeth ground to the same diameter. Therefore, these teeth remove very little material and rubbing is the rule rather than the exception. In addition, final sizing may be accomplished through a pure rubbing action by a series of polished burnishing elements.

Control of size of cut in each of the above operations is somewhat limited. In broaching, the chip thickness is determined in the tool design stages by the diameter changes between successive teeth. Once the broach is made, the only possible variation in cutting conditions is cutting speed. In tapping, the helical path of the cutting edges is fixed by the tap diameter and the pitch of the threads. Chip thickness can be controlled in two ways, however: (1) variations in original hole size, and (2) variations in chamfer angle at the end of the tap. Variations in hole size affect the percent of thread which remains and influence not only the amount of metal removal, but also the amount of rubbing surface between the tap and the hole. Variations in chamfer angle affect the length of cutting edge available for a given hole size and therefore influence the thickness of the chip. Small chamfer angles may give the undesirable characteristic of a wedging action and high normal forces during cutting, while large chamfer angles may lead to excessive chip thicknesses. Reaming permits the greatest control of size

of cut among these operations because both depth of cut and feed are independent variables as far as reamer function is concerned.

In general, broaching and reaming involve thin chips whereby, by comparison, tapping is a thick-chip operation. The size of cut in these operations can be of prime importance because of the resultant behavior in the cutting zone during chip formation. The effect that this may have upon the formation of built-up edge and normal cutting forces can influence the degrees of rubbing that takes place between the tool and the work. All chip formation is accompanied by elastic deformation in the cutting zone. Therefore, in the absence of built-up edge or in the event of high normal forces, or both, it is possible that the leading cutting edges can produce a hole that is smaller than the body of the tool. Rubbing, therefore, is an obvious result. On the other hand, excessive formation of a built-up edge may result in sufficiently oversize holes to eliminate or at least minimize the amount of rubbing between the body of the tool and the hole surface.

In light of the considerations discussed above, a series of reaming, tapping, and broaching investigations was carried out on the seven materials and each of the cutting fluids listed in Appendix B. Cutting forces, cutting torques, dimensional variations, surface quality, and general performance were all recorded as data relevant for evaluations of the fluids. The relative effectiveness of the various fluids in these operations must be judged according to their ability to: (1) reduce or eliminate built-up edge, and (2) provide adequate lubrication between the tool flanks and the work surfaces. As might be expected, not all fluids were able to fulfill either or both of the requirements, nor were they equally effective on all materials. Above all, it was found that even very slight variations in tool geometry resulted in differences which were far greater than any of those attributed directly to the fluids themselves.

REAMING

Reaming investigations were carried out with 3/4-inch-diameter reamers on a Fosdick Jig Borer with the setup illustrated in the photograph of Fig. 4.1. The Jig Borer was selected to take advantage of the greater rigidity and greater spindle accuracy than would be found on a conventional drill press. One-inch-long specimens were prepared from 1-inch-diameter bar stock of each of the seven materials. These were held in a collet chuck which was, in turn, mounted on a torque dynamometer to permit continuous torque records for each test.

Reamers and General Conditions

Standard 3/4-inch-diameter straight shank, 8-flute, spiral machine reamers were used in all final test sequences. In general, two approaches

were used. At the beginning of the test program, one reamer was assigned to each of the ten fluids and identified by the fluid number. Thus Reamer No. 1 was used exclusively with Fluid No. 1; Reamer No. 2 with Fluid No. 2, and similarly through all ten fluids. In this series of tests, nine sizes of cut were tested on each material with each fluid-reamer combination. These sizes of cut are listed in Table 4.1 and are identified by Nos. 1 through 9. Straight-flute reamers of .735 inch, .740 inch, and .745 inch diameter were used to establish the initial hole size for variations in depth of cut, where depth of cut is identified as the radial difference between the reamer size and the hole size. All cuts were made at a constant spindle speed of 65 rpm, which gave a peripheral velocity of 12.8 fpm for the 3/4-inch-diameter reamers. The velocity was deliberately low to emphasize the lubricating properties of the fluids.

The second shorter series of tests was made at a single cutting condition in which two of the ten reamers were used with all fluids on four of the seven materials. In the course of these investigations, it was found that the major share of the differences in torque values which were found among some of the fluids in the first series of tests had to be attributed to variations in the reamers themselves.

Reaming Behavior

A sketch identifying reamer nomenclature is shown in Fig. 4.2. As was pointed out earlier, the machine reamer does all of its cutting on the end and, specifically, along the chamfer which is usually at 45°. The rubbing referred to takes place between the margins and the hole surface after full depth of cut is reached at the chamfer corner. The margins are narrow bands running along the flutes and, in cross-section, are circular arcs which establish reamer diameter.

A typical reaming torque chart is shown in Fig. 4.3 and illustrates the pattern of behavior when rubbing occurs. The cutting torque, T_1, is identified as the torque required to remove the material at full depth of cut at a specific feed rate. The magnitude is a function of material properties but is also influenced by tool wear and the condition of the cutting edges. During cutting, a built-up edge develops along the chamfer, but the critical location is right at the corner between the chamfer and the margins. A large built-up edge at this point would produce an oversize hole and the torque level could remain at T_1 as cutting progressed since rubbing would not occur. At the opposite extreme, in the complete absence of built-up edge, elastic deformation in the cutting zone would result in a hole smaller than the diameter of the margins; rubbing would occur between the margins and the hole surface, and additional torque would be required to overcome friction. The torque would, of course, continue to rise as the reamer advanced into the workpiece because of the increasing length of rubbing contact. The slope, K_1, which represents the rate of torque increase, would be a function not

only of the amount of elastic deformation but also the effectiveness of the lubricant in reducing friction between the margins and the workpiece. Thus, with all the effects, the slope could range from zero under conditions of (1) large built-up edge or (2) perfect lubrication or zero friction at one extreme, to infinity with complete seizure at the other.

A number of significant factors relative to fluid and material behavior will be noted among the data presented, but the most significant relationships arise as a result of variations among reamers. The most important aspect of these reamer variations is that some of the reamers will distinguish very markedly among fluids on certain materials where others will show very little difference. Not all aspects could be investigated in time for this report, but the approach seems to be a very promising method for fluid evaluation and should be developed further.

Test Results For Cutting Torques

Cutting torques are significant in that they reveal material response to cutting and to variations in size of cut. Cutting torque values can also be used to calculate cutting horsepower, or more basic, unit or specific horsepower which is the horsepower required per cubic inch of material removed per minute. The cutting torques for all materials and all sizes of cut are summarized in Table 4.2. Listed, also, are slopes which indicate the effect of feed and depth for each material, and unit horsepower values for magnesium and 1042 steel. These values were derived from standard log-log plots, a sample of which is shown in Fig. 4.4. The listed cutting torques are actually averages from all ten reamers and fluids for each cutting condition. There were some differences in cutting torque values among the various reamers, as indicated at one cutting condition in Table 4.4, but the various fluids did not appear to alter the relative values appreciably. The averages, therefore, should be quite representative.

The results indicate, first, that in general the higher the mechanical properties, the higher the cutting torque for a given condition. Copper and stainless steel deviate somewhat from this general rule, copper because of its softness and high ductility, stainless steel because of its high strain hardening characteristics. Secondly, even though torque values go up with an increase in feed or depth of cut, unit horsepower values go down, indicating better cutting efficiency with thicker chips.

The above relationships are perhaps of only minor importance in reaming since rubbing torques can change the picture quite drastically. A look at the data in Table 4.7 will show that under certain cutting conditions magnesium requires almost twice as much torque as does stainless steel, yet the cutting torque for magnesium is approximately only 1/10 that for stainless steel.

Effect of Reamer Variations

It was indicated earlier that reamer variations contributed significantly to the separation of fluid behavior among the work materials. Inspection of the reamers revealed two types of variations among them: (1) slight variations in the condition of the cutting edges and rounding of the chamfer corner, and (2) variations in diameter or taper along the body. It is believed that the variations in the cutting edges and chamfer corners contributed to the variations in cutting torques and to the rubbing rates immediately after full depth of cut was reached, but that the most pronounced effects came from the body tapers.

The results of body diameter measurements in short increments over the working length of the reamer are shown in Table 4.3. It is noted that only two reamers, No. 1 and No. 4, did not have a smaller diameter at the end than at some point further along the body. All of the others had tapers of at least some degree for varying distances. Six of the ten reamers had total diameter variations of less than .00015 inch while Reamer No. 9 had the greatest variation of .0014 inch with a taper over the entire working length.

To illustrate the nature and the magnitude of the effects of the reamer variations, the results of a series of tests on magnesium and brass with Fluid No. 5 and Cut No. 8 are summarized in Table 4.4. The torque traces for the first 1/8 inch of reamer travel on magnesium are reproduced in Fig. 4.5. It can be seen that the reamers which were relatively straight had the lowest rubbing rates with the exception of Reamer No.1. The results for Reamer No. 1 are included as recorded in this test sequence but are not typical of previous behavior. In preparation for this series of tests, the leading edges of this reamer were stoned lightly to remove built-up edge deposits from 1018 steel of another test series. This resulted in a slight taper which was, nevertheless, sufficient to change the torque results by a factor of 8.5 in a repeat test on brass at Cut No. 5. This was the only test series which was affected by the stoning.

It is important to note that while there are similar trends in the response of the magnesium and the brass to the individual reamers, brass is by far the most sensitive to reamer variations, at least with Fluid No. 5. With the straighter reamers, the maximum rubbing torque (maximum torque less cutting torque) on brass is substantially less than that on magnesium. With the tapered reamers, however, the relative torque levels are reversed. Hole diameters and surface quality follow the same general pattern. Comparing the extreme results among the reamers, the cutting torques varied by a factor of 1.8 and 1.4 for magnesium and brass, respectively. However, the rubbing torques were in some cases more than 100 times the cutting torques and varied by a factor of 10 and 43, respectively.

Some additional tests were made with Reamers Nos. 1, 3, 8, 9, and 10 on aluminum under the conditions shown in Fig. 4.6. The fluid combinations of

Nos. 1 and 3, and Nos. 8 and 2, were used to note the effect of additions to the base fluid. Under the conditions in (a) there is very little difference in torque level among the fluids with Reamer No. 1, but there is a distinctive difference in the appearance of the traces. Fluids Nos. 2 and 8 show slightly more erratic and higher amplitude oscillations than do Fluids Nos. 1 and 3. Yet, they produced the smallest holes—.7508 inch, and .7510 inch for Fluids Nos. 8 and 2, respectively, compared with .7516 inch for both Fluids Nos. 1 and 3—and gave the most consistent surface quality. Inspection of the surface revealed that there were definite burnished bands produced with Fluids Nos. 1 and 8 in spite of the smaller hole size.

The same general trends prevailed among the fluids in the tests with the various reamers even though the size of cut was at the other extreme. The results in (c) of Fig. 4.6 again show very pronounced effects among reamers but, as distinguished from the results on magnesium and brass, the reamers do not separate the fluids as well on this material. One reason is undoubtedly due to built-up edge behavior. This is shown quite clearly in the traces with Reamer No. 8 and to some extent with Reamer No. 1. The results with Reamer No. 8 and Fluid No. 8 can be compared with the values in Table 4.7 for the same reamer-fluid combination, and it is found that they show only about 1/8 the original value.

The effect of built-up edge is also illustrated by the dry results in (b). Reamer No. 9, which very obviously has the highest torque levels in (c) has even a lower torque value than the straight reamer, No. 1, under dry conditions. Both reamers had a noticeable built-up edge at the chamfer corners.

Results With Several Reamers and All Fluids

Reamers Nos. 1 and 9, the two extremes with regard to body taper, were tested at a single size of cut on four materials—magnesium, brass, copper, and 1018 steel. These materials cover a fair range of properties, including a low and a high modulus of elasticity. They vary with respect to tendencies to form a built-up edge also. The torque traces for each reamer and each material are shown in Figs. 4.9 through 4.16, and the results are tabulated in Table 4.5. Maximum cutting torques for each reamer, fluid and material combination are plotted in Fig. 4.8 for convenience.

Results from the .740-inch-diameter preparatory reamer have also been included in Table 4.6 and Figs. 4.17 through 4.20 for comparison. First, the feed rates were higher for this reamer than they were for Reamers Nos. 1 and 9, and second, this was a straight-fluted reamer instead of spiral fluted. The combination of higher feed and straight flutes should accent the formation of built-up edge, and perhaps sort out the effectiveness of a fluid to reduce built-up edge or provide lubrication for the reamer margins.

Strong evidence of this possibility is shown in Fig. 4.7. The torque traces were made with a .745 inch diameter straight-fluted reamer on aluminum at Cut No. 8 with Fluids Nos. 1 and 9. The test conditions were repeated a number of times, and each time the traces were identical to those shown in the figure.

The traces do not distinguish between the fluids as far as maximum torque level is concerned, but they do indicate two different types of behavior. Fluid No. 1 seems to give rise to unstable built-up edge formation but prevents seizure between the margins and the hole surface, while Fluid No. 9 is effective in reducing built-up edge but shows poor lubricating qualities. This is evidenced by three general observations of the traces: (1) the break in the trace of Fluid No. 1 occurs much earlier, more abruptly, and at a much lower level than that of Fluid No. 9, indicating the possibility of built-up edge; (2) as rubbing torque increases beyond the break in the curve, the trace with Fluid No. 9 shows high-frequency peaks such as would be encountered with momentary seizure between the margins of the reamer and the hole surface. The erratic rises and falls or leveling off of the torque values indicate that some material is being removed by the seizure; (3) what appears to be most significant, the oscillations of the trace for Fluid No. 1 stop abruptly as the cutting edges reach the end of the hole as indicated by the arrow. This indicates rather pointedly that the oscillations originated in the cutting zone. With Fluid No. 9, however, the trace is very similar even after the cutting edges break through the end of the piece and only the margins are in contact. The torque levels shortly after the cutting edges leave the piece substantiate another characteristic of fluid behavior. Approximately 80% of the maximum torque level achieved with Fluid No. 1 was due to rubbing friction between the margins and the work, while 60% of the maximum torque with Fluid No. 9 was contributed by approximately the first 1/16 inch of the reamer.

The above characteristics can be noted among a number of fluid, reamer, and material combinations in Figs. 4.9 through 4.20, particularly for the 1018 steel. Fluid No. 9 with Reamers Nos. 1 and 9 on the 1018 steel, and Fluids Nos. 4 and 5 with Reamer No. 9 on brass give rise to very sharp drops in torque values during one revolution of the reamer. This is actually a result of metal being removed by the margins on the reamer as the fluids breakdown under obviously high normal and friction forces. The removal was in the form of smear on the margins with brass, but actual chips were cut away on the 1018 steel.

General observations of the results show that copper gives the widest dispersion among the fluids with both Reamers Nos. 1 and 9. Fluids Nos. 2, 4, and 5 give the highest torque levels with the straight reamer, but Fluids Nos. 7 and 8 show torque increases of over 400% to give the highest torque levels with Reamer No. 9. Fluids Nos. 1 and 3 consistently gave the lowest torque levels for all three reamers and caused very pronounced discoloration of the surface. Fluid No. 5 gave the best and most consistent surface quality

regardless of reamer. Fluids Nos. 2 and 4 seemed to give the next best overall quality, but were subject to some seizure and resultant tears in the surface. The problem of seizure on copper is pretty well defined by the dry trace in Fig. 4.13. Practically all surfaces had some tears and those from Fluids Nos. 9 and 10 seemed to be the most prominent.

The results on brass and 1018 steel ran somewhat parallel with Reamer No. 1 except for Fluid No. 9. This fluid was, by far, the most effective in minimizing built-up edge on steel and gave the highest torque values by as much as a factor of ten. Its poor lubricating qualities led to seizure at the high torque values and the surface quality was rather erratic because of it. Reamer No. 9 separated the fluids substantially and Fluids Nos. 1, 3, 4, 5, and 6 all gave comparable surface quality. Burnishing and some tearing was evident. The traces in Figs. 4.15 and 4.16 show more pronounced seizure tendency with Reamer No. 1 with all but Fluid No. 9. This is reflected in the surface roughness measurements listed in Table 4.5 where all fluids gave better surface quality with Reamer No. 9, even the dry. As they did with the copper, Fluids Nos. 1 and 3 stayed pretty well together through this series indicating that perhaps the additive is not particular effective on these materials. They gave the lowest torque values with the .740-inch-diameter reamer and Reamer No. 1, but torque values increased by a factor of almost 20 with Reamer No. 9. If anything, Fluid No. 1 showed less tendency for seizure than did Fluid No. 3.

It is interesting to note that in spite of the lower modulus of elasticity and the lower cutting torque requirements, the maximum reaming torques with all reamers and all but one fluid were consistently higher for magnesium than they were for steel. The only exception was Fluid No. 9. Where this fluid always gave the maximum torque values on steel, it gave the lowest torque values on magnesium. Some flaky smear was found along the margins near the chamfer corner when Fluid No. 9 was used, very similar to what was found in reaming dry. The reamed surface was rather dull in appearance but was one of the most consistent. Fluids Nos. 2 and 8 gave the highest torque values with Reamer No. 1 with Fluid No. 8 giving a somewhat more erratic behavior. With Reamer No. 9, Fluids Nos. 2 and 3, and their basefluids 8 and 1 gave comparable torques, the base fluids occupying a slightly lower level. All of the surfaces produced by Reamer No. 9 show that some seizure or smearing took place to at least some degree. The surfaces produced with Fluids Nos. 1 and 9 seem to be most consistent.

Of the four materials tested, the most pronounced changes between Reamers Nos. 1 and 9 occurred on brass. The torques with the straight reamer were, in general, the lowest of any of the materials. The torque results from seven of the ten fluids varied by no more than two pound inches. With Reamer No. 9, there was a substantial increase in torque level with all fluids, the Fluid No. 5 results increasing by a factor of more than 30. The effect of the fluids upon surface quality seems to be less pronounced on brass than on the other materials. With Reamer No. 1 all of the surfaces looked pretty much the

same with the exception of the one produced with Fluid No. 10. The surface was relatively uniform, but of greater roughness. The surfaces produced by Reamer No. 9 were discolored and streaked with burnished bands and were unattractive in appearance. The dry results looked much better.

The .740-inch-diameter reamer results help to verify the results with Reamers Nos. 1 and 9. On magnesium, the results approach those of Reamer No. 9 show, generally, the same instabilities among the fluids. On brass, the results are much closer to Reamer No. 1 than they are to Reamer No. 9, illustrating that brass is more sensitive to reamer taper than to size of cut. As expected, however, the results on the 1018 steel are far more emphatic than they are on brass and magnesium, which do not have a pronounced tendency to form a built-up edge. The results in Fig. 4.20 illustrate the same general trends as those found with Reamer No. 1 in Fig. 4.15, but they separate the fluids to a far greater degree. Seizure is very evident with Fluids Nos. 7, 8, and 10, almost paralleling the dry results. The instability of Fluids Nos. 2, 4, 5, and 6 is also very much in evidence. In each instance, metal removal by the margins of the reamers was observed during momentary seizure.

Effect of Size of Cut

All of the size of cut variations were made with single fluid-reamer combinations with all fluids on all materials, and produced the cutting torque relationships given in Table 4.2. As was indicated earlier, neither the fluids nor the reamer variations affected the cutting torques appreciably. However, the results in Tables 4.4 and 4.5 show that all other factors—rubbing rates and torques, hole diameters, and surface roughness, for example—do vary from reamer to reamer. Therefore, a direct comparison of results among fluids in this series of tests cannot be made with any assurance that relative values are not altered by reamer taper. Also, cutting torques were averages of ten readings and, thus, were fairly representative. All other values in this series, however, are results from single tests at each condition and subject to at least some variation.

Even though the effect of reamers is difficult to separate from the effect of the fluids themselves, there were general trends that appeared within and among the fluid-reamer combinations. The values in Table 4.7 represent the maximum rubbing torques for each condition. These values were derived by subtracting the respective cutting torques listed in Table 4.2 from the maximum reaming torques at each size of cut. This eliminates cutting torque as a variable from among the materials as well as from the size of cut, and allows a comparison on the basis of a common unit. The results show, first of all, that rubbing torques are consistently higher on magnesium, copper, and stainless steel over most of the combinations. Also, these materials show a reasonably consistent trend of increasing rubbing torque with increasing feed, although they appear to differ in their reaction to depth of cut.

Magnesium seems to be more sensitive to rubbing torques at the light feeds but relatively stable at the medium and high feeds. Stainless steel shows trends of slightly increasing rubbing torques in the light and medium feed ranges but has definite signs of decreasing rubbing torques at the high feeds, probably because of built-up edge. Similar trends exist for copper, although there seems to be a tendency for rubbing torques to rise with an increase in either depth or feed through the full range of conditions. On the average, copper gives the highest rubbing values, but it is interesting to note that magnesium, the easiest material to cut, requires as much or more torque than either copper or stainless steel with many of the cut combinations.

Hole diameter measurements tend to substantiate the above relationships. On stainless steel, the hole diameters decrease with an increase in depth at low feeds, but increase with depth variations at high feeds. Low depth and high feed combinations also produce smaller holes. On copper, the smallest holes were produced consistently by the highest feed and depth combinations. Feed seems to be more effective than depth, however. The greatest effect upon hole diameters on magnesium took place in the middle feed ranges, Cuts Nos. 4, 5, and 6, where increasing depths gave smaller holes. Increasing feeds gave very slight decreases in diameter, but ranges in depth at the high and low feeds did not seem to have any effect.

On materials forming built-up edge (with the exception of stainless steel), the results are not consistent. The 1018 steel shows higher rubbing torques at higher feeds and depths, such as Cuts Nos. 3, 6, and 9; yet hole diameters, though not always the smallest, were more consistent at the lower feeds. On 1042 steel, the highest rubbing torques were usually found among the smallest feed and depth of cut combinations. Hole sizes were inconsistent and inconclusive.

Aluminum and brass both show a sensitivity to reamer taper, but not always in the same manner. With the Fluid No. 9 and Reamer No. 9 combination, brass shows the highest rubbing torques with the light feeds, Cuts No.s 1, 2, and 3, while at high feeds aluminum has a value of more than twice the rubbing torque of brass. With The Reamer No. 7 and Fluid No. 7 combination, however, it is brass that has a substantially higher rubbing torque value at the high feeds. This appears to be more of an effect of fluid, since Reamer No. 9 gave about four times the rubbing torque of Reamer No. 7 in the tests summarized in Table 4.5.

The results in Table 4.7 give a reasonable picture of the relative effects of the fluids as far as rubbing torques are concerned, but they do not reveal the character of the torque behavior. On stainless steel the fluid-reamer combinations 1, 2, 4, 7, and 8, for example, all gave reasonably comparable values; yet there was a noticeable difference in fluid behavior. Fluid No. 1 gave the most stable torque behavior at all cuts. Fluid No. 2 was relatively stable at light feeds, but from Cut No. 3 on,

seizure tendencies were evident. Fluid No. 4 gave rise to erratic performance at all conditions and exhibited seizure or stick-slip tendencies at high feeds. Fluids Nos. 7 and 8, especially 7, gave seizure or stick-slip tendencies at all conditions.

On 1042 steel, the similarities among fluids revealed by the rubbing torque values are pretty valid. Fluids Nos. 1 and 5 had very similar traces over the full range, although Fluid No. 5 seemed to be more effective in the cutting zone region because of less erratic torque behavior. Fluids Nos. 2, 4, and 7 also had similar behavior, particularly in the middle feed ranges. Fluids Nos. 2 and 4 were more effective at light feeds and Fluid No. 7 at the heavy feed-fine depth combination. The only fluids that did not show at least some similarities were Fluids Nos. 3, 8, and 9 and this was undoubtedly due to reamer effect to a great extent. Seizure tendencies were far less pronounced on the 1042 steel than they were on either the stainless or 1018 steels.

Residual Stresses

The results and a brief description of a technique that was used to illustrate the effect of the various fluids upon residual stresses induced in the remaining hole surface are given in Table 4.8. The results are not intended to be conclusive, because only one specimen was tested at each condition, but they do show rather convincingly that there is a difference in the behavior among materials and, more important, among the fluids.

The numbers in the table represent the relative effects of the stresses rather than the stresses themselves. They denote the difference in the amount of change in a gage width between a reference unreamed specimen and the reamed specimen after they have been split between the gage marks. The slotting causes the stresses to relax and exert their influence on either spreading out or closing in the gage marks depending upon the effective stress distribution. The unreamed specimens on the three materials all had inherent stresses which closed in the gage marks after slotting. The positive numbers in Table 4.8 indicate that the stresses in the reamed specimen kept the gage marks from closing in as much as they did in the unreamed specimen by the given amount. Negative numbers indicate that the gage marks closed in even more than they did on the reference specimens.

The most important effects represented by the results are thos showing the influence of the fluids, even to the point of a complete reversal of behavior by Fluids Nos. 1, 2, and 10 on aluminum which was affected most by the fluid changes. Magnesium shows the smallest range of variations which is fairly consistent with the results of rubbing torques in Table 4.5.

Surface roughness and hole diameters measurements were also made in this series, and the relative positions of the fluids in order of increasing

surface roughness and increasing hole diameter are tabulated below:

FLUID NUMBERS

Fluid	Magnesium		Brass		Aluminum	
Rating	Surface	Hole	Surface	Hole	Surface	Hole
1	10	9	3	9	1	9
2	9	8	9	3	3	3
3	8	3	1	8	8	8
4	3	2	8	1	2	10
5	1	10	10	10	10	1
6	2	1	2	2	9	2

Magnesium gave the smallest holes with all fluids, and had the smallest range of surface roughness, but the roughness level with practically all fluids was higher than it was on the other two materials. Aluminum had the lowest surface roughness but the greatest range among the fluids and gave, generally, the largest hole sizes. The ranges in hole diameters were no more than 0.001 inch between the fluids rated highest and lowest for each material so the relative positions on this basis are open to question. There was no doubt about the effect of Fluid No. 9, however. The diameters were all distinctly smaller with this fluid. It is interesting to note that the fluids that gave the better surface quality generally gave the smaller hole. The only major exceptions were Fluid No. 10 on magnesium, Fluids Nos. 1 and 9 on aluminum. These fluids, on the respective materials, gave directly opposite effects.

In summary, the reaming results show (1) a difference in fluids in their effectiveness on various materials, and (2) a very high degree of sensitivity to very slight changes in tool geometry. The latter effect is so dominant that analyses and comparisons of results of information from several sources should be made with caution. Usual comparisons are made on the basis of reaming torques, surface quality, and diameter variations. However, surface quality, for example, can improve or deteriorate with increasing torques even for a given material, depending upon the effectiveness of a fluid. This effect is noted in Table 4.5.

To summarize the relative effects of fluids, materials, and reamer variations, the results for rubbing torques from Table 4.5 have been put in ratio form and listed in Table 4.9. The ratio of rubbing torques on each material as a result of reamer change is shown in Table 4.9A. In general, brass shows the greatest sensitivity to reamer variations, particularly with Fluids Nos. 5, 4, and 2, in order. The 1018 steel, however, shows the greatest change with Fluids Nos. 3 and 1. The magnitudes of some of these changes are enormous.

The ratios in Table 4.9B show the relative effects of the fluids among the various materials, and were derived by using the Reamer No. 1 rubbing torque values on brass as a base. These results show that with Reamer No. 1 all fluids, except one, exerted the greatest influence on copper. The only exception was Fluid No. 9 which had the greatest effect upon 1018 steel. With Reamer No. 9, Fluids Nos. 1 and 3 exerted the greatest influence upon magnesium, although these two fluids came reasonably close to having an equal influence on all materials. Fluid No. 9 still had the greatest influence on 1018 steel and the rest of the fluids on copper.

The relative order of influence of the fluid on each material is given in Table 4.9C in sequence of decreasing rubbing torques. This table shows that relative orders of fluids can change with changes in tool geometry. On brass, for example, Fluids Nos. 9 and 10 gave the highest torque levels with Reamer No. 1, but gave the lowest rubbing torque levels with Reamer No. 9. Fluids Nos. 1 and 3 had just the opposite effect on 1018 steel. The influence of fluid additives is also indicated.

TAPPING

Tapping tests were performed on a Detroit Tap and Tool Company tapping machine equipped with a precision lead screw to advance the tap at the helix angle of the thread and an automatic spindle reverse for tap backout. The setup, similar to the one used in reaming, is shown in Fig. 4.21. Specimens, 3/4 inch long, were inserted in a specially made holder, which was held in a torque dynamometer. A slot was machined in the specimens to fit over a key in the holder to prevent rotation at high tapping torques. Cutting fluids were applied from a pump-type oil can.

The tapping tests were designed to investigate the behavior during a complete tapping cycle—tap advance and tap backout. Continuous torque values were recorded for all conditions with all fluids and all materials. Torque values, thread dimensional stability, thread surface appearance, and general observation of performance were used for evaluation.

Taps and General Conditions

The majority of tests covering all materials and all fluids were made with Greenfield Tap and Die Company 1/2 inch-13NC, G-H3 machine taps. These are ground taps that are to have a size .001 inch to .0015 inch above basic thread pitch diameter. Besly "X-Press" taps were used on a second shorter series of tests on brass, aluminum, and magnesium. These taps actually form the thread by plastic deformation of the material rather than by cutting.

For the longer series of tests, specimens were prepared in five different hole sizes to represent different percentages of full thread. The

sizes are identified by numbers 1 through 5, and are listed in Table 4.10 along with the percent thread they represent. Only the recommended size, Hole No. 5, was used for the "X-Press" tap. All tests were carried out at a constant speed of 74 rpm.

In the first series of tests one tap was assigned to each material and was used with all fluids. This eliminated the tap as a variable in the results. All five hole sizes were run with a given fluid in a sequence starting with the largest hole. Tap breakage made it impossible to run some of the tests with the smaller holes on 1018 steel and, particularly, on stainless steel. Only one "X-Press" tap was used in the short test series. All tapped holes were gaged with "Go" and "No Go" gages in Classes 1 through 4.

Tapping Behavior

Many similarities in cutting behavior exist between reaming and tapping, except that tapping involves a much more severe operation. Built-up edge, rubbing, and seizure are generally much more pronounced. Also, a solid tap cannot be withdrawn from the hole like a reamer, but must be backed off by reversing the direction of rotation. Thus, a static condition exists at the point of reversal which means that friction characteristics could be quite different under high normal forces.

Tap nomenclature is identified in Fig. 4.22. As in reaming, cutting is done only by the cutting edges created by chamfering or pointing the end of the tool. Rubbing takes place between the tap body and the newly created thread surface. The rubbing surface area is much greater than that in reaming because contact is made not only at the periphery of the body, but along the sides of the vees as well. For a given tap size and a given hole diameter, the severity of chip formation is determined by the chamfer angle. Large angles given very thick chips because the full depth of cut must be made by one or two threads. This presents not only built-up edge problems on many materials but, because taps have limited torque resisting capacity, can lead to tap breakage at high torque levels. Small chamfer angles thin out the chips but increase length of contact and may give more severe rubbing in the cutting zone as a result of higher normal forces.

Tapping relationships among torque, volume rate of metal removal, and lengths of rubbing and cutting edges should prove useful in the analysis of the torque records, and are illustrated in the composite chart of Fig. 4.23. Calculations, which are quite complex because of thread geometry, were made for conditions with Hole No. 1. The values for volume rate of metal removal, length of cutting edge, and length of rubbing edge would all change with a change in the percent thread.

The full distance of tap advance has been divided into four separate areas of behavior, which also apply to tap backout after reversal. Zone-A

represents the portion of tap advance from the initial point of contact of the chamfer with the edge of the hole to the point where full tap diameter is reached in a matter of just less than four revolutions or four threads. During this portion volume rate of metal removal rises as more of the chamfer is engaged to remove additional material. Rubbing edge length rises in a nonlinear manner because of the varying depth of the thread vee and because there is some rubbing associated with the flanks of the cutting edges. Both the volume rate of metal removal and the length of cutting edge are a maximum at this point and remain constant through Zone-B which represents the tap advance from the start of full tap diameter to the position where the edge of the chamfer is at the edge of the exit side of the hole. Length of rubbing edge rises linearly over this portion as more threads enter the holes since advance is constant per revolution and the body is at full diameter.

In Zone-C, length of cutting edge and rate of volume removal drop to zero as the chamfer exits to the point of full body diameter. Rubbing edge length continues to rise, however, this time in a nonlinear manner which is determined by the difference between the increase due to full threads entering the hole and the partial threads of the chamfer leaving the hole. During overtravel, only the body is in contact and the rubbing edge length does not change since full teeth are leaving as well as entering the hole.

From the time of initial contact with the workpiece, the torque continues to rise until the reference point on the chamfer starts to exit at the end of the hole. This rise is due, first, to cutting and rubbing in Zone-A, then rubbing alone in Zone-B. The deviation from linearity in Zone-B is due partially to plastic deformation due to rubbing, but also to tap design. As pointed out in Fig. 4.22, taps have a back taper for the very purpose of relieving the rubbing problem. Thus, as the tap enters the hole the diameter of the tap is decreasing slightly. This results in a lower rate of increase of rubbing torque. It also accounts for the decrease in torque level during overtravel, as well as the torque increase during tap backout. The torque during backout is all rubbing torque.

The variations that can occur in torque behavior and in torque levels are similar to those that occur in reaming.

Variations in Tap Geometry

This phase has not been studied specifically in tapping as it was in reaming, but there was evidence that taps had a fair degree of influence on the results. First, there were differences in diameters, back tapers, and in one case, even a negative relief angle on the body threads of the tap used on magnesium. The measured values of four of the taps used are shown in Table 4.11, along with identifying symbols. The original taps used on 1018 steel, copper, and stainless steel were broken before measurements were made.

Taps B and M were tested on brass and magnesium with Hole No. 2 and Fluids Nos. 6 and 9. The torque traces from these tests are shown in Fig. 4.24. The results are tabulated in Table 4.12. Tabulated, also, are maximum torque values on aluminum from a series of eight taps not used in the test program. These results were found with Fluid No. 3 and Hole No. 4. Taps B and M do not show spectacularly different maximum torque results, but they do show differences in behavior as revealed by the torque traces. The most pronounced effects occur with Fluid No. 9. The results on aluminum show a range of torque increase of 60%. Even more pronounced, are the results of repeat tests on stainless steel as shown in Fig. 4.25. The traces on the left in the figure were made with the tap initially designated for this material. The ones on the right were made with a replacement tap after the original fractured on one of the test series. There is a 100% change in the repeat with Fluid No. 2 and more than a 50% change with Fluid No. 6.

Test Results—Tapping Torques

Two sets of cutting torques have been tabulated for the various materials. One set of values has been taken directly from the torque traces for each of the hole sizes and each of the fluids. These were read at the point of full chamfer engagement as represented by the boundary between Zones-A and B in Fig. 4.23, and are tabulated in Tables 4.14 through 4.20 for the various materials. These torque values, however, do include some rubbing torque as was indicated in the discussion on the chart in Fig. 4.23. To separate rubbing from true cutting, the information from the original reaming results was used to calculate equivalent unit horsepower values for tapping, and these values were then used to calculate the minimum cutting torques. The results of these calculations are listed in Table 4.13.

As was indicated, the object of the calculations was to separate rubbing from cutting torques so that maximum friction torques could be found. The results tabulated in Table 4.22 are the differences between the maximum recorded torques for each condition and the minimum cutting torques for the respective hole sizes. These values represent the maximum frictional torques at each condition. On the other hand, the cutting torques listed in Tables 4.14 through 4.20 were found by subtracting the recorded cutting torque from the maximum torque, and represent the frictional torque between the body of the tap and the workpiece. Thus, in one case the friction torques represent the combined effects of the cutting zone and the body of the tap, while in the other only the body effects are considered.

Backout torques are listed for each material and each hole size in Tables 4.14 through 4.20 along with the other torque values. They are listed again separately in Table 4.21 in more convenient form for a comparison among materials. Caution must be used in making too direct a comparison because a different tap was used on each material and, as was shown, some differences among taps do exist.

The calculated values of unit horsepower and minimum cutting torque in Table 4.13 indicate the severity of the tapping operation as compared with reaming. The thicker chips lead to more efficient metal removal, as indicated by the lower unit horsepower values, but cutting torques increase by a factor of about ten for the respective conditions used in the tests. Because of the high initial values, the percent increase in torque due to rubbing friction is not as great in tapping, generally, as it is in reaming. Where exceptionally high values did occur, they were the result of seizure, which was usually accompanied by tap breakage.

The calculated minimum cutting torque values and the maximum frictional torques can be useful in forming a comparison between the body rubbing torque, as listed in Tables 4.14 through 4.20 for the various materials, and the friction torque originating in the cutting zone. As might be expected, there are some discrepancies among the various results because of the limited number of tests, but for the most part they show a logical pattern.

The friction torque in the cutting zone can be determined by subtracting the minimum cutting torque from the measured torque at full chamfer depth, or by subtracting the rubbing torque from the maximum frictional torque. When this is done, variations in behavior among materials and among fluids are noted. On magnesium, for example, the body rubbing torque with all fluids is always higher than cutting-zone friction torque but with a decreasing ratio from Hole No. 5 to Hole No. 1, where the ratio between the two is practically one. On 1018 steel, however, these are reversals of behavior. With the smallest hole, Hole No. 1, the body rubbing torque is at least twice the cutting-zone friction torque with Fluids Nos. 1, 3, and 4 which were the only ones run at this condition because of tap breakage. With Hole No. 2, however, only Fluids Nos. 1, 2, and 3 show slightly higher body torques while the rest show higher cutting-zone friction by as much as a factor of two with Fluids Nos. 4, 7, and 10. Fluids Nos. 7 and 8 continue to give higher cutting-zone friction torque with Hole No. 3 as the other fluids reverse behavior once more. The variations in behavior are undoubtedly due to the effect upon built-up edge or lubricating qualities, or both. On magnesium, aluminum, and brass, Fluid No. 9 gave the highest cutting-zone friction torques by far. Fluid No. 2 gave the lowest values. Fluid No. 10 gave the highest values on copper, and also on magnesium. On brass, however, it was on a par with Fluid No. 2. Fluid No. 9, which was so dominant on the other nonferrous materials, gave, in general, the lowest values of cutting-zone friction torque on copper along with Fluids Nos. 1, 2, and 3. Fluid No. 9 also gave among the lowest values on the two steels, as did Fluid No. 1. On these materials, Fluids Nos. 7, 8, and 10 had the greatest effect, with Fluid No. 8 giving particularly high values on 1018 steel. When the fluids are compared on the basis of body rubbing torques, there is a slight shift in relative position among most of the materials. On 1018 steel, for example, Fluids Nos. 1 and 5 have a higher relative position and Fluids Nos. 6 and 7 have a lower relative position on the basis of rubbing torques than they have on the basis of cutting-zone friction effects.

The backout torques listed in Table 4.21 show that magnesium, copper, and stainless steel had the more consistently higher values, with Fluid No. 9 again being the most effective on all but 1018 and stainless steel, particularly with the smaller hole sizes. Fluid No. 10 showed the greatest effect on copper and stainless steel with the larger hole sizes.

Thread Quality

The backout torques seemed to be consistent with the gaging results. Class 4 threads were produced with all fluids on magnesium, aluminum, copper, and brass. As a matter of fact, some of the tapped holes on copper were so small that even the thread "Go" gage would enter only part way. There were, however, two holes in copper that were gaged as Class 1. These were on Hole No. 1 with Fluids Nos. 8 and 10, which showed pronounced seizure tendencies at this condition. Dry tests also produced Class 4 threads on magnesium and brass, but only Class 3 threads on aluminum. The fluids were, thus, effective in permitting Class 4 threads on this material. Dry tests were not made on the other materials.

The threads produced on the ferrous materials were, for the most part, of Class 3. With Fluid No. 9 on 1042 steel, Class 4 threads were produced with all five hole sizes. All other fluids had a definite trend of producing Class 3 threads with hole sizes 1, 2, and 3 and giving or approaching Class 4 with hole sizes 4 and 5. On 1018 steel and stainless steel, some opposite trends were observed. The two No. 1 holes that were tapped with Fluids Nos. 1 and 4 were gaged as Class 2 and Class 1 respectively, as seizure occurred during tapping. With Holes Nos. 2, 3, 4, and 5, Fluids Nos. 1, 2, and 3 gave better thread quality with increasing hole size. Fluids Nos. 4, 5, 6, and 9 gave better quality with the smaller hole sizes. The threads produced with Fluids Nos. 7, 8, and 10 were gaged as Class 3 but were rougher than the others. On stainless steel, Fluids Nos. 1, 2, 4, and 9 gave the tightest threads with the larger hole sizes. The other fluids had opposite trends. The effect of tap change was very pronounced with Fluid No. 6. One tap produced Class 3 threads with Holes Nos. 3 and 4, and Class 2 threads with Hole No. 5. The other tap produced Class 4 threads with all three holes.

Visual inspection of thread surface quality showed results reasonably similar to those found in reaming. There were some variations with the more severe conditions. For the most part, there seemed to be few differences in surface quality with the larger hole sizes. Brass, magnesium, and aluminum, in order, were particularly difficult to judge in quality. Fluids Nos. 3, 4, 5, and 7 seemed to give better surfaces than the others on brass but the margin, if any, was very small. Fluids Nos. 3 and 6 gave very obvious discoloration of the surface. On magnesium, Fluid No. 7 gave the brightest surface, and appeared to be the best. Fluids Nos. 5 and 10 were very close. Fluid No. 9 gave the dullest surface but in terms of roughness was similar to the others. On aluminum, Fluids Nos. 1, 2, 3, and 10 were distinguished

from Fluids Nos. 4, 5, 6, 7, and 8. Within each group the variation was minor. Without question, Fluid No. 9 gave the poorest and dullest surface. On copper, Fluid No. 4 seemed to be the best followed by Nos. 3, 5, and 1 in order. Fluids Nos. 7, 8, and 10 seemed to give excellent surfaces, but were subject to seizure. Discoloration was noted with Fluids Nos. 1, 2, 3, and 5.

In the ferrous group of materials, Fluid No. 9 gave the best results on all three, 1018, 1042, and stainless steel. There were very obvious differences among groups of fluids on the 1018 steel. Fluid No. 6 followed No. 9, and this was followed by a group composed of Fluids Nos. 4, 5, 3, and 2, in that order. Fluids Nos. 1, 7, and 8 were judged last with a rather wide gap among the three. Fluid No. 8 was definitely inferior for the surface had considerable tears. The effect of additives to Fluids Nos. 1 and 8 was very pronounced on this material. On 1042 steel, the relative ratings were about the same with one exception. Fluid No. 1, which was somewhat inferior on 1018 steel gave a surface quality only a little worse than what was found with Fluid No. 9. Fluid No. 2 also had a slightly higher relative rating.

General Fluid Behavior During Tapping

Torque behavior on aluminum and brass was almost identical. All fluids, but No. 9 on brass, showed similar behavior over the range from Hole No. 5 through Hole No. 2. These behaviors are typical of the traces in Fig. 4.24. Fluids Nos. 2 and 4 were the only fluids that did not show some tendency for seizure on aluminum. All others showed slight tendencies with Holes Nos. 1, 2, and 3. Fluids Nos. 2, 6, 8, and 10 had similar tendencies on brass with the smallest hole. Typical behavior on magnesium is also represented in Fig. 4.24. There were very light seizure tendencies with Fluids Nos. 4, 5, 7, and 9 on Hold No. 1, but there was little difference in general behavior. Except for torque levels and seizure behavior, copper and magnesium had very similar traces. All fluids on copper showed seizure tendencies, with Fluids Nos. 8, 9, and 10 being particularly susceptible with Hole No. 1.

Typical fluid behavior on stainless steel is shown in Fig. 4.25. Fluid No. 10 gave the most violent reaction, causing seizure even with Hole No. 5. Other fluids did not give such pronounced reaction, but it was impossible to tap any hole smaller than Hole No. 3 without breaking the tap.

The most representative fluid behavior on 1018 steel is shown in Fig. 4.26. Fluids Nos. 1, 2, 4, 7, 8, and 10 were most susceptible to seizure and several taps were broken with Hole No. 1. Fluid No. 5 appeared to have the least tendency for seizure although Hole No. 1 was not tapped. The higher carbon content of the 1042 steel was very effective in reducing seizure tendencies to a minimum. There was no pronounced seizure tendencie with any of the fluids, and all holes were tapped without difficulty.

In an attempt to study seizure and stick-slip phenomena, an accelerometer was mounted on the specimen holder to pick up high frequency variations during tapping. To date, these investigations have been of exploratory nature to develop techniques, to find most effective accelerometer locations, and, in general, to determine the extent of the problem associated with the phenomena. Sample oscilloscope traces are shown in Fig. 4.27 for several materials. These records show frequencies of about 25,000 cycles per second at varying amplitudes among the materials.

Tests With "X-Press" Taps

As was indicated, "X-Press" taps literally form the thread by plastically displacing the material from the region of the root of the thread causing it to flow and form the crest portion. This technique has been referred to as "chipless" tapping and is used primarily on brass and aluminum. Since rubbing is very severe in this operation, tests were made to see if differences among fluids would be accented. The tests were conducted on three materials, aluminum, brass, and magnesium. The results on aluminum and brass are given in Table 4.23 and typical traces are shown in Fig. 4.28. The magnesium is not included because it reacts very badly to plastic deformation, and the threads were all badly cracked and distorted.

Aside from the results with Fluid No. 9, the differences among fluids were more pronounced on the brass, but were not of the magnitudes expected. Surface qualities were again difficult to judge, but behaviors similar to reaming were noted. Fluids Nos. 1, 2, and 3 seemed to give the better surface quality on brass. Fluids Nos. 4, 5, 7, and 8 gave poorer quality by comparison. Smear on the thread surfaces was noted with the latter fluids. On aluminum, Fluids Nos. 1, 7, and 4 gave the cleanest surfaces. Fluids Nos. 3 and 9 were definitely inferior to the others, but there was even a wide gap between these two. The surface with Fluid No. 9 was badly smeared and distorted. Fluid No. 3 showed similar tendencies but to a much lesser degree.

BROACHING

Broaching investigations were carried out on a six-ton capacity American Hydraulic Vertical Broaching Machine, with the setup illustrated in Fig. 4.29. They were designed to measure and record the effect of fluids upon two criteria during cutting: (1) broaching or cutting forces, and (2) normal forces. These forces were measured by two specially designed dynamometers, and the relationships among the broach, the specimen, and the dynamometers is shown in the closeup photographs of Figs. 4.30 and 4.31.

The lower dynamometer supported the specimen and the upper assembly. It consisted of two parts which pivoted about a pin at one end and were separated at the other by a sensitive Kistler load cell which served as a direct

pickup for the broaching forces. The upper unit consisted of six sensing fingers in the form of cantilever beams which spanned the work specimen in pairs, three to each side. A very sensitive semiconductor strain-gage was mounted on each finger to sense the variations in bending which occurred with diameter changes in the specimen. These diameter changes represented the stresses or normal forces imposed on the workpiece during broaching. The position of the specimen relative to the fingers is illustrated in Fig. 4.31. As seen in Fig. 4.30, the fingers were spaced to measure the diameter changes at the top, middle, and bottom of the specimen. The sensitivity of diameter change was as little as 6 millionths of an inch for each millimeter of deflection on the recorder chart.

The work specimens were in the form of bushings, .980 inch outside diameter, and .730 inch inside diameter. They were 1 inch long. Specimens were prepared from six of the seven work materials. Stainless steel was not tested in this series of investigations.

Broaches and General Conditions

A series of two pull-type round hole broaches was used for each test sequence. These are shown in Fig. 4.30. One broach, without burnishing elements and identified as Broach No. 1, enlarged the hole from .730 inch to .740 inch diameter. The second broach, Broach No. 2, enlarged the hole from .740 inch to .750 inch diameter and contained burnishing elements for final finishing. Other than the burnishing elements and the difference in size, design specifications for the two broaches were the same. Each broach had three roughing teeth and four finishing teeth with specified diameter increment changes of .002 inch and .001, respectively. The last finishing tooth was followed by three dwell teeth at the same diameter. Relief angles were 2°, 1°, and 1/2° for the roughing, finishing, and dwell teeth, in order. Hook angle, corresponding to rake angle of single point tools, was 12° on all teeth. All cutting edges were left unnotched and produced continuous circular chips.

The actual diameters, diameter increments, and pitch of successive teeth are given in Tables 4.24 and 4.25. It is seen that there are random variations from the original specifications. The oversize diameter on the burnishing elements conforms to standard practice to account for elastic deformations. Tooth pitch varied (design specifications called for alternate 5/16 inch, 11/32 inch, and 3/8 inch pitch) but was designed so that at some given time only roughing, or finishing, or dwell teeth or burnishing elements alone were in contact with the specimen.

Two specimens were tested with each broach and each fluid on all materials. Broaching velocity was approximately 6.5 fpm on all tests. Permanent records were made of cutting forces and the behavior characteristics of each

of the three sets of fingers. In addition, an accelerometer was mounted directly to specimens of magnesium, brass, aluminum, and 1018 steel to record radial accelerations. Traces from these tests are shown in Fig. 4.44.

Broaching Behavior

Broach cutting behavior is exemplified by the photograph of the first broach in Fig. 4.30. Of particular note is the behavior of the dwell teeth. It can be seen that even though these teeth are within .0001 inch of being the same diameter, they still remove some material. This illustrates very well the effect of elastic deformations during cutting at greater chip thicknesses.

As was pointed out in the introduction to this section of the report, chip thicknesses in broaching are fixed quantities determined in the design stages. Therefore, the rate of initial removal per unit of cutting speed versus broach position relative to the specimen is a constant at any given point. The theoretical values for Broaches Nos. 1 and 2 were calculated and are plotted in Figs. 4.32 and 4.33, respectively. The two are, of course, very similar and the differences in levels for given broach positions are due to differences in diameter increments. The step changes that occur are due to teeth entering and leaving the work specimen. The horizontal spaces between steps are lags between the time one tooth leaves and another tooth enters and are represented by the difference between the sum of three consecutive tooth pitches and the specimen length. The lag distances for Broach No. 1 and the identity of teeth leaving and entering the work specimen are shown in Fig. 4.32. The types of teeth and the combinations that determine the level for the rate of metal removal are identified in Fig. 4.33. Except for the burnishing elements, they are common to both broaches. It should be pointed out that the rate of metal removal represented by the first three steps on each chart will be affected by the initial hole diameter and the resultant volume that will be removed by the first tooth. The changes between steps, however, and the rates of metal removal following, would not be affected.

Theoretically, the broaching forces should be proportional to the rate of metal removal and should follow the same general pattern. Any deviation by actual forces would have to be attributed to rubbing and cutting characteristics. The burnishing forces would also be affected by cutting characteristics and how they affected hole size, and by fluid properties.

To illustrate generally typical behavior, broaching force results with each broach on four material-fluid combinations were superimposed, to scale, on rate of metal removal charts identical to those in Figs. 4.32 and 4.33. These results with Fluid No. 7 on aluminum, copper, and 1018 steel; and Fluid No. 9 on magnesium are illustrated in Figs. 4.34 through 4.41 for the two broaches. The force examples on aluminum, copper, and 1018 steel were,

for the most part, typical of all fluids. Fluid No. 9 on magnesium emphasized the lack of lubrication in finishing and burnishing more than the others. The plots, themselves, are very interesting, for they show distinct differences in behavior among the materials. Broaching forces on the 1018 steel follow the rate of metal removal charts most closely. The effect of built-up edge is shown by the relatively lower forces with the finishing teeth and little, if any, force with the dwell teeth. The entry and exit of the cutting teeth is well pronounced over most of the broach travel. The forces on aluminum follow the rate of metal removal proportionally until the finishing teeth enter. Beyond this point, the forces tend to be higher in proportion, indicating that rubbing friction is contributing to the force level. This is illustrated by the relatively high level of force with the dwell teeth and the burnishing elements. Magnesium shows a similar behavior, but the friction forces are much more pronounced during the finishing, dwell, and burnishing sequence. Prior to that, the force plateaus are very distinct and follow the rate of metal removal plots quite well. This kind of behavior was typical of most of the fluids, but as was pointed out, was most pronounced with Fluid No. 9, pronounced enough in this case to give, with practically no metal removal, higher force levels than those encountered during roughing. Copper is somewhat unique among this group of materials in that its behavior tends to follow the rate of metal removal values, but the plateaus are distorted and the tooth changes are less abrupt. This emphasizes the gummy behavior and the high distortion that accompanies chip formation in most cutting operations on this material.

Another characteristic of broaching behavior which substantiates some of the characteristics mentioned above is the influence of cutting forces upon workpiece diameter as the individual teeth of the broach pass along the length of the specimen. The inherent cutting characteristics of broaching imply that high normal forces exist during chip formation. High rubbing forces also imply that normal forces must exist. In the broaching of thin-walled specimens, such as were used in the test series, the normal forces can cause not only the work diameter to expand, which is the most obvious result, but can also cause the diameter to contract in certain portions of the length.

In the beginning of the broaching program, theoretical calculations of diameter change in relative units were made assuming that the normal forces from each tooth exerted a uniformly distributed tensile stress and a bending stress upon the specimen. The results of these calculations for relative diameter changes at the top and the bottom of the specimen are shown in Figs. 4.42 and 4.43. The vertical lines represent teeth entering or leaving. The short slanting lines show the effect during the time interval between leaving and entering teeth. As can be seen, the results predict that the diameters will expand or contract, depending upon the position of the teeth with respect to the specimen length and the chip load taken by each tooth.

That the above calculations are not too far from actual behavior is substantiated by the accelerometer results shown in Fig. 4.44. These results actually represent radial accelerations at a point 3/8 inch from the top of the specimen. The accelerations are, however, proportional to diameter changes at the given point, and it is seen that they give characteristics which are intermediate between the calculated results for the top and bottom of the specimen. The "fingers" of the dynamometer also gave similar trends, but the changes were not sharply defined. Also, because of the extreme sensitivity of the gages to any movement, some difficulty was encountered in keeping the original reference due to slight shift in the specimen during broaching. The magnitude of the shift was usually less than .001 inch but it was enough to cast some doubt on the true total levels of diameter change. Vibrations during cutting, also contributed to erratic behavior. The results did show, however, that changes in diameter of as much as .0015 inch took place during many of the tests. On the steel specimens, this change in diameter would give a stress of 52,000 psi at a normal force equivalent of about 12,000 lbs. In addition, the broached hole diameters given in Table 4.29 show that all diameters are less than the diameters of the broach teeth or burnishing elements, and in one case, Broach No. 1 on brass with Fluid No. 7, the hole diameter was .0025 inch less than the diameter of the dwell teeth on the broach.

The influence of the normal forces upon diameter changes, undoubtedly contribute to some of the taper which seems to be inherent in the broaching of thin-walled specimens. Magnesium, which has the lowest modulus of elasticity of the materials tested, had the smallest average hole size but also showed the most consistent taper between the top and bottom of the hole, averaging about .0001 inch on all the specimens. The steels, particularly the 1018 material, had negligible taper. Part of the taper may have been due to residual stresses, because in general the taper was a litte greater with the burnished hole, on the brass especially.

Test Results—Forces

As was mentioned previously, the pitch of the broach teeth was designed so that at some time during broaching only certain sets of teeth would be in contact with the work specimen. As a result, it was possible to separate the roughing, finishing, dwell, and burnishing forces. These are tabulated individually for each material and each fluid in Tables 4.26 and 4.27. All forces and the resultant hole diameters have been grouped for each material in Table 4.28. The roughing and finishing tooth forces are considered cutting forces, while dwell tooth forces, for all practical purposes, and burnishing forces result primarily from rubbing.

In general, the cutting forces follow the cutting torque behavior established in reaming. The 1018 steel, 1042 steel, and copper have the highest roughing and finishing forces, followed by brass, aluminum and magnesium in

order. One noticeable deviation from general trends appears with Fluid No. 9 on aluminum. This fluid consistently gave the highest forces among the fluids on aluminum, and resulted in the highest dwell and burnishing forces of any of the materials. The dwell and burnishing forces were both higher than the finishing forces, and the burnishing force with Fluid No. 9 was even higher than the roughing force. The hole diameters were, however, the smallest and the surface finish the roughest, which is consistent with results on tapping and reaming.

Fluid No. 9 also gave similar behavior on magnesium. Both burnishing and dwell forces were higher than finishing forces with the burnishing force again higher than the roughing force. Surface roughness was obviously worse only with the burnishing elements, however, and the hole sizes were still among the lowest with this fluid. Fluids Nos. 2, 3, and 8 also gave higher dwell than finishing forces on magnesium, but only Fluids Nos. 1, 3, and 6 gave higher dwell than burnishing forces. On brass, however, Fluids Nos. 1, 3, and 6 had just the opposite effect and were the only fluids to give higher burnishing than dwell forces. It may be noted, also, that Fluid No. 5 gave the highest burnishing force on brass and was the only fluid to give a higher dwell than finishing force. This appears to be consistent with the reaming results.

The results on copper and the 1018 and 1042 steels appear to follow the more expected results of lower dwell than burnishing forces. Only Fluids Nos. 5 and 10 on 1018 steel reverse the normal trends. Except for results with Fluid No. 9, the steels give the lowest forces in the rubbing group, reflecting built-up edge characteristics during cutting. The steels and copper allow distinctions to be made among the fluids fairly well at all force levels, with copper showing perhaps the greatest deviations. Aluminum, brass, and magnesium do not allow distinctions to be made as well, particularly in the cutting force group. Brass shows a wider spread among the rubbing forces, which again appears to be consistent with reaming behavior.

Surface Roughness and Dimensional Stability

These results are listed in Tables 4.29 and 4.30 as average values for both broaches. In general, those fluids which gave the poorest finishes also gave the widest diameter variations, with the exception of Fluid No. 9 on aluminum with both broaches and on magnesium with Broach No. 1. Except for isolated cases, the differences in diameters for a given material are quite small. There is a very obvious effect of Fluid No. 9 on aluminum and the two steels. On aluminum it gave the smallest holes with by far the best surface. As a matter of fact, the measured surface roughness values are somewhat misleading on copper and the steels particularly. On the steels, there was a much wider difference between Fluid No. 9 and the others than what is indicated by the relative differences in roughness levels. There was

no comparison in visual appearance. Fluids Nos. 10, 8, 7, and 2 in that order were worse than the others. The differences were less pronounced on the 1042 steel. The same fluids gave the highest roughing forces, as well. On copper, there is no question that the major portion of the hole surface carried the surface quality as listed in Table 4.30. However, Fluids Nos. 2, 4, 7, 8, and 10 particularly gave seizure tendencies which resulted in at least partially torn surfaces. It is interesting to note that these fluids also gave the highest roughing forces on copper. Surfaces on the other materials appear to be fairly well represented by the surface roughness values.

Summary

The results of the reaming, tapping, and broaching tests seems to be in general agreement with each other as well as with the results from other test series. Where heavier cutting is concerned, fluid effects seemed to be similar in tapping, broaching, and turning. On the steels, for example, Fluids Nos. 2, 4, 7, 8, and 10 gave, in general, the highest forces on all three of the operations. The higher force levels seemed to be due to seizure tendencies and cutting zone behavior. Friction wear results show most of these fluids as having among the highest coefficients of friction. On the other hand, Fluid No. 5 gave the lowest or among the lowest forces or torques on all materials but brass and possibly magnesium. Friction wear results again correlate fairly well, for Fluid No. 5 has among the lowest coefficients of friction on all but brass and magnesium. Like similarities may be found among the other materials and between surface roughness and dimensional stability.

A very significant finding is the influence of tool geometry upon test results, particularly where rubbing is accented as it was in reaming. This is particularly important with materials without tendencies to form built-up edges or with fluids that are effective in reducing built-up edge. Normal forces may rise to a level where even an effective fluid will breakdown and give widely varying results.

TABLE 4.1

SIZES OF CUT TESTED WITH ALL FLUIDS ON EACH MATERIAL

(Numbers in parentheses identify combinations of feed and depth)

Feed, ipr	Radial Depth of Cut, in. .0025	.005	.0075
.0023	(1)	(2)	(3)
.0036	(4)	(5)	(6)
.0087	(7)	(8)	(9)

TABLE 4.2

AVERAGE CUTTING TORQUES AND SLOPES FOR ALL CUTTING CONDITIONS ON ALL TEST MATERIALS*

Material	Cutting Torque, lb in. Cut Number 1	2	3	4	5	6	7	8	9	Slope Variable Feed	Depth
Magnesium	.50 (.58)**	.89 (.52)	1.26 (.49)	.77 (.44)	1.08 (.49)	1.51 (.44)	1.12 (.35)	2.06 (.31)	2.83 (.29)	.61	.84
Aluminum	.57	1.05	1.51	.94	1.44	2.18	1.87	3.17	4.48	.80	.80
Brass	.60	1.20	1.77	1.05	1.70	2.41	1.86	3.29	4.77	.77	.86
Copper	1.28	2.51	3.62	2.20	4.52	6.81	4.27	7.79	11.12	.85	.80
1018 Steel	1.40	2.37	3.18	1.68	3.44	4.81	3.82	7.28	10.3	.84	.88
1042 Steel	1.47 (1.70)	2.60 (1.49)	3.52 (1.38)	2.19 (1.61)	3.75 (1.41)	5.08 (1.30)	4.52 (1.45)	8.26 (1.27)	11.9 (1.18)	.88	.81
Stainless Steel	2.64	4.85	8.20	4.71	7.85	12.9	11.5	19.0	24.3	.98	.76

*Average values for all reamers and all fluids. Fluids did not appear to affect cutting torques appreciably. See Table 4.4 for variations among reamers on magnesium and brass. Slopes were determined by plotting torque versus the variables feed and depth as in Fig. 4.4.

**Numbers in parentheses represent unit horsepower values as calculated from results in Fig. 4.4.

TABLE 4.3

REAMER DIAMETER MEASUREMENTS ALONG AXIS

IN ONE-QUARTER INCH INCREMENTS FOR WORKING LENGTH OF ONE INCH

Reamer No.	Body Diameters, in.				
	1/16	1/4	1/2	3/4	1
	Distance from Chamfer End, in.				
1	.7504	.7504	.7504	.7504	.7504
2	.7502	.7502	.75025	.7503	.7503
3	.7502	.7502	.7503	.75035	.75035
4	.7504	.7504	.7504	.75035	.75035
5	.75025	.75035	.7503	.7503	.7503
6	.7502	.75025	.7503	.7503	.7503
7	.7499	.7501	.7503	.75035	.75035
8	.7498	.7499	.7502	.7504	.7504
9	.7486	.7490	.7496	.7498	.7500
10	.7501	.7502	.75035	.75035	.7504
.740*	.7411	.7412	.7412	.7412	.7412

TABLE 4.4

COMPARISON OF REAMER BEHAVIOR ON BRASS AND MAGNESIUM WITH FLUID NO. 5 AT A SINGLE CUTTING CONDITION

Feed = .0087 ipr Radial Depth of Cut = .005 rpm = 65 Velocity = 12.8 fpm

Material	Measurement	Reamer Number									
		1*	2	3	4	5	6	7	8	9*	10
Magnesium	Cutting torque, lb in.	2.75	1.75	1.75	1.88	2.75	2.0	1.56	1.56	2.50	2.75
	Torque at .015 in. depth, lb in.**	8.0	3.0	3.5	3.2	8.3	5.8	5.3	3.8	10.0	7.0
	Max. rubbing torque, lb in.	153	47	50	23	64	52	109	75	229	85
	Initial rubbing rate, lb in./in.	396	21.9	158	11.7	181	80	354	117***	457	364
	Hole diameter, in.	.75010	.75035	.75025	.75045	.75025	.75020	.75020	.75045	.74890	.75010
	Surface roughness, µin.	15-35-25	30-20	80-30-30	35-60	45-30	10-22	25-25	40-20	25-35	20-16
Brass	Cutting torque, lb in.	3.0	3.62	3.0	2.62	3.75	3.25	2.75	3.0	3.50	3.75
	Torque at .015 in. depth, lb in.**	8.0	4.0	4.5	5.0	9.6	6.5	6.8	3.7	9.4	7.3
	Max. rubbing torque, lb in.	217	7.8	82	8.4	16	17	89	31	361	153
	Initial rubbing rate, lb in./in.	325	11.2	51.6	0	23.4	15.6	315	37.4***	458	340
	Hole diameter, in.	.74980	.75055	.75015	.75060	.75060	.75035	.75040	.75085	.74850	.74995
	Surface roughness, µin.	20-12	17-27	105-30-20	15-40	50-80	20-30-30	45-35	35-25	23-15	4-9

*Torque results are probably higher than normal. Leading edges were stoned very lightly to remove built-up edge from 1018 steel on previous series of tests. This resulted in a change of .0001 inch in diameter near the chamfer. A repeat test on brass at a feed of .0036 ipr with Reamer No. 1 and Fluid No. 5 gave a maximum torque value of 160 lb in. compared with an initial value of 19 lb in.

**Torque after reamer travels .015 inch at full diameter. To illustrate effect of chamfer corner condition.

***Slope increased after about 5 revolutions to 273 and 187 for magnesium and brass, respectively.

TABLE 4.5

RESULTS OBTAINED WITH REAMER NO. 1 (STRAIGHT) AND REAMER NO. 9 (SLIGHT TAPER) WITH ALL FLUIDS AT A SINGLE CUTTING CONDITION

Feed = .0036 ipr | Radial Depth of Cut = .005 inch | RPM = 65 | Velocity = 12.8 fpm

Fluid No.	Measurement*	Work Material: Magnesium (Reamer 1)	Magnesium (Reamer 9)	Brass (Reamer 1)	Brass (Reamer 9)	Copper (Reamer 1)	Copper (Reamer 9)	1018 Steel** (Reamer 1)	1018 Steel** (Reamer 9)
1	Max. Torque, lb in.	20	148	8.0	85	31	127	8	115
	Hole Diameter, in.	.75065	.74965	.75080	.74975	.75055	.75980	.75115	.74945
	Surf. Rough., µin.	30-50-35	25→20	8→15	40→60	28→15	35-65-60	170→180	50→40
2	Max. Torque, lb in.	49	182	75	158	230	375	16	73
	Hole Diameter, in.	.75040	.74990	.75080	.74975	.75000	.74925	.70595	.74965
	Surf. Rough., µin.	25-35-35	20→35	15→15	50→65	6—9—9	8→8	200→150	60→95
3	Max. Torque, lb in.	26	168	10.5	108	40	142	7.5	150
	Hole Diameter, in.	.75060	.74945	.75065	.74990	.75055	.75025	.75095	.74960
	Surf. Rough., µin.	45→25	17→25	10→7	35→45	21→13	38→38	65—110—65	45→30
4	Max. Torque, lb in.	26	88	9.5	250	173	375	15	57
	Hole Diameter, in.	.75060	.74950	.75080	.74955	.75020	.74885	.75210	.74975
	Surf. Rough., µin.	75→20	17→32	30→20	25→35	2→5	3→10	150→140	45→65
5	Max. Torque, lb. in.	18	105	9.0	300	163	350	13	40
	Hole Diameter, in.	.75060	.74935	.75080	.74950	.75000	.74925	.75125	.74970
	Surf. Rough., µin.	40→30	15→25	15→35	20→25	5.5→5.5	5.5→7.5	145→145	45→45
6	Max. Torque, lb in.	19	102	9	125	60	155	14	67
	Hole Diameter, in.	.75060	.74935	.75070	.74965	.75050	.74945	.75145	.74950
	Surf. Rough., µin.	35→35	25→40	13—19	20→25	8→3	16—19—16	130-230-200	40→25
7	Max. Torque, lb in.	31	125	9.0	108	83	456	12	33
	Hole Diameter, in.	.75055	.74975	.75070	.74990	.75035	.74945	.75125	.74975
	Surf. Rough., µin.	40→30	20→40	15→22	40→80	4.5—7.5—6	20—40-20	120→150	80→110
8	Max. Torque, lb in.	49	152	9.0	58	100	512	14	19
	Hole Diameter, in.	.75050	.74940	.75075	.75005	.75030	.74885	.75150	.74980
	Surf. Rough., µin.	30→40	25→40	14→22	55→95	5.5—10—8	12→22	100-220-150	70→70
9	Max. Torque, lb in.	10	34	19	90	55	202	145	500
	Hole Diameter, in.	.75065	.75005	.75070	.75005	.75060	.74955	.75010	.75000***
	Surf. Rough., µin.	22→25	18→25	20→17	55→80	50—150—50	15—90-50	95—30—50	70-130-70
10	Max. Torque, lb in.	34	87	12	40	100	270	10	42
	Hole Diameter, in.	.75055	.74990	.75085	.75015	.75030	.74945	.75140	.74980
	Surf. Rough., µin.	30→30	20→20	30→60	65→85	10→25	10—60-50	150→230	90→130
Dry	Max. Torque, lb in.	80	165	6.2	13	90**	53**	27	360
	Hole Diameter, in.	.75150	.7516	.75165	.75045	.75110	.74995	.75095	.74975
	Surf. Rough., µin.	45→45	50→35	70→95	50-80-60	280-150-375	60-180-90	250→275	40—60-40

*Hole diameter—Middle of specimen. Surface Roughness—Variation from top, to middle, to bottom of hole. Two numbers indicate gradual change over length.

**Torque values are average of maximum and minimum of fluctuations. Very pronounced stick-slip and seizure tendency, particularly with straight reamer.

***Hole enlarged by margins on reamer just before end of travel. Torque value rose to 725 lb in. when seizure took place then dropped to 150 lb in. when metal was removed.

TABLE 4.6

MAXIMUM REAMING TORQUES ON MAGNESIUM, BRASS, COPPER, AND 1018 STEEL WITH .740 INCH DIAMETER STRAIGHT-FLUTE REAMER

Feed = .0087 ipr Radial Depth of Cut = .005 inch RPM = 65

Material	Torque, lb in. Fluid Number										
	1	2	3	4	5	6	7	8	9	10	Dry
Magnesium	54	92	70	62	59	54	69	94	26	75	44
Brass	25	16	20	20	20	27	24	16	37	16	14
Copper	42	50	43	57	58	47	46	47	60	61	63
1018 Steel	13	40	13	30*	42*	32	33	31	140	30	40

*Peak before seizure and eventual drop in torque.

TABLE 4.7

MAXIMUM RUBBING TORQUES FOR EACH REAMER-FLUID COMBINATION, ALL CUTS, ALL MATERIALS

Cut Number—Rubbing Torque, lb in.									Work Material	Cut Number—Rubbing Torque, lb in.								
1	2	3	4	5	6	7	8	9		1	2	3	4	5	6	7	8	9
			Fluid No. 1—Reamer No. 1										Fluid No. 2—Reamer No. 2					
13	12	12	34	43	35	24	27	29	Magnesium	7.6	9.1	8.8	20	19	15	26	24	27
5.0	5.6	.96	2.4	1.1	.96	7.7	7.6	7.0	Aluminum	1.9	2.7	2.2	1.8	1.1	1.6	5.9	3.2	2.9
6.3	3.6	3.4	5.0	2.8	2.7	5.5	4.8	3.4	Brass	8.8	5.4	5.9	5.3	3.2	4.0	6.2	5.5	6.0
25	8.6	8.4	22	23	22	78	64	59	Copper	14	18	31	70	70	77	34	57	78
1.8	.71	6.2	1.2	3.4	5.2	1.0	2.7	2.1	1018 Steel	2.9	2.6	5.6	1.9	2.8	4.6	2.3	3.3	6.5
5.0	4.6	2.5	2.7	6.7	15	9.7	2.7	3.4	1042 Steel	11	4.6	7.5	18	2.4	5.3	2.8	2.7	2.8
46	36	39	58	62	57	76	32	10	Stainless Steel	38	33	34	43	47	40	69	52	61
			Fluid No. 3—Reamer No. 3										Fluid No. 4—Reamer No. 4					
25	32	36	37	46	39	40	45	45	Magnesium	10	7.8	9.4	14	15	15	27	27	27
28	29	31	44	44	43	33	19	18	Aluminum	2.5	.62	2.2	1.6	1.7	1.3	3.3	2.6	1.3
>40*	70	47	39	30	33	173	135	117	Brass	1.9	1.6	1.2	2.8	1.2	.96	8.8	4.8	4.1
49	47	35	75	50	50	84	70	62	Copper	19	42	43	69	69	77	22	32	49
5.4	2.0	4.3	1.9	2.8	3.3	3.5	1.4	6.5	1018 Steel	2.3	.71	1.8	1.2	.31	2.7	0	5.8	2.7
32	32	28	94	2.3	18	18	16	5.3	1042 Steel	16	2.8	1.2	18	3.6	5.3	.35	2.1	2.8
51	46	44	58	54	44	57	61	50	Stainless Steel	30	26	25	32	32	30	51	48	13
			Fluid No. 5—Reamer No. 5										Fluid No. 6—Reamer No. 6					
3.2	5.9	5.0	11	10	12	14	18	20	Magnesium	8.2	13	10	18	23	19	29	30	32
1.9	.88	0	.39	.88	.59	1.5	1.9	1.6	Aluminum	2.7	1.1	0	2.4	1.8	1.3	3.7	2.0	2.0
1.9	1.4	1.5	5.0	7.2	4.6	5.6	8.0	6.0	Brass	1.6	.75	.91	3.2	1.9	.84	2.5	1.7	.95
6.1	19	26	41	42	48	3.2	3.4	1.9	Copper	6.1	6.2	5.9	11	14	18	57	45	42
1.7	1.1	1.8	1.6	4.7	7.7	1.7	2.4	6.5	1018 Steel	1.7	.71	3.7	1.1	.56	.84	0	.80	4.6
23	2.1	3.1	6.5	1.7	11	8.8	.86	1.6	1024 Steel	1.6	7.1	1.2	2.1	1.1	2.6	.35	.25	1.6
21	34	38	38	38	36	61	50	51	Stainless Steel	28	20	28	45	58	44	47	61	63
			Fluid No. 7—Reamer No. 7										Fluid No. 8—Reamer No. 8					
13	13	13	22	22	19	36	35	35	Magnesium	49	67	63	>50*	80	72	>100*	110	147
1.9	.62	2.2	1.4	1.7	.34	6.1	5.1	5.7	Aluminum	23	38	46	44	55	52	92	112	99
.28	.50	.54	4.7	6.6	5.2	34	27	18	Brass	13	9.2	5.9	7.8	6.5	6.7	11	4.7	13
3.6	27	45	89	87	92	22	32	54	Copper	248	285	315	322	358	---	---	---	---
4.2	2.0	1.8	.61	2.2	1.5	1.0	1.4	6.5	1018 Steel	4.2	9.5	6.2	6.9	6.6	6.5	8.5	2.8	13
1.6	2.1	2.5	18	3.0	2.8	26	1.5	3.4	1042 Steel	67	141	99	60	44	43	70	37	28
27	30	27	29	45	48	64	33	30	Stainless Steel	62	54	54	60	72	73	97	88	124
			Fluid No. 9—Reamer No. 9										Fluid No. 10—Reamer No. 10					
6.1	6.6	5.0	12	12	12	23	21	22	Magnesium	7.0	11	19	26	28	31	>50*	98	103
33	29	28	41	46	44	95	107	104	Aluminum	6.9	3.0	4.1	4.1	5.5	6.6	9.8	12	17
46	53	47	40	40	35	44	43	47	Brass	3.8	5.1	3.4	2.8	2.6	2.7	3.1	4.2	5.8
96	94	97	98	210	220	316	---	---	Copper	6.1	67	68	2.6	19	37	81	130	164
250	345	---	---	---	---	---	---	---	1018 Steel	1.8	.71	2.5	1.2	2.2	3.3	1.7	2.7	5.8
248	216	221	248	308	345	370	---	---	1042 Steel	2.8	2.1	3.1	2.1	1.5	2.2	6.0	2.7	5.3
372	---	---	---	---	---	---	---	---	Stainless Steel	43	49	51	53	65	67	90	43	40

*Off scale

TABLE 4.8

EFFECT OF FLUID AND SIZE OF CUT ON RESIDUAL STRESS*

Fluid No.	Change in Gage Length After Slotting, .001 inch														
	Magnesium					Brass					Aluminum				
	Cut Number														
	1	2	3	5	8	1	2	3	5	8	1	2	3	5	8
1	16	14.8	16.7	14.9	22.2	3.6	1.4	4	3	7.2	.1	- .6	- .1	-2.1	.9
2	12.2	16.6	19.6	21.4	20.6	4.8	3.2	---	4.5	5	- .8	- .6	- .1	- .4	- .1
3	16.2	15.2	15.8	23.2	18	5	---	7.2	5.5	7.5	.9	2.4	2.9	.9	1.2
8	22.6	22	24.2	20.8	21.4	8.2	5.8	4.5	9.9	6.5	4.9	4.5	7.4	4.7	6.2
9	7.8	13	12	20.2	19.9	9.7	9.4	9	13.2	12.2	5.4	6.9	7.9	8.9	4.9
10	20.8	16	18.6	16.8	18.8	8.7	6.9	7.1	7.6	8.9	1.9	4.6	3.9	.9	- .1

*Residual stress represented by relative change in gage width after slotting of reamed and unreamed specimen:

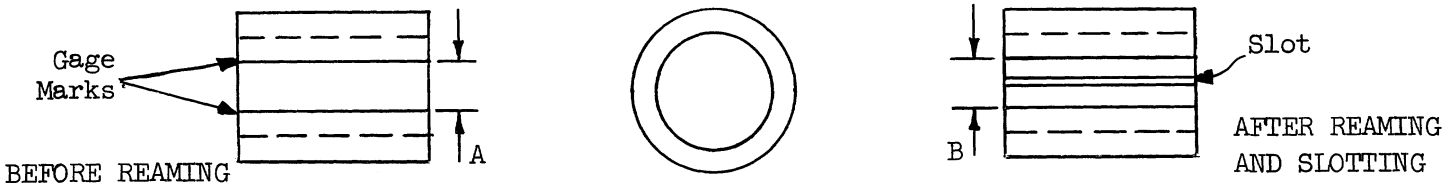

Reference value for each material is found by slotting unreamed specimen and measuring change. Numbers in above table = original chnage of representative unreamed specimens—(A-B). Positive numbers indicate a widening of gage marks relative to original. Negative numbers indicate a closing. Widening would be due to what would be in effect a compressive stress.

TABLE 4.9

SUMMARY OF RELATIVE EFFECTS OF REAMER CHANGE,

FLUIDS, AND MATERIALS BASED ON RESULTS IN TABLE 4.5

(A) Ratio of Rubbing Torques Between Reamers Nos. 9 and 1

Material	Fluid Number									
	1	2	3	4	5	6	7	8	9	10
Magnesium	7.8	3.7	6.5	3.4	5.8	5.4	4.0	3.1	3.4	2.6
Brass	13	27	12	32	41	17	15	7.7	5.1	3.7
Copper	4.6	1.6	3.9	2.2	2.2	2.7	5.7	5.3	3.9	2.8
1018 Steel	24	5.5	36	4.6	3.8	6.0	3.4	1.5	3.5	5.8

(B) Relative Rubbing Torque Ratios Based Upon Results with Reamer No. 1 on Brass*

Material	Reamer Number	Fluid Number									
		1	2	3	4	5	6	7	8	9	10
Magnesium	1	3.0	8.3	2.8	3.2	2.3	2.6	4.1	6.6	.52	3.2
	9	23	32	19	11	14	14	17	20	1.9	8.5
Brass	1	1	1	1	1	1	1	1	1	1	1
	9	13	27	12	32	41	17	15	7.7	5.1	3.7
Copper	1	4.2	29	3.9	22	22	7.6	11	13	2.9	9.3
	9	19	62	15	48	48	20	63	69	11	26
1018 Steel	1	.7	2.2	.47	1.5	1.3	1.5	1.2	1.6	8.2	.62
	9	17	12	17	6.9	5	9	4	2.2	29	3.6

*Values for Reamer No. 9 found by multiplying respective ratios in A by respective ratios for Reamer No. 1 in B.

(C) Relative Fluid Ratings Based Upon Decreasing Effect on Rubbing Torque (from B above)

Material	Reamer Number	Order									
		Fluid Number									
		1	2	3	4	5	6	7	8	9	10
Magnesium	1	2	8	7	4 or 10		1	3	6	5	9
	9	2	1	8	3	7	5 or 6		4	10	9
Brass	1	9	10	3	4	5,	6,	7, or 8		1	2
	9	5	4	2	6	7	1	3	8	9	10
Copper	1	2	4 or 5		8	7	10	6	1	3	9
	9	8	7	2	4 or 5		10	6	1	3	9
1018 Steel	1	9	2	4,	6, or 8		5	7	1	10	3
	9	9	1 or 3		2	6	4	5	7	10	8

TABLE 4.10

HOLE SIZES AND PERCENT THREADS USED IN TEST SEQUENCE

Percent Thread	94	78	62	47	31
Hole Size, in.	13/32	27/64	7/16	29/64	15/32
Identifying No.	1	2	3	4	5

TABLE 4.11

TAP PITCH DIAMETER AND BODY RELIEF MEASUREMENTS OF TAPS USED*

Material On Which Used and Identification	Position of Measurement From End—No. of Threads					
	5 and 6		12 and 13		20 and 21	
	Dia, in.	Relief, in.	Dia, in.	Relief, in.	Dia, in.	Relief, in.
Magnesium (M)	.4504	-.0002	.4500	-.0003	.4490	-.0003
Aluminum (A)	.4501	.0002	.4496	.0003	.4492	.0004
Brass (B)	.4503	.0003	.4498	0001	.4494	.0001
1042 Steel (42)	.4501	.0001	.4499	.0002	.4494	.0004

*Measured by 3-wire method on supermicrometer. Values to nearest 10^{-4}. Relief indicated by amount of diameter change along land width away from cutting edge. Positive numbers indicate relief in proper direction. Negative numbers indicate that tailing edges are at greater diameter than leading edges.

TABLE 4.12

VARIATIONS IN TAPPING TORQUES WITH VARIOUS TAPS ON MAGNESIUM, BRASS, AND ALUMINUM

(A) Magnesium and Brass, Hole No. 2, Maximum Torque, lb in.

Fluid No.	Magnesium		Brass	
	Tap B	Tap M	Tap B	Tap M
6	50	50	52	55
9	84	95	98	74

(B) Aluminum, Hole No. 2, Fluid No. 3

	Tap Numbers*							
	1	2	3	4	5	6	7	8
Maximum Torque, lb in.	48	31	33	30	33	36	31	36

TABLE 4.13

UNIT HORSEPOWER AND MINIMUM CUTTING TORQUE FOR TAPPING AS CALCULATED FROM ORIGINAL REAMING DATA

Hole Size	Work Material					
	Magnesium	Aluminum	Brass	Copper	1018	1042
	(A) Unit Horsepower					
1	.111	.276	.240	.575	.650	.800
2	.114	.280	.243	.590	.656	.810
3	.119	.288	.250	.626	.670	.832
4	.126	.296	.259	.690	.685	.855
5	.145	.321	.282	.770	.725	.922
	(B) Minimum Cutting Torque, lb in.					
1	18.1	45.0	39.0	94.0	106	130
2	12.9	31.6	27.5	66.7	74.3	91.5
3	10.7	26.0	22.5	56.5	60.5	75.0
4	8.25	19.4	17.0	45.0	44.8	56.0
5	4.15	9.2	8.05	22.0	20.8	26.4

TABLE 4.14

TAPPING TORQUE DATA FOR MAGNESIUM

(Torque units, lb in.)

Hole No.	Type of Torque	Fluid Number									
		1	2	3	4	5	6	7	8	9	10
1	Maximum	48	42	46	50	49	60	60	60	104	98
	Cutting	30	30	32	32	36	40	36	38	60	52
	Rubbing	18	12	14	18	13	20	24	22	44	46
	Backout	10	20	16	16	16	20	25	34	120	48
2	Maximum	39	36	38	36	36	44	42	50	90	64
	Cutting	25	21	22	26	16	28	28	28	40	36
	Rubbing	14	15	16	10	20	16	14	22	50	28
	Backout	8	15	12	16	16	18	24	30	68	28
3	Maximum	32	29	33	30	31	39	33	47	88	52
	Cutting	16	16	16	20	22	18	18	20	24	24
	Rubbing	16	13	17	10	9	21	15	27	64	28
	Backout	12	14	13	11	13	16	24	26	60	28
4	Maximum	27	26	27	26	28	35	28	33	76	38
	Cutting	11	12	11	12	10	12	10	13	16	16
	Rubbing	16	14	16	14	18	23	18	20	60	22
	Backout	9	12	12	12	10	14	18	21	42	26
5	Maximum	21	21	22	19	21	33	20	23	60	24
	Cutting	6	8	8	8	6	8	6	8	10	10
	Rubbing	15	13	14	11	15	25	14	15	50	14
	Backout	8	4	6	4	4	8	10	8	32	14

TABLE 4.15

TAPPING TORQUE DATA FOR ALUMINUM

(Torque units, lb in.)

Hole No.	Type of Torque	Fluid Number									
		1	2	3	4	5	6	7	8	9	10
1	Maximum	84	78	76	76	76	84	88	85	132	88
	Cutting	68	65	72	70	68	70	72	64	86	64
	Rubbing	16	14	4	6	8	14	16	21	46	24
	Backout	2	6	4	12	1	2	4	4	10	4
2	Maximum	56	51	56	53	58	55	57	57	78	52
	Cutting	50	44	50	48	48	50	52	52	64	48
	Rubbing	6	7	6	5	10	5	5	5	14	4
	Backout	4	3	4	6	4	0	2	3	12	4
3	Maximum	41	40	42	41	40	46	41	42	60	44
	Cutting	36	40	38	32	34	34	36	36	44	40
	Rubbing	5	8	2	3	8	12	5	6	16	4
	Backout	2	2	3	3	2	0	3	4	10	4
4	Maximum	28	28	28	27	27	29	29	26	44	28
	Cutting	22	22	26	24	24	24	26	22	32	26
	Rubbing	6	6	2	3	3	5	3	4	12	2
	Backout	2	2	1	2	2	0	0	4	10	4
5	Maximum	22	20	23	20	20	21	21	--	30	20
	Cutting	12	16	16	8	10	16	16	--	20	16
	Rubbing	10	4	7	12	18	5	5	--	10	4
	Backout	0	2	2	2	0	0	0	--	4	3

TABLE 4.16

TAPPING TORQUE DATA FOR BRASS

(Torque units, lb in.)

Hole No.	Type of Torque	Fluid Number									
		1	2	3	4	5	6	7	8	9	10
1	Maximum	76	80	78	84	80	76	80	88	116	90
	Cutting	64	62	64	72	68	68	68	72	80	52
	Rubbing	12	18	14	12	12	8	12	16	36	28
	Backout	3	4	4	4	4	5	5	3	16	0
2	Maximum	64	49	54	58	56	56	56	55	88	49
	Cutting	50	44	48	50	50	48	50	48	60	44
	Rubbing	14	5	6	8	6	8	6	7	28	5
	Backout	4	2	4	4	2	5	4	4	14	1
3	Maximum	43	37	32	44	36	38	40	39	64	34
	Cutting	36	32	30	38	32	34	36	36	42	32
	Rubbing	7	5	2	6	4	4	4	3	22	2
	Backout	3	2	0	2	3	4	2	2	8	0
4	Maximum	33	27	31	34	30	32	32	28	48	26
	Cutting	22	22	22	23	21	22	23	20	24	24
	Rubbing	11	5	7	11	9	10	9	8	24	2
	Backout	0	1	0	0	3	2	0	3	6	0
5	Maximum	20	20	22	24	20	20	20	18	32	18
	Cutting	12	11	12	12	12	14	16	12	16	16
	Rubbing	8	9	10	12	8	6	4	6	16	2
	Backout	0	1	2	0	3	1	1	1	5	0

TABLE 4.17

TAPPING TORQUE DATA FOR COPPER

(Torque units, lb in.)

Hole No.	Type of Torque	Fluid Number									
		1	2	3	4	5	6	7	8	9	10
1	Maximum	144	256	168	210	180	215	250	430	545	280
	Cutting	112	144	116	160	144	160	160	164	140	168
	Rubbing	32	112	52	50	36	55	90	266	405	112
	Backout	26	20	28	28	26	28	24	32	---	---
2	Maximum	132	160	112	124	116	160	132	168	132	192
	Cutting	90	108	92	100	100	120	114	112	104	144
	Rubbing	42	52	20	24	16	40	18	56	28	48
	Backout	23	6	19	16	16	19	3	25	42	20
3	Maximum	85	96	88	104	96	100	104	132	112	134
	Cutting	64	68	70	80	68	76	84	83	76	96
	Rubbing	21	28	18	24	28	24	20	49	36	38
	Backout	20	12	15	13	14	18	26	20	35	35
4	Maximum	64	68	68	72	72	72	88	92	88	108
	Cutting	40	48	48	52	50	48	60	55	44	64
	Rubbing	24	20	20	20	22	24	28	37	44	44
	Backout	14	15	12	9	11	16	20	13	24	26
5	Maximum	44	36	50	54	50	56	64	60	68	76
	Cutting	20	28	28	24	32	32	36	28	32	26
	Rubbing	24	8	22	30	18	24	28	32	36	50
	Backout	8	32	9	7	6	14	14	12	16	20

TABLE 4.18

TAPPING TORQUE DATA FOR 1018 STEEL

(Torque units, lb in.)

Hole No.	Type of Torque	Fluid Number									
		1	2	3	4	5	6	7	8	9	10
1	Maximum	354	---	368	560	---	---	---	---	---	---
	Cutting	176	---	192	224	---	---	---	---	---	430
	Rubbing	178	---	176	336	---	---	---	---	---	---
	Backout	12	---	6	14	---	---	---	---	---	---
2	Maximum	176	184	154	144	224	176	265	610	128	280
	Cutting	120	128	108	112	96	112	160	160	96	176
	Rubbing	56	56	46	32	128	64	105	450	32	104
	Backout	0	2	2	0	0	0	0	0	0	0
3	Maximum	96	136	92	116	112	104	132	143	98	190
	Cutting	72	80	76	70	80	80	108	108	76	120
	Rubbing	24	56	16	46	32	24	24	35	22	70
	Backout	3	1	2	2	0	0	0	0	1	0
4	Maximum	52	64	51	64	68	60	88	92	68	100
	Cutting	40	44	44	40	56	48	64	62	48	64
	Rubbing	12	20	7	24	12	12	24	30	20	36
	Backout	1	4	0	0	0	0	0	0	8	0
5	Maximum	35	44	34	34	44	39	48	56	38	52
	Cutting	20	24	22	20	28	32	28	28	24	24
	Rubbing	15	20	12	14	16	7	20	28	18	18
	Backout	2	2	2	0	0	0	0	0	0	0

TABLE 4.19

TAPPING TORQUE DATA FOR 1042 STEEL

(Torque units, lb in.)

Hole No.	Type of Torque	Fluid Number									
		1	2	3	4	5	6	7	8	9	10
1	Maximum	240	240	240	208	176	208	224	224	172	176
	Cutting	160	160	176	160	160	160	192	192	152	160
	Rubbing	80	80	64	48	16	48	32	32	20	16
	Backout	0	0	0	0	0	0	0	0	64	0
2	Maximum	128	128	140	128	128	128	144	160	144	240
	Cutting	112	120	128	120	112	112	128	128	112	144
	Rubbing	16	8	12	8	16	16	16	32	32	96
	Backout	16	2	0	0	0	0	0	0	80	0
3	Maximum	96	96	92	100	88	96	108	112	128	112
	Cutting	80	88	86	84	80	80	100	100	82	100
	Rubbing	16	8	6	16	8	16	8	12	46	12
	Backout	6	2	8	0	0	0	0	0	96	0
4	Maximum	80	76	76	--	72	72	76	84	100	88
	Cutting	52	52	52	52	52	56	56	64	48	60
	Rubbing	28	24	24	--	20	16	20	20	52	28
	Backout	6	3	4	16	0	0	0	0	56	3
5	Maximum	36	44	40	36	40	44	48	52	60	48
	Cutting	24	28	28	32	32	36	38	38	32	32
	Rubbing	12	16	12	4	8	8	10	14	28	16
	Backout	8	0	4	0	0	0	0	0	32	2

TABLE 4.20

TAPPING TORQUE DATA FOR STAINLESS STEEL

(Torque units, lb in.)

Hole No.	Type of Torque	1	2	3	4	5	6	7	8	9	10
1	Maximum Cutting Rubbing Backout	Tests not run because of tap breakage.									
2	Maximum Cutting Rubbing Backout	Tests not run because of tap breakage.									
3	Maximum	240	288	---	240	240	192	400	272	256	---
	Cutting	96	120	100	112	112	112	144	112	104	---
	Rubbing	144	168	---	128	128	80	256	160	152	---
	Backout	32	2	4	0	16	0	---	---	---	---
4	Maximum	92	--	96	108	108	120	120	120	120	---
	Cutting	72	80	80	80	84	100	100	76	68	144
	Rubbing	20	--	16	28	24	20	20	44	52	---
	Backout	6	8	2	2	4	13	35	9	12	48
5	Maximum	52	56	60	60	60	76	64	64	52	120
	Cutting	36	36	40	44	44	68	60	32	32	68
	Rubbing	16	20	20	16	16	8	4	32	20	52
	Backout	5	16	8	10	3	7	7	4	10	14

TABLE 4.21

BACK-OUT TORQUES FOR ALL CONDITIONS ON ALL MATERIALS

(Values, lb in.)

Fluid No.	Work Material													
	Magnesium	Aluminum	Brass	Copper	1018 Steel	1042 Steel	Stainless Steel	Magnesium	Aluminum	Brass	Copper	1018 Steel	1042 Steel	Stainless Steel
	Hole No. 1							Hole No. 4						
1	10	2	3	26	12	0	--	9	2	0	14	1	6	6
2	20	6	4	20	--	0	--	12	2	1	15	4	3	8
3	16	4	4	28	6	0	--	12	1	0	12	0	4	2
4	16	12	4	38	14	0	--	12	2	0	9	0	16	2
5	16	1	4	26	--	0	--	10	2	3	11	0	0	4
6	20	2	5	28	--	0	--	14	0	2	16	0	0	13
7	25	4	5	24	--	0	--	18	0	0	20	0	0	35
8	34	4	3	32	--	0	--	21	4	3	13	0	0	9
9	120	10	16	seizure	--	64	--	42	10	6	24	8	56	12
10	48	4	0	tap broke	--	0	--	26	4	0	26	0	3	48
	Hole No. 2							Hole No. 5						
1	8	4	4	23	0	16	--	8	0	0	8	2	8	5
2	15	3	2	6	2	2	--	4	2	1	32	2	0	16
3	12	4	4	19	2	0	--	6	2	2	9	2	4	8
4	16	6	4	16	0	0	--	4	2	0	7	0	0	10
5	16	4	2	16	0	0	--	4	0	3	6	0	0	3
6	18	0	5	19	0	0	--	8	0	1	14	0	0	7
7	24	2	4	32	0	0	--	10	0	1	14	0	0	7
8	30	3	4	25	0	0	--	8	--	1	12	0	0	4
9	68	12	14	42	0	80	--	32	4	5	16	0	32	10
10	28	4	1	20	0	0	--	14	3	0	20	0	2	14
	Hole No. 3													
1	12	2	3	20	3	6	32							
2	14	2	3	12	1	2	2							
3	13	3	0	15	2	8	4							
4	11	3	2	13	2	0	0							
5	13	2	3	14	0	0	16							
6	16	0	4	18	0	0	0							
7	24	3	2	26	0	0	--							
8	26	4	2	20	0	0	--							
9	60	10	8	35	1	96	--							
10	28	4	0	35	0	0	--							

TABLE 4.22

MAXIMUM FRICTIONAL TORQUE FOR ALL CONDITIONS ON ALL MATERIALS*

(Values, lb in.)

Fluid No.	Work Material													
	Magnesium	Aluminum	Brass	Copper	1018 Steel	1042 Steel	Stainless Steel	Magnesium	Aluminum	Brass	Copper	1018 Steel	1042 Steel	Stainless Steel
	Hole No. 1							Hole No. 4						
1	30	39	37	50	248	110	--	19	9	16	24	12	28	--
2	24	33	41	162	---	110	--	18	9	10	23	20	24	--
3	28	31	39	74	262	110	--	19	9	12	23	7	24	--
4	32	31	45	116	454	78	--	18	8	17	27	24	0	--
5	29	31	41	86	---	46	--	20	8	13	27	23	20	--
6	42	39	37	121	---	78	--	27	10	15	27	15	16	--
7	40	43	51	156	---	94	--	20	10	15	40	43	20	--
8	40	40	48	336	---	94	--	25	7	11	47	47	28	--
9	86	87	77	451	---	42	--	68	25	31	44	23	52	--
10	80	43	51	226	---	46	--	30	9	9	63	55	32	--
	Hole No. 2							Hole No. 5						
1	26	24	36	44	102	36	--	17	13	12	24	15	12	--
2	23	19	21	69	110	36	--	17	11	12	14	23	18	--
3	25	24	26	35	80	48	--	18	14	14	29	13	14	--
4	23	21	30	57	70	36	--	15	12	16	32	14	10	--
5	23	26	28	61	150	36	--	17	18	12	28	23	14	--
6	31	23	28	77	102	36	--	29	12	12	34	18	18	--
7	29	25	28	67	191	52	--	16	12	12	42	27	24	--
8	37	25	27	77	537	68	--	19	--	10	38	35	26	--
9	77	46	60	73	54	52	--	56	21	24	46	17	34	--
10	51	20	21	115	206	148	--	20	11	10	54	31	22	--
	Hole No. 3													
1	21	15	20	28	35	21	--							
2	18	14	14	39	75	21	--							
3	22	16	9	31	31	17	--							
4	19	15	21	47	55	25	--							
5	20	14	13	49	51	13	--							
6	28	20	15	43	43	21	--							
7	22	15	17	47	71	33	--							
8	36	16	16	75	82	37	--							
9	77	34	41	55	37	53	--							
10	41	18	11	77	139	37	--							

*Values derived by subtracting calculated minimum cutting torque from maximum torques from charts.

TABLE 4.23

MAXIMUM TAPPING AND BACK-OUT TORQUES

WITH "X-PRESS" TAPS ON ALUMINUM AND BRASS

Material, lb in.		Fluid Number*								
		1	2	3	4	5	6	7	8	9
Aluminum	Maximum Torque	144	176	179	195	192	165	176	---	368
	Maximum Back-out Torque	128	152	157	163	160	138	144	---	248
Brass	Maximum Torque	144	104	136	152	160	176	116	128	184
	Maximum Back-out Torque	68	60	104	112	136	160	84	92	180

*Fluid No. 10 was not tested; nor was Fluid No. 8 on aluminum.

TABLE 4.24

BROACH SPECIFICATIONS—BROACH NO. 1

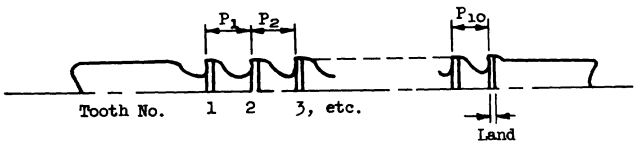

Roughing Teeth, Nos. 2-4
Finishing Teeth, Nos. 5-8
Dwell Teeth, Nos. 9-11

Tooth	Tooth Diameter, inch	Rise/Tooth, dia. change inch	Tooth Pitch, P, inch
1	.7305		
		.0019	.3047
2	.7324		
		.0025	.3703
3	.7349		
		.0020	.3489
4	.7369		
		.0010	.3150
5	.7379		
		.0009	.3672
6	.7388		
		.0010	.3443
7	.7398		
		.0010	.3300
8	.7408		
		.0001	.3647
9	.7409		
		.0001	.3501
10	.7410		
		.0001	.3056
11	.7411		

TABLE 4.25

BROACH SPECIFICATIONS—BROACH NO. 2

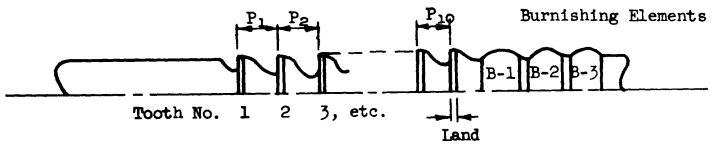

Roughing Teeth, Nos, 2-4
Finishing Teeth, Nos. 5-8
Dwell Teeth, Nos. 9-11

Tooth	Tooth Diameter, inch	Rise/Tooth, dia. change, inch	Tooth Pitch, P, inch
1	.7402		
		.0019	.3259
2	.7421		
		.0017	.3547
3	.7438		
		.0024	.3434
4	.7462		
		.0010	.3316
5	.7472		
		.0010	.3645
6	.7482		
		.0008	.3431
7	.7490		
		.0011	.3204
8	.7501		
		000	.3742
9	.7501		
		000	.3442
10	.7501		
		000	.3220
11	.7501		
			.5223
B-1	.7504	000	.3463
B-2	.7504	000	.3414
B-3	.7504		

TABLE 4.26

BROACHING FORCES—ROUGHING AND FINISHING

Fluid No.	Roughing Forces, lb						Finishing Forces, lb					
	Work Material											
	Aluminum	Brass	Magnesium	Copper	1042 Steel	1018 Steel	Aluminum	Brass	Magnesium	Copper	1042 Steel	1018 Steel
1	2130	2490	1330	3680	5850	8000	1290	1440	1060	2200	3160	3180
2	2100	2600	1320	5420	6240	8560	1410	1510	1050	3410	3150	3140
3	2090	2640	1330	3300	5720	7240	1440	1490	1050	2570	3160	3180
4	2260	2580	1300	5110	5990	6910	1440	1590	1060	3580	2950	3280
5	2280	2480	1380	3860	5410	6250	1540	1530	1060	2940	3050	3060
6	2320	2690	1400	3410	5380	6620	1460	1500	1060	2220	3020	3320
7	2310	2590	1360	4920	6350	8750	1400	1570	1070	3310	3160	3430
8	2290	2640	1370	5600	6630	8860	1510	1570	1060	3480	3260	3830
9	2800	2440	1430	4090	5300	7560	1510	1570	1060	3480	3260	3830
10	2260	2650	1330	5740	6560	9070	1480	1580	1050	3760	3010	4440

TABLE 4.27

BROACHING FORCES—DWELL AND BURNISHING

Fluid No.	Maximum Dwell Forces, lb						Maximum Burnishing Forces, lb					
	Work Material											
	Aluminum	Brass	Magnesium	Copper	1042 Steel	1018 Steel	Aluminum	Brass	Magnesium	Copper	1042 Steel	1018 Steel
1	330	1100	990	880	250	270	620	1280	970	1190	490	480
2	360	1330	1140	1010	330	170	610	1260	1200	1380	470	450
3	490	1300	1070	840	270	200	780	1410	1030	1190	470	430
4	440	1460	980	1130	170	370	790	1280	1090	1230	490	440
5	460	1630	940	980	170	420	750	1490	1020	1060	420	300
6	390	1070	870	810	270	370	670	1250	710	1200	470	520
7	600	1280	1070	1200	400	200	800	1080	1150	1360	500	350
8	540	1430	1110	1430	200	350	810	1300	1190	1880	370	490
9	2370	1520	1730	1120	1380	1830	3240	1200	1900	1150	2320	2720
10	760	1350	1050	880	300	420	860	1100	1070	980	400	220

TABLE 4.28

SUMMARY OF ALL BROACHING FORCES FOR EACH MATERIAL

Material		Force, lb									
		Fluid Number									
		1	2	3	4	5	6	7	8	9	10
Aluminum	Roughing	2130	2100	2090	2260	2280	2320	2310	2290	2800	2260
	Finishing	1290	1410	1440	1440	1540	1460	1400	1510	2270	1480
	Dwell	330	360	490	440	460	390	600	540	2370	760
	Burnishing	620	610	780	790	750	670	800	810	3240	860
	Hole Dia, in.	.74990	.74982	.74980	.74970	.74962	.74967	.74975	.74972	.74940	.74967
Brass	Roughing	2490	2600	2640	2580	2480	2690	2590	2640	2440	2650
	Finishing	1440	1510	1490	1590	1530	1500	1570	1570	1530	1580
	Dwell	1100	1330	1300	1460	1630	1070	1280	1430	1520	1350
	Burnishing	1280	1260	1410	1280	1490	1250	1080	1300	1200	1100
	Hole Dia, in.	.74940	.74928	.74925	.74940	.74928	.74942	.74942	.74938	.74930	.74938
Magnesium	Roughing	1330	1320	1330	1300	1380	1400	1360	1370	1430	1330
	Finishing	1060	1050	1050	1060	1060	1060	1070	1060	1210	1050
	Dwell	990	1140	1070	980	940	870	1070	1110	1730	1050
	Burnishing	970	1200	1030	1090	1020	710	1150	1190	1900	1070
	Hole Dia, in.	.74920	.74928	.74930	.74938	.74925	.74930	.74935	.74932	.74930	.74935
Copper	Roughing	3680	5420	3300	5110	3860	3410	4020	5600	4090	5740
	Finishing	2200	3410	2570	3580	2940	2220	3310	3480	2760	3760
	Dwell	880	1010	840	1130	980	810	1200	1430	1120	880
	Burnishing	1190	1380	1190	1230	1060	1200	1360	1880	1150	980
	Hole Dia, in.	.74965	.74980	.74965	.74968	.74968	.74955	.74990	.74972	.74962	.74990
1042 Steel	Roughing	5850	6240	5720	5990	5410	5380	6350	6630	5300	6560
	Finishing	3160	3150	3160	2950	3050	3020	3160	3260	2780	3010
	Dwell	250	330	270	170	170	270	400	200	1380	300
	Burnishing	490	470	470	490	420	470	500	370	2320	400
	Hole Dia, in.	.75034	.75028	.75031	.75022	.75031	.75028	.75032	.75025	.74996	.75028
1018 Steel	Roughing	8000	8560	7240	6910	6250	6620	8750	8860	7560	9070
	Finishing	3180	3140	3180	3280	3060	3320	3430	3830	2820	4440
	Dwell	270	170	200	370	420	370	200	350	1830	420
	Burnishing	480	450	430	440	300	520	350	490	2720	220
	Hole Dia, in.	.75022	.75031	.75028	.75020	.75038	.75026	.75036	.75034	.74960	.75055

TABLE 4.29

AVERAGE BROACHED HOLE DIAMETERS*

Fluid No.	Hole Diameters,* in.—Broach No. 1						Hole Diameters,* in.—Broach No. 2					
	Increments, 10^{-5} in. (avg dia less base dia of .7390 inch)						Increments, 10^{-5} in. (avg dia less base dia of .74900 inch)					
	Work Material											
	Aluminum	Brass	Magnesium	Copper	1042 Steel	1018 Steel	Aluminum	Brass	Magnesium	Copper	1042 Steel	1018 Steel
1	96	85	38	86	133	140	89	36	10	71	134	122
2	95	54	40	91	134	137	87	32	28	90	128	131
3	89	46	32	84	148	140	74	28	35	62	131	128
4	88	60	31	89	141	151	72	38	36	70	122	120
5	106	55	54	111	149	146	65	31	28	65	131	138
6	98	51	44	104	140	148	61	35	31	56	128	126
7	90	-50**	20	100	141	143	66	42	34	88	132	136
8	79	51	32	85	141	157	69	36	32	75	125	138
9	58	38	22	84	84	72	36	35	28	65	96	60
10	91	62	30	99	142	175	66	42	36	82	128	155

*Diameters expressed in terms of increments to be added to base value.
**Note negative value to make hole diameter of .7385, approximately .0025 inch less than dwell teeth diameter.

TABLE 4.30

AVERAGE SURFACE ROUGHNESS OF BROACHED HOLES

Fluid No.	Surface Roughness, in., rms—Broach No. 1						Surface Roughness, in., rms—Broach No. 2					
	Work Material											
	Aluminum	Brass	Magnesium	Copper	1042 Steel	1018 Steel	Aluminum	Brass	Magnesium	Copper***	1042 Steel	1018 Steel
1	6.3	4.0	2.2	3.2	36	34	3.2	3.5	2.2	4.8	35	40
2	7.0	3.7	2.5	4.0(20)*	35	24	3.8	2.5	2.0	1.8	25	28
3	6.0	3.7	2.5	2.0	31	30	2.8	2.8	3.5	5.2	30	25
4	4.7	4.7	4.4	3.0(45)*	32	36	4.0	4.2	2.3	2.0	20	25
5	5.0	7.7	1.8	2.5	30	31	4.8	3.5	3.0	13	28	20
6	2.8	3.2	1.8	4.8	41	38	3.0	5.2	2.3	2.9	20	20
7	4.5	4.2	2.2	20	35	45	5.5	13	4.5	25	25	45
8	5.2	4.2	2.1	5.5(30)*	41	48	2.4	1.9	2.5	1.9	25	70
9	11.0	2.2	2.5	6.8	5.2**	8.5**	15	14	8	7.0	4.0**	9.0**
10	3.5	4.0	1.8	5.0(17)*	59	82	3.0	4.2	3.2	25(100)	42	75

*Smear or seizure tendency. Number in parentheses indicates roughness in torn area.
**Only one that does not show pronounced smearing.
***Almost all fluids show at least a trace of smear and tears. Most pronounced with Fluids Nos. 2, 4, 8, and 10.

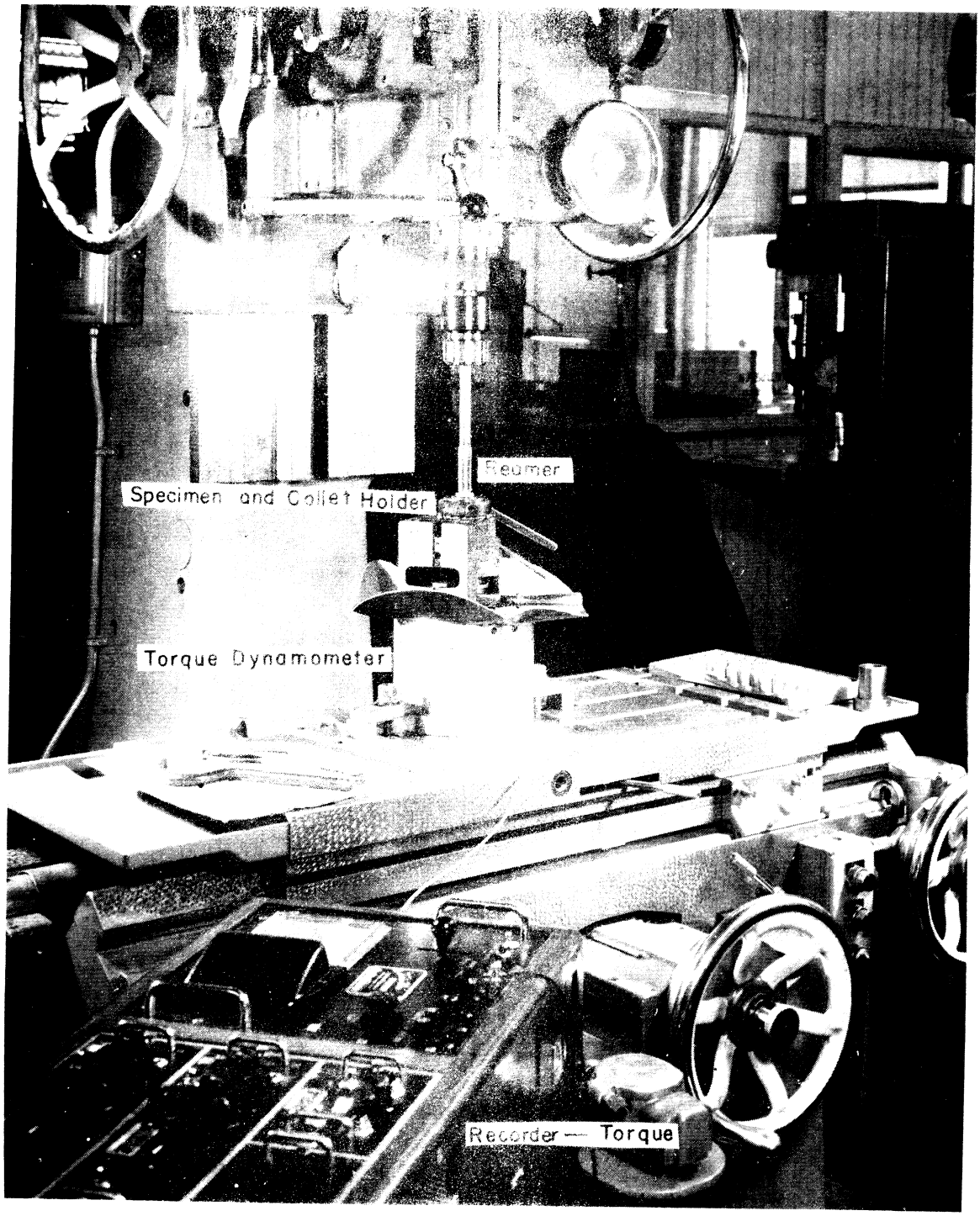

Fig. 4.1. [illegible] Continuous torque records were made [illegible] different feeds for all fluids on [illegible] pump-type oil cans.

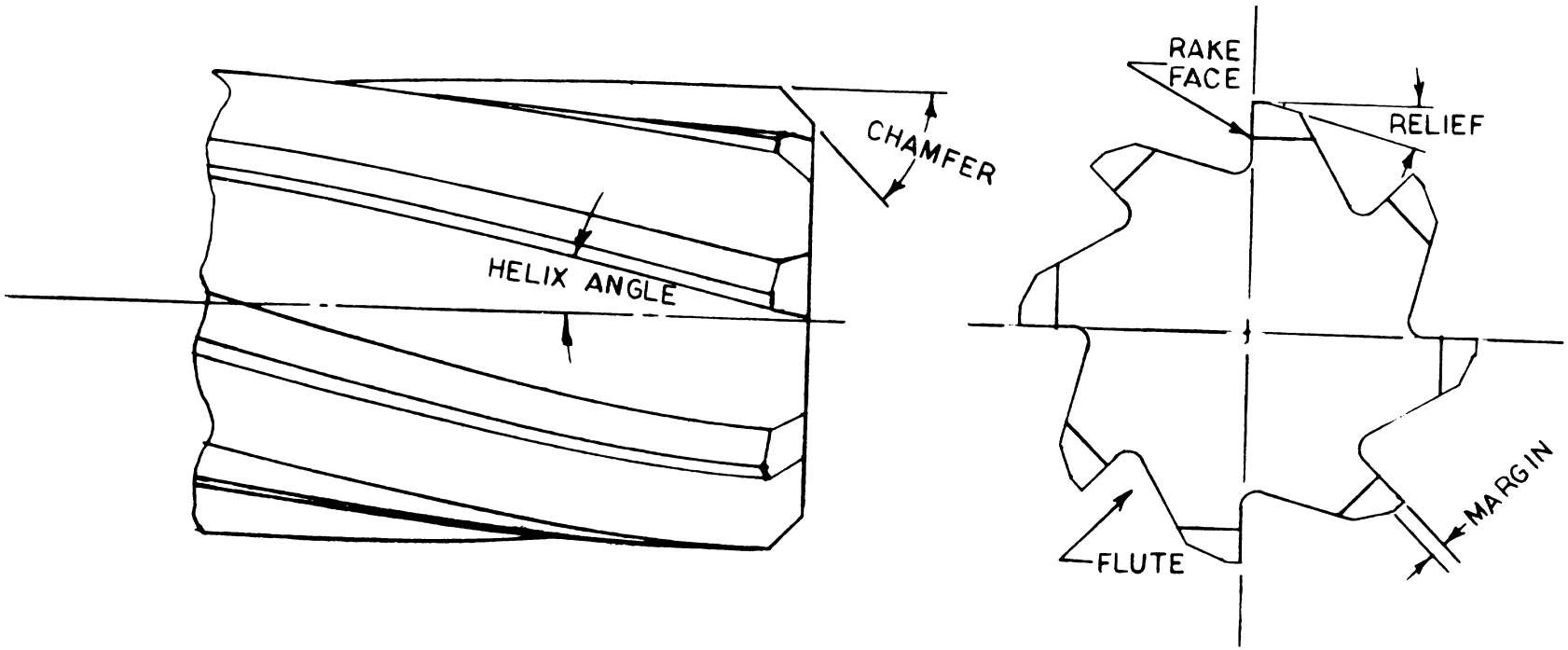

Fig. 4.2. Reamer nomenclature. All cutting done by chamfer. Helix angle corresponds to rake angle of single point tool. Peripheral relief angle reduces area of contact between reamer body and hole surface.

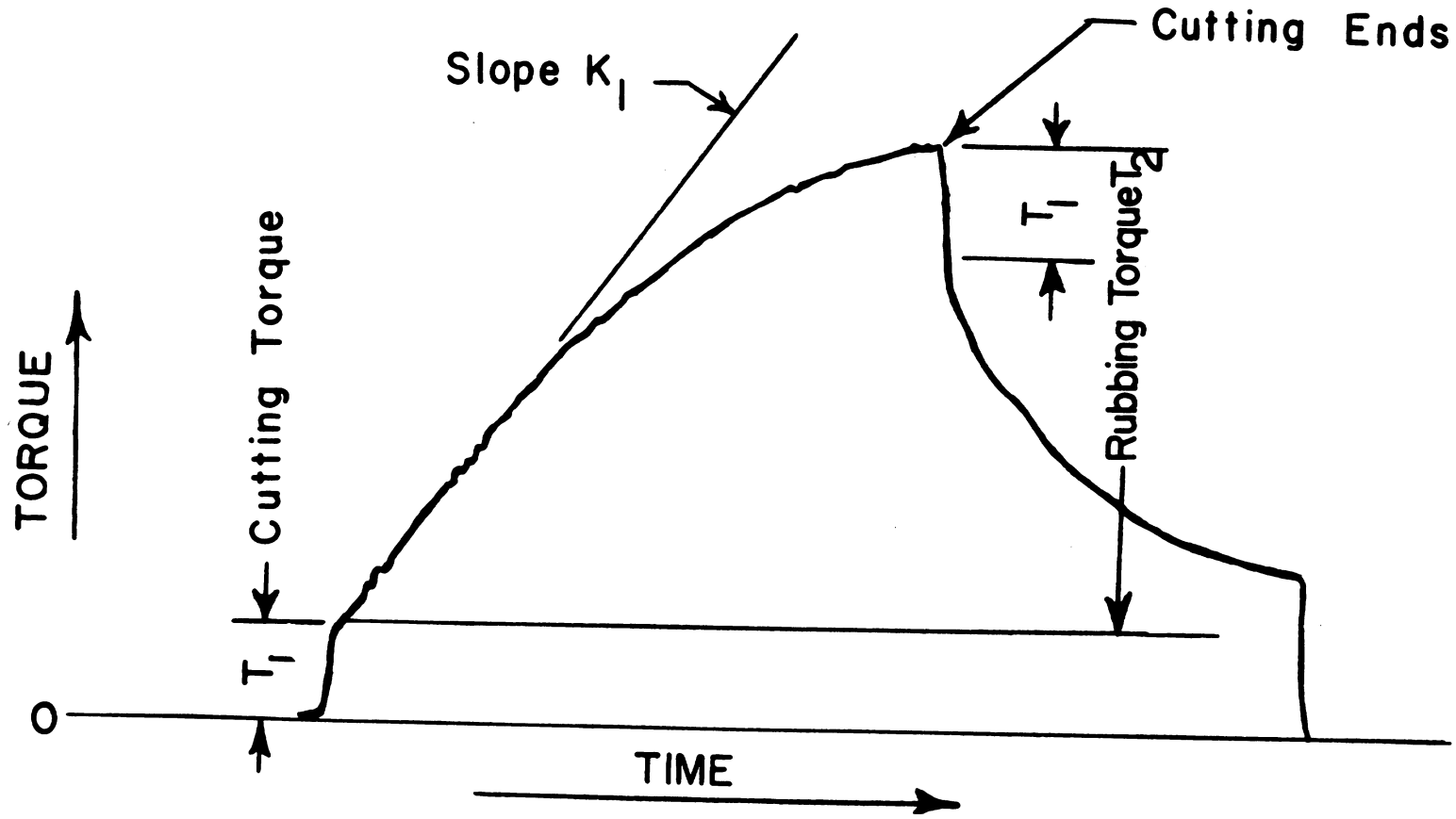

Fig. 4.3. Typical torque-time chart for reaming when rubbing occurs. Rate of torque increase deviates from linear trend due to plastic flow or burnishing of work material. With no rubbing, torque remains constant at T_1 level.

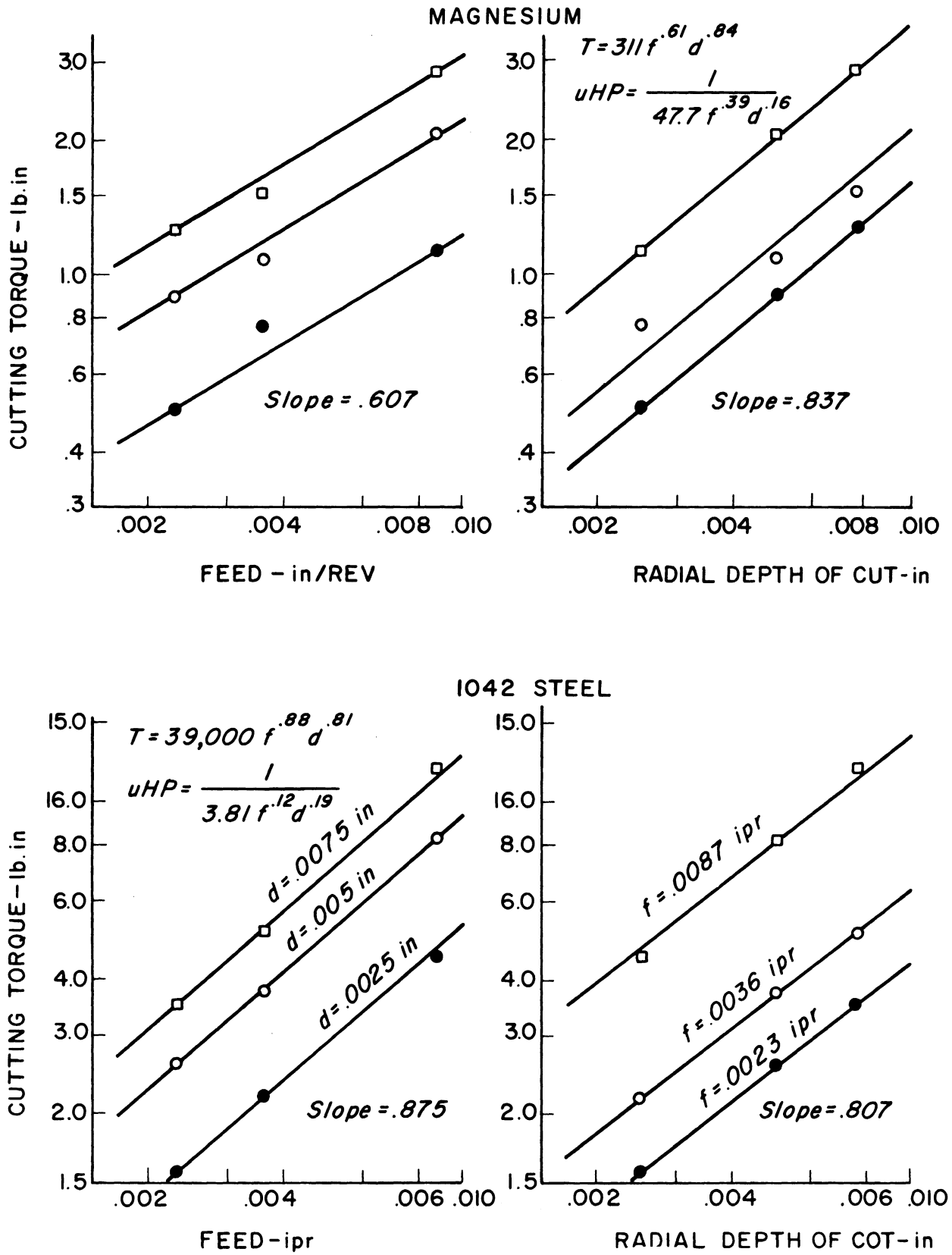

Fig. 4.4. Sample plots of cutting torque versus feed and depth for magnesium and 1042 steel from data in Table 4.2.

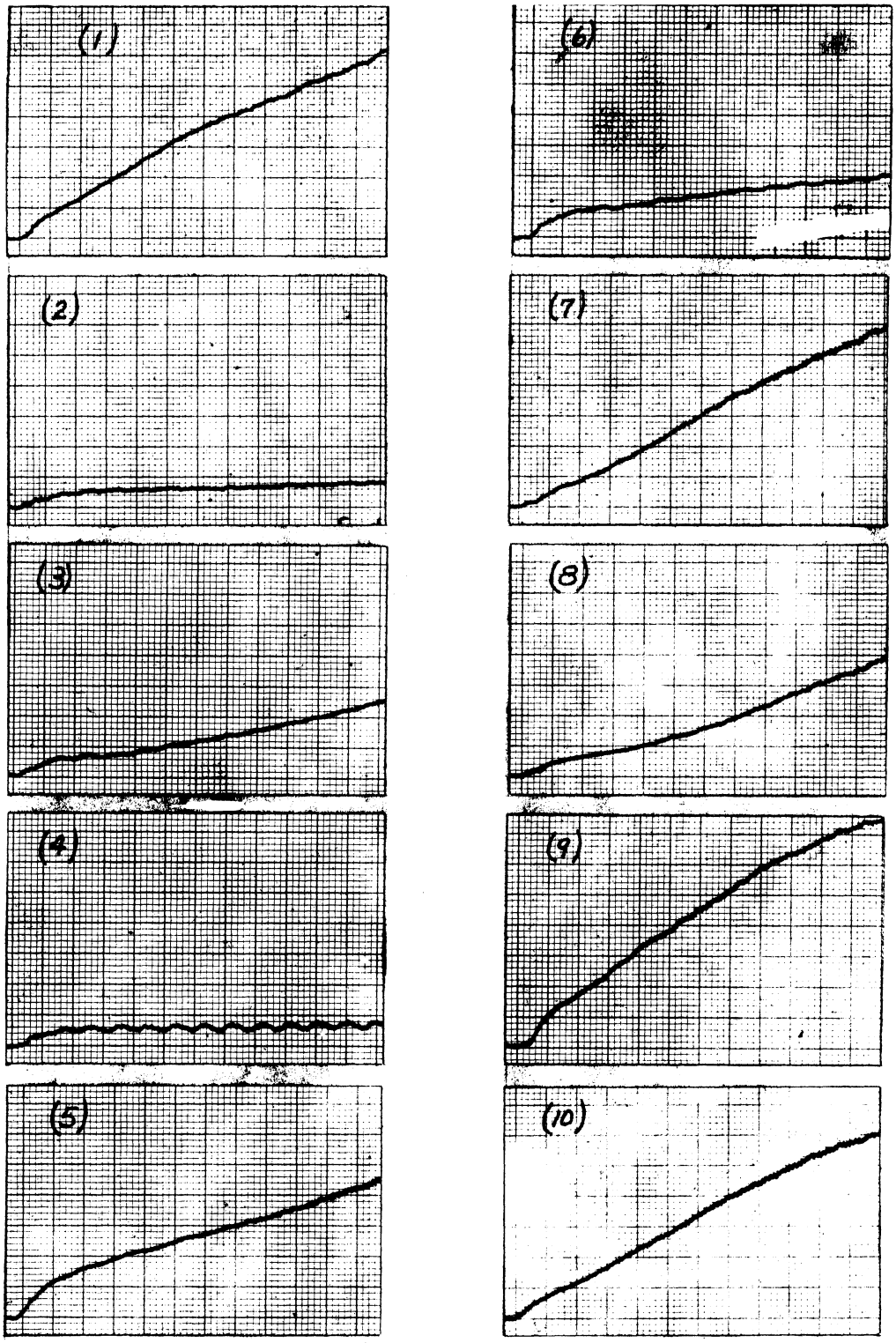

Fig. 4.5. Torque records showing variations among reamers when reaming at constant conditions with Fluid No. 5. Material is magnesium; f = .0087 ipr, d = .005 in (radial), V = 12.8 fpm. Numbers in parentheses identify reamers. Records traced from left to right. Vertical scale: 1.25 lb in./mm. Chart speed, 5 mm/sec. Horizontal length of trace represents 1/8 in. of reamer travel at full diameter. Similar behavior found on brass. Results summarized in Table 4.4.

ALUMINUM

(a) Reamer No. 1 f= .0023 ipr d= .0025 in

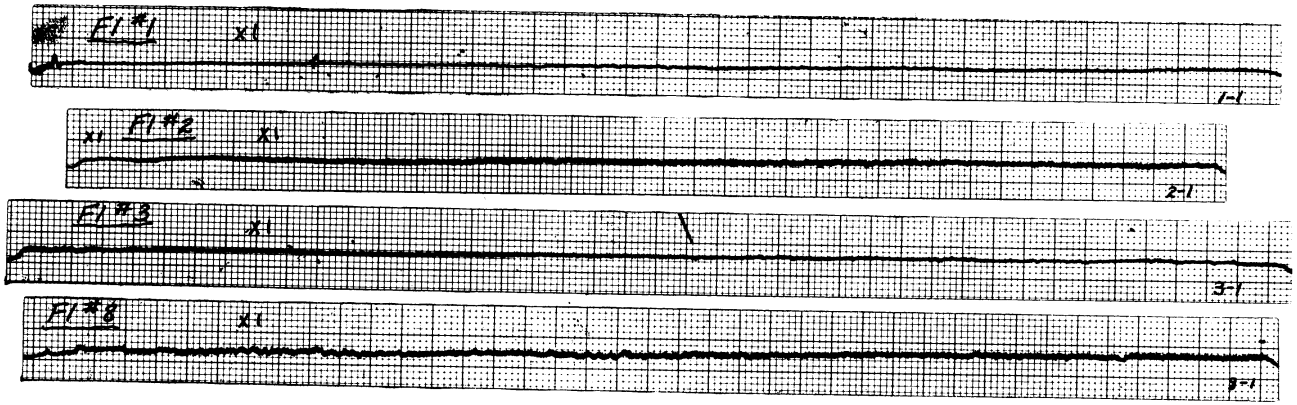

(b) Dry - f= .0036 ipr d= .005 in

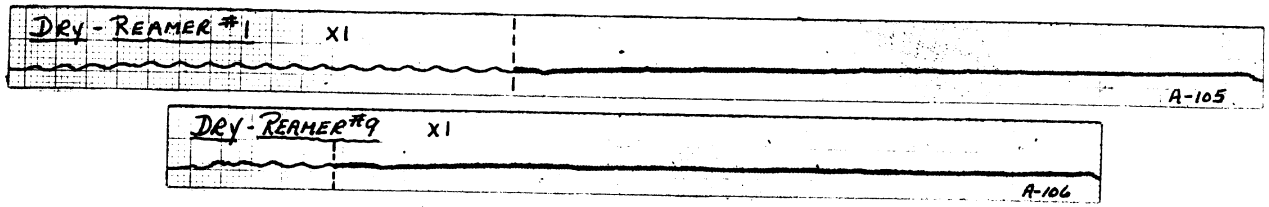

f= .0087 d= .005 in

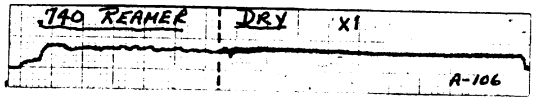

(c) Effect of Various Reamers and Fluids

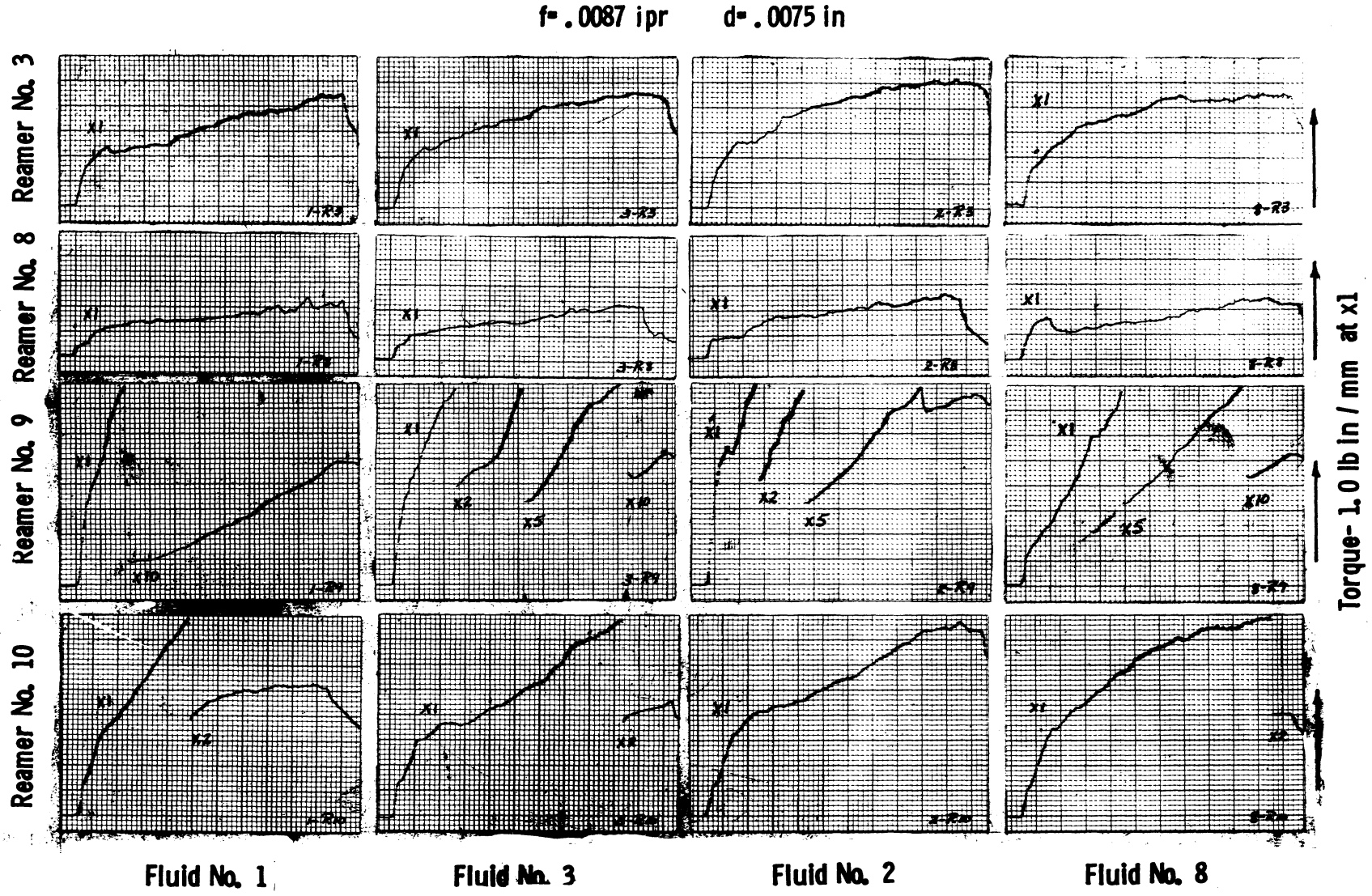

Fig. 4.6. Torque traces of various reamer-fluid combinations on aluminum. Vertical scale in (a) and (b): 1.25 lb in. torque/mm at X1. Where vertical dashed line appears, it denotes point of change of chart speed from 5 mm to 0.5 mm/sec. All other traces start at 0.5 mm/sec. Charts traced from left to right.

ALUMINUM - Effect of Fluid

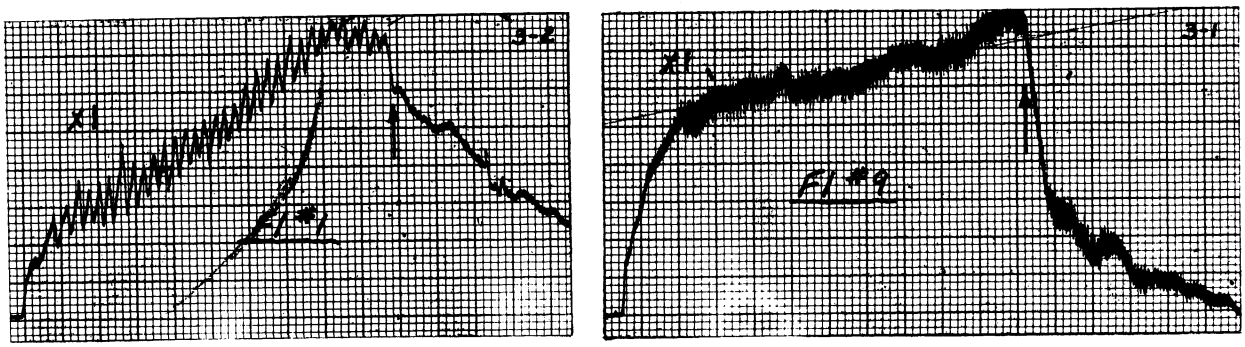

Fig. 4.7. Torque traces on aluminum with 0.745-in.-diameter straight-fluted reamer showing differences in fluid behavior. f = .0087 ipr, d = .005 in., V = 12.8 fpm. Vertical scale: 1.25 lb in. torque/mm. Chart speed: 5 mm/sec. 53 mm = 1 in. of reamer travel. Curves traced from left to right. Arrows denote end of cutting.

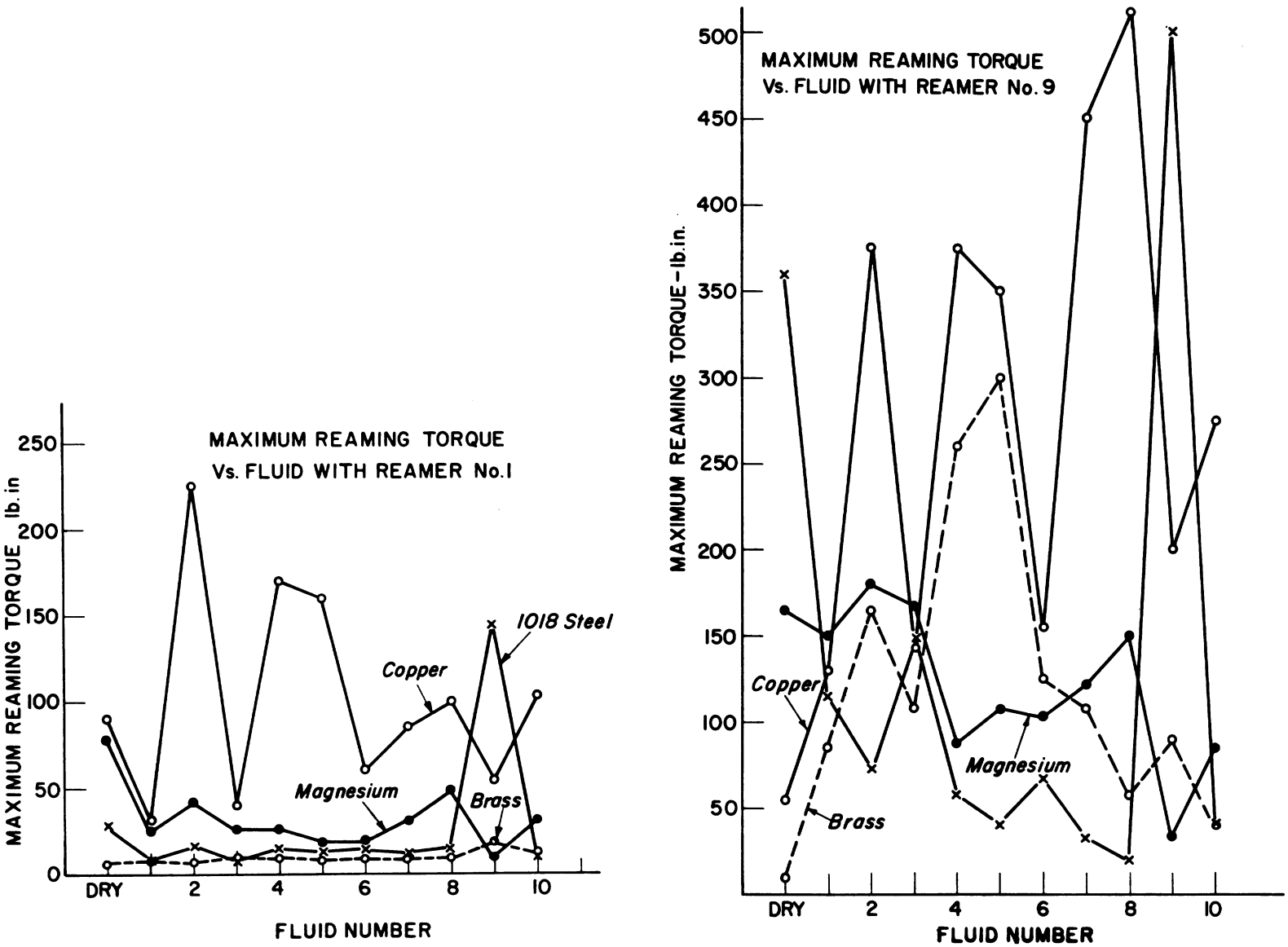

Fig. 4.8. Plots of maximum torque values for each fluid and each material for Reamers Nos. 1 and 9. From data in Table 4.5.

MAGNESIUM - Reamer No. 1

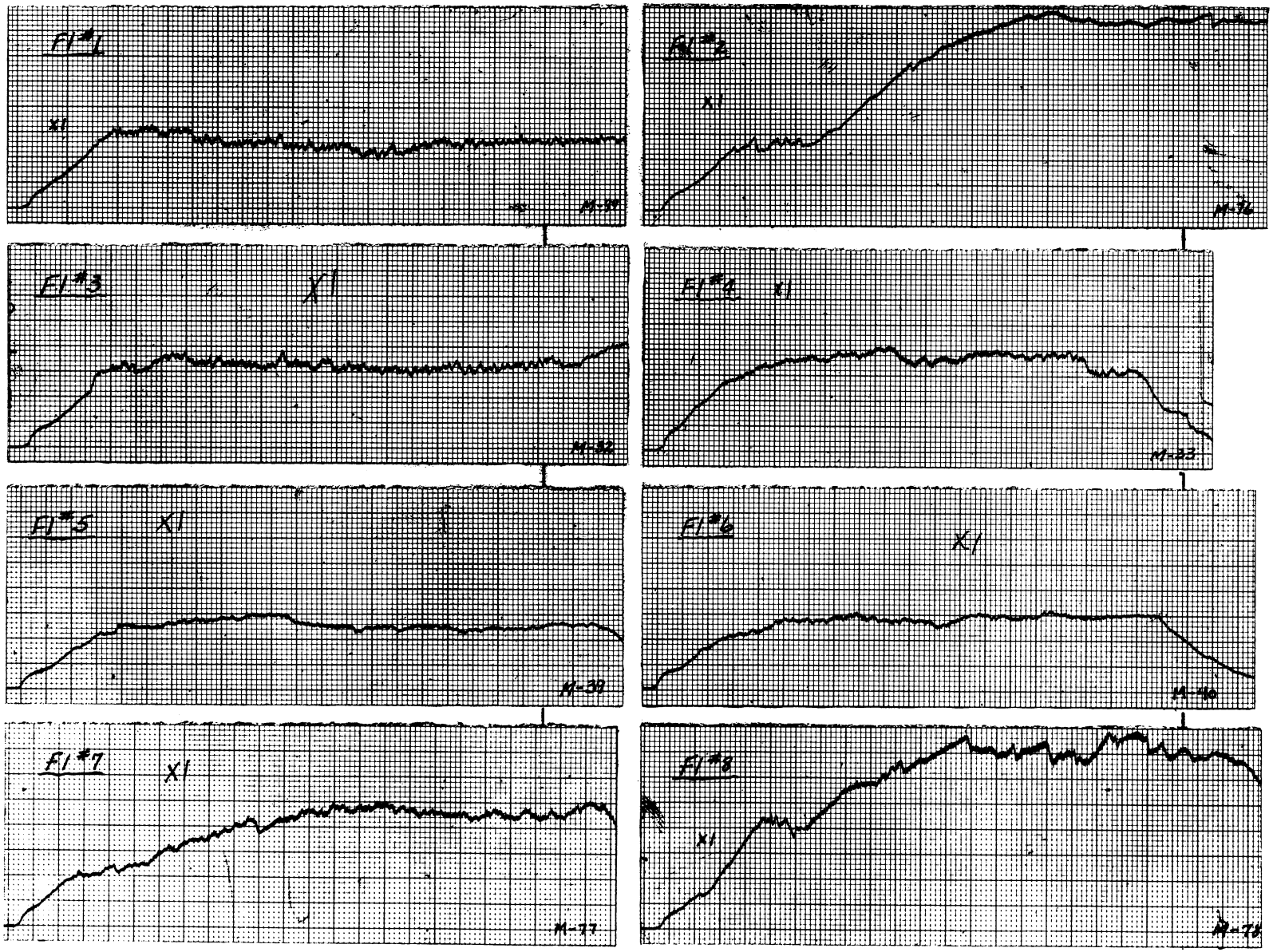

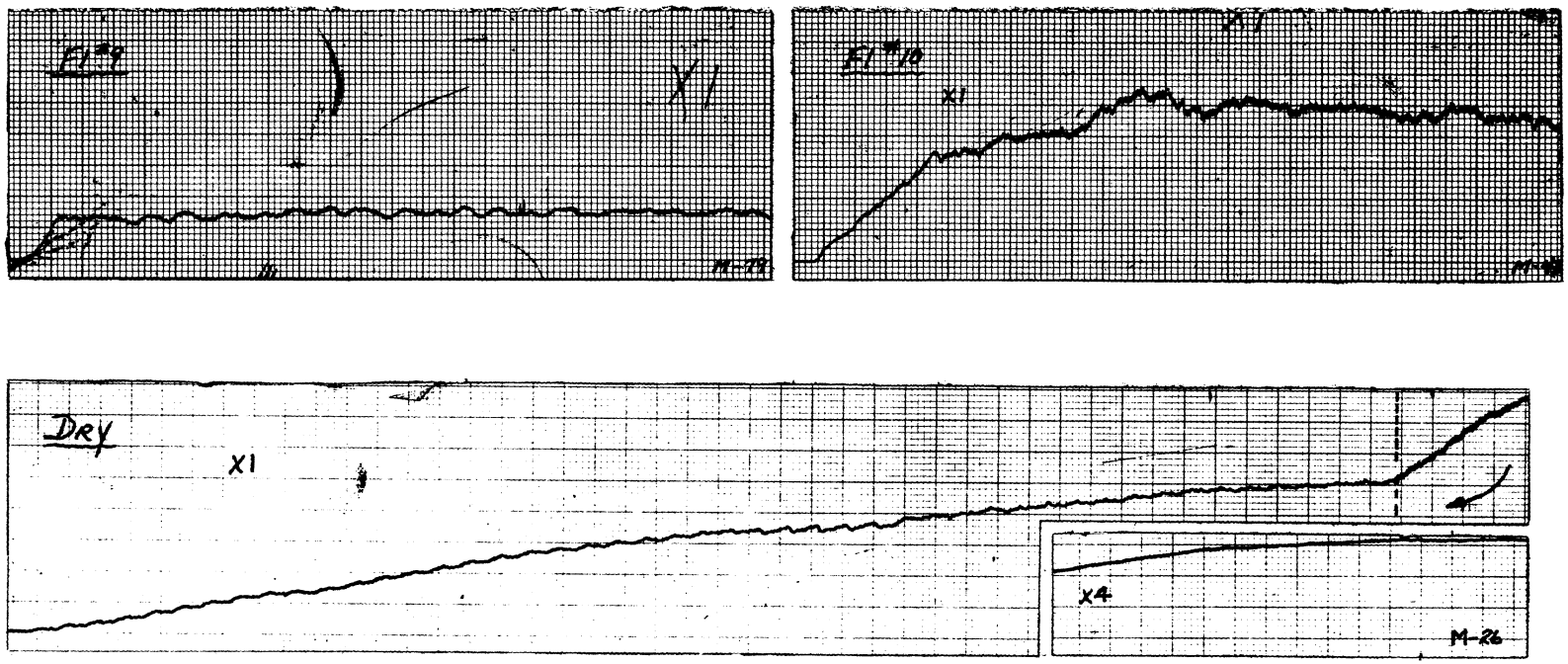

Fig. 4.9. Torque traces on magnesium with Reamer No. 1 and all fluids. f = .0036 ipr, d = .005 inch, V = 12.8 fpm. Records traced from left to right. Vertical scale = 1.25 lb in./mm at X1. Where vertical dashed line appears on trace, it denotes change of chart speed from initial value of 5 mm/sec to 0.5 mm/sec. All other chart speeds at 0.5 mm/sec. Conditions apply to Figs. 4.10 through 4.16.

MAGNESIUM - Reamer No. 9

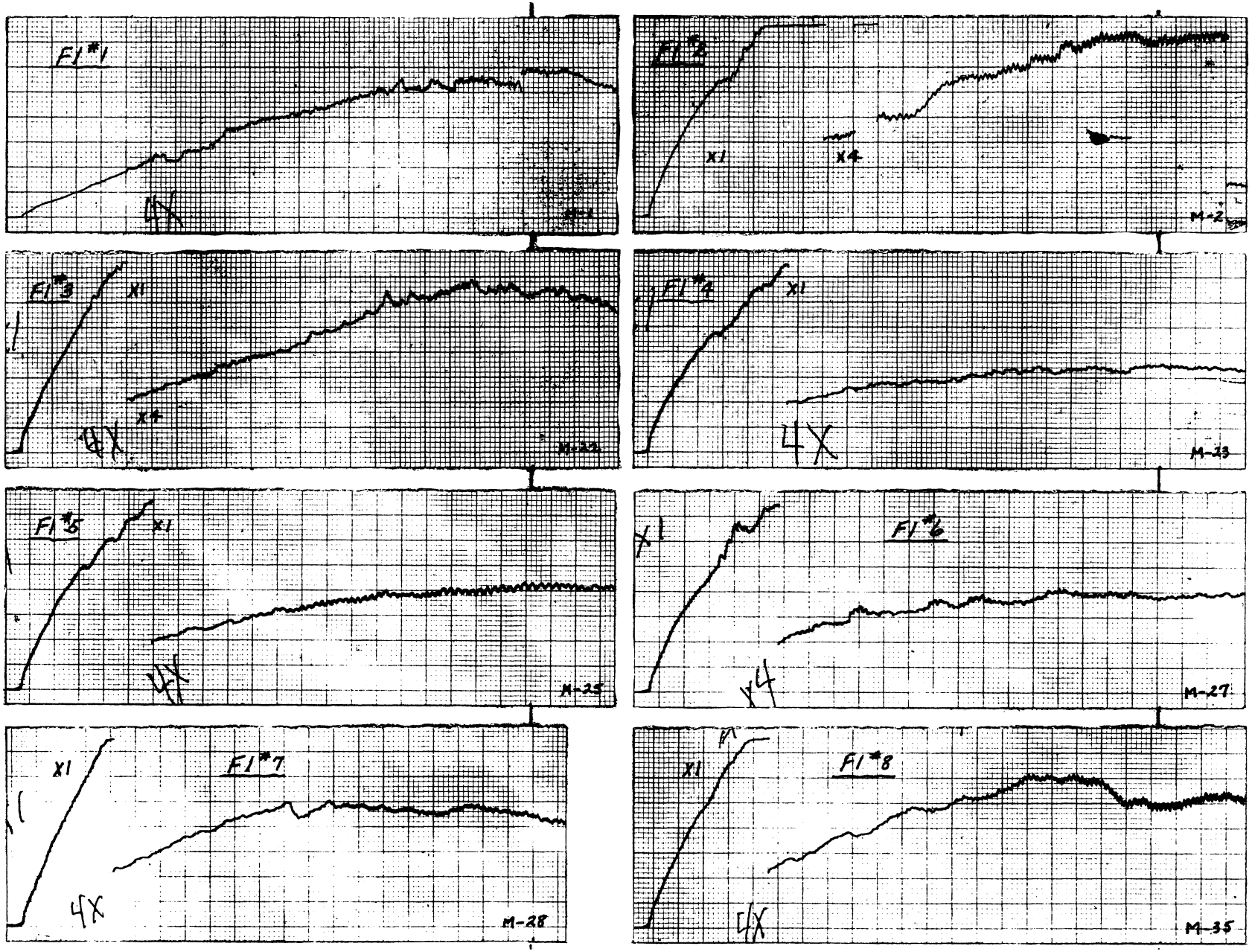

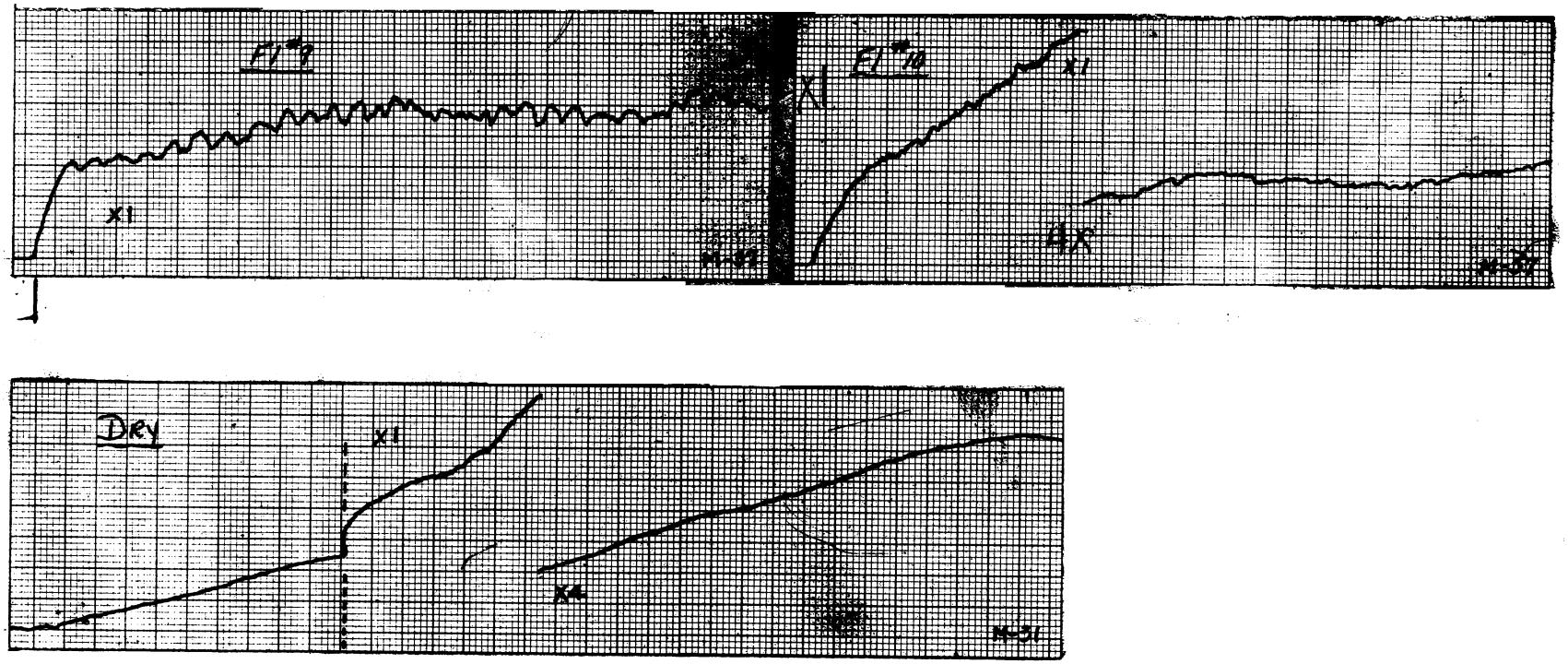

Fig. 4.10. Torque traces on magnesium with Reamer No. 9 and all fluids. Condition and chart designations same as for Fig. 4.9.

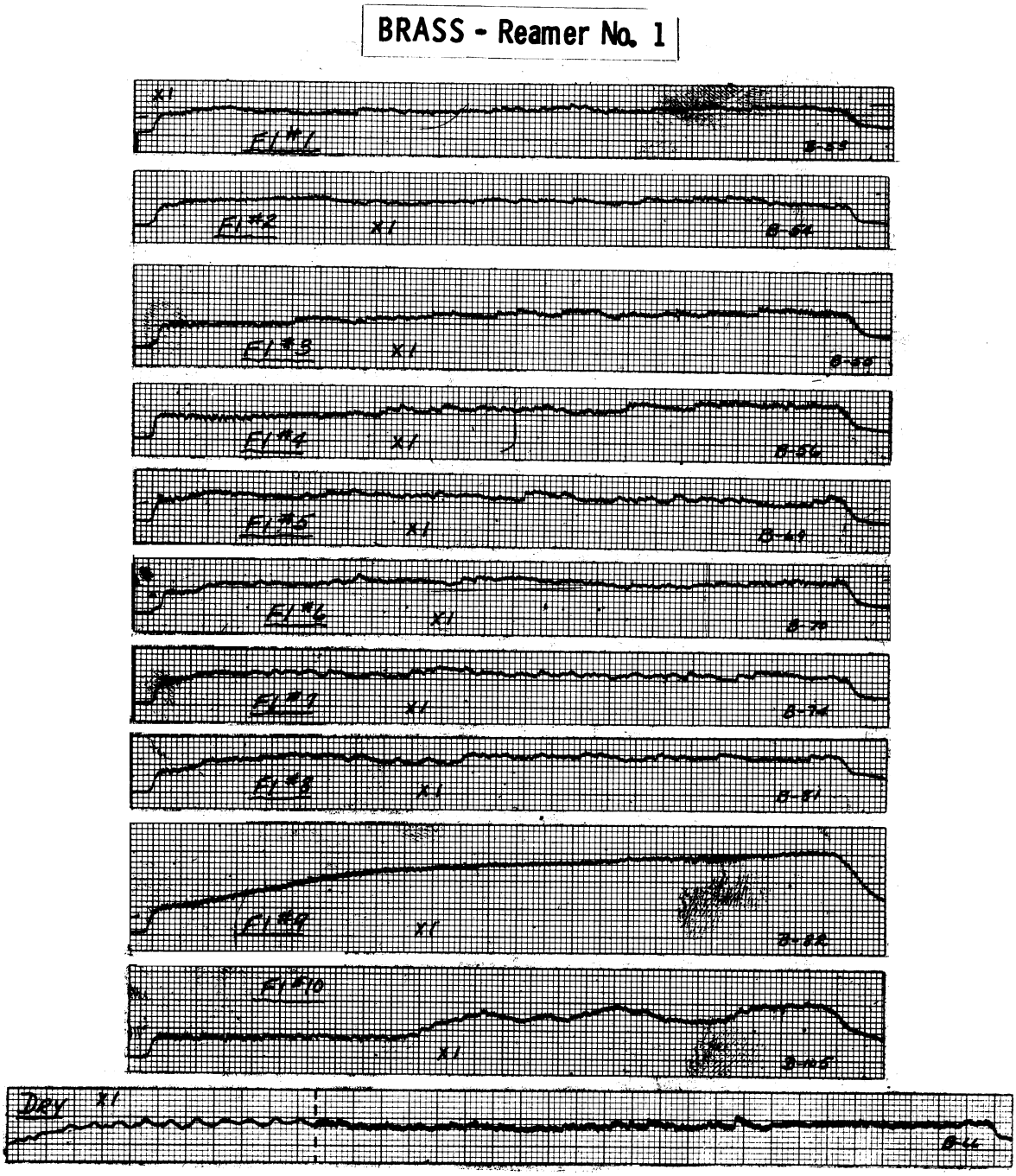

Fig. 4.11. Torque traces on brass with Reamer No. 1 and all fluids. Conditions and chart designations same as for Fig. 4.9.

BRASS - Reamer No. 9

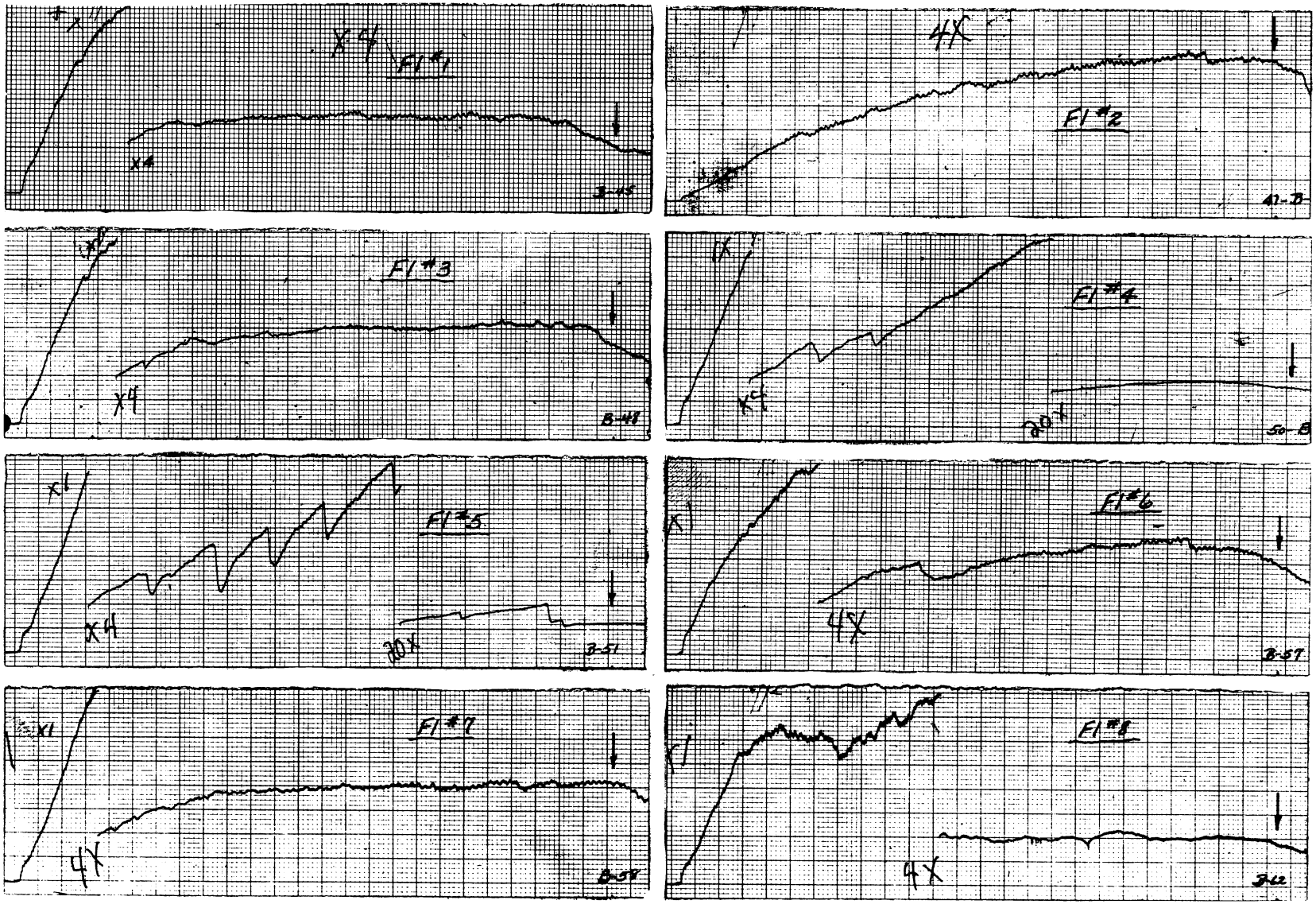

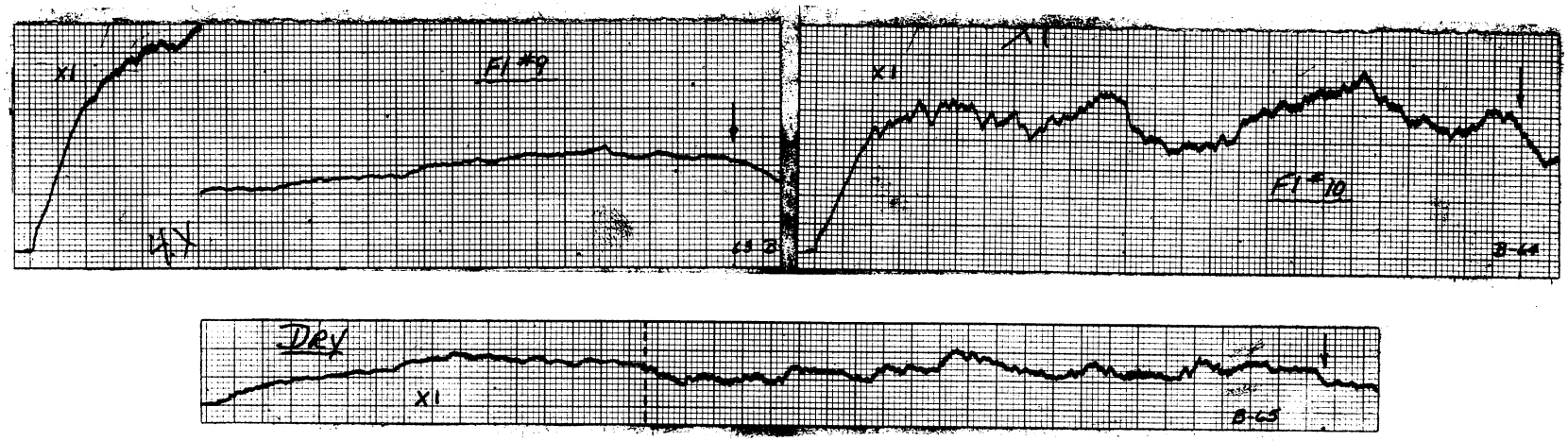

Fig. 4.12. Torque traces on brass with Reamer No. 9 and all fluids. Conditions and chart designations same as for Fig. 4.9.

COPPER - Reamer No. 1

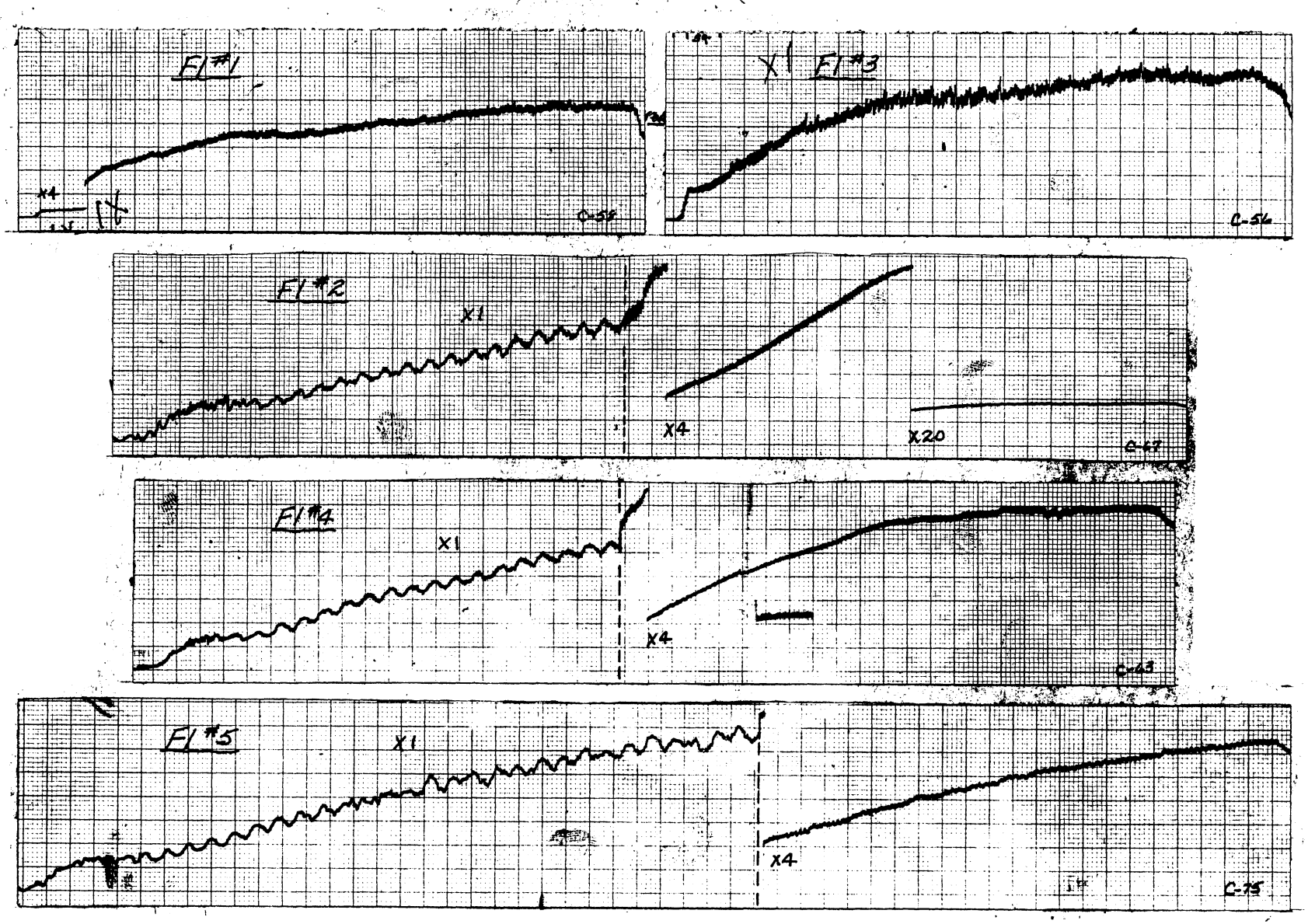

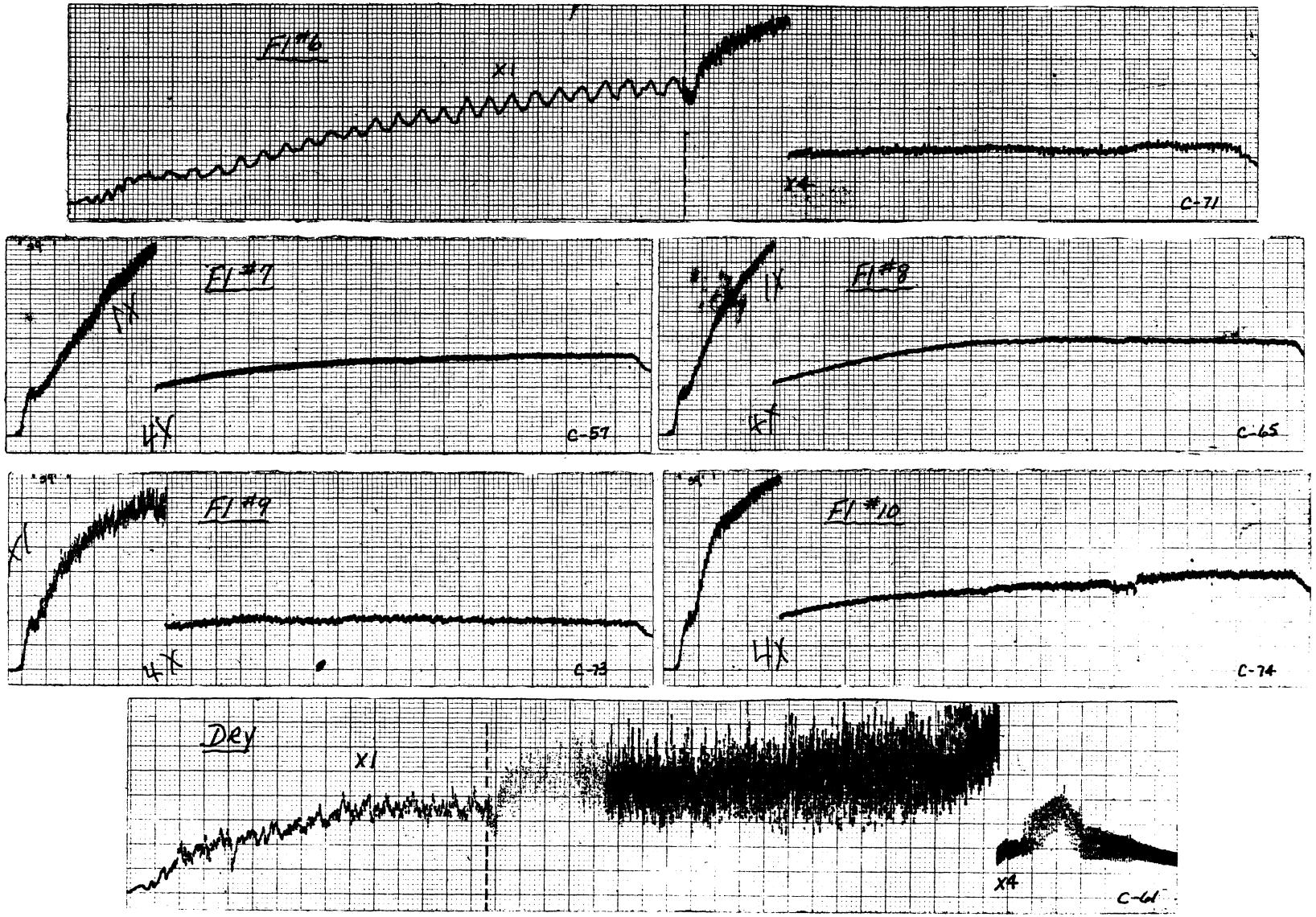

Fig. 4.13. Torque traces on copper with Reamer No. 1 and all fluids. Conditions and chart designations same as for Fig. 4.9.

COPPER - Reamer No. 9

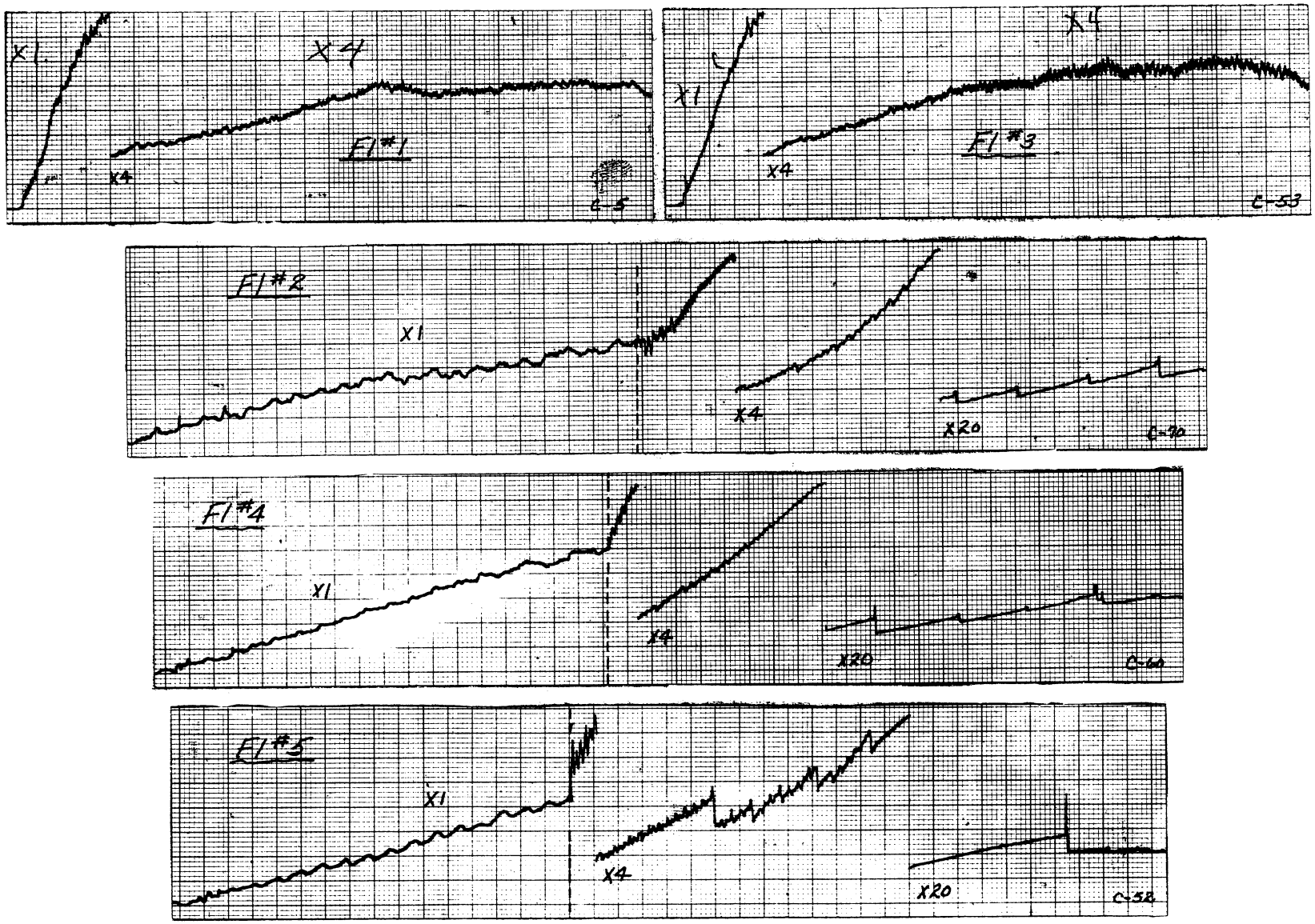

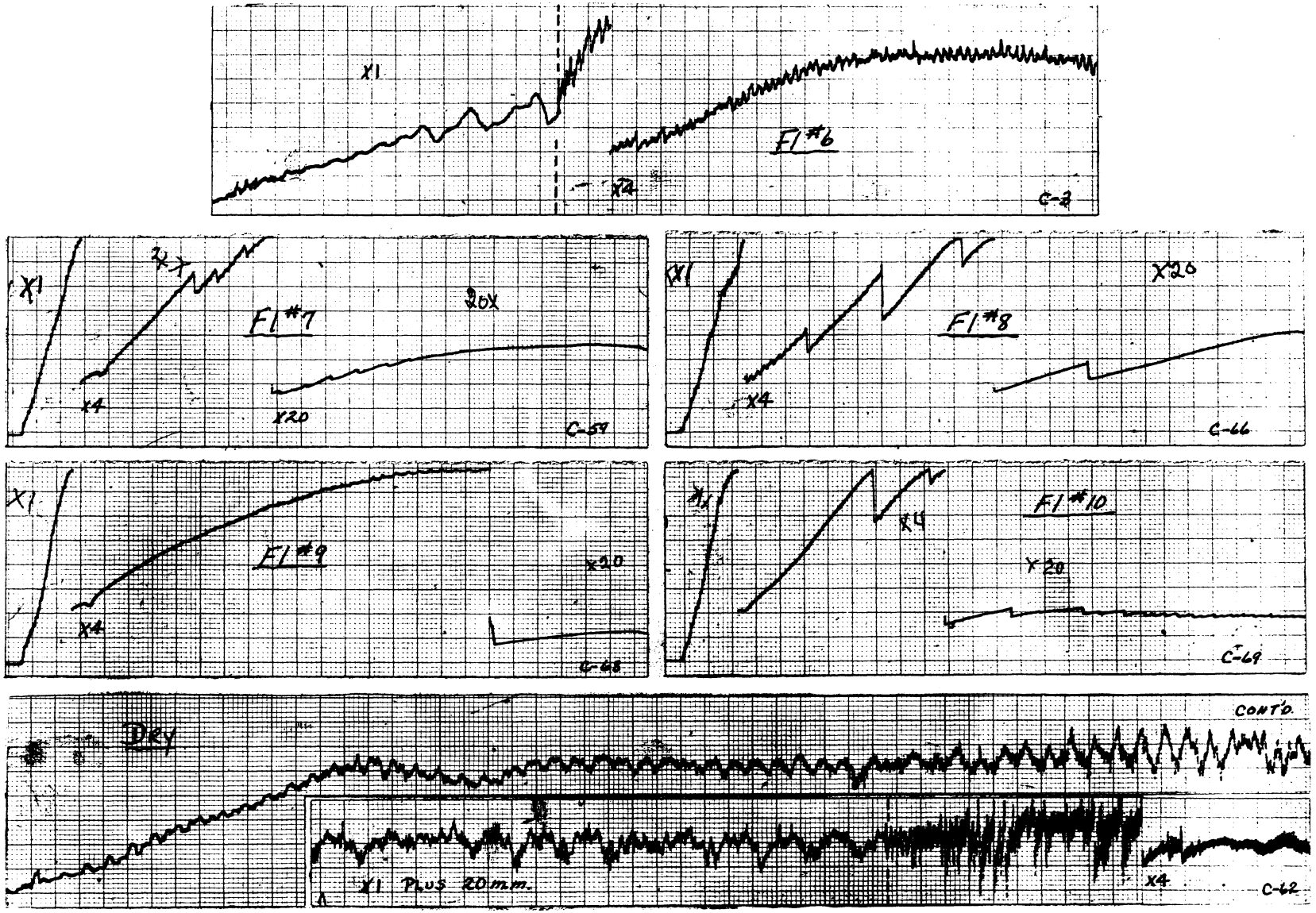

Fig. 4.14. Torque traces on copper with Reamer No. 9 and all fluids. Conditions and chart designations same as for Fig. 4.9.

1018 STEEL - Reamer No. 1

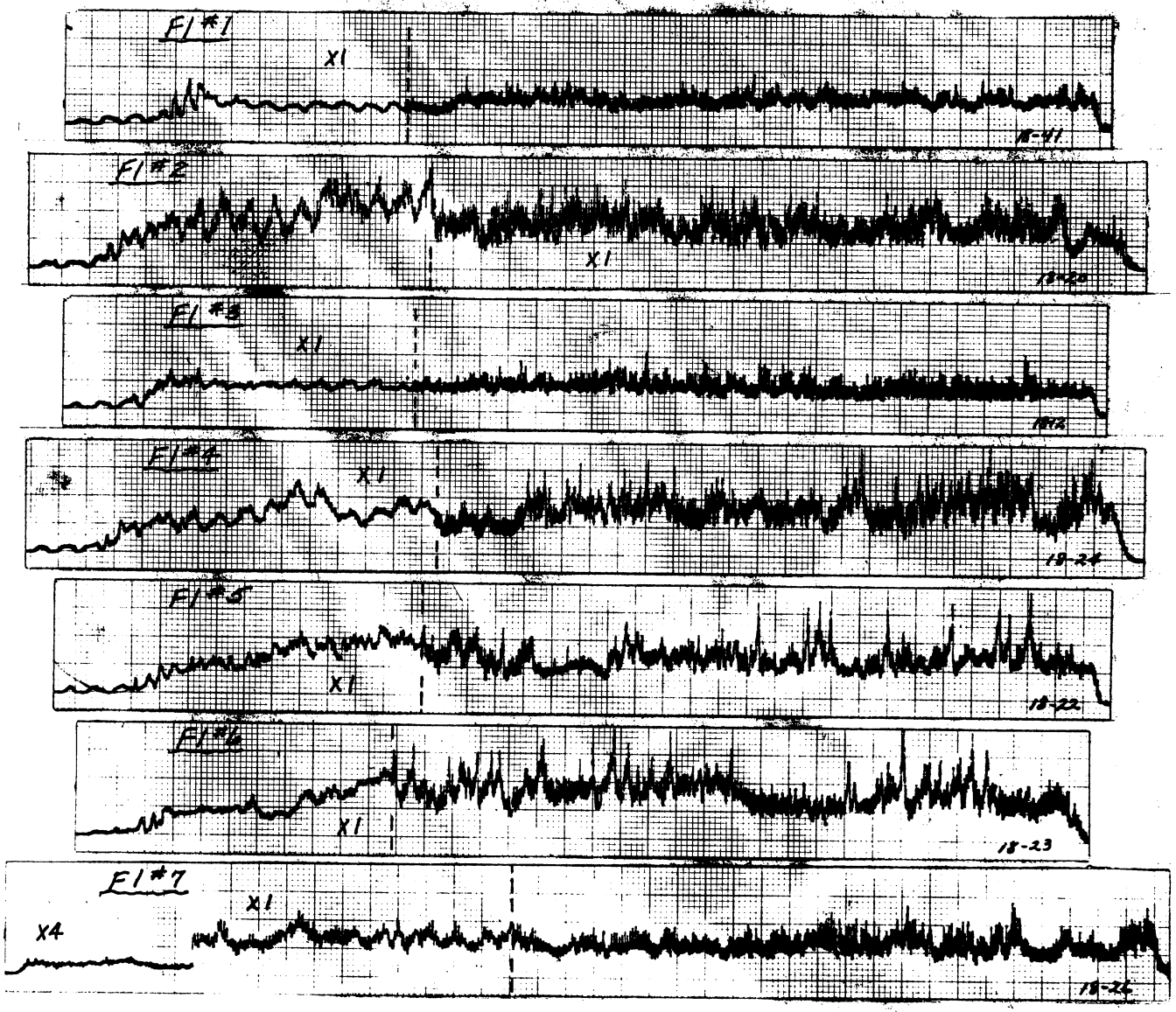

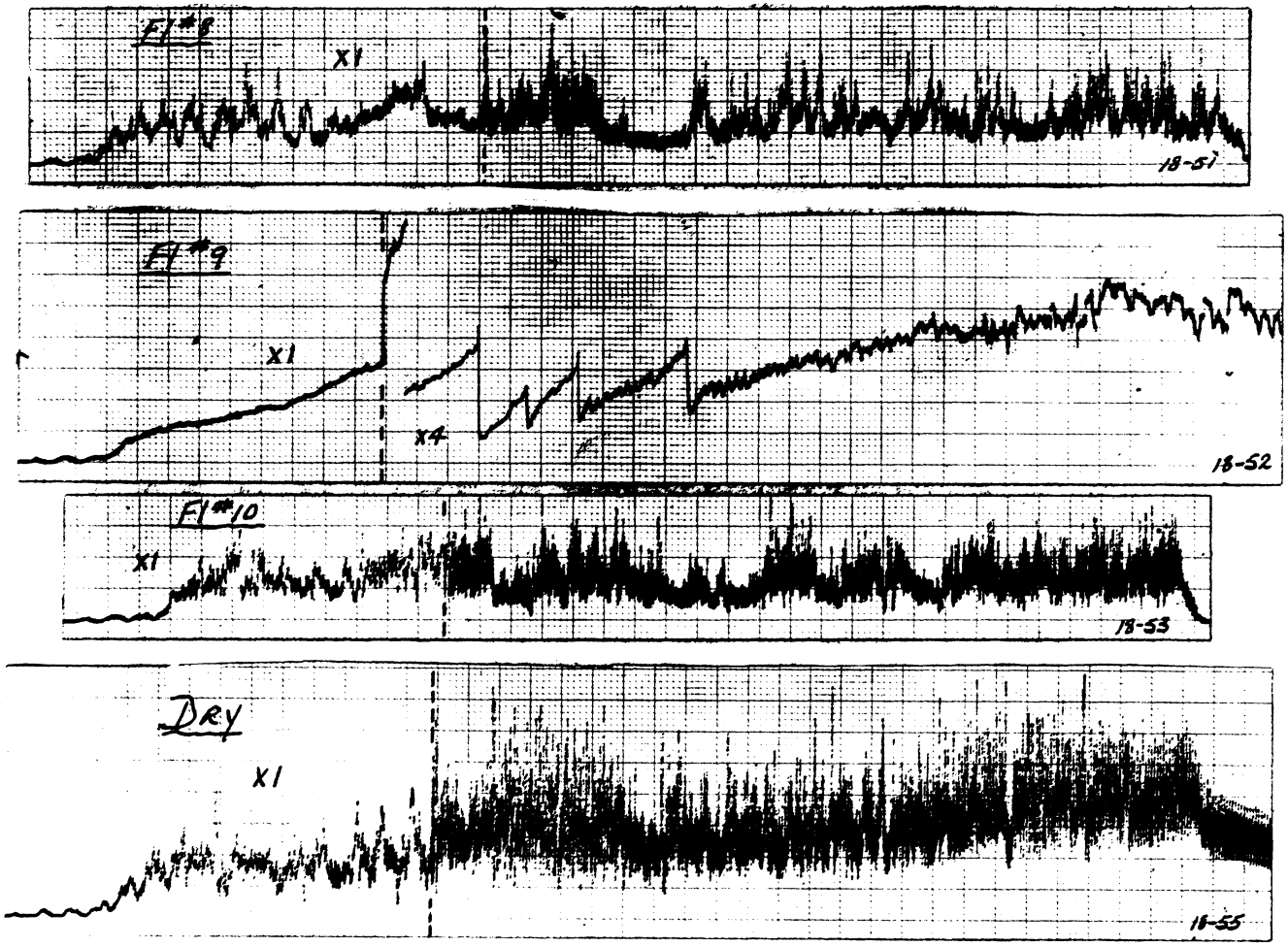

Fig. 4.15. Torque traces on 1018 steel with Reamer No. 1 and all fluids. Conditions and chart designations same as for Fig. 4.9.

1018 STEEL - Reamer No. 9

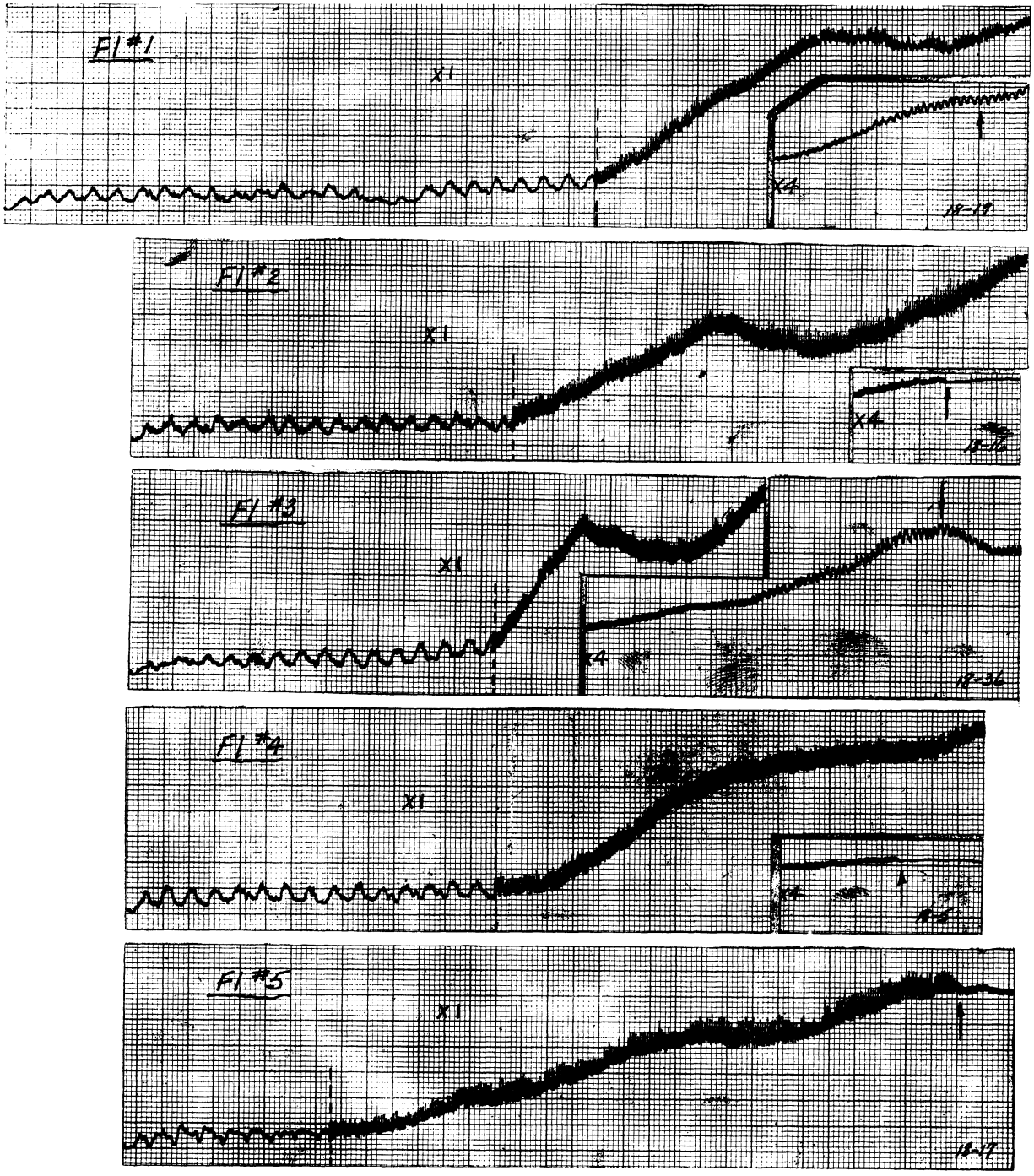

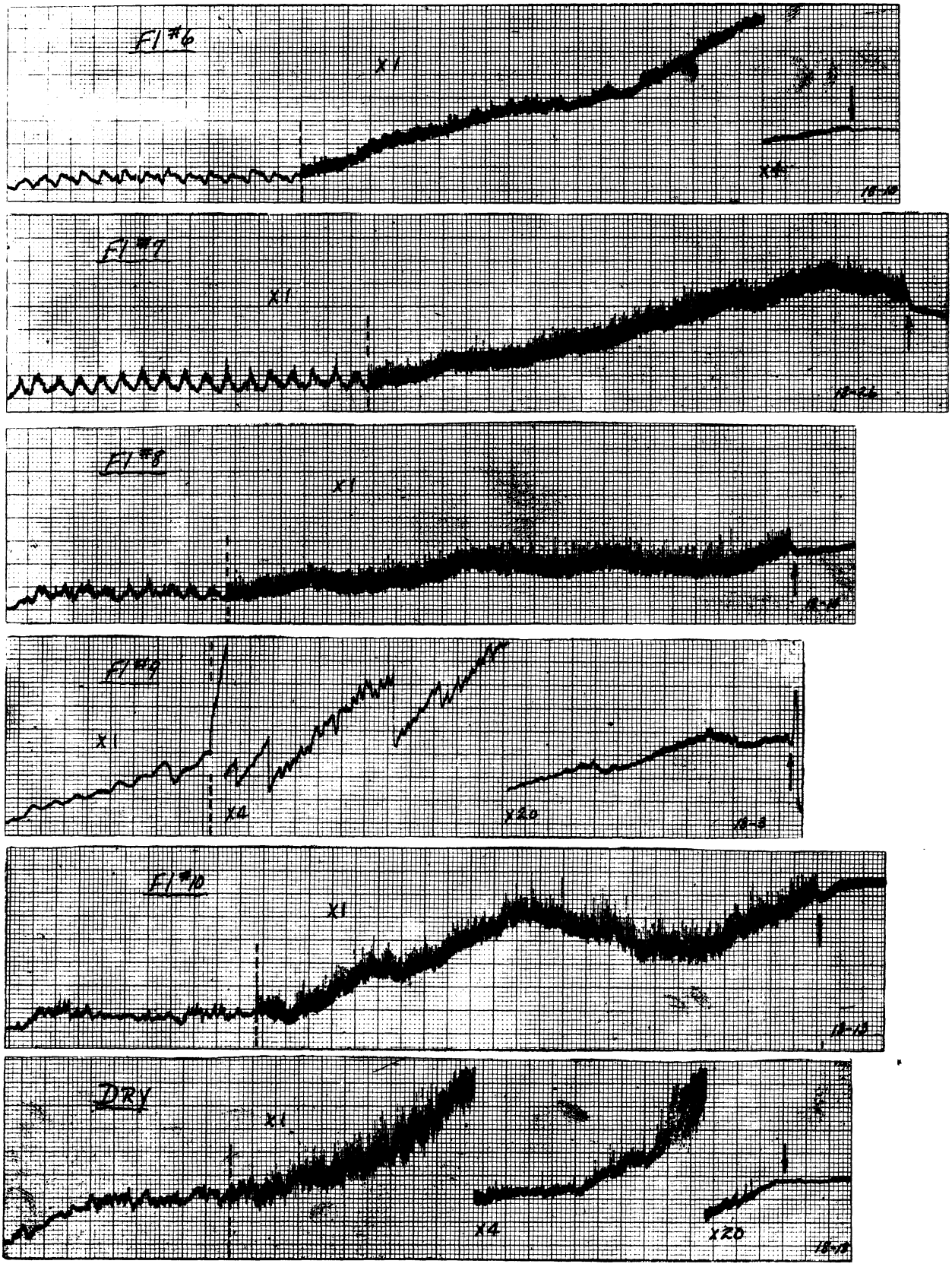

Fig. 4.16. Torque traces on 1018 steel with Reamer No. 9 and all fluids. Conditions and chart designations same as for Fig. 4.9.

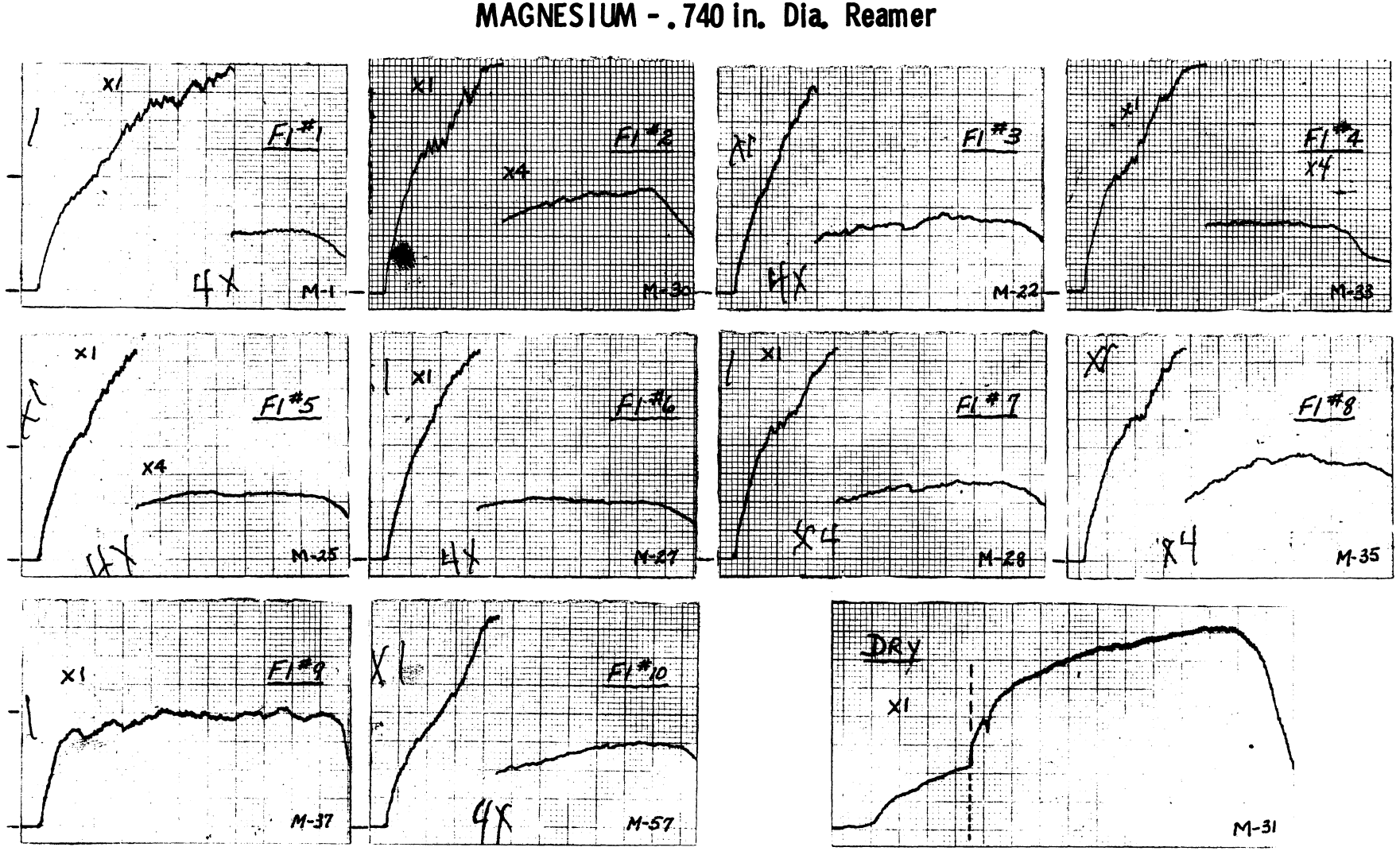

Fig. 4.17. Torque traces on magnesium with .740-in.-diameter straight-fluted reamer and all fluids. f = .0087 ipr, d = .005 inch, V = 12.8 fpm. Records traced from left to right. Vertical scale = 1.25 lb in./mm at X1. Where dashed vertical line appears on trace it denotes change in chart speed from 5 mm/sec to 0.5 mm/sec. All other chart speed 0.5 mm/sec.

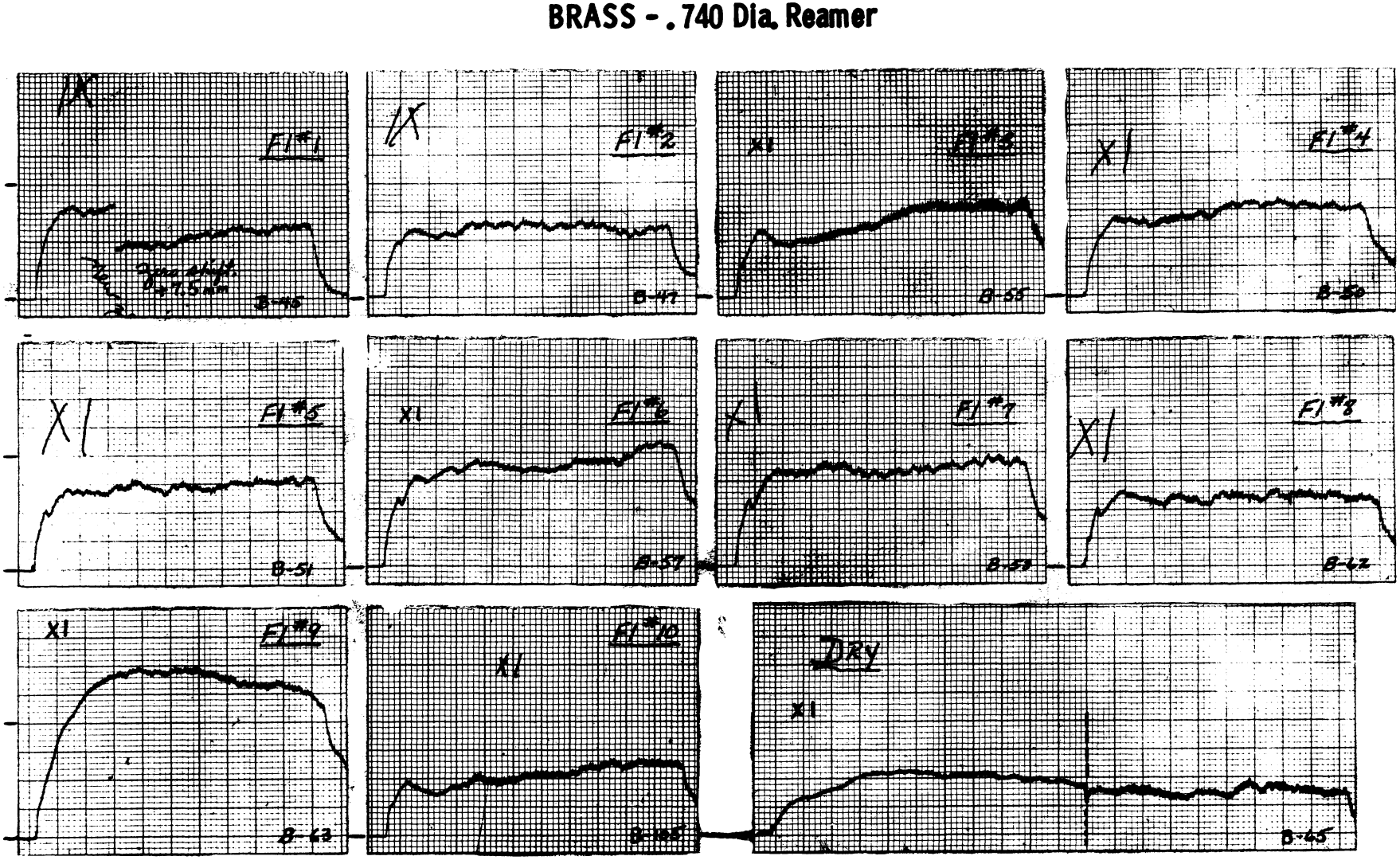

Fig. 4.18. Torque traces on brass with .740-in.-diameter reamer and all fluids. Conditions and chart designations same as for Fig. 4.17.

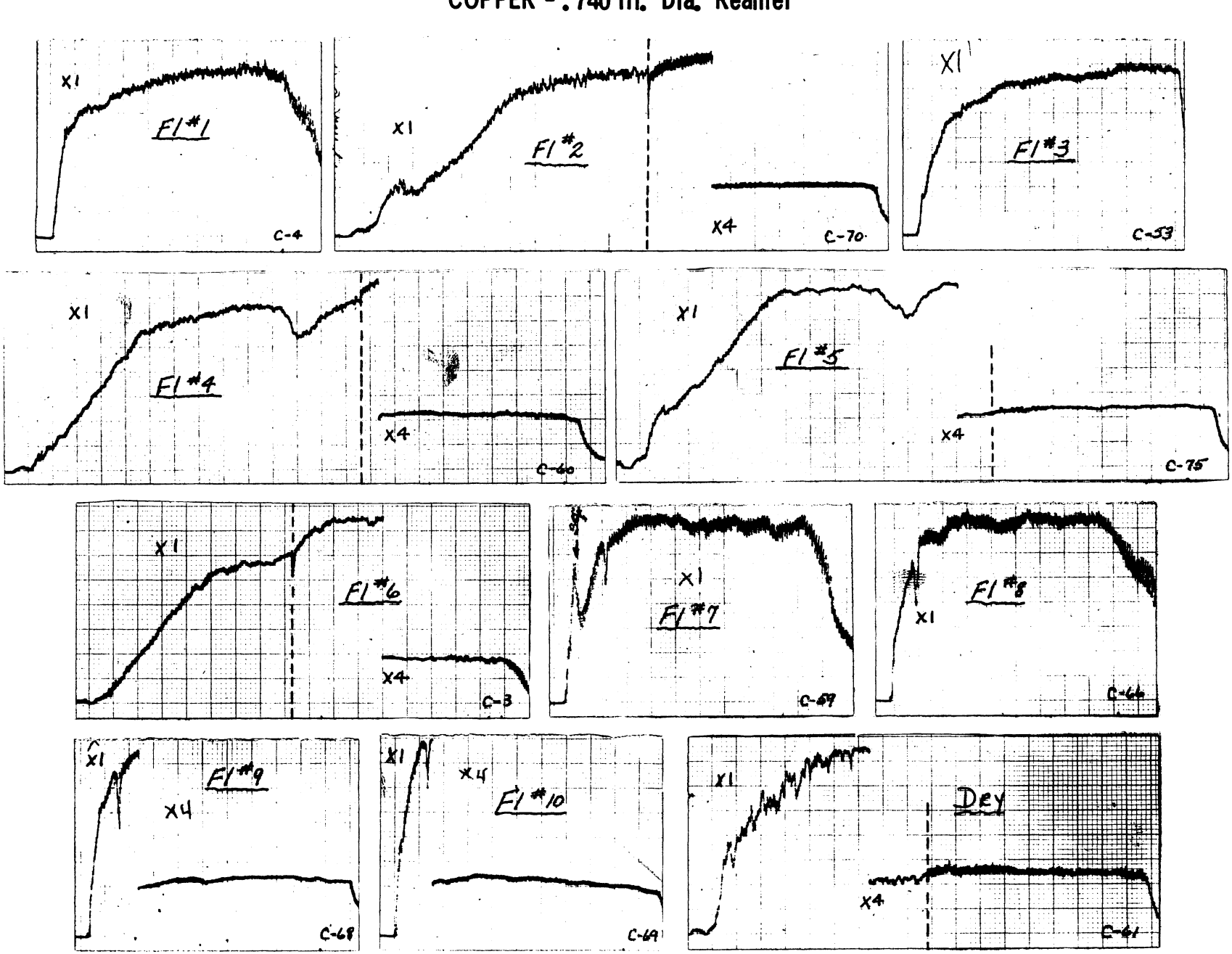

Fig. 4.19. Torque traces on copper with .740-in.-diameter reamer and all fluids. Conditions and chart designations same as for Fig. 4.17.

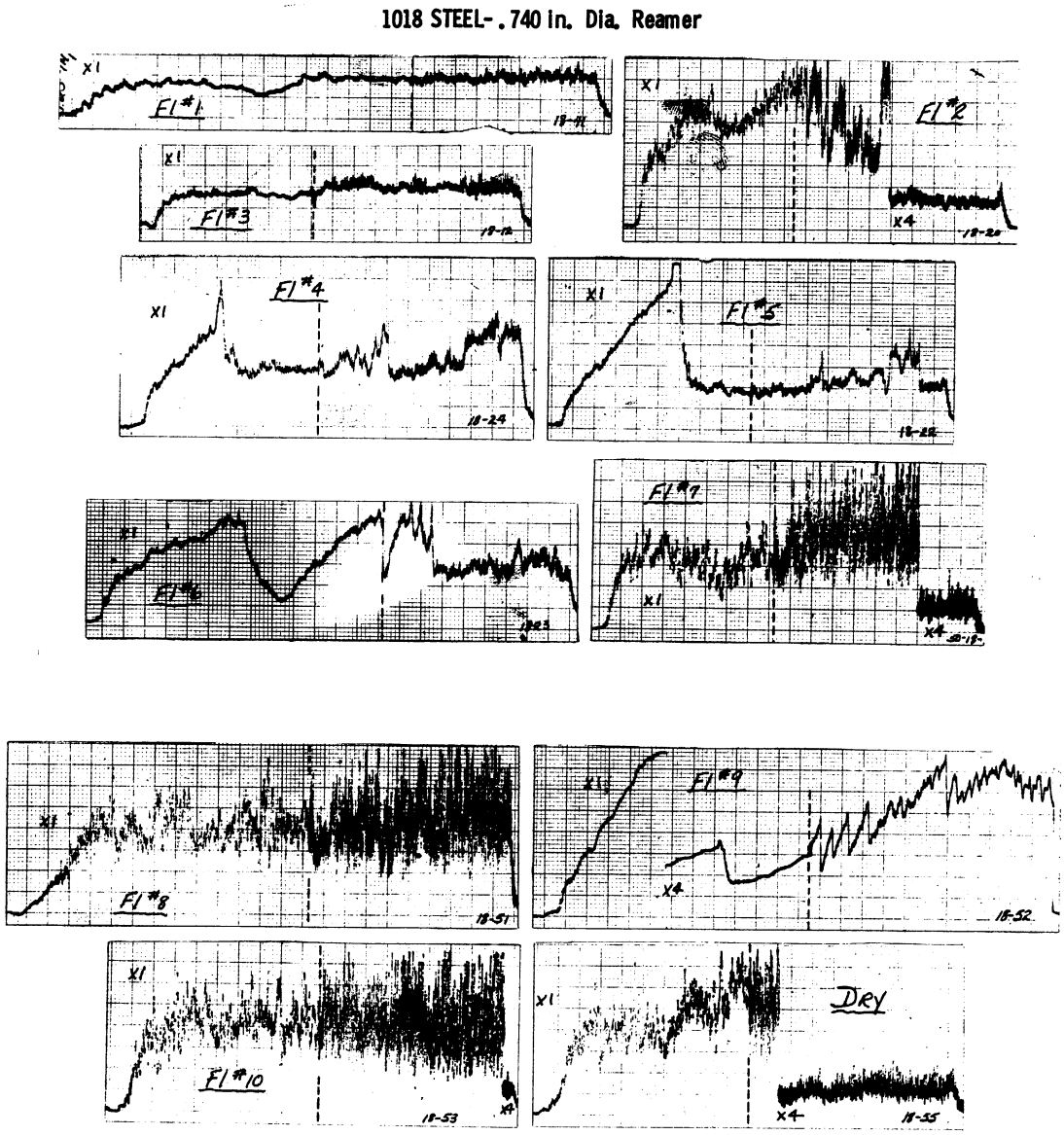

Fig. 4.20. Torque traces on 1018 steel with .740-in.-diameter reamer and all fluids. Conditions and chart designations same as for Fig. 4.17.

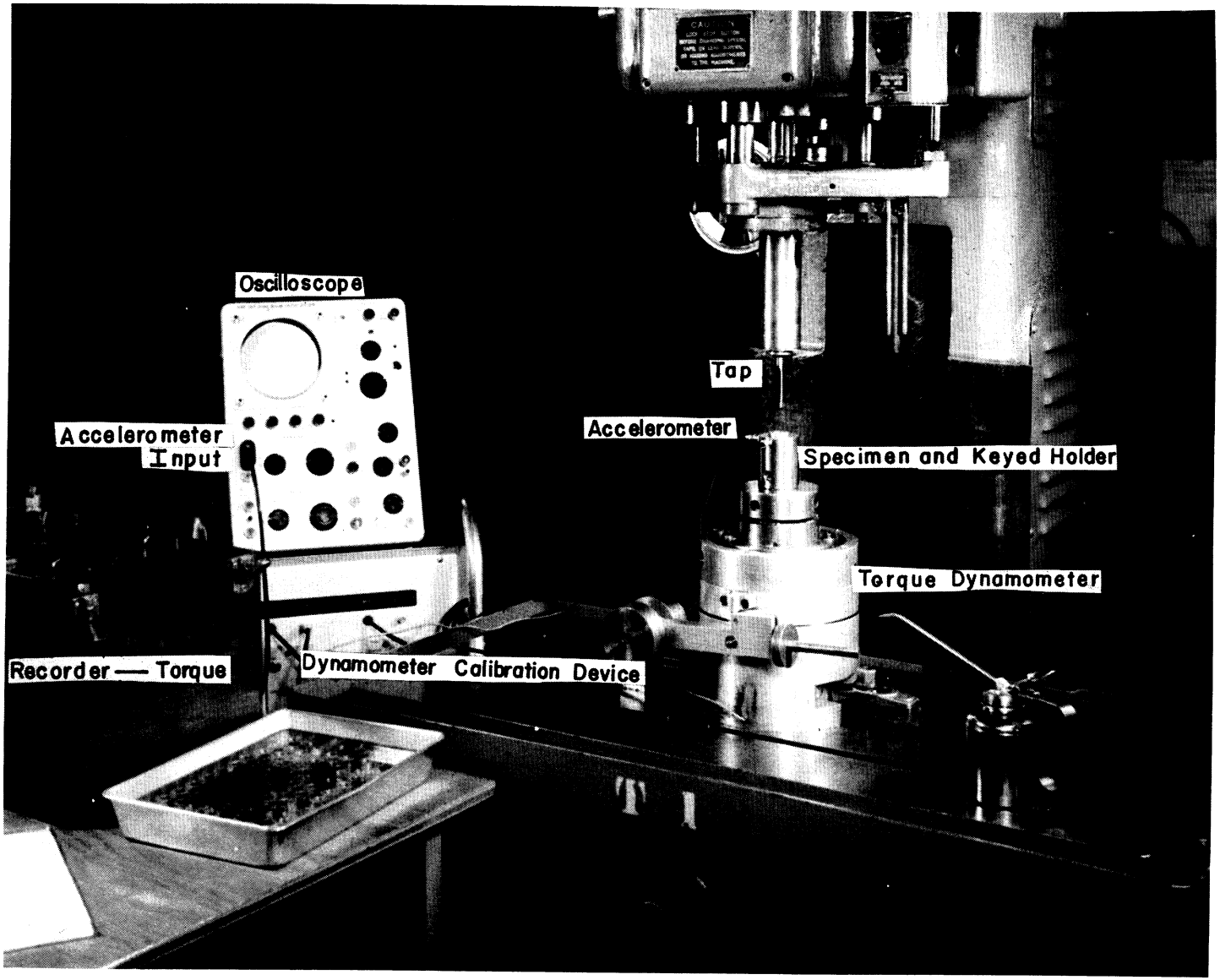

Fig. 4.21. Equipment and instrumentation used in tapping tests. Accelerometer was used in exploratory investigations of stick-slip phenomena. It was mounted in the holder, radial to and at the midpoint of the specimen.

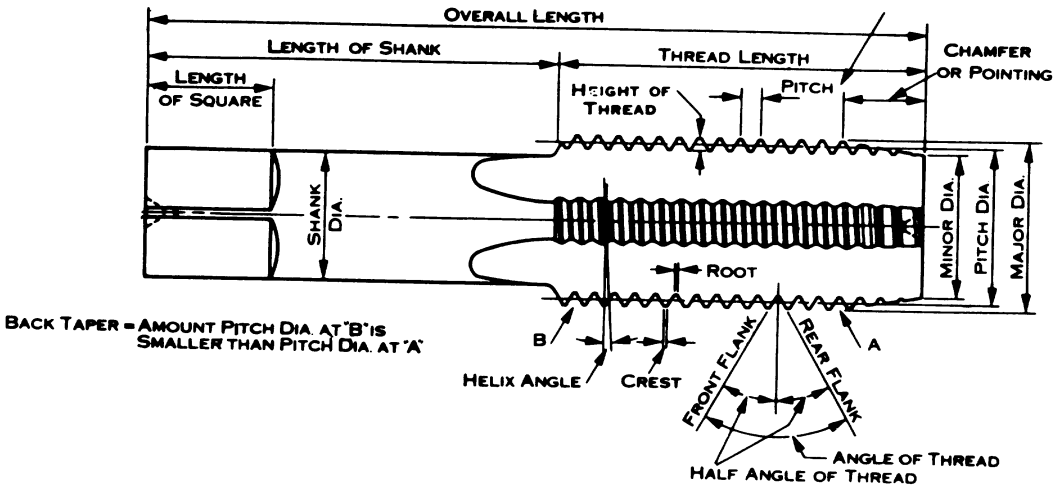

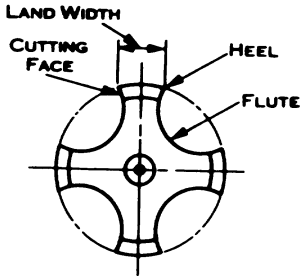

TAP

Fig. 4.22. Sketch identifying nomenclature of standard tap used in tapping tests. Cutting is done only by the cutting edges created by chamfer or pointing. Length of cutting edges and rubbing surface area is greater than corresponding counterparts in reaming.

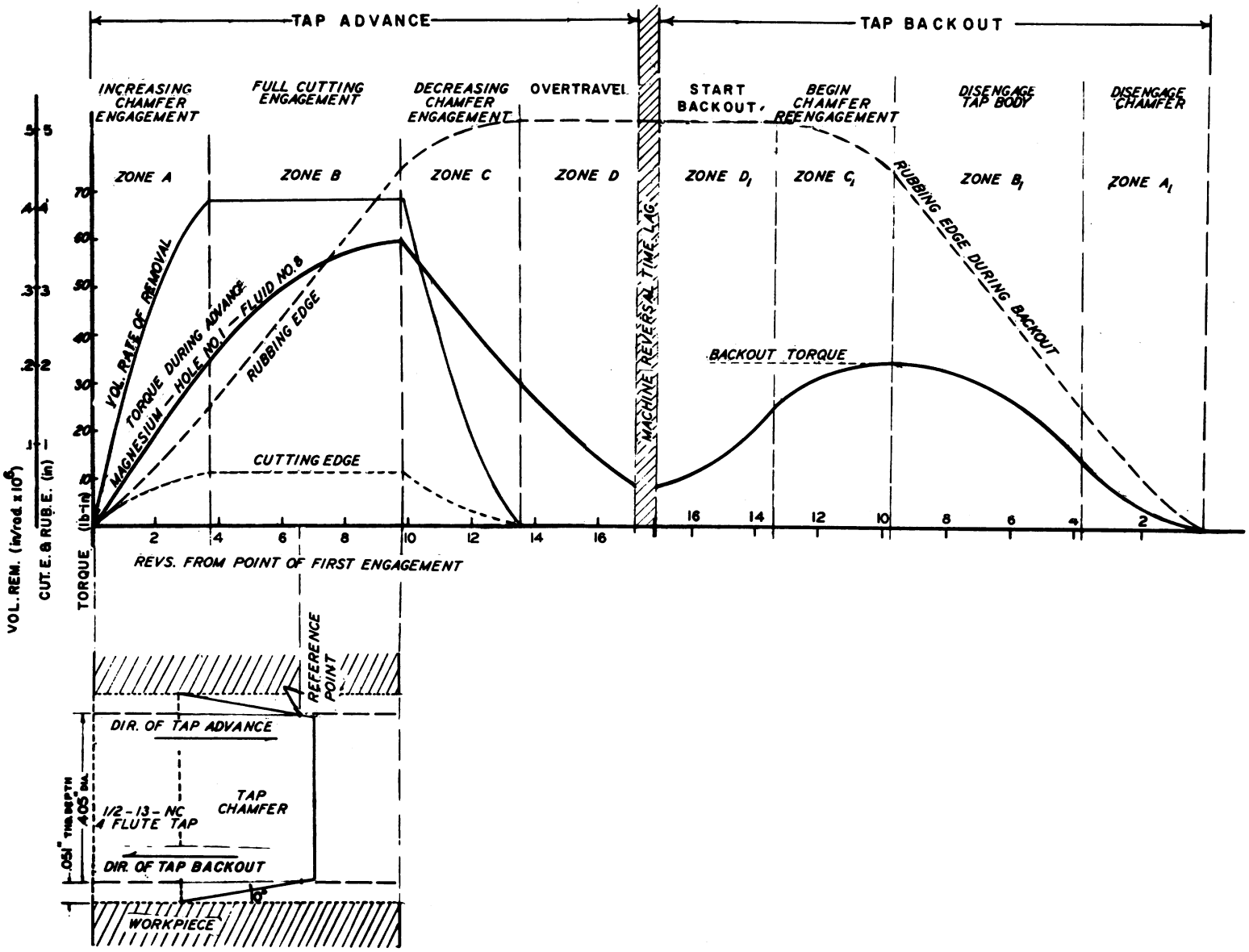

Fig. 4.23. Chart showing relationship between typical tapping torque behavior, volume rate of metal removal, and lengths of cutting and rubbing edges during tap advance and tap backout.

BRASS

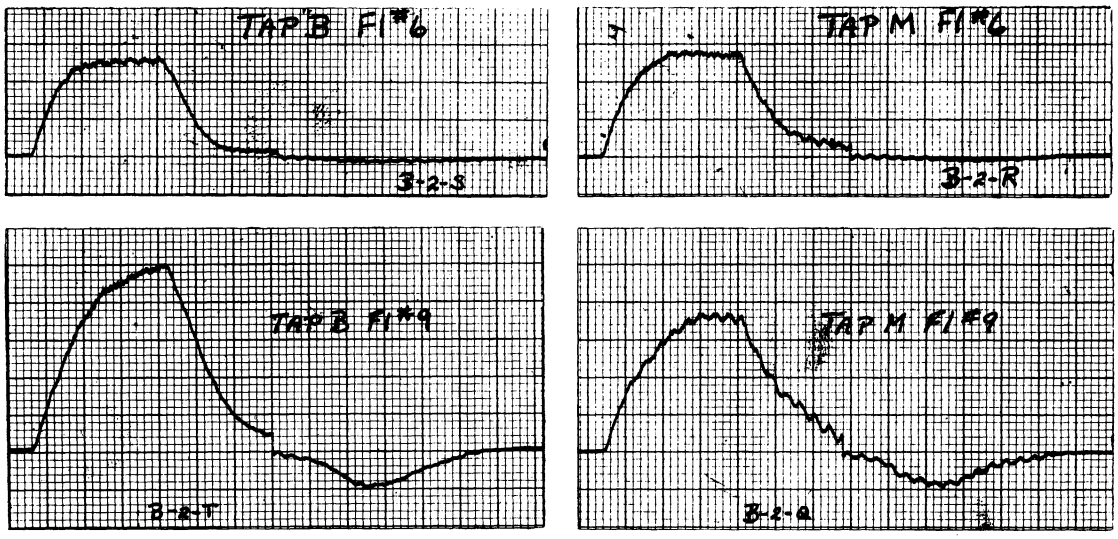

MAGNESIUM

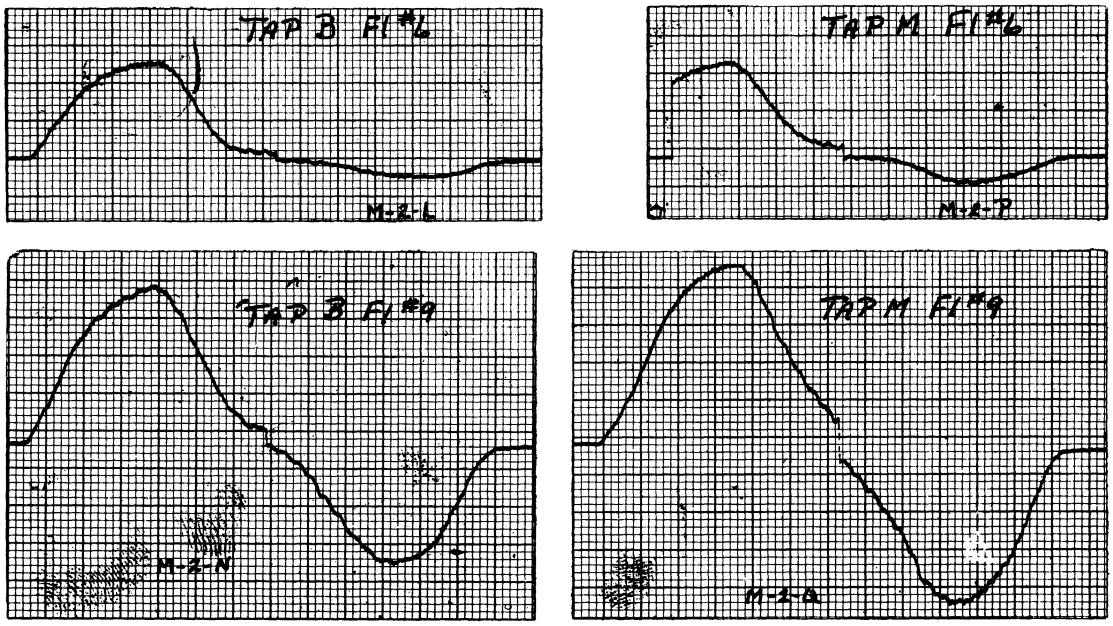

Fig. 4.24. Torque traces showing effect of Taps B and M on brass and magnesium, Hole No. 2, with Fluids Nos. 6 and 9. Note reversal of behavior with Fluid No. 9. Vertical scale, torque, 4 lb in./mm. Chart speed: 2.5 mm/sec. Traces from left to right.

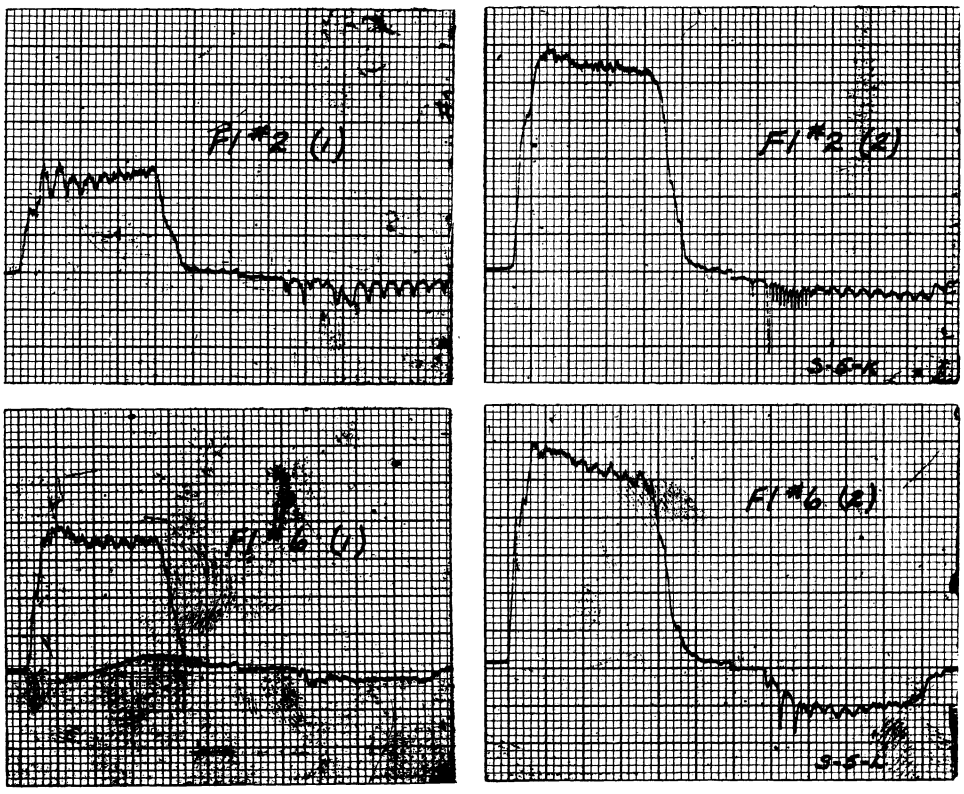

Fig. 4.25. Torque traces showing effect of tap change on stainless steel, Hole No. 5, with Fluids Nos. 2 and 6. Both taps new, taken out of box as received. Vertical scale, torque, 4 lb in./mm. Chart speed: 2.5 mm/sec. Traces from left to right. Tapped hole size went from Class 2 to Class 4 with change from (1) to (2) with Fluid No. 6.

(A) Effect of Fluids - Hole No. 2

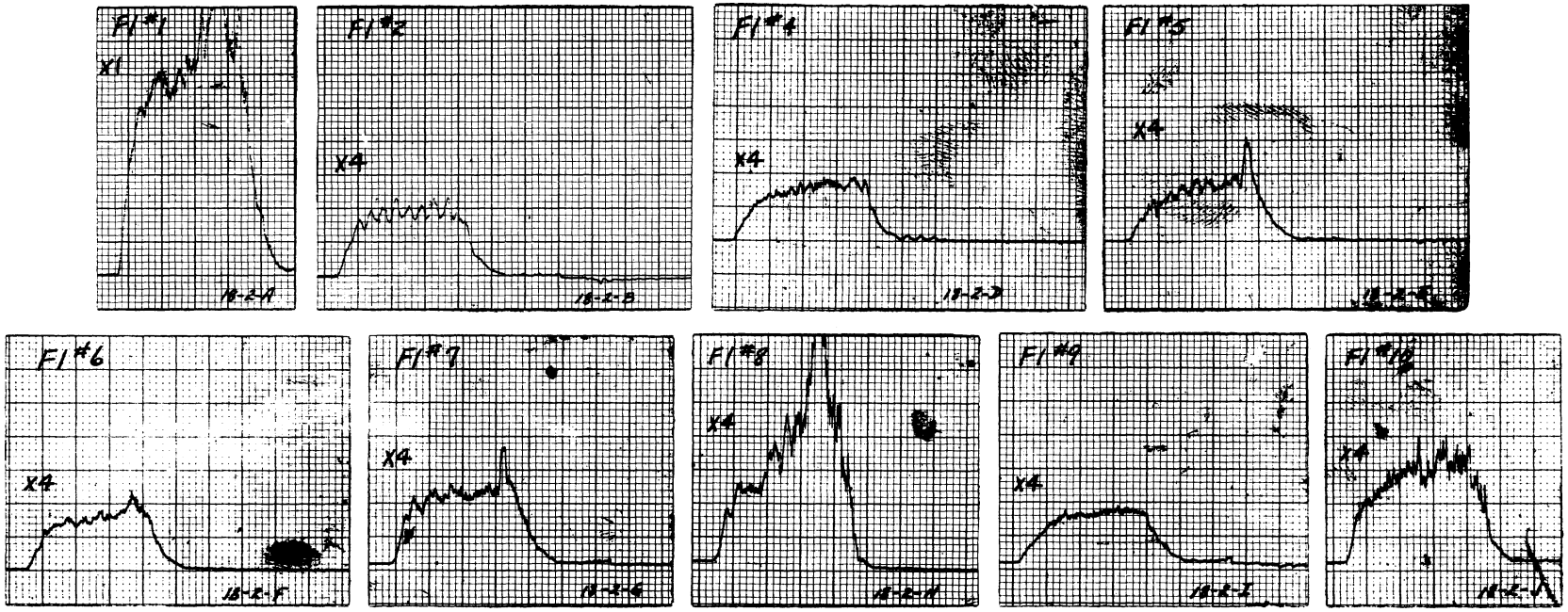

(B) Effect of Hole Size - Fluid No. 3

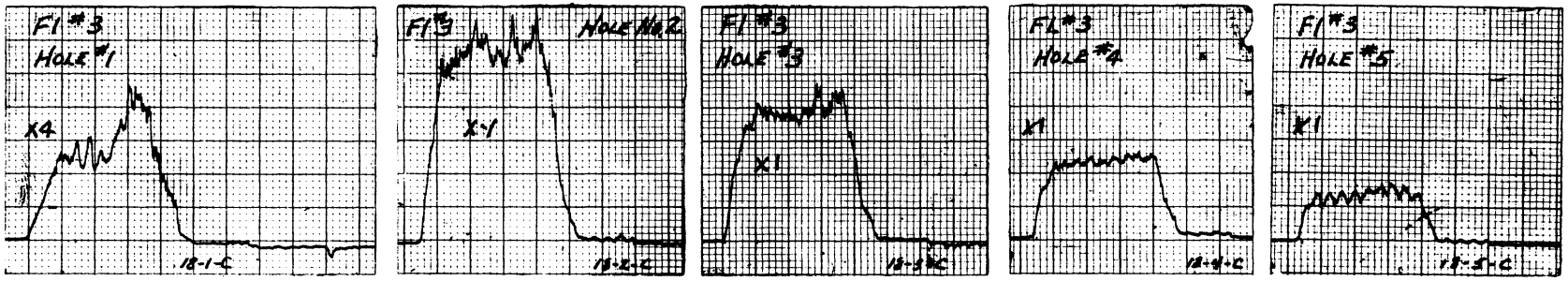

Fig. 4.26. Tapping torque traces on 1018 steel showing effect of fluids (A) and hole diameter (B). Vertical trace, torque, 4 lb in./mm at X1. Chart speed = 2.5 mm/sec. Traces from left to right.

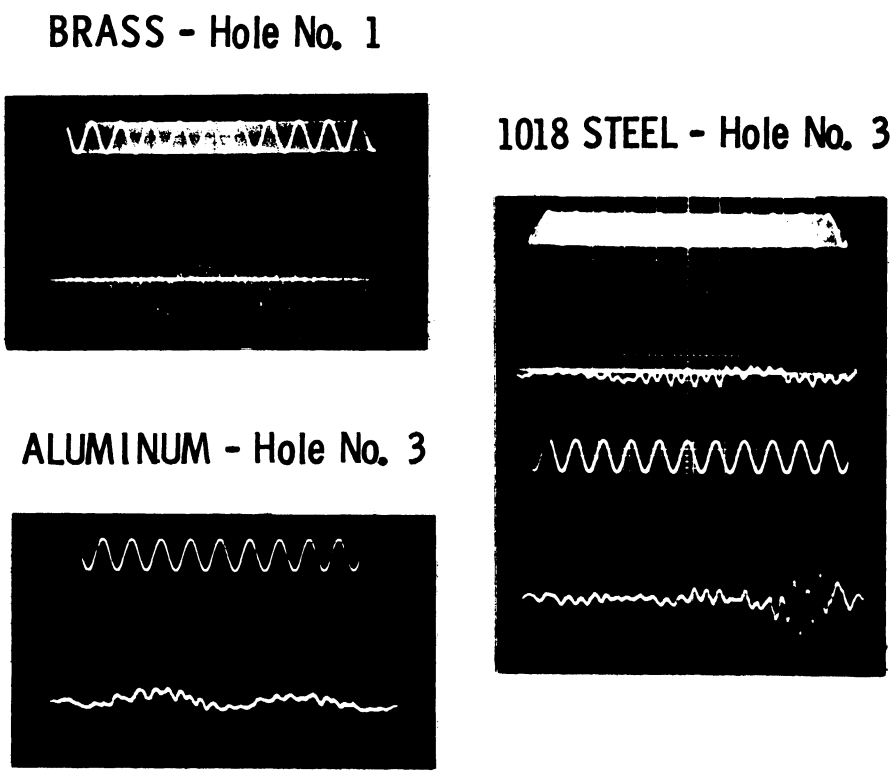

Fig. 4.27. Representative oscilloscope traces of exploratory tests of stick-slip phenomena in tapping. Traces represent output from accelerometer mounted radially on specimen holder. Reference sine wave at frequency of 10,000 cps. On 1018 steel lower trace taken at approximately full depth of tap chamfer, upper trace at maximum torque level. All tests with Fluid No. 2.

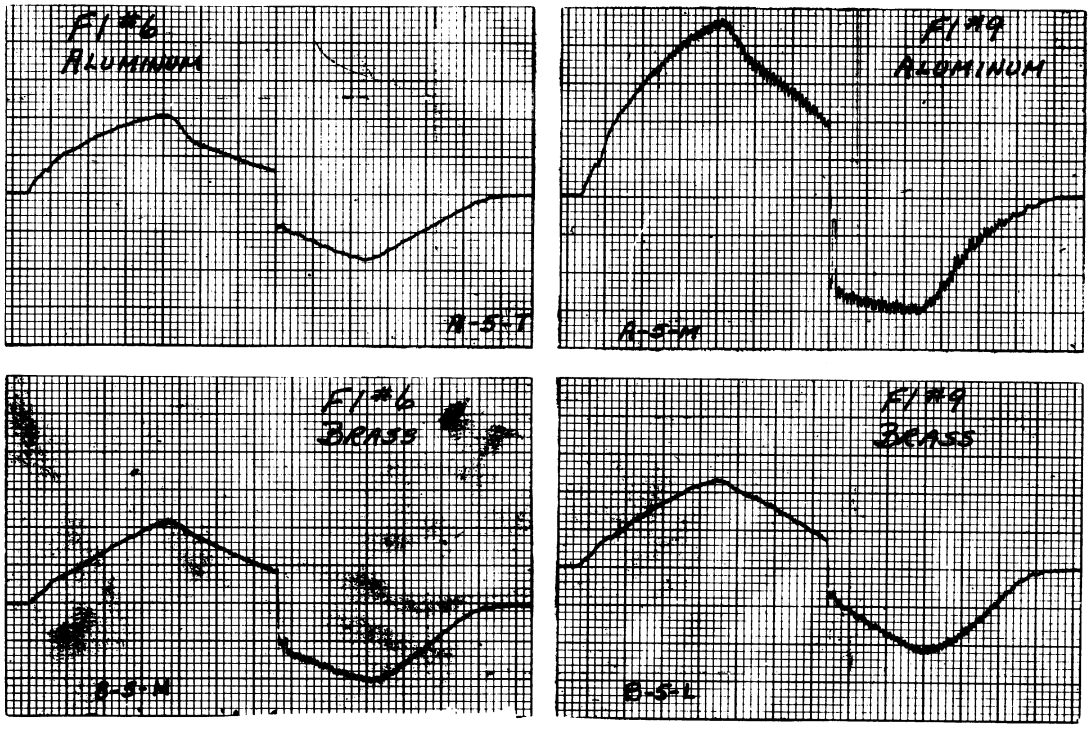

Fig. 4.28. Typical torque traces on aluminum and brass with "X-Press" tap on Hole No. 5. Trace with Fluid No. 9 on aluminum is most distinctive. Other traces typical of all fluids. Vertical scale, torque, 16 lb in./mm. Chart speed: 2.5 mm/sec. Traces from left to right.

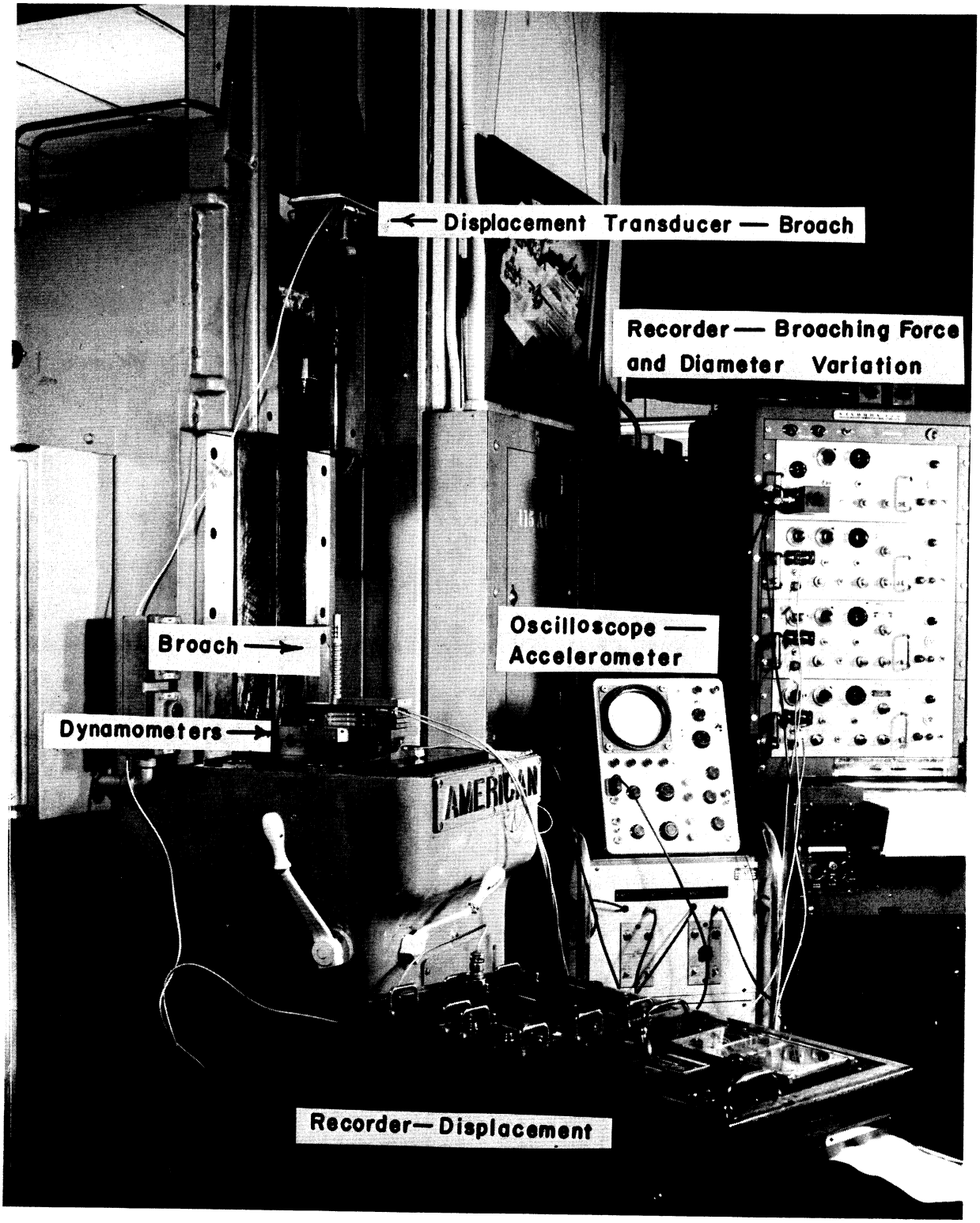

Fig. 4.29. Photograph of broaching setup showing equipment and instrumentation used.

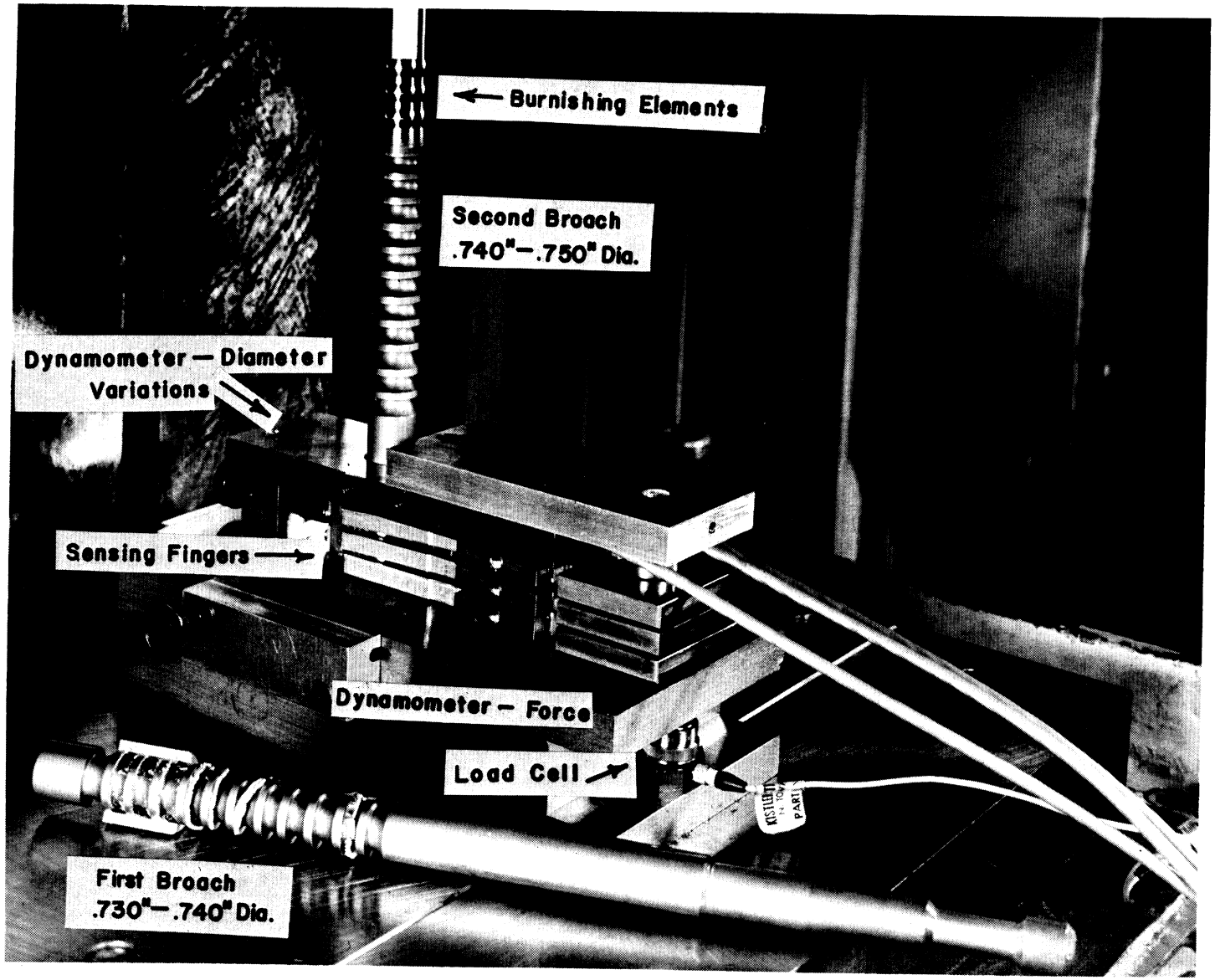

Fig. 4.30. Closeup of working zone showing broach, specimen, and dynamometers in position for cutting. Note type of chips produced by roughing, finishing, and dwell teeth of first broach. See Fig. 4.31 for position of specimen.

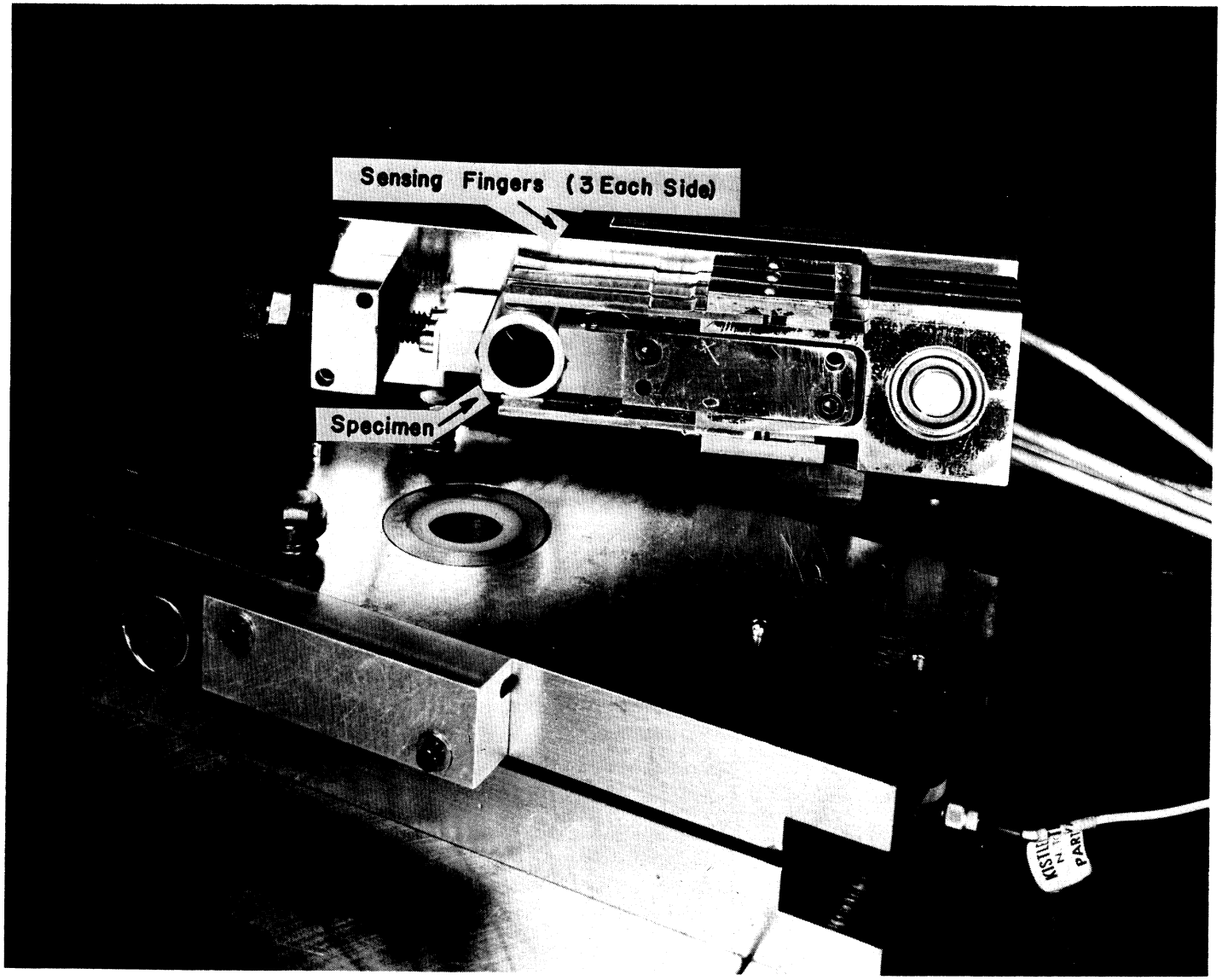

Fig. 4.31. Upper dynamometer turned on its side to show location of specimen and sensing fingers. V-blocks and clamp are used only to locate specimen and not for clamping against broaching forces. Specimen is supported by lower dynamometer during broaching.

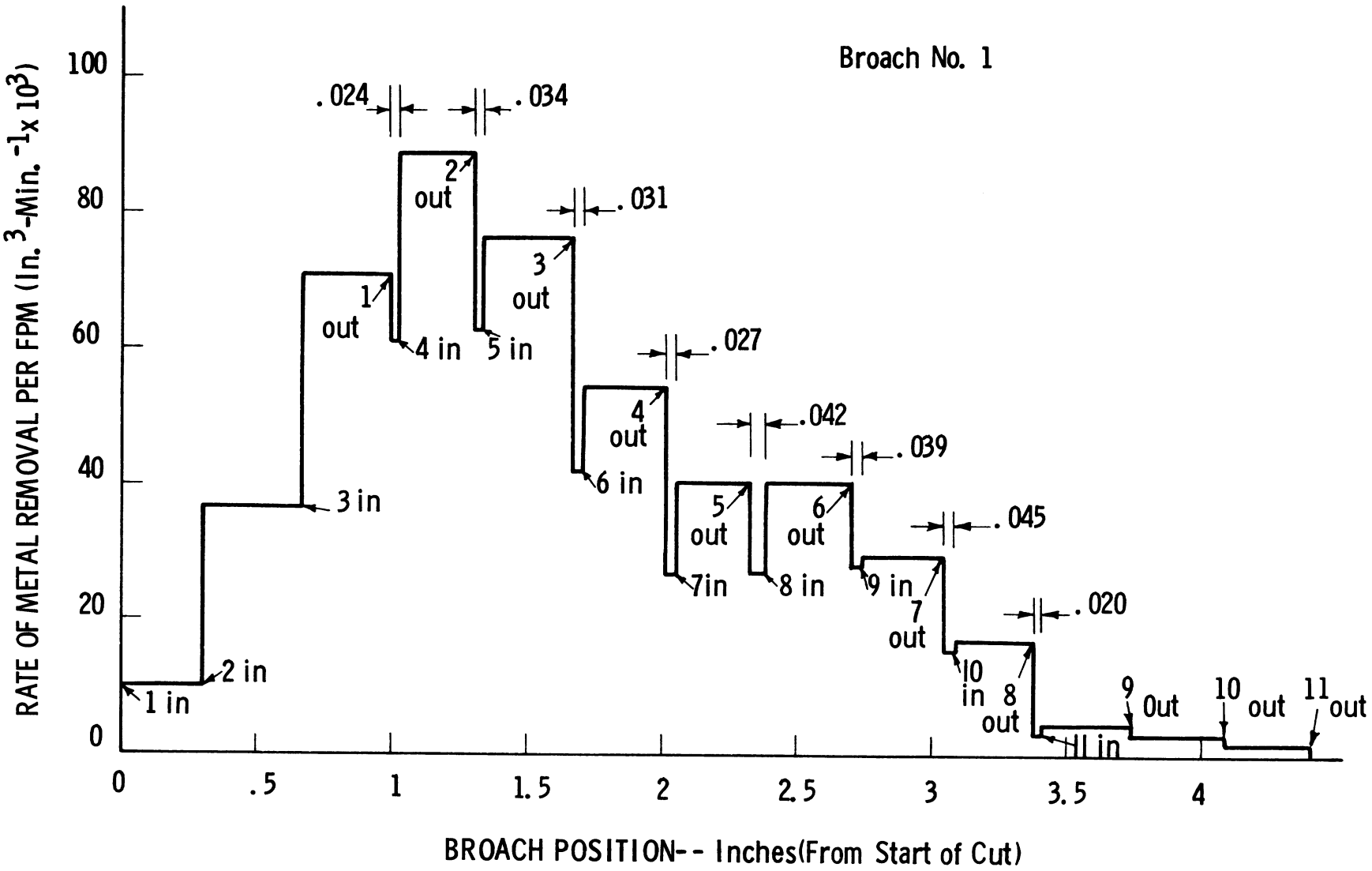

Fig. 4.32. Rate of metal removal vs. broach position for Broach No. 1. Steps result from different teeth entering and leaving work specimen. Horizontal gaps represent lag between leaving and entering teeth. Tooth combinations described in Fig. 4.33.

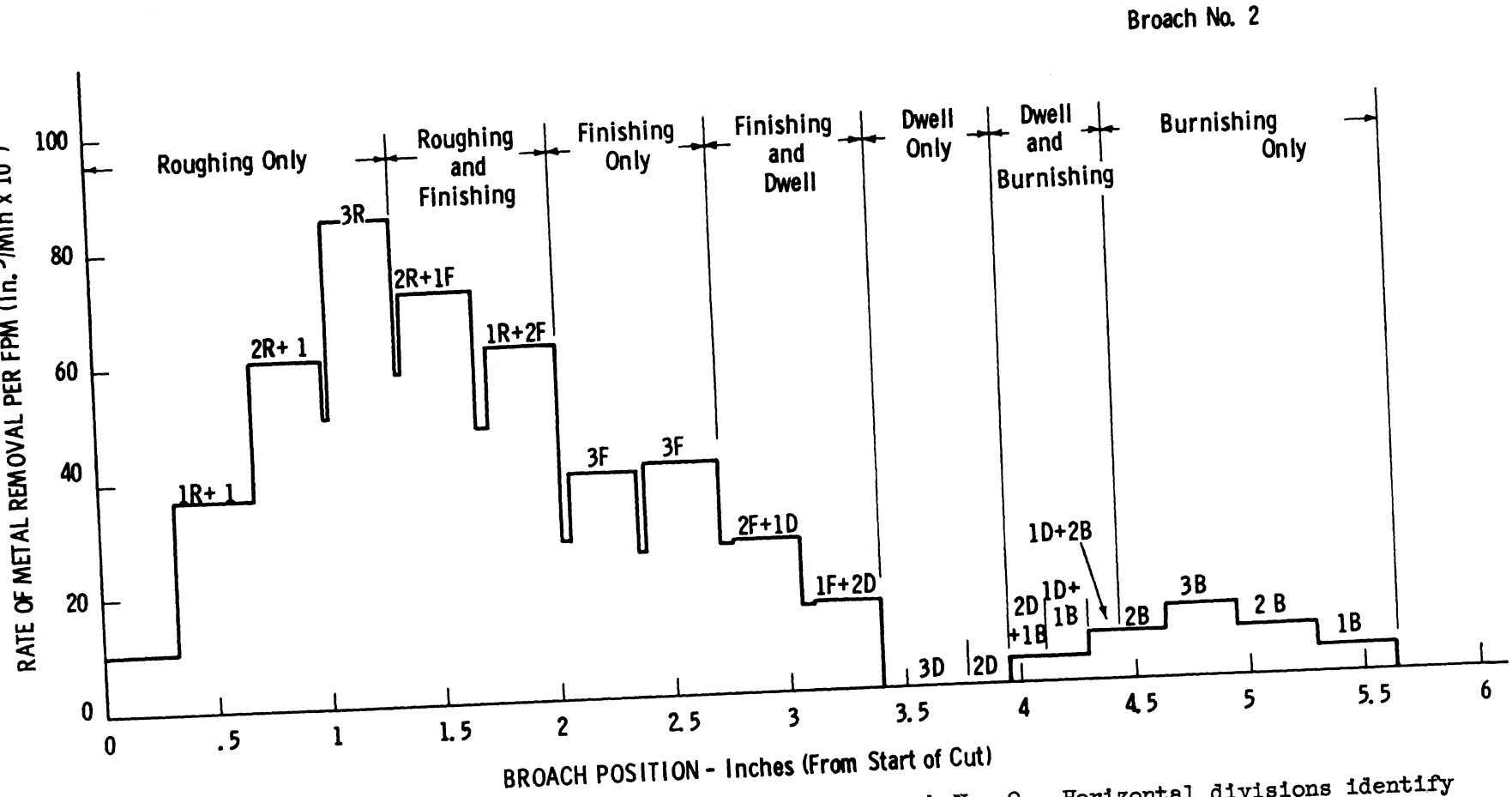

Fig. 4.33. Rate of metal removal vs. broach position for Broach No. 2. Horizontal divisions identify the type of teeth in contact with work specimen. Symbols: R, roughing tooth; F, finishing tooth; D, dwell tooth; and B, burnishing tooth. Burnishing tooth does not actually remove material. Values based on theoretical diameter change.

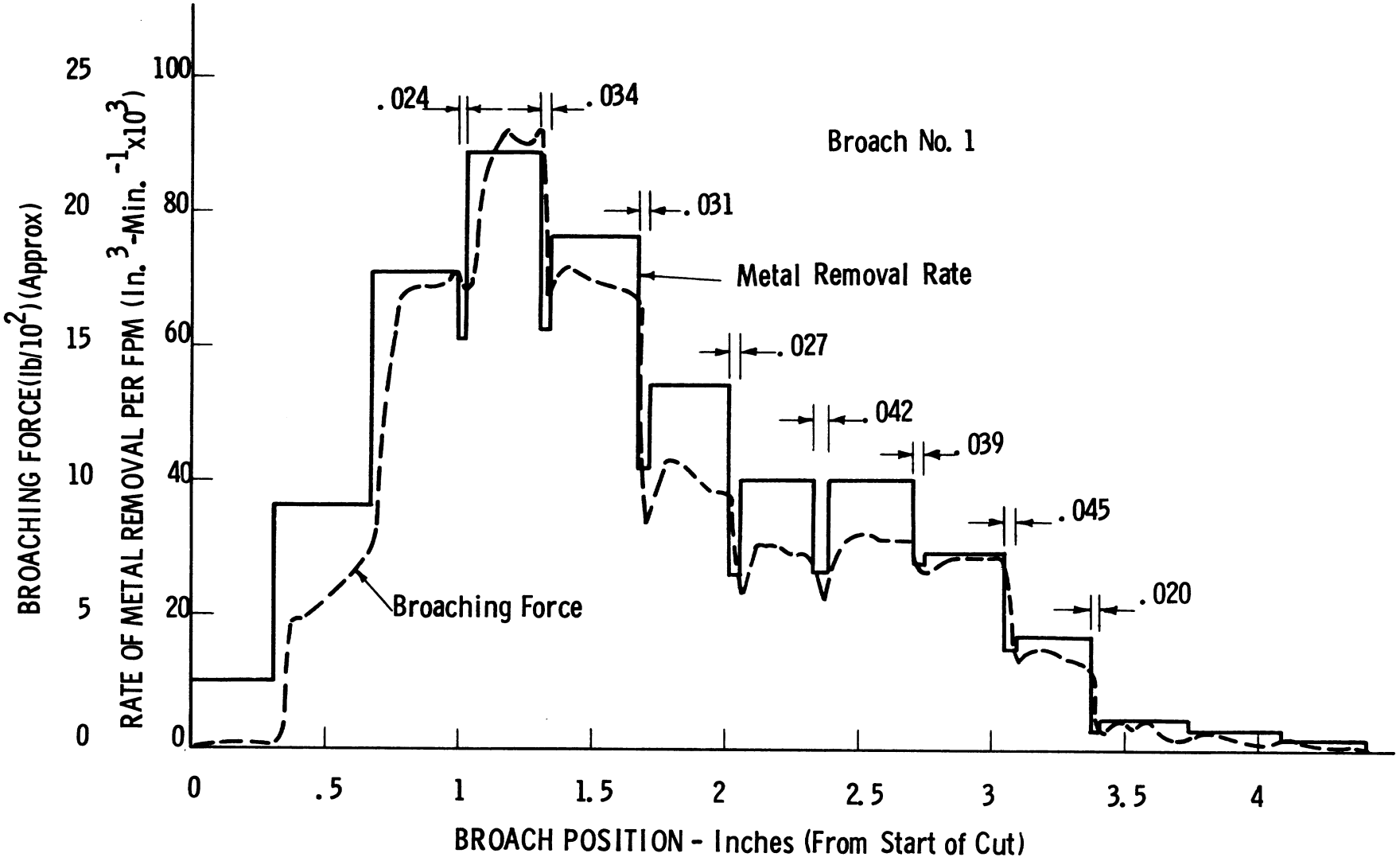

Fig. 4.34. Comparison of metal removal rates with broaching force behavior at corresponding broach positions. 1018 steel, Broach No. 1, Fluid No. 7. Note negative slopes after finishing tooth entry. Typical of built-up edge behavior.

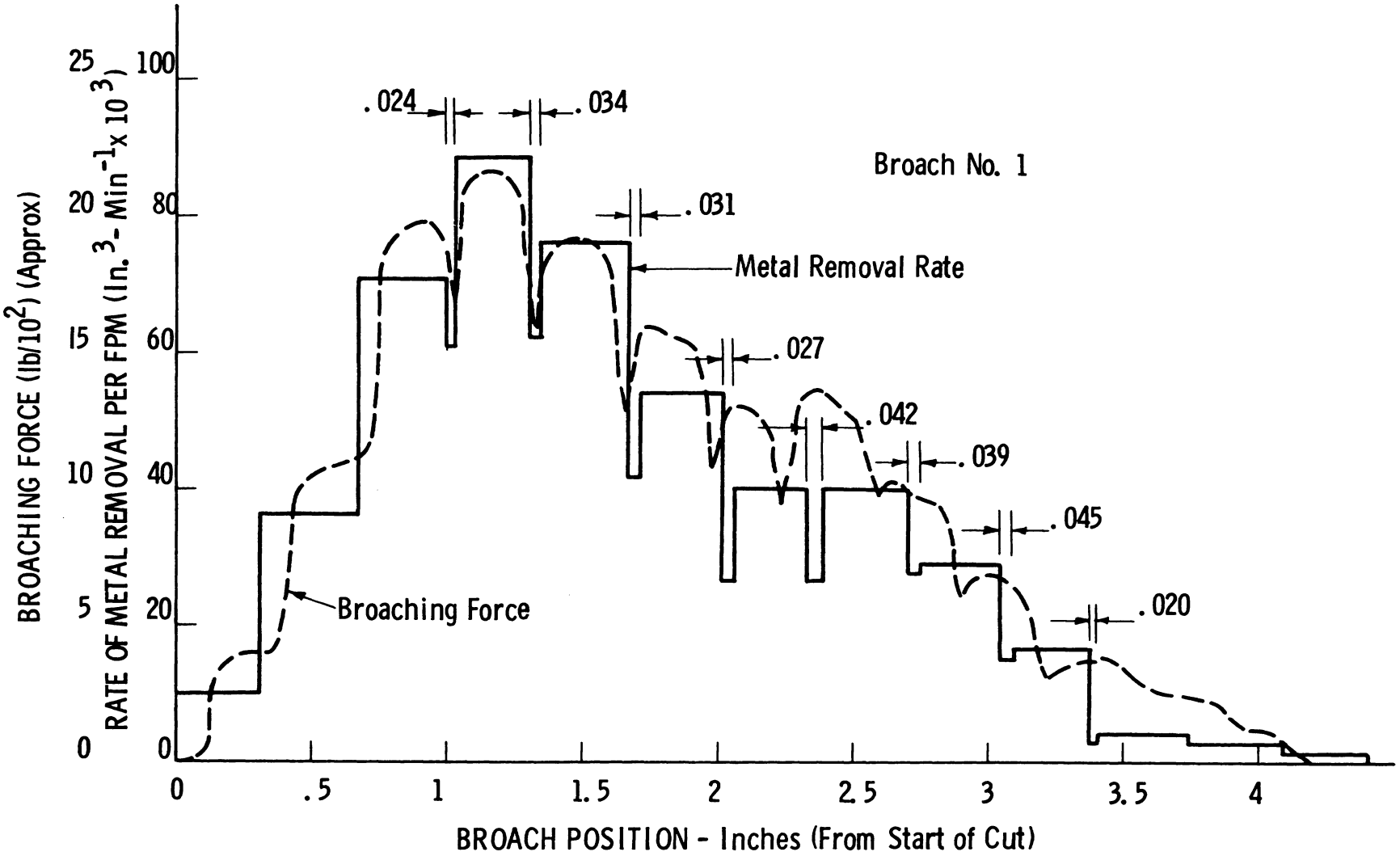

Fig. 4.35. Comparison of metal removal rates with broaching force behavior at corresponding positions of the broach. Aluminum, Broach No. 1, Fluid No. 7. Note slightly higher relative force level with low metal removal rates.

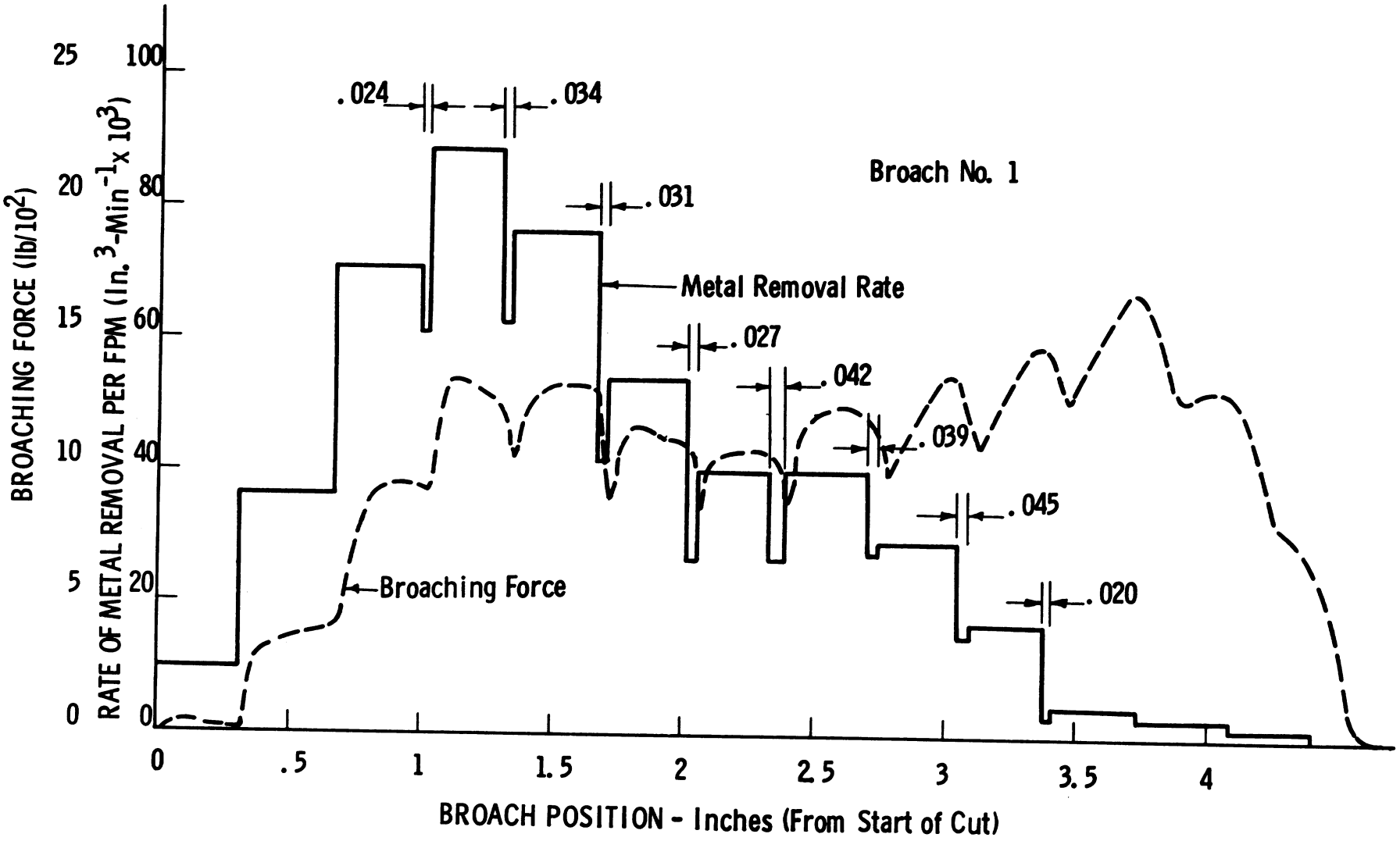

Fig. 4.36. Comparison of metal removal rates with broaching force behavior at corresponding positions of the broach. Magnesium, Broach No. 1, Fluid No. 9. Note higher force level with dwell than with roughing.

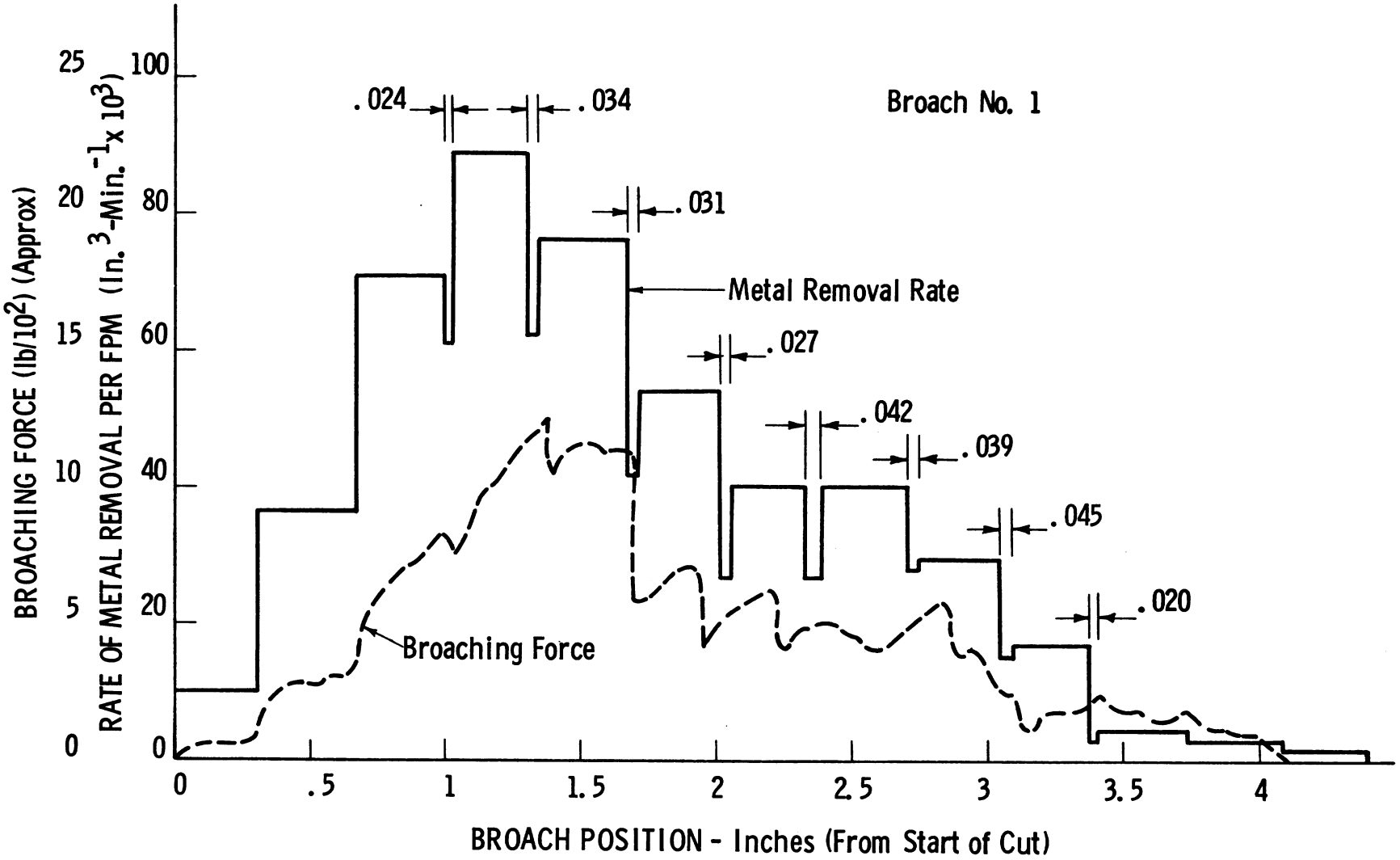

Fig. 4.37. Comparison of metal removal rates with broaching force behavior at corresponding positions of the broach. Copper, Broach No. 1, Fluid No. 7. Note distortion of plateaus and high rates of force increase after tooth entry.

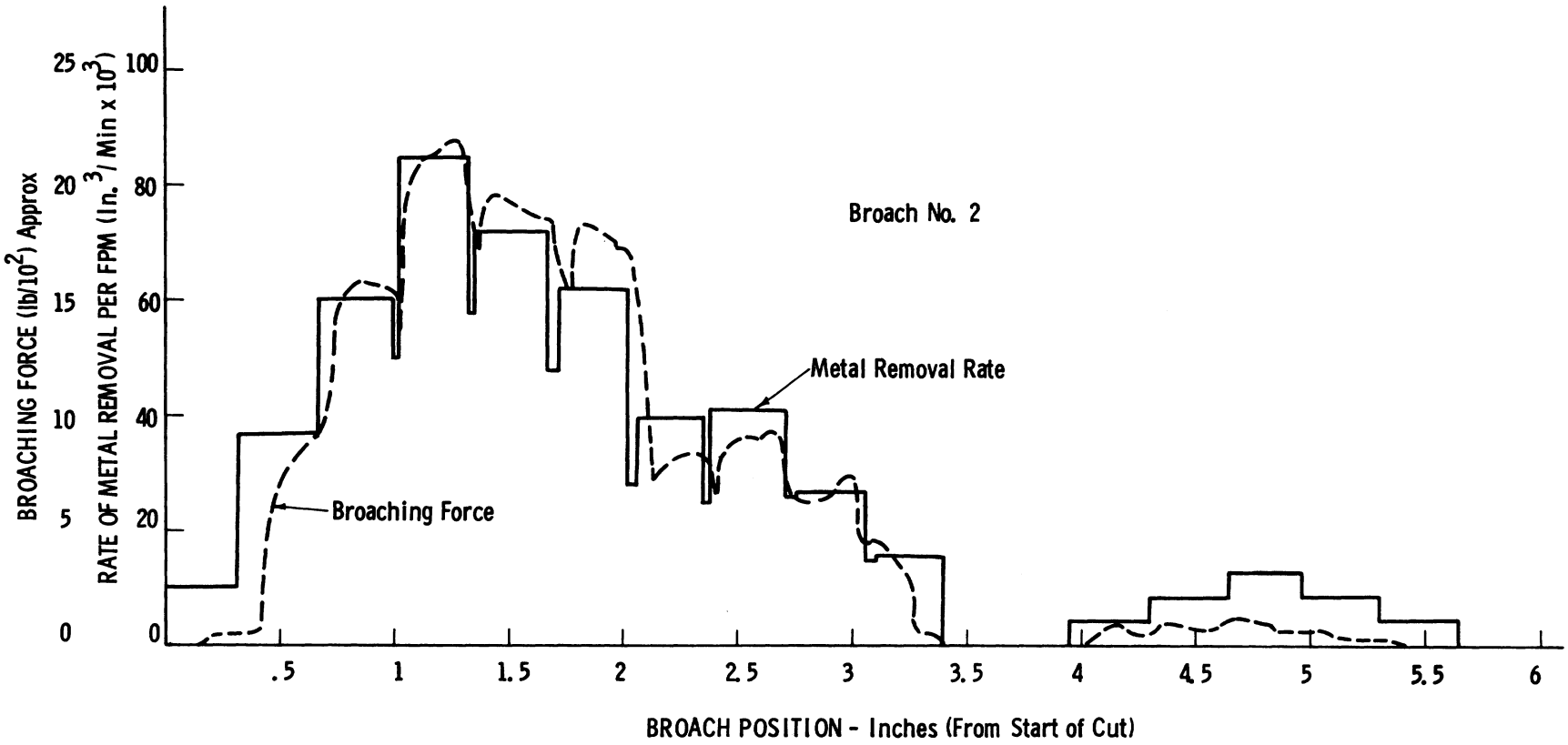

Fig. 4.38. Same as Fig. 4.34 but with Broach No. 2. Note absence of dwell tooth forces. Hole diameter was larger than diameter of dwell teeth.

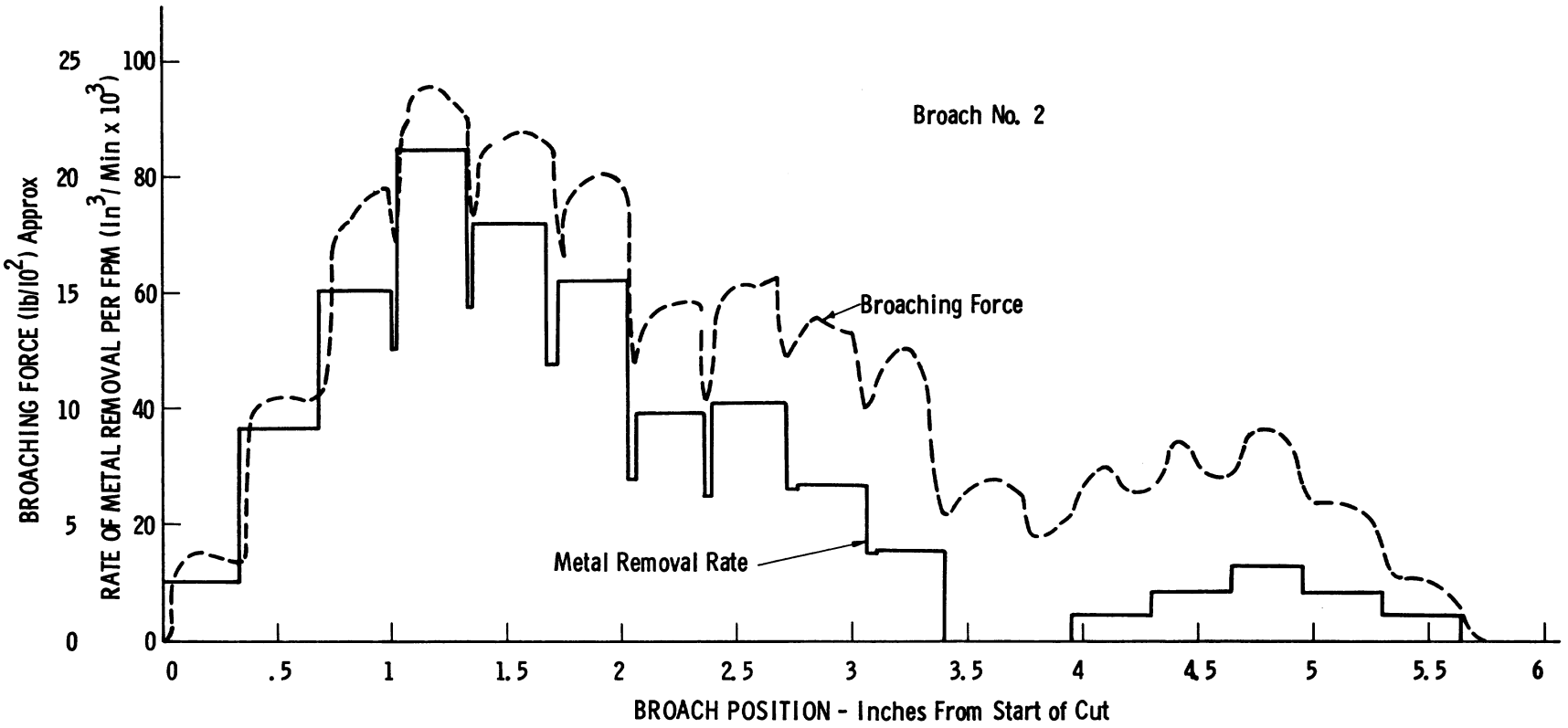

Fig. 4.39. Same as Fig. 4.35 but with Broach No. 2. Note change in force scale.

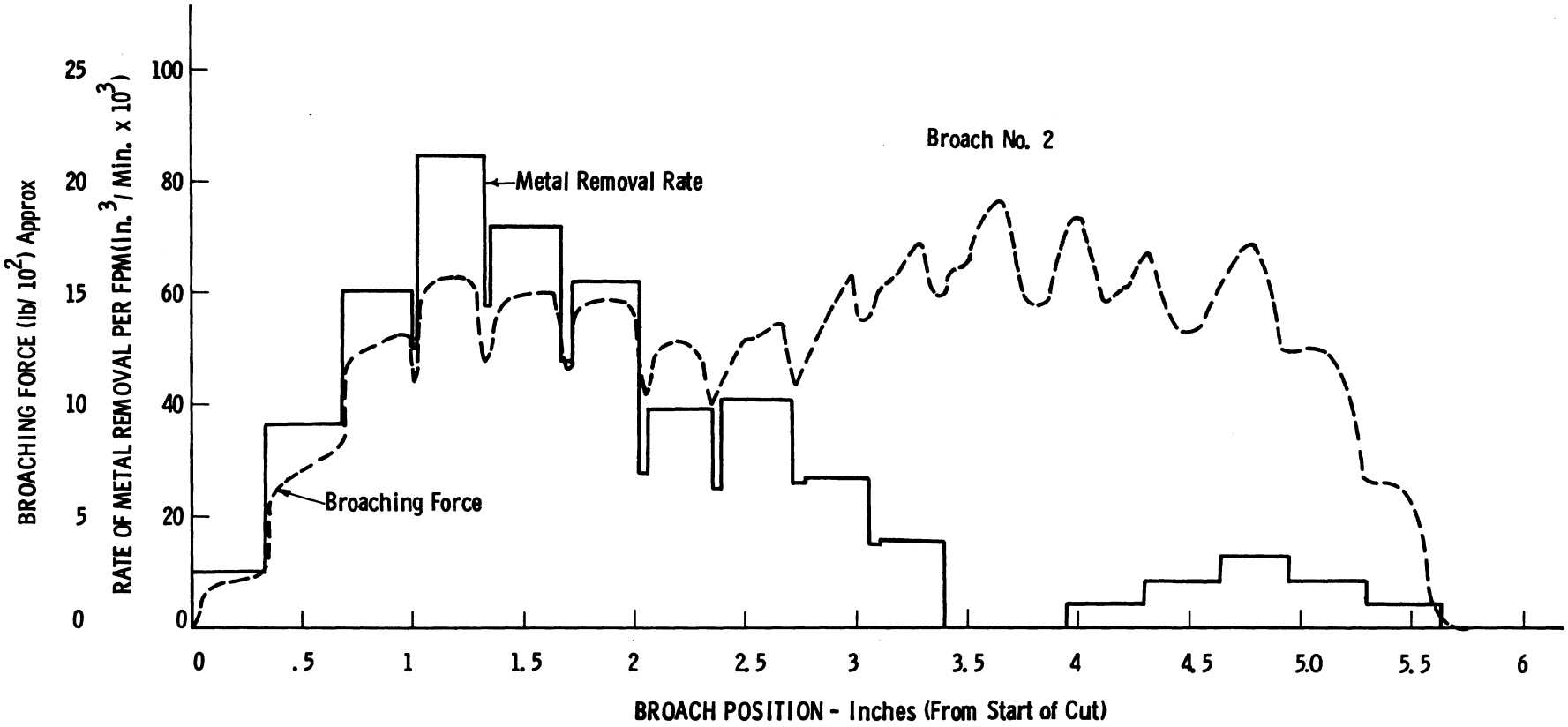

Fig. 4.40. Same as Fig. 4.36 but with Broach No. 2. Note that dwell forces are higher than either roughing or burnishing. Note, also, change in scale.

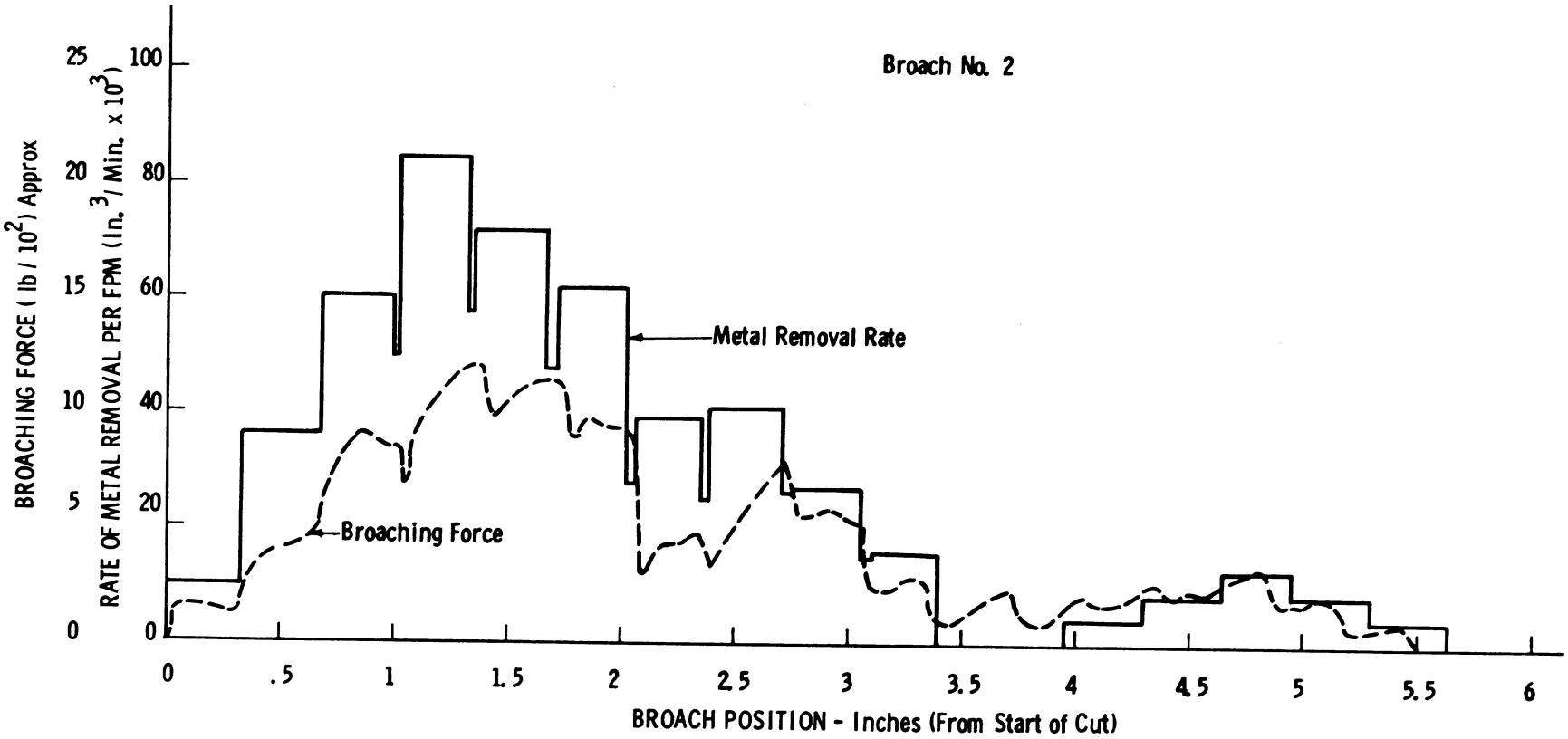

Fig. 4.41. Same as Fig. 4.37 but with Broach No. 2.

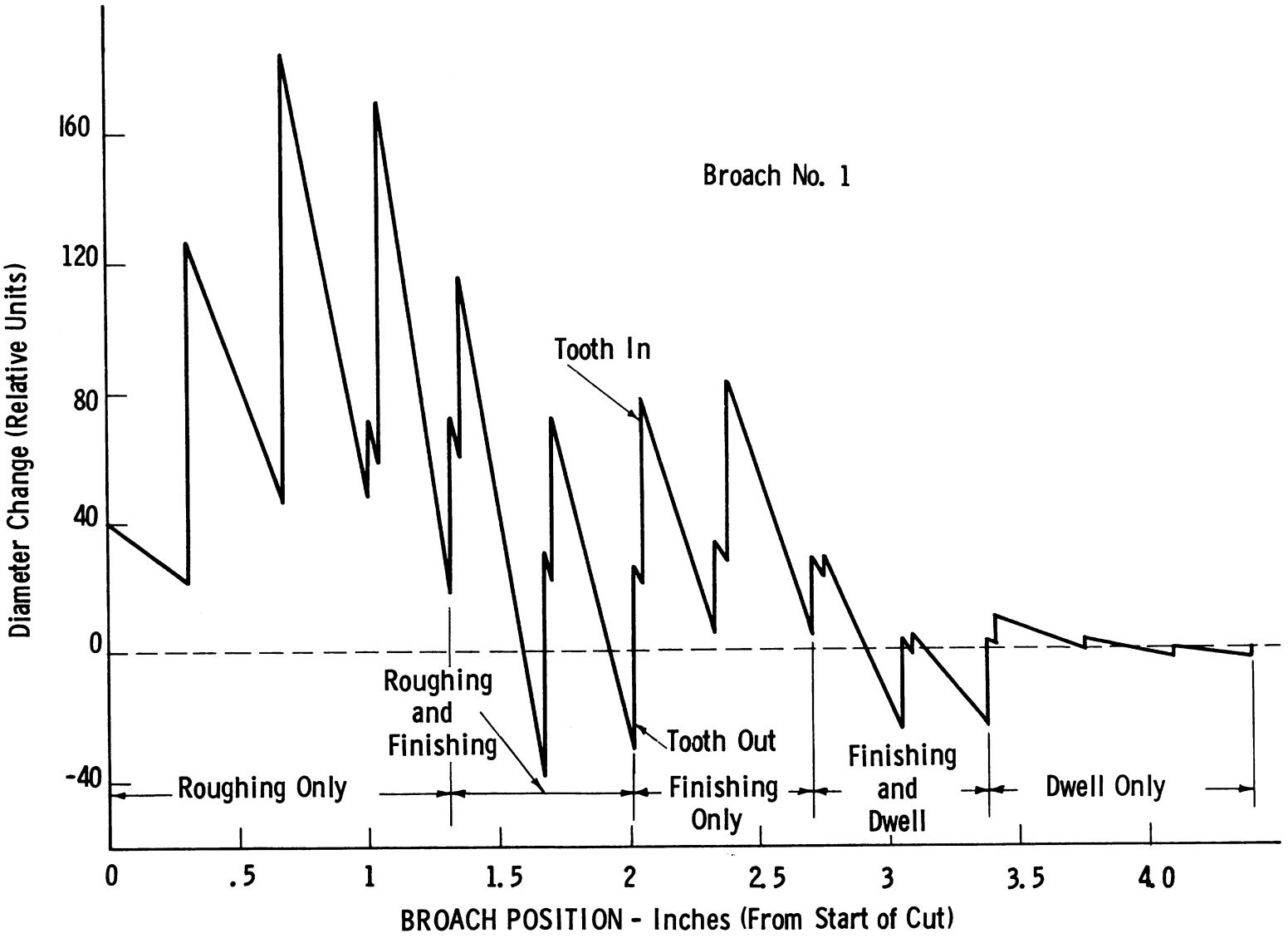

Fig. 4.42. Relative theoretical diameter changes at top of bushing vs. broach position. Changes due to normal forces. Calculations based upon assumption that normal force gave rise to direct tensile and bending stresses.

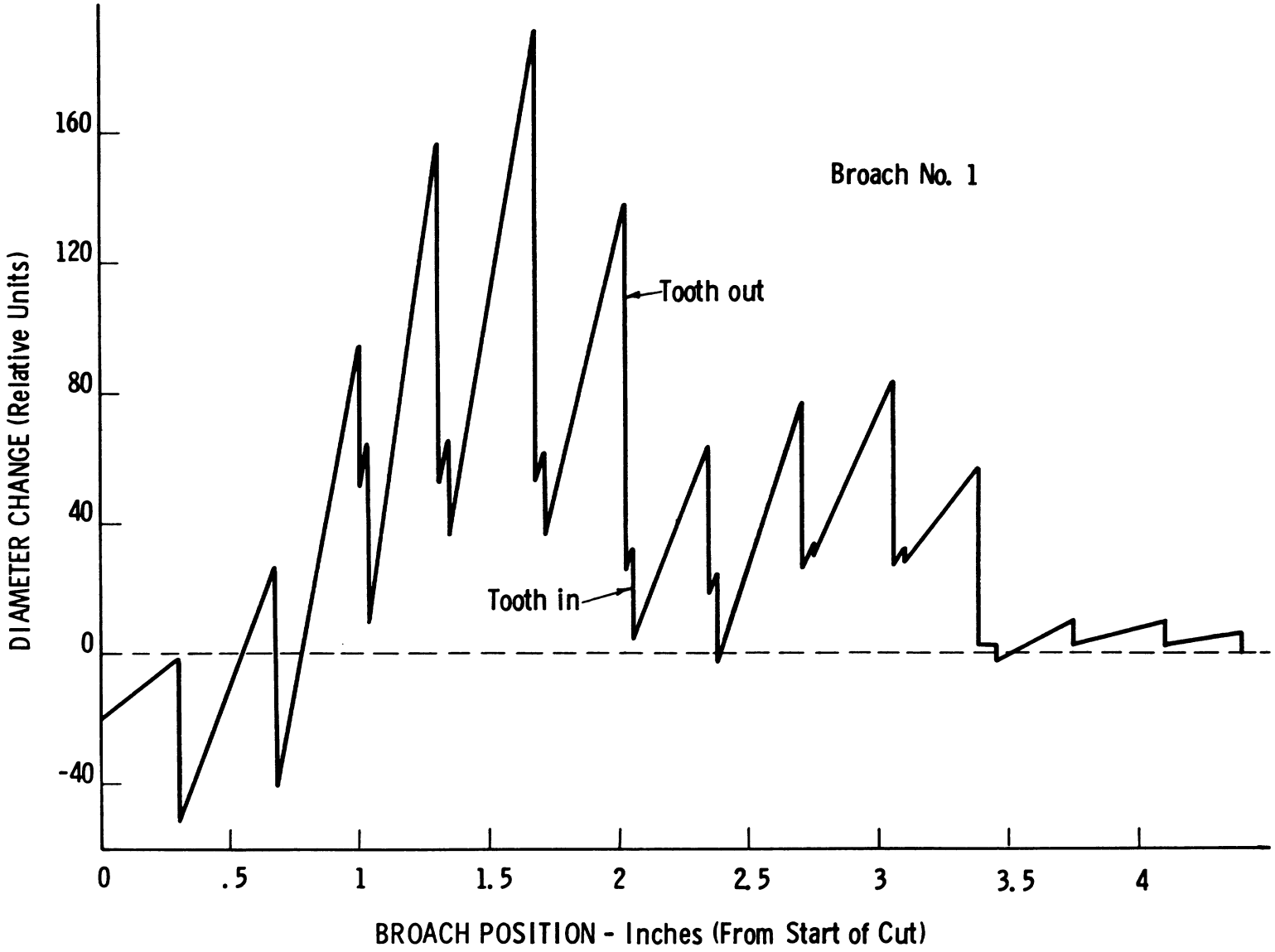

Fig. 4.43. Same as Fig. 4.42 but at bottom of specimen. Note reduction in diameter at start of cut.

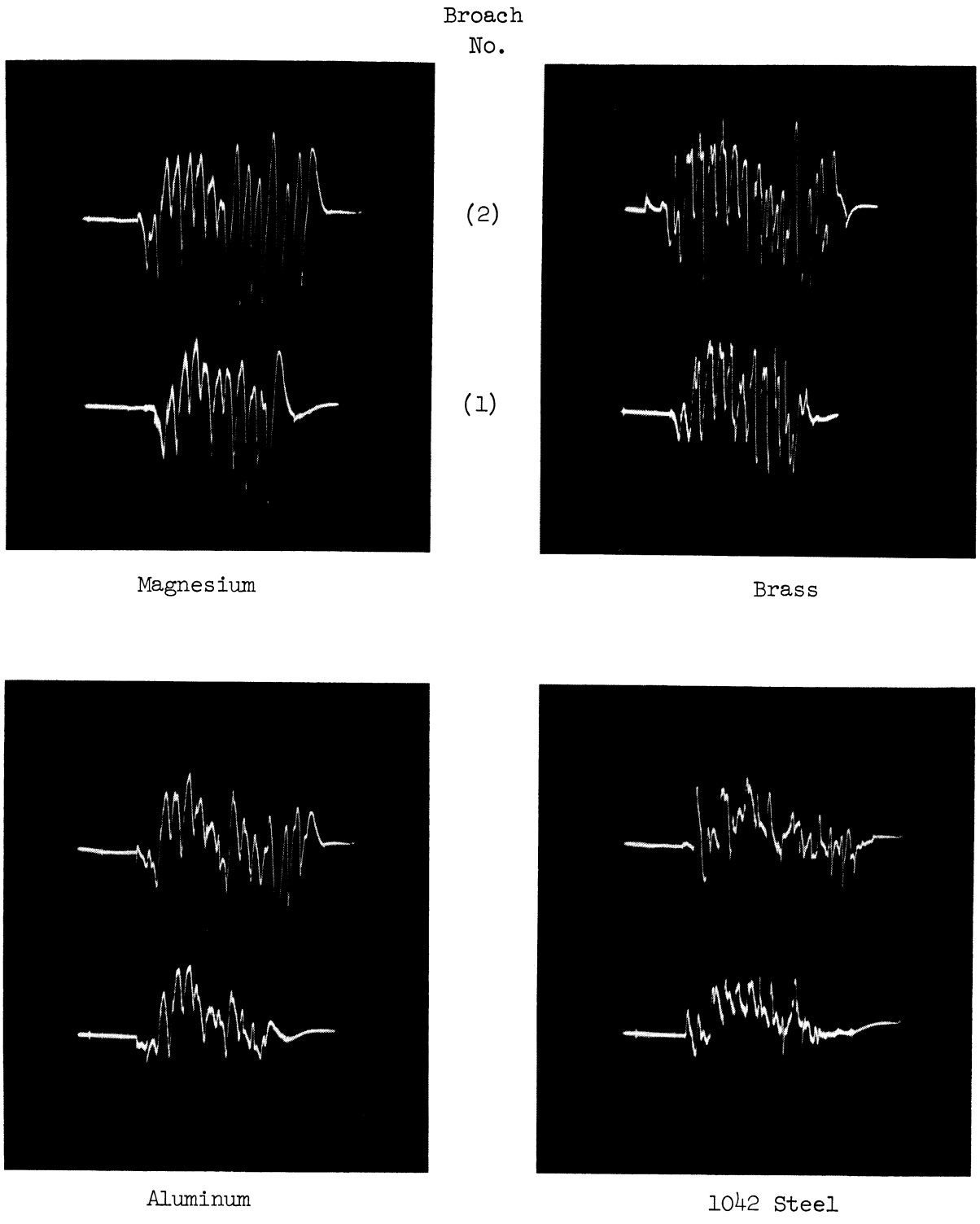

Fig. 4.44. Radial acceleration of broaching specimen. Time increases from left to right at 1/2 sec/centimeter. Deflection upward represents increase in diameter at the accelerometer which was located 3/8 inch from entering end. One centimeter of vertical deflection of trace equals 5 g's of acceleration. Note rapid rise on entrance of teeth into steel.

SECTION V

LABORATORY STUDY INVOLVING THE SHEAR ZONE

There has been some interest recently in the possibility of a cutting fluid having beneficial effects by direct action on the shear zone. Considerable work with carbon tetrachloride has already been done. Most of the results appear to indicate that the chlorine is very effective in preventing rewelding of cracks that develop as the result of shear strain. However, there is no evidence that carbon tetrachloride is capable of spontaneous propagation of such a crack or dislocation. It is exceedingly difficult in any metal-cutting operation to restrict carbon tetrachloride to the shear zone. Therefore, a great deal of the effect of carbon tetrachloride in metal-cutting operations can be attributed to action in the chip-tool interface.

Despite the disappointing results to date in investigating direct action on the shear zone, it was decided to take yet another look at the problem while cutting in the presence of superimposed stress. It was theorized that the spontaneous propagation of any sort of crack, microscopic or otherwise, in the shear zone would require an energy source. Such a source could be the presence of residual stresses in the vicinity of the shear zone. Therefore, a series of tests was carried out with an orthogonal cut in a planer equipped with a fixture which made it possible to superimpose either compressive stress or tensile stress in the surface to be machined.

The apparatus for this investigation is illustrated in Fig. 5.1. The single-point cutting tool was mounted in a two-component dynamometer which made it possible to monitor the cutting forces during the actual cut. The work specimen was in the form of a narrow beam which could be prestressed by the application of a bending moment. Numerous tests were carried out with this arrangement while cutting annealed AISI 1020 steel with a 30° rake-angle high-speed steel-cutting tool. Cuts were made with no superimposed stress as well as at compressive and tensile stresses of 40,000 pounds per square inch. This was done not only for dry cutting but also with Fluids Nos. 6 and 10 representing extremes of lubrication capability. These results yielded no evidence of direct action of the cutting fluid on the shear zone. Typical cutting force data for all three stress conditions are shown plotted in Figs. 5.2, 5.3, and 5.4; for dry cutting, Fluids Nos. 6 and 10, respectively. There was some evidence that superimposing compressive stress on the work surface reduced the cutting force. However, numerous tests did not yield a statistically valid trend to confirm this. Furthermore, such evidence appeared only with dry cutting and not with the cutting fluids. Thus, one must conclude that there is no significant direct action of the cutting fluid on the shear zone, at least under the conditions of this investigation. The machined surface had many small cracks and tears which represent areas of stress con-

centration upon which a direct-acting fluid would have an excellent opportunity to assert itself. If such direct action is possible, then it must be that the highly strained condition of the metal immediately adjacent to the work surface must so distort the lattice structure that the necessary energy for crack propagation is no longer available.

Tests were carried out with the orthogonal planing cut with all ten fluids and dry cutting with no superimposed stress. Typical results are summarized in Table 5.1 for a cut thickness of 0.006 inch on workpieces 0.208 inch wide. It will be noted that the more effective cutting fluids reduce the cutting component of force and therefore the energy requirements between 30 and 40%. However, at twice the thickness of cut, the energy requirements are reduced only about 20% by the most effective fluids. Therefore, the lubrication effectiveness has decreased with the heavier cuts, thus supporting the suggestion made in the last section concerning saturation as a limitation on lubrication.

TABLE 5.1

COMPARISON OF FLUIDS BY FORCES AND FINISH

Fluid No.	Force Components, %		Surface Finish
	Cutting	Normal	
			Very poor
Dry	100.0	100.0	(Badly torn,
10	97.3	82.3	erratic, with
8	90.0	76.0	large built-up edge)
			Poor
2	85.6	72.0	(More uniform
7	85.5	65.8	but torn;
4	79.3	57.3	small built-up edge)
9	75.2	52.7	
			Fair
5	71.3	52.0	(Slightly torn;
6	71.3	50.4	small built-up edge)
1	67.1	42.6	
3	63.8	42.6	

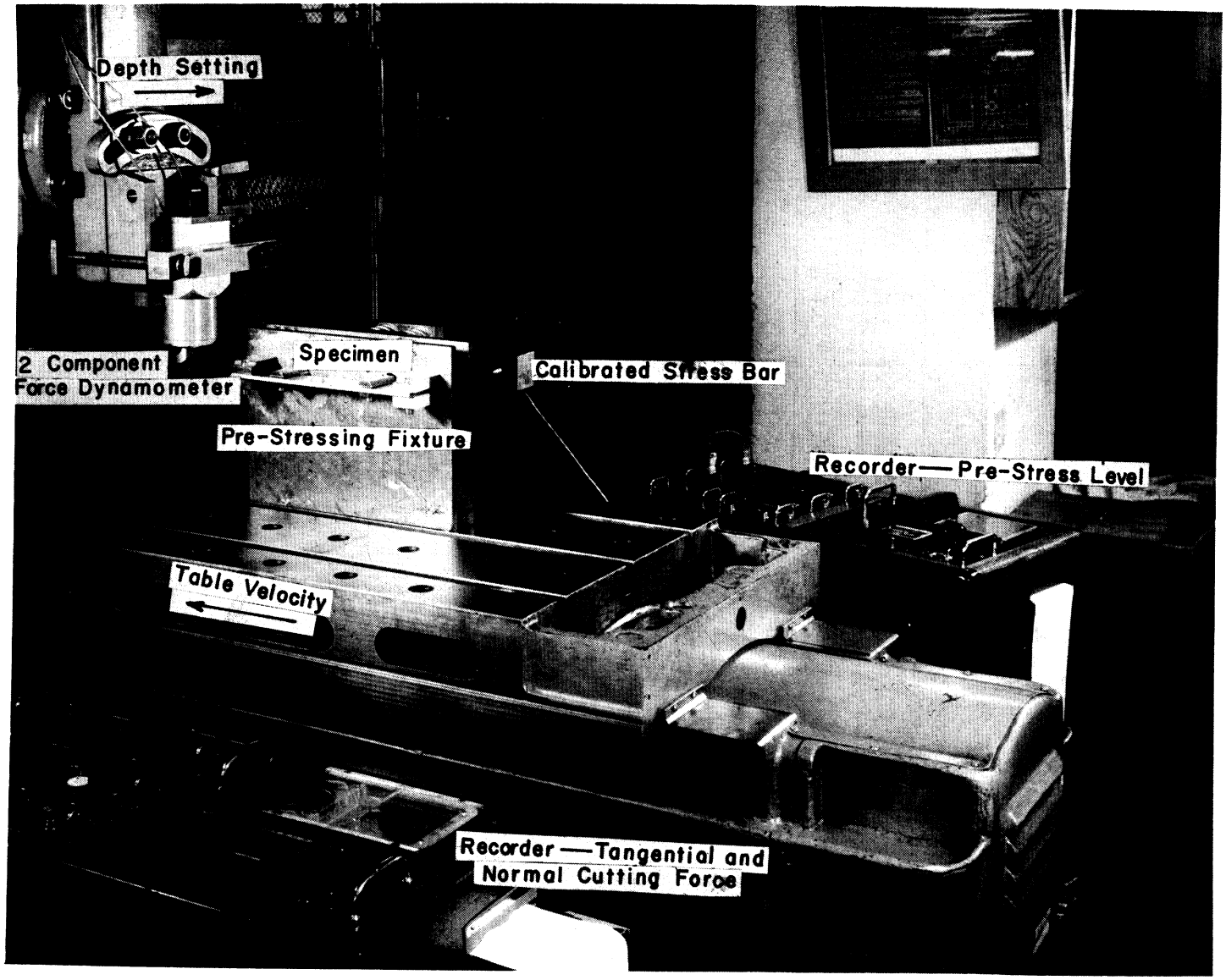

Fig. 5.1. Rockford hydraulic planer equipped with a two-component cutting-force dynamometer and workpiece prestressing fixture. A spring-induced bending load provides either tensile or compressive stresses in surface being cut.

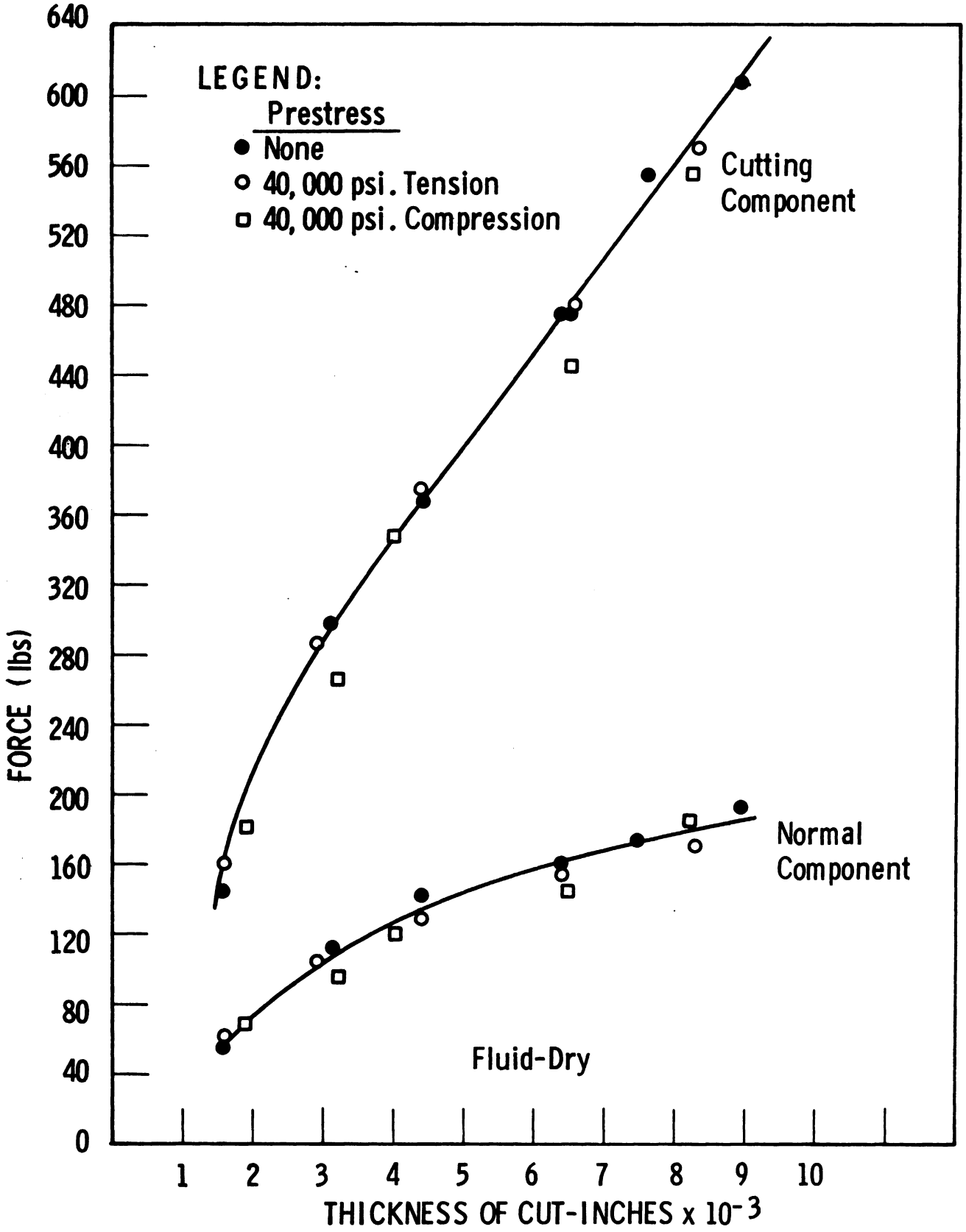

Fig. 5.2. Cutting forces with and without prestress in work surface with 30° rake angle. Width of cut = 0.208 inch. Cutting speed = 14 fpm.

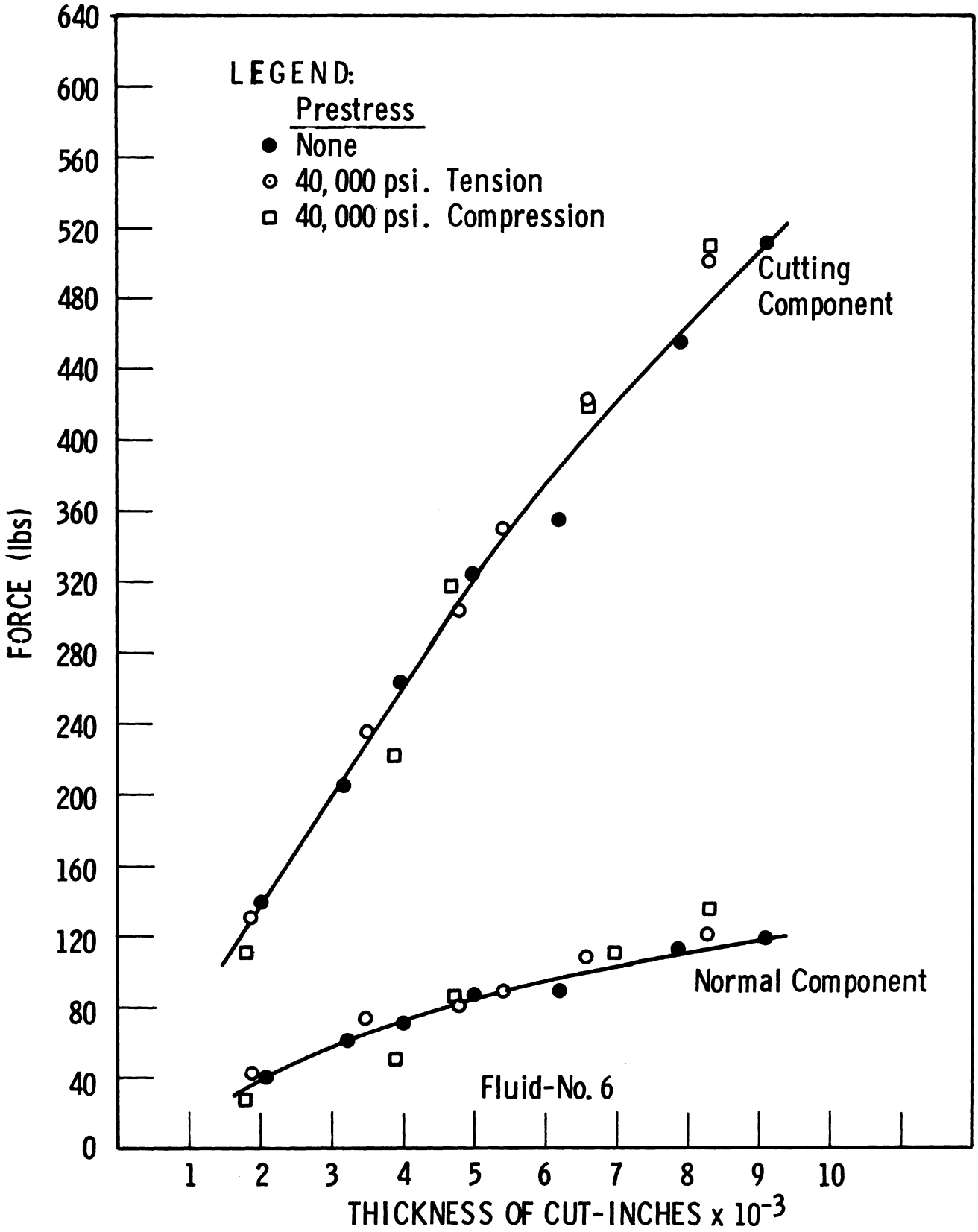

Fig. 5.3. Cutting forces with and without prestress in work surface with 30° rake angle. Width of cut = 0.208 inch. Cutting speed = 14 fpm.

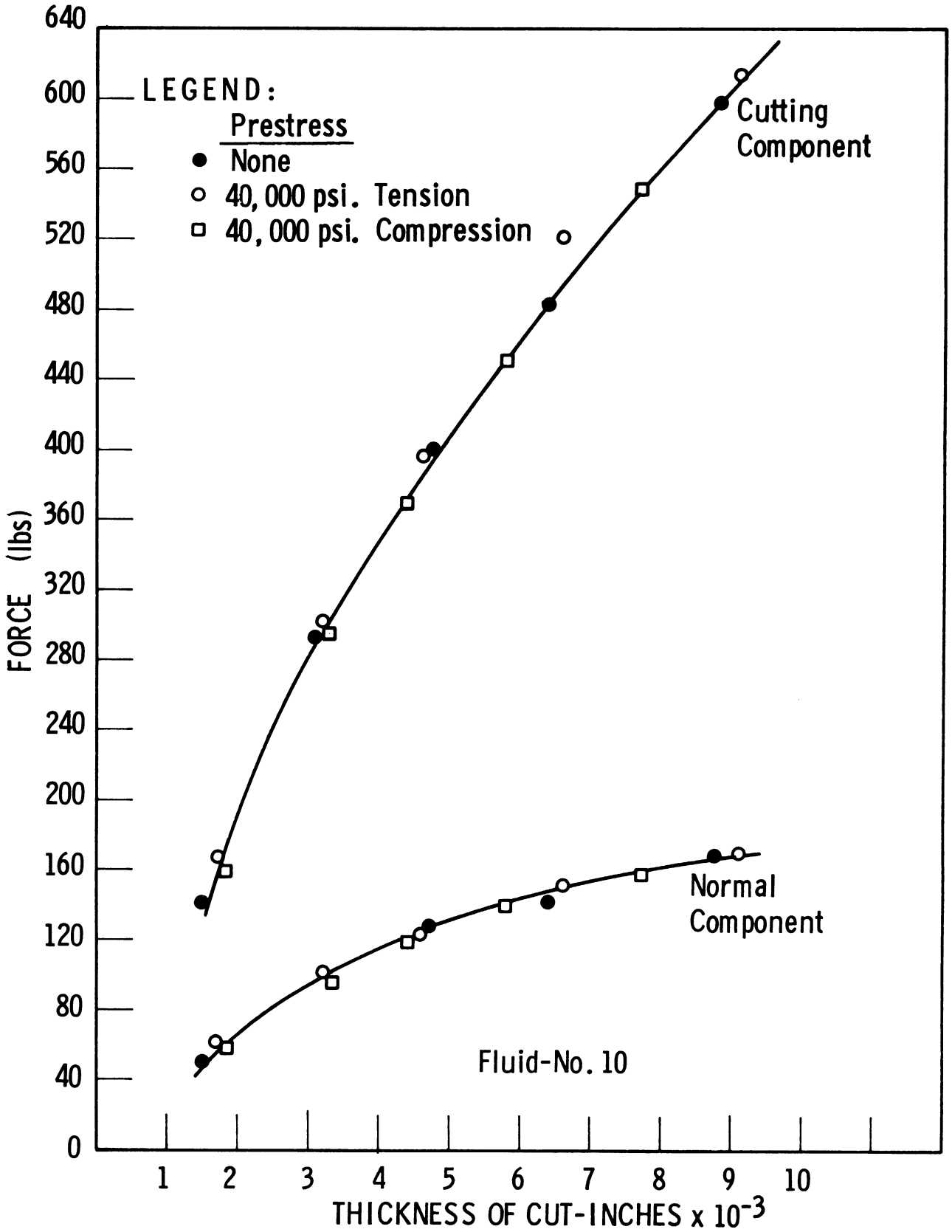

Fig. 5.4. Cutting forces with and without prestress in work surface with 30° rake angle. Width of cut = 0.208 inch. Cutting speed = 14 fpm.

SECTION VI

CONVENTIONAL FRICTION STUDIES

FRICTION-WEAR MACHINE

Wear Studies

Figure 6.1 shows the friction-wear machine in which the ten fluids under study were evaluated. The results were obtained by observing the wear and determining the coefficient of friction for pairs which were run under continuously varying loads while immersed in the fluids. One constant member of the friction pair was a standard hard chrome-plated 1.182 inch diameter spherical surface carried on the rotating spindle of the machine. The other stationary member was one of the seven metals used throughout the various project studies. The load on the stationary member was continuously varied for 10 cycles between a maximum normal load of 40 pounds and a minimum of 20 pounds. All specimens were ultrasonically cleaned before and after each test to assure maximum cleanliness. Records of the normal load and torque reaction were taken continuously throughout the tests.

The wear results are tabulated in Table 6.1. It is obvious that mere observation of wear patterns themselves is not sufficient to draw final conclusions from these tests. Because of the nature of some of the fluids, the chemical reactions that can and must take place between the newly worn surfaces and the fluids have an important influence on wear rates. Therefore, final interpretation must be based on more knowledge of the chemistry of the fluids and their reactions with the metals used.

With respect to the fluids, the following was noted:

Fluid No. 1: Aluminum wore significantly more than other metals, while copper exhibited about half as much wear and was corroded. Very moderate wear on magnesium and 1042 steel.

Fluid No. 2: Very moderate wear on all metals except 1042 steel, on which there was none.

Fluid No. 3: Equal wear on brass, magnesium, and copper—equivalent to wear on copper with Fluid No. 1. Moderate wear on aluminum. Steels virtually unaffected.

Fluid No. 4: Copper wore the most—equivalent to the wear with Fluid No. 1. Aluminum and magnesium wore about half as much. Brass wore very moderately. 1018, 1042, and stainless steels were virtually unaffected.

Fluid No. 5: Very little wear on any metals. Copper and aluminum were worn most, and 1042 steel exhibited no wear.

Fluid No. 6: Aluminum wore considerably, with copper a bit less and corroded. Magnesium wore about half as much as copper; brass wore moderately, and steels not at all.

Fluid No. 7: Magnesium wore moderately; aluminum, brass, and copper wore very little. Steels showed even less wear.

Fluid No. 8: Moderate wear on aluminum, much less on copper and magnesium. Negligible wear on all others.

Fluid No. 9: Magnesium wore very heavily and the fluid turned black. Aluminum wore about half as much, while copper wore half as much as aluminum, with stainless steel a little less than aluminum. Brass, and 1018 and 1042 steels showed virtually no wear.

Fluid No. 10: Very moderate on magnesium, with very little on copper, aluminum, brass and 1018 steel. Virtually none on 1042 and stainless steel.

The following observations were made with respect to the additives and the measured wear results:

1. 2.5% Chlorafin 40—added to Fluid No. 1 (Sunicut 100):
   Reduced the wear on aluminum but appeared to increase wear on brass and magnesium significantly.

2. 2.5% Chlorafin 40—added to Fluid No. 8 (98G):
   Reduced the wear on aluminum.

3. 11% Sulchlor 99—added to Fluid No. 8 (98G):
   Reduced the wear on aluminum. Significantly increased wear on copper. Moderately increased wear on magnesium and 1042 steel. Significantly greater wear on copper and 1042 steel compared with Chlorafin 40. Somewhat less wear on aluminum and magnesium compared with Chlorafin 40.

4. 2.5% Ortholeum 162—added to Fluid No. 8 (98G):
   Reduced wear on aluminum. Significantly increased wear on magnesium and to a lesser extent, wear on brass.

These conclusions were drawn regarding the fluids:

1. Fluid No. 9 was the least effective, although it had little effect on the wear on 1018 and 1042 steels.

2. Fluid No. 10 was the most effective and caused the least wear.

3. Fluid No. 8 was next in effectiveness in minimizing wear.

4. Fluid No. 2 was third in effectiveness in minimizing wear.

The following visual observations with respect to the wear on the metals were made:

Aluminum:	Fluids Nos. 2, 5, 7, and 10 caused the least wear. Fluids Nos. 3, 4, and 8 were next. Fluid No. 9 caused the most wear, and with Fluid No. 1 the next most.
Brass:	Fluids Nos. 5 and 10 caused virtually no wear. Fluids Nos. 1, 6, 8, and 9 caused about equal wear, but only a little more than the first two. Fluids Nos. 2 and 4 were next, and Fluids Nos. 3 and 7 next but causing only slightly greater wear.
Magnesium:	Fluid No. 5 caused very little wear, with No. 8 very close. Fluids Nos. 1, 2, and 10 were similar, with little more wear caused. Fluids Nos. 4, 3, 6, and 7 were ranked in that order, but all caused little wear. Fluid No. 9 caused extreme wear and the fluid turned black.
Copper:	Fluids Nos. 4 and 10 caused the least wear, with Fluids Nos. 2, 7, and 8 very close in that order. Fluids Nos. 1 and 3 caused some wear and corroded the specimens. Fluid No. 5 caused more wear, while Fluid No. 6 both corroded the specimen and caused even more wear. Fluid No. 9 caused the most wear.
1042 Steel:	Fluids Nos. 2, 5, and 8 caused no wear. Fluids Nos. 1, 3, 6, 9, and 10 caused insignificant wear. Fluids Nos. 4 and 7 caused very little wear.
1018 Steel:	Fluids Nos. 1, 4, and 7 caused insignificant wear, as did Fluids Nos. 3, 6, 8, and 9. Fluids Nos. 2 and 5 caused very little wear.
Stainless Steel:	Fluids Nos. 1, 6, 8, and 10 caused insignificant wear, as did Fluids Nos. 2, 3, 4, and 7. Fluids Nos. 5 and 9 caused very little wear.

Coefficient of Friction Studies

The results of the study showed that the coefficient of friction varied for the same friction pair when the fluid varied. However, the variation in friction coefficient did not appear to have any reasonable correlation with the variation in wear noted in the various friction pairs when they were operated in different fluids. It is to be noted also that the coefficient of friction was not constant throughout each test run.

An analysis of the geometry of the friction-wear tests developed in Appendix C gives rise to the simple relationship that the coefficient of friction, $\mu = 2T/ND$, where T is the torque reaction in pounds-inches, N is the normal load between the pair, and D is the diameter of the rotating sphere in inches. Thus, if μ is a constant for a particular pair and fluid, then the torque is directly proportional to μ since both N and D are also constants. μ may then be directly computed from the recorded values of torque at the load conditions of the test.

Table 6.2 is a tabulation of computed values of the coefficient of friction under the conditions of test. Figure 6.2 is a typical chart of the normal load and torque variations for a representative test cycle, in which the normal load was varied between 40 and 20 pounds for ten cycles. Because of the change in torque between the first cycle of a test and the last cycle of a series, the friction coefficient was computed for both the beginning and end of the series, which accounts for the two values of μ for each fluid and metal combination. There is a dual tabulation because μ was also computed for both the 40- and the 20-pound normal load, using the resultant torque for both the beginning and the end of the ten cycles.

The plots given in Figs. 6.3 through 6.16 show the effect of the fluid on the wear for each metal tested, and the effect of the fluid on the coefficient of friction for each pair at the beginning and at the end of each test run.

The following observations with respect to friction coefficient by fluids should be noted:

Fluid No. 1: Lowest for aluminum, with greatest change on brass. Little change for steels.

Fluid No. 2: Lowest on magnesium; highest on steels, but without much change. Values at minimum load more erratic but generally followed same trend.

Fluid No. 3: Highest on steels, but with little change. Large changes on nonferrous metals.

Fluid No. 4: Little change; highest on steels.

Fluid No. 5: Large change on copper; little change on others. Low on aluminum.

Fluid No. 6: Large change on aluminum and magnesium. Little change on others.

Fluid No. 7: Large change on aluminum and magnesium. Little change on others.

Fluid No. 8: Large changes on nonferrous metals with little on steels at maximum load but more at minimum load.

Fluid No. 9: High values for all, with magnesium very high.

Fluid No. 10: Large changes in magnesium which had the lowest friction coefficient. Little change in others.

The following observations on friction coefficients with respect to additives to the fluids are pertinent:

1. 2.5% Chlorafin 40—Fluids Nos. 8 and 2 (8+2.5% Chlorafin 40): Had no major effect on 1018 and stainless steels. Reduced wear somewhat on 1042. Its principal effect was an increase in the friction coefficient of aluminum and brass, which indicated a probable chemical reaction.

2. 11% Sulchlor 99—Fluids Nos. 8 and 4 (8+11% Sulchlor 40): Reduced friction coefficient of brass, and 1018 and 1042 steels. Reduced initial friction coefficient of aluminum.

3. .25% Ortholeum 162—Fluids Nos. 8 and 7 (8+.25% Ortholeum 162): Little effect on aluminum. Increased friction coefficient of brass markedly at all conditions. Decreased friction coefficient of magnesium initially but increased it at end and at minimum load.

4. 2.5% Chlorafin 40 and .25% Ortholeum 162—Fluids Nos. 2 and 7: Fluid No. 2 reduced the friction coefficient of copper after running, and reduced the friction coefficient of 1018 steel. Fluid No. 7 reduced the aluminum and magnesium friction coefficient after cycling. It also reduced the friction coefficient of 1042 steel.

5. 2.5% Chlorafin 40 and 11% Sulchlor 99--Fluids Nos. 2 and 4:
Fluid No. 4 reduced the friction coefficient of aluminum appreciably compared to Fluid No. 2. Fluid No. 2 reduced the friction coefficient of 1018 steel appreciably compared to Fluid No. 4. Fluid No. 4 caused an appreciable drop in the friction coefficient of magnesium and copper after running, and brass to a lesser degree. Fluid No. 2 caused a drop in the friction coefficient of stainless steel after running.

6. 11% Sulchlor 99 and .25% Ortholeum 162—Fluids Nos. 4 and 7:
Fluid No. 4 reduced the friction coefficient of aluminum and copper; Fluid No. 7 reduced it for brass and 1042 steel.

7. 2.5% Chlorafin 40 and Sunicut 100—Fluids Nos. 1 and 3:
Addition of Chlorafin 40 to Sunicut 100 increased the friction coefficient of aluminum markedly, and that of 1018 and 1042 steel to a lesser degree. It decreased the friction coefficient of brass.

8. 2.5% Chlorafin 40—Fluids Nos. 2 and 3:
Chlorafin 40 added to 98G effectively reduced the friction coefficient of copper, and of 1018 and stainless steel, particularly by the end of the runs. Chlorafin 40 added to Sunicut 100 reduced the friction coefficient of aluminum, brass, and magnesium at the end of the runs.

Graphical plots of the coefficient of friction and the wear for each metal with respect to the fluid are shown in the appendix. These plots illustrate the observations made above.

Lack of correlation between wear data and coefficients of friction may be attributed to a change in the basic geometry of the friction pair. The change may be due to both elastic relaxation and to the total wear that has occurred. Chemical reactions between the fluids and the worn surfaces also will influence the wear and the friction, as evidenced by both data and observations. There may also be some effects from the temperatures generated that would influence chemical reactions, wear, and friction.

CONSTANT-ENERGY APPARATUS

Another method of evaluating the fluids under study is to determine how they influence the damping of a constant-energy system by increasing or decreasing the frictional forces present. Those fluids which cause the dynamic system to dampen more quickly tend to be less beneficial in reducing friction while those fluids which aid in maintaining the motion of a dynamic system are more beneficial in reducing friction.

The constant-energy system used in this study is shown in Fig. 6.17. It is heavy steel table mounted on vertical cantilever beams to which are bonded electrical resistance wire strain gages which monitor the motion of the table. One member of a friction pair is mounted on the table. The other member is a balanced 1/2-inch hardened precision steel ball which may be loaded onto the table-mounted member with known weights. The fluid to be evaluated is dropped on the specimen, a suitable load is applied to the ball and the table is displaced a measured amount. It is released and the decay of its motion is recorded by suitable strain gage measurements.

The theory developed to interpret the results of these tests is completely explained in the appendix. Because of the light loads, which ranged from no load to 150 grams, and the fact that the system was not heavily damped, the log-decrement relationship developed was of a form which permitted the use of an arbitrary number of cycles for evaluating the damping curves. The relationship is:

$$\delta = \frac{\ln \frac{X_1}{Xn}}{n-1}$$

where

δ = log-decrement
X_1 = amplitude of first cycle
Xn = amplitude of first cycle in which dampout was 80%
n = number of cycles in which 80% dampout occurred.

If n is then plotted on log-log paper against the load applied to the friction pair, a series of graphs which compare the influence of the fluids on the friction characteristics of the pair is obtained. Those fluids which reduce friction more will have a larger number of cycles to 80% dampout than those which have less effect and permit the system to dampen out sooner.

The results of the tests show that Fluid No. 5 was most effective in reducing friction except in the case of magnesium and stainless steel. It was quite satisfactory with the magnesium and compared favorably with the other fluids. It was somewhat better than Fluid No. 8 with stainless steel but considerably below the other fluids except at a 10-gram load.

Fluid No. 5 provided consistently more cycles to 80% dampout for aluminum, brass, copper, 1042 steel (except at 10 grams), and 1018 steel.

Fluid No. 6 was consistently second best for brass except at 10 grams, while Fluid No. 4 was second best for copper except at 10 grams and was generally second best for 1018 steel. Fluid No. 7 was second best for stainless steel except at 20- and 10-gram loads. Fluid No. 1 was second best for aluminum except at 20 and 10 grams, where Fluid No. 7 was second best. No fluid was consistently second best for magnesium.

It is evident from the data taken that the chemical action of the fluid upon the surfaces in contact must play an important part in the friction, and therefore in the damping relations that exist. It would appear that the inconsistent results obtained at lower loads must also be related to the film strength of the fluids and the relative roughness of the surfaces.

TABLE 6.1

TEST SPECIMEN WEAR MEASUREMENT

(The increase in chord length of the spherical test surface is measured in inches.)

Fluid No.	Aluminum	Brass	Magnesium	Copper	1042 Steel	1018 Steel	Stainless Steel
1	.0265	.0016	.0048	.0130	.0041	.0014	0
2	.0035	.0033	.0040	.0025	0	.0036	.0027
3	.0055	.0118	.0130	.0135	.0023	0	.0005
4	.0085	0038	.0075	.0145	.0065	0	0016
5	.0050	.0008	0	.0020	0	.0007	.0096
6	.028	.0006	.0135	.0225	.0023	.0010	0
7	.0035	.0069	.0120	.0010	.0043	0	.0018
8	.0115	.0002	.0020	.0020	.0004	0	.0007
9	.0360	.0006	.0835	.0185	.0007	.0010	.0170
10	.0010	0020	.0075	.0016	.0032	.0020	.0010

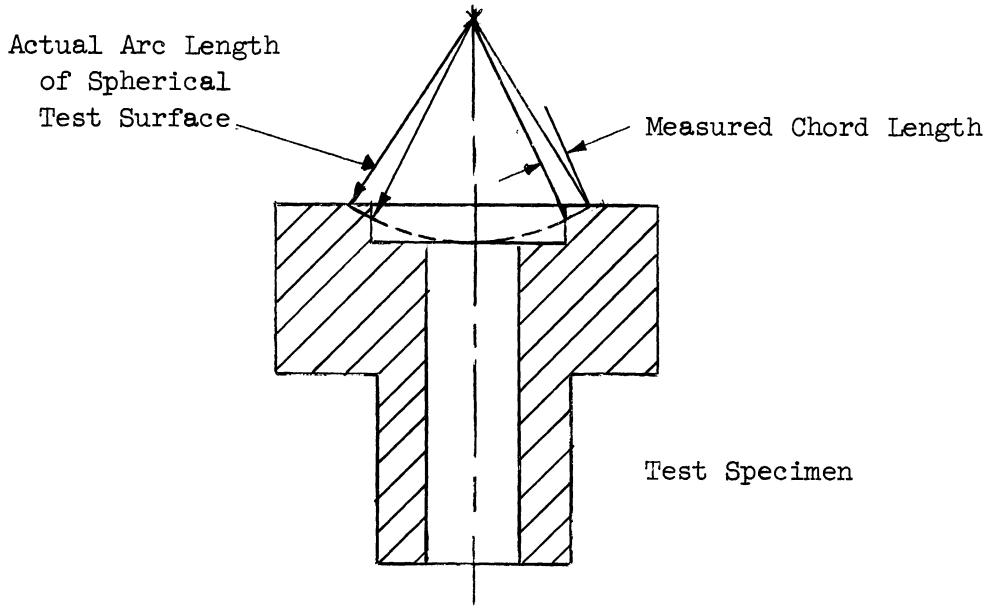

TABLE 6.2

FRICTION-WEAR TESTS

Fluid No.	Normal Load (lb)	Dynamic Friction Coefficients (Type B Specimens)													
		Aluminum		Brass		Magnesium		Copper		1042 Steel		1018 Steel		Stainless Steel	
		B*	E*	B	E	B	E	B	E	B	E	B	E	B	E
1	40	.101	.046	.220	.169	.195	.165	.246	.110	.195	.165	.203	.199	.233	.228
	20	.063	.017	.199	.131	.127	.085	.228	.101	.170	.110	.177	.148	.195	.212
2	40	.165	.152	.182	.169	.140	.140	.165	.119	.228	.212	.186	.190	.228	.186
	20	.161	.148	.182	.148	.093	.093	.123	.068	.212	.152	.170	.136	.177	.136
3	40	.169	.131	.190	.148	.174	.131	.198	.097	.246	.233	.246	.220	.233	.224
	20	.177	.098	.177	.085	.161	.103	.220	.119	.228	.220	.254	.220	.245	.245
4	40	.110	.122	.199	.177	.161	.101	.182	.119	.237	.220	.237	.220	.199	.203
	20	.051	.055	.199	.085	.123	.059	.115	.059	.220	.186	.245	.212	.140	.161
5	40	.122	.114	.186	.165	.182	.169	.161	.114	.190	.182	.144	.148	.169	.178
	20	.106	.098	.161	.127	.144	.110	.089	.042	.170	.136	.110	.110	.085	.063
6	40	.140	.072	.182	.165	.140	.076	.161	.157	.203	.173	.199	.182	.203	.212
	20	.114	.034	.195	.140	.072	.017	.115	.101	.190	.148	.203	.182	.224	.228
7	40	.161	.106	.165	.161	.148	.093	.165	.169	.199	.178	.233	.212	.212	.212
	20	.131	.084	.170	.186	.144	.103	.144	.136	.199	.148	.262	.220	.203	.190
8	40	.165	.098	.174	.127	.161	.127	.169	.122	.186	.182	.182	.174	.203	.190
	20	.136	.059	.136	.059	.098	.076	.115	.059	.148	.118	.136	.106	.136	.114
9	40	.232	.241	.254	.309	.677	.677	.381	.424	.275	.339	.330	.339	.338	.364
	20	.228	.228	.237	.296	.590	.508	.373	.407	.220	.246	.245	.372	.338	.313
10	40	.140	.161	.184	.182	.190	.045	.157	.140	.233	.233	.212	.212	.260	.275
	20	.085	.127	.140	.270	.042	.004	.135	.123	.199	.228	.170	.190	.237	.237

*B - Beginning of tests
E - End of 10 cycles

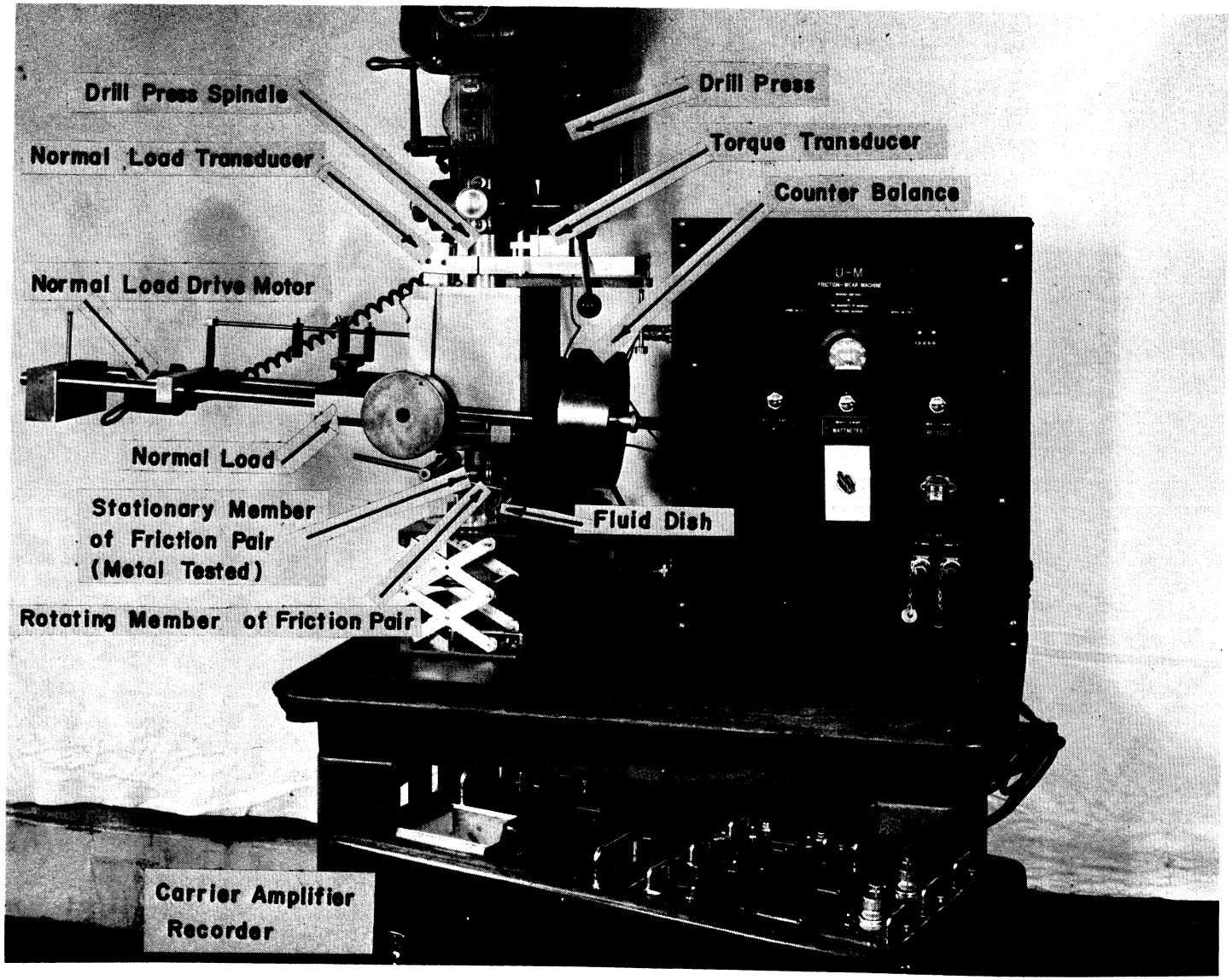

Fig. 6.1. Friction-wear machine.

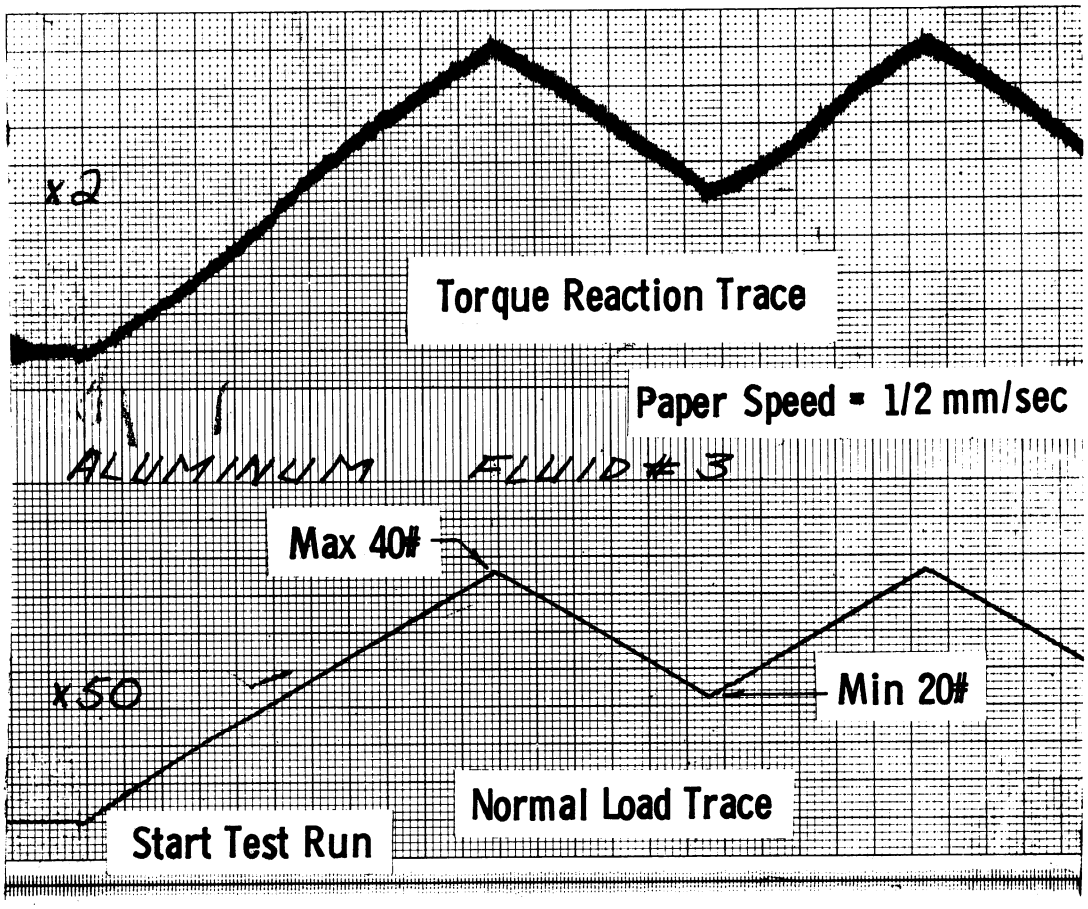

Fig. 6.2. Typical Sanborn Recorded trace.

Calibration:

1. Tangential
   10 lb-in. at 10X = 20 mm
   1 mm = 0.5 lb-in. at 10X
   1 mm = 0.05 lb-in. at 1X
   Elec. Gain = 15 mm at 1X
   Run at 2X

   } Channel No. 916

2. Thrust
   8 lb at 10X = 32 mm
   1 mm = .25 lb at 10X
   1 mm = .025 lb at 1X
   Elec. Gain = 7 mm at 1X
   Run at 50X—1 mm = 1.25 lb

   } Channel No. 921

Set normal load for 0 → 40 lb → 20 lb

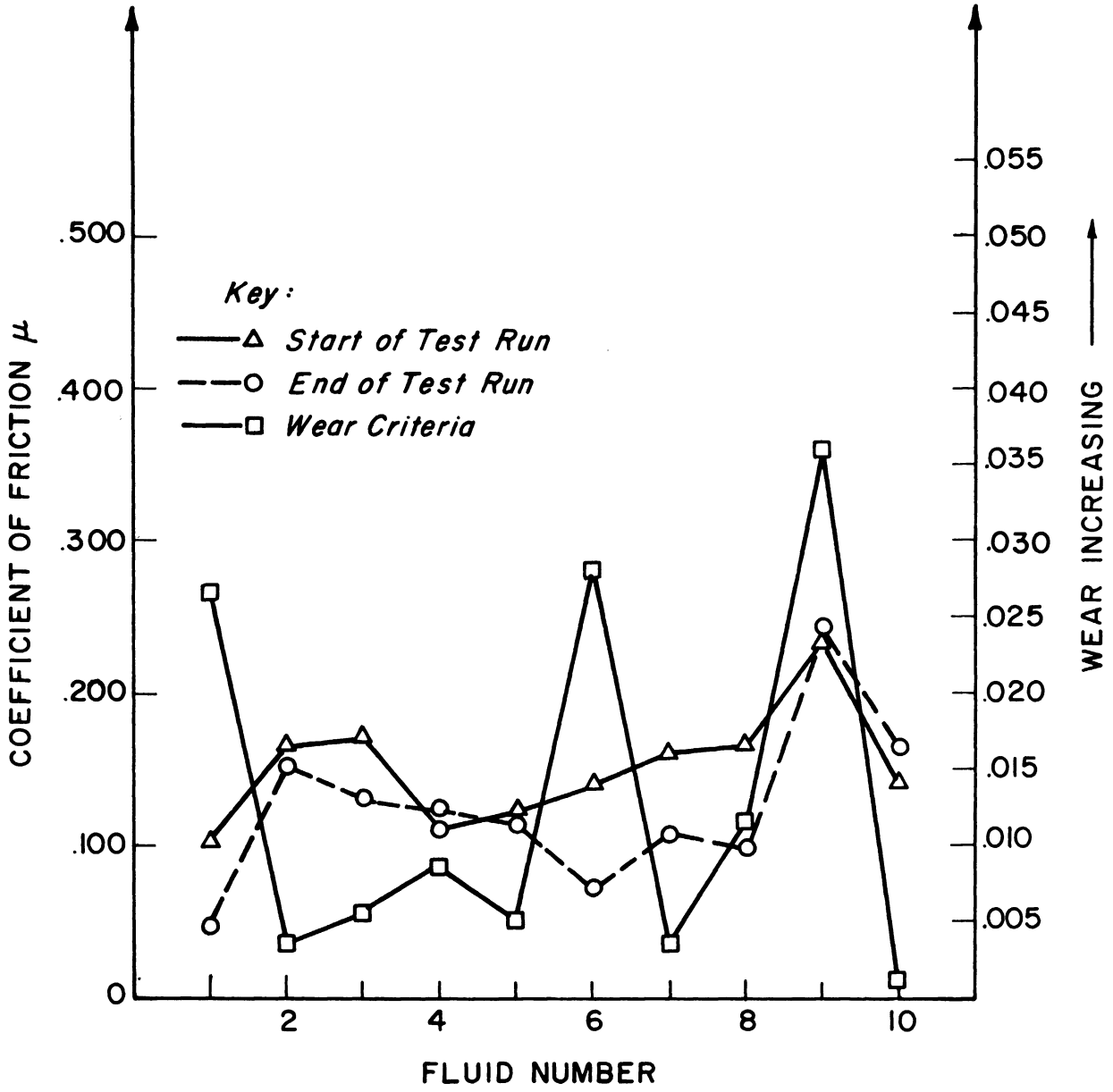

Fig. 6.3. Aluminum specimen coefficient of friction and wear measurement vs. fluid number at maximum normal load—40 lb.

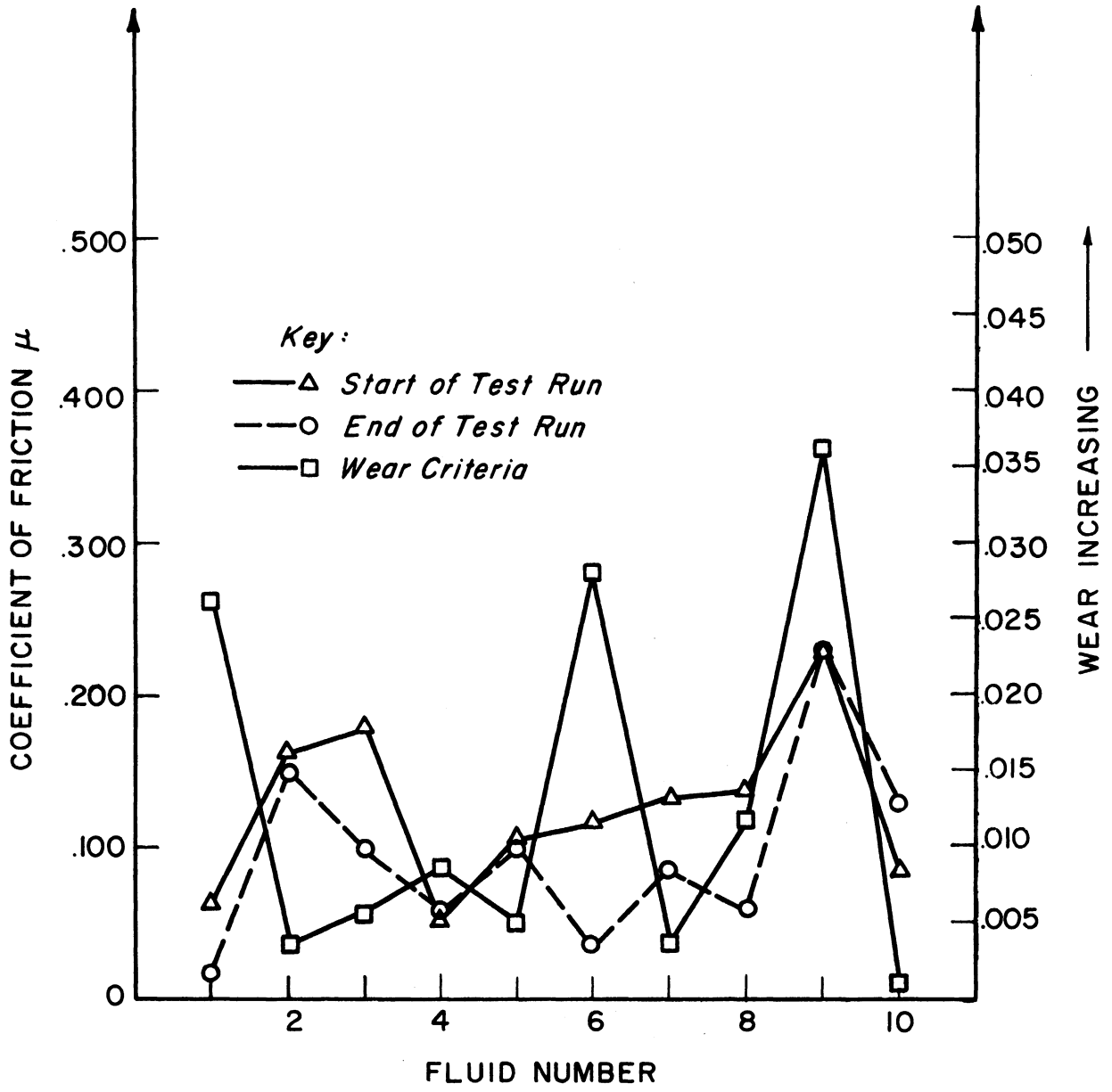

Fig. 6.4. Aluminum specimen coefficient of friction and wear measurement vs. fluid number at minimum normal load—20 lb.

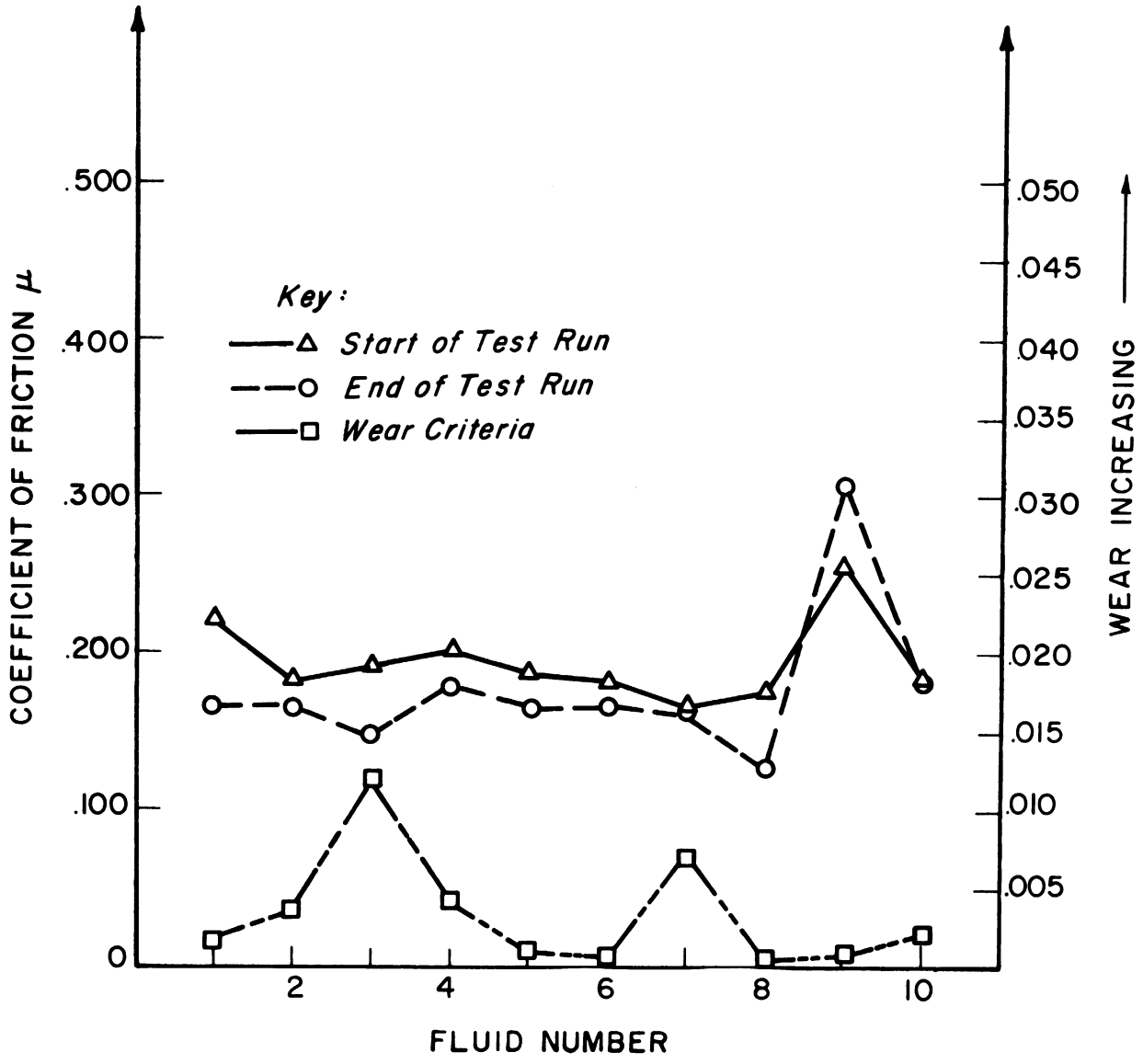

Fig. 6.5. Brass specimen coefficient of friction and wear measurement vs. fluid number at maximum normal load—40 lb.

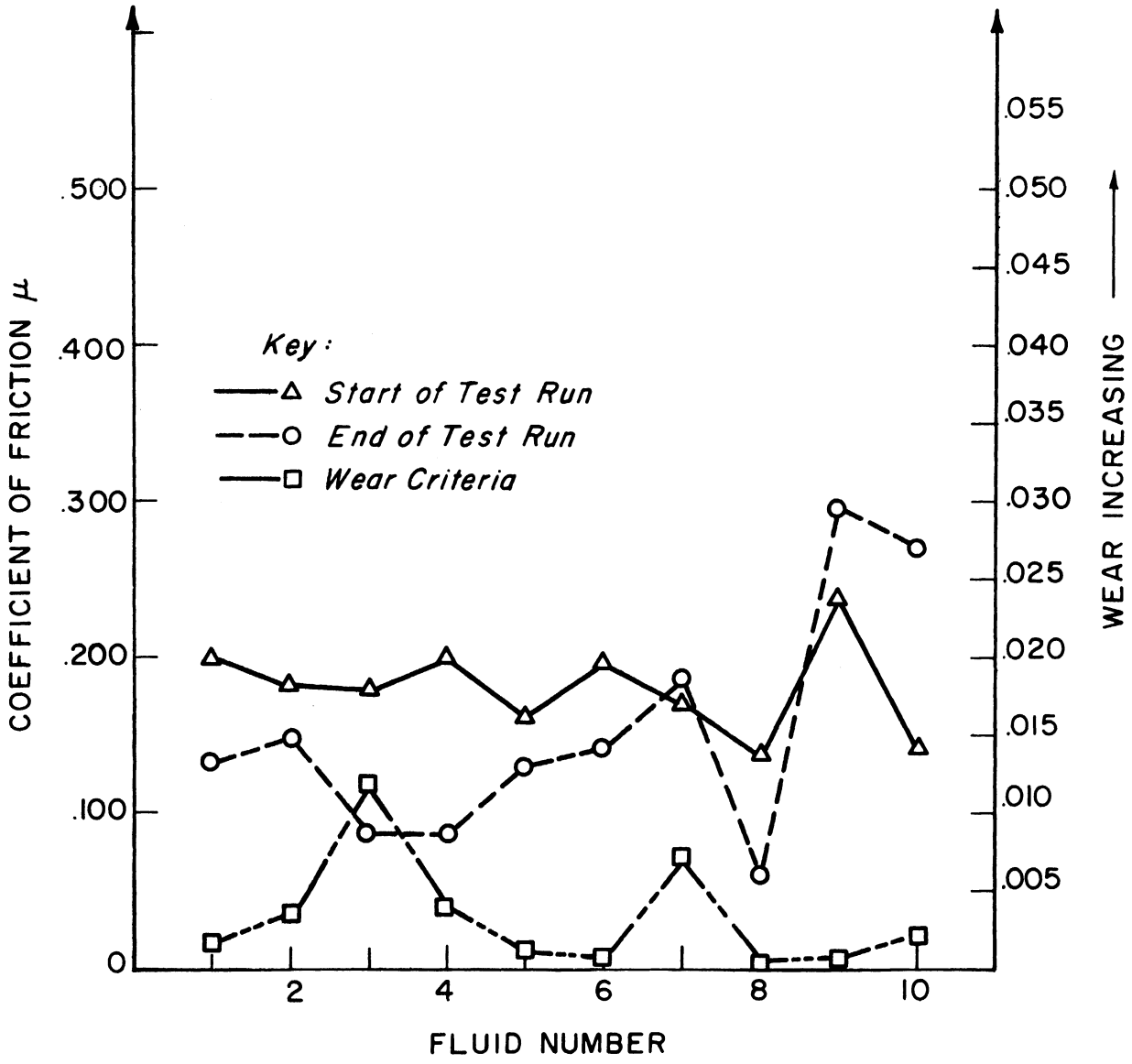

Fig. 6.6. Brass specimen coefficient of friction and wear measurement vs. fluid number at minimum normal load—20 lb.

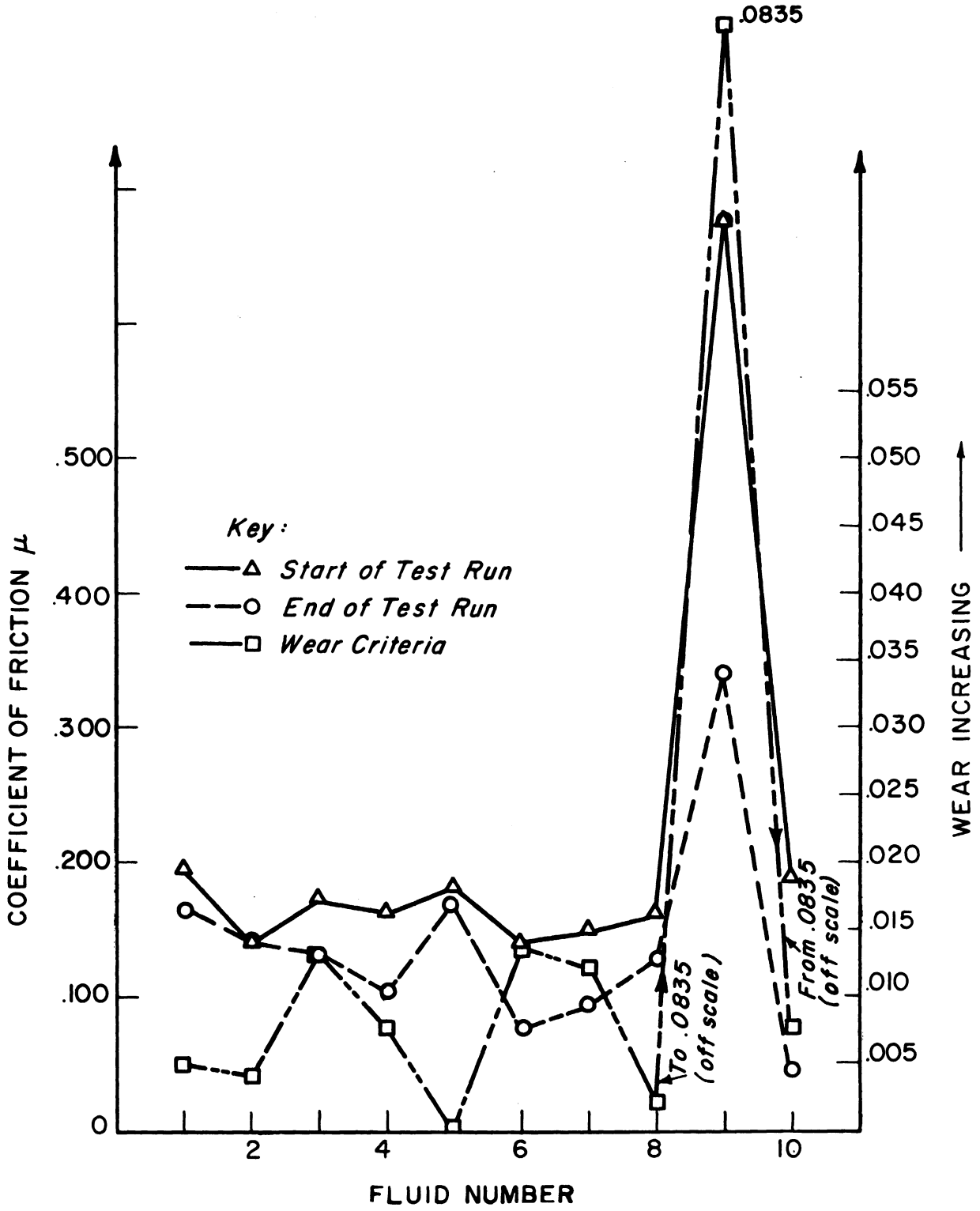

Fig. 6.7. Magnesium specimen coefficient of friction and wear measurement vs. fluid number at maximum normal load—40 lb.

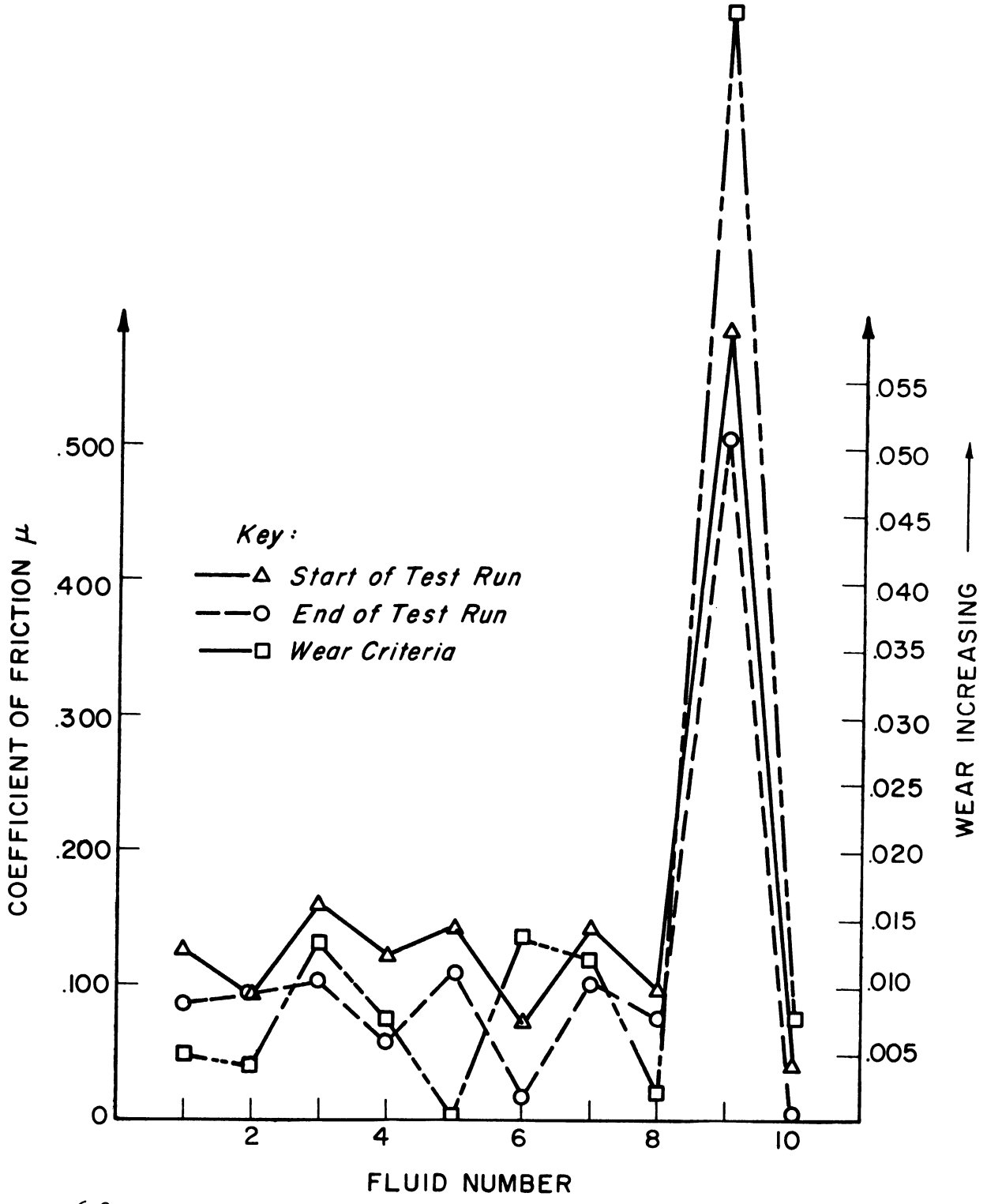

Fig. 6.8. Magnesium specimen coefficient of friction and wear measurement vs. fluid number at minimum normal load—20 lb.

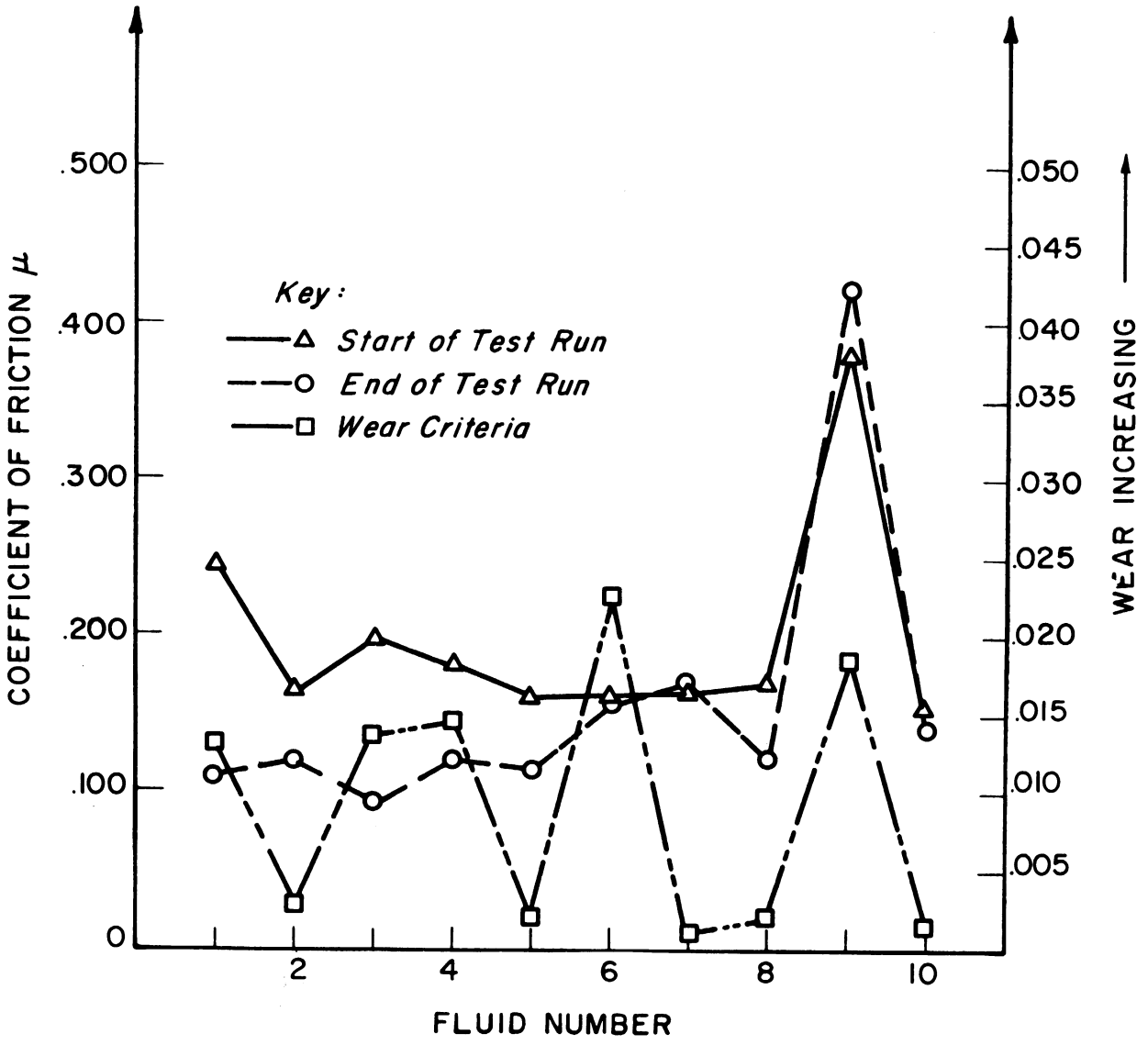

Fig. 6.9. Copper specimen coefficient of friction and wear measurement vs. fluid number at maximum normal load—40 lb.

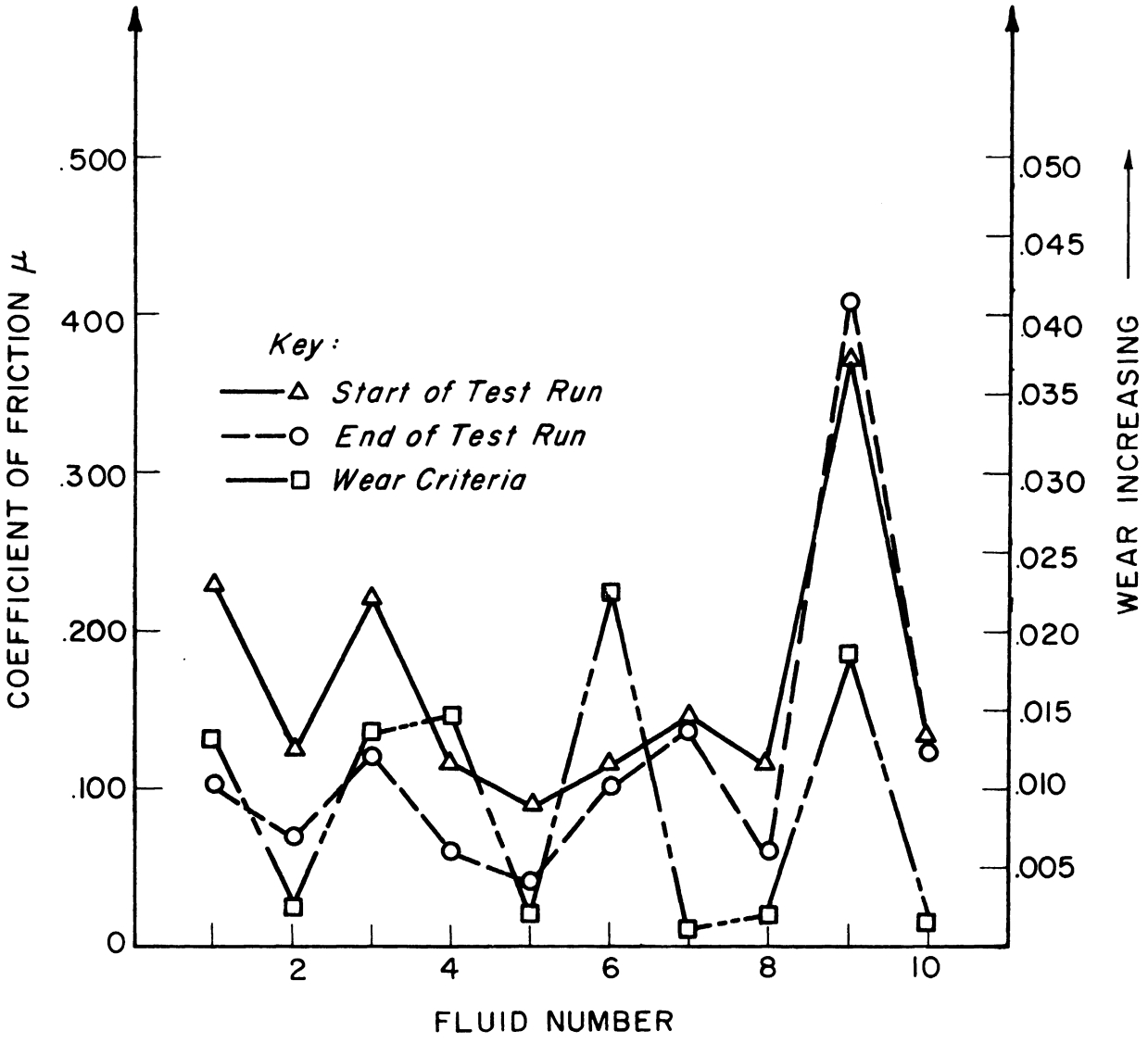

Fig. 6.10. Copper specimen coefficient of friction and wear measurement vs. fluid number at minimum normal load—20 lb.

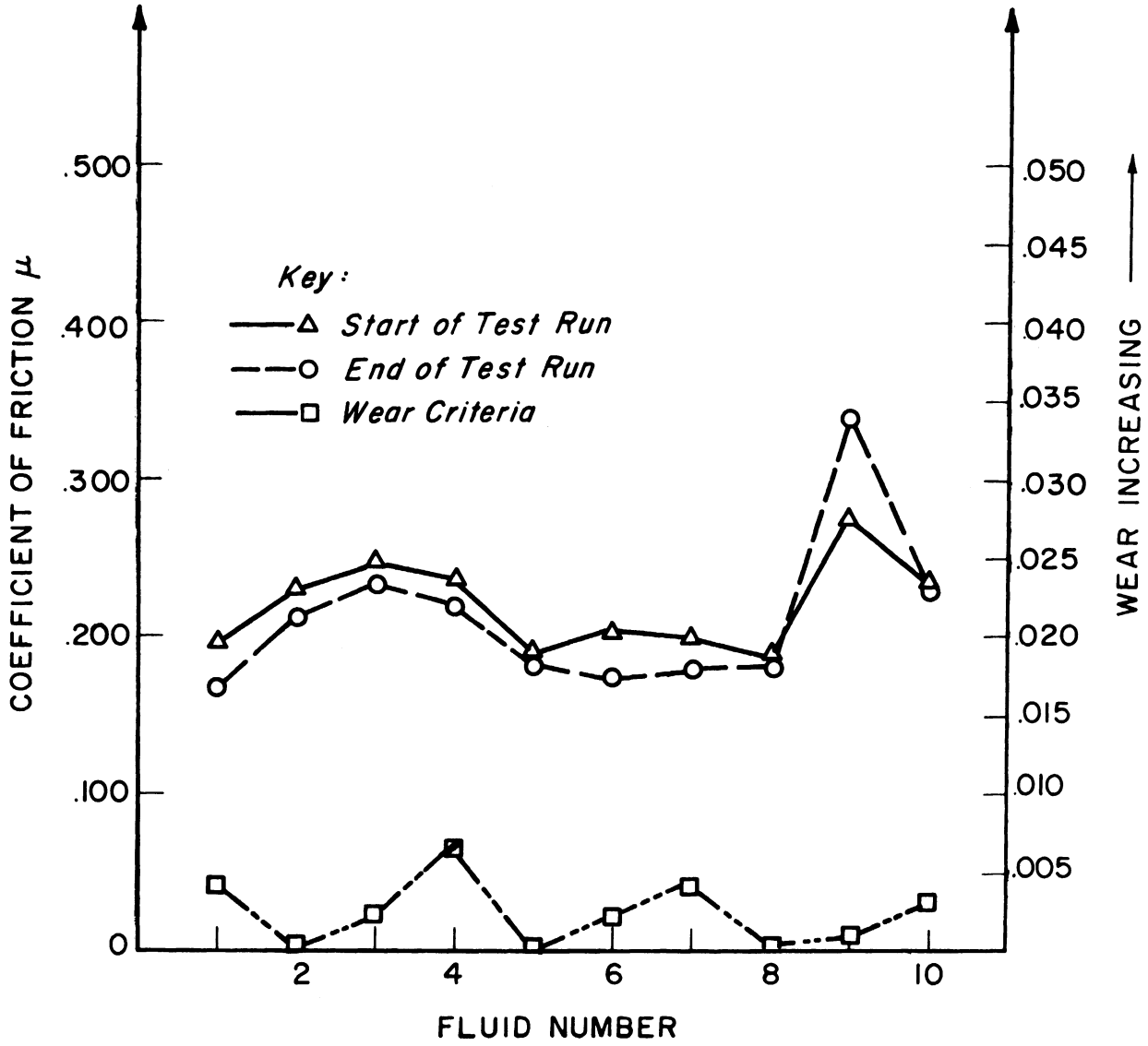

Fig. 6.11. 1042 steel specimen coefficient of friction and wear measurement vs. fluid number at maximum normal load—40 lb.

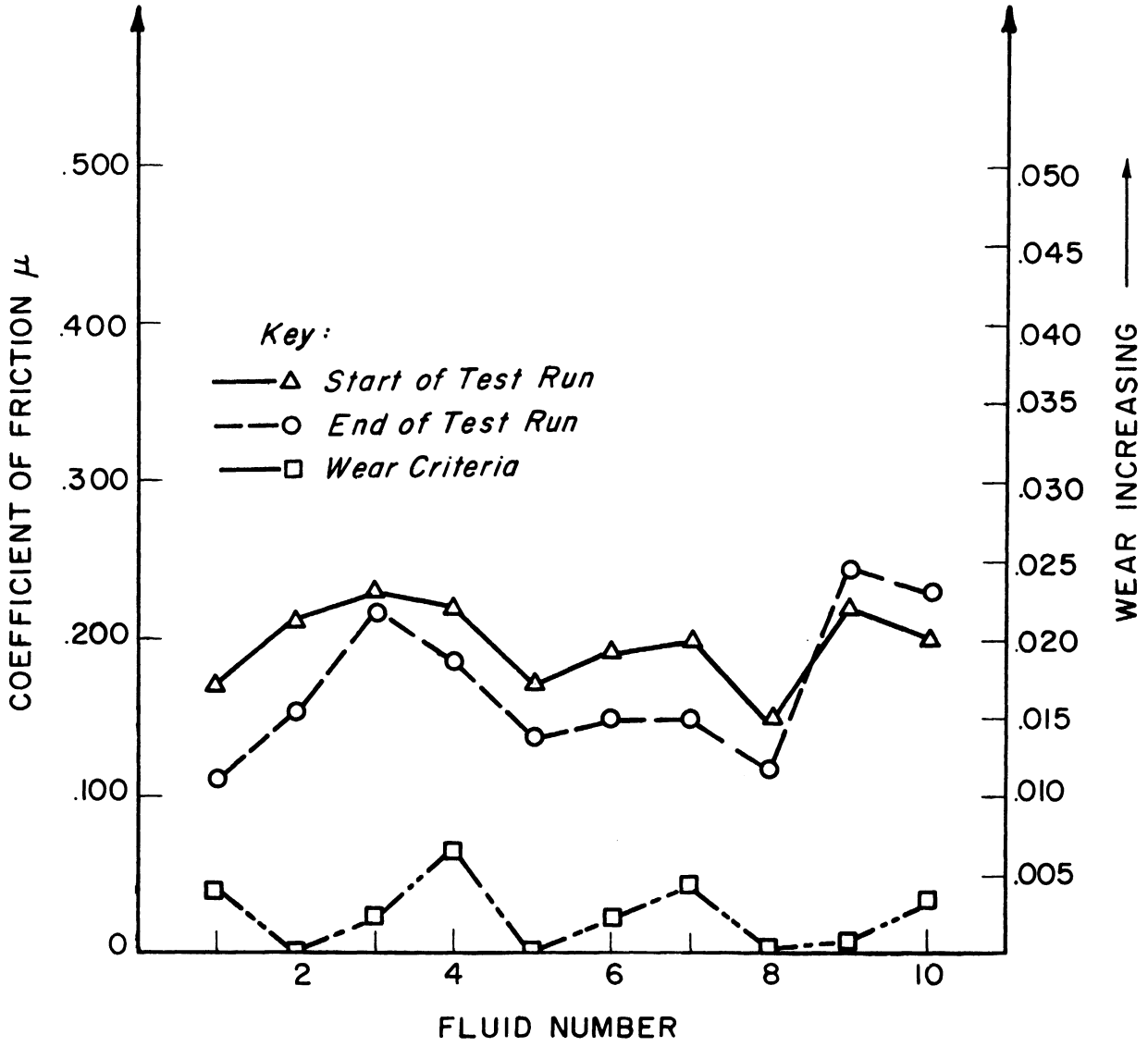

Fig. 6.12. 1042 steel specimen coefficient of friction and wear measurement vs. fluid number at minimum normal load—20 lb.

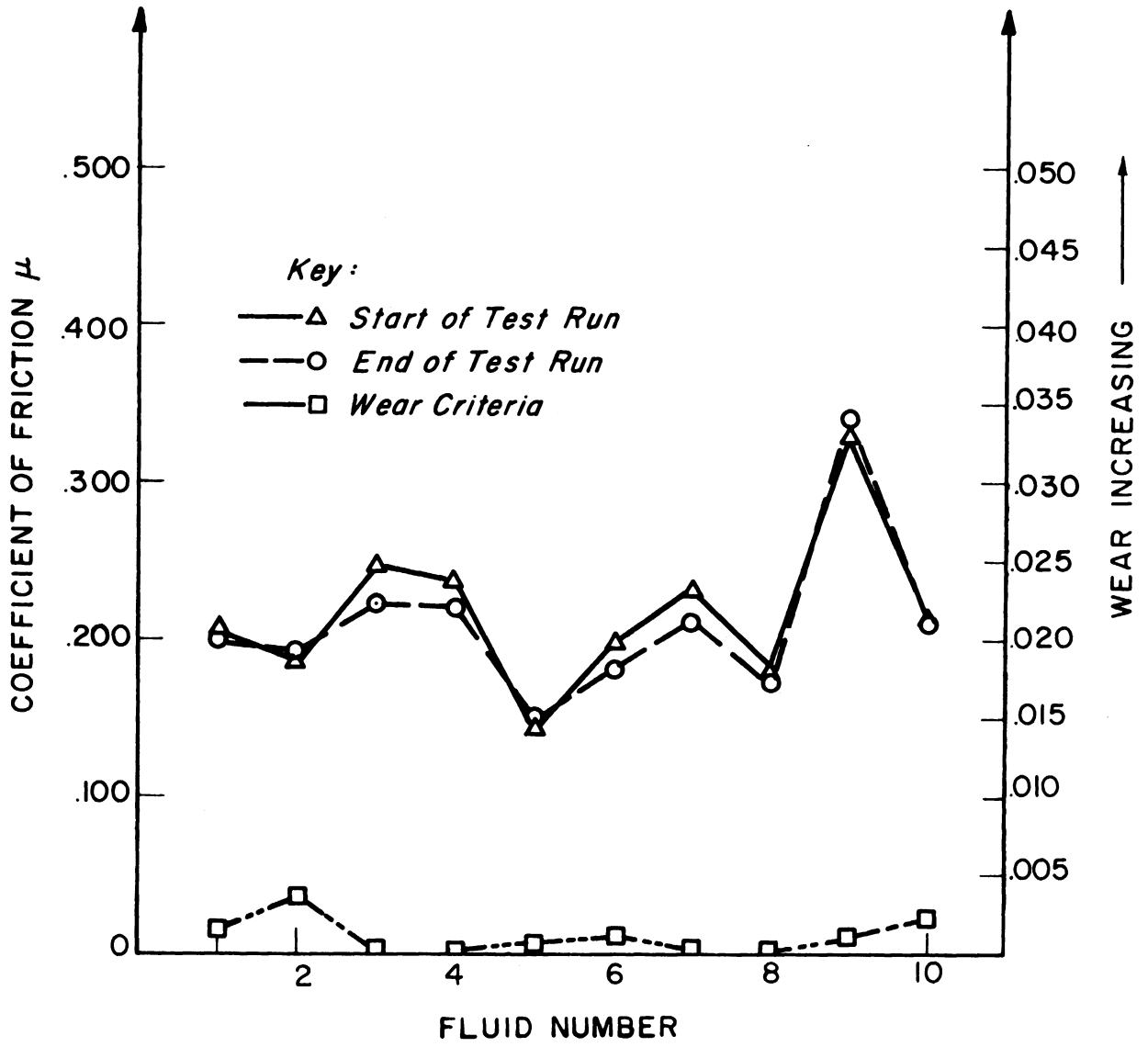

Fig. 6.13. 1018 steel specimen coefficient of friction and wear measurement vs. fluid number at maximum normal load—40 lb.

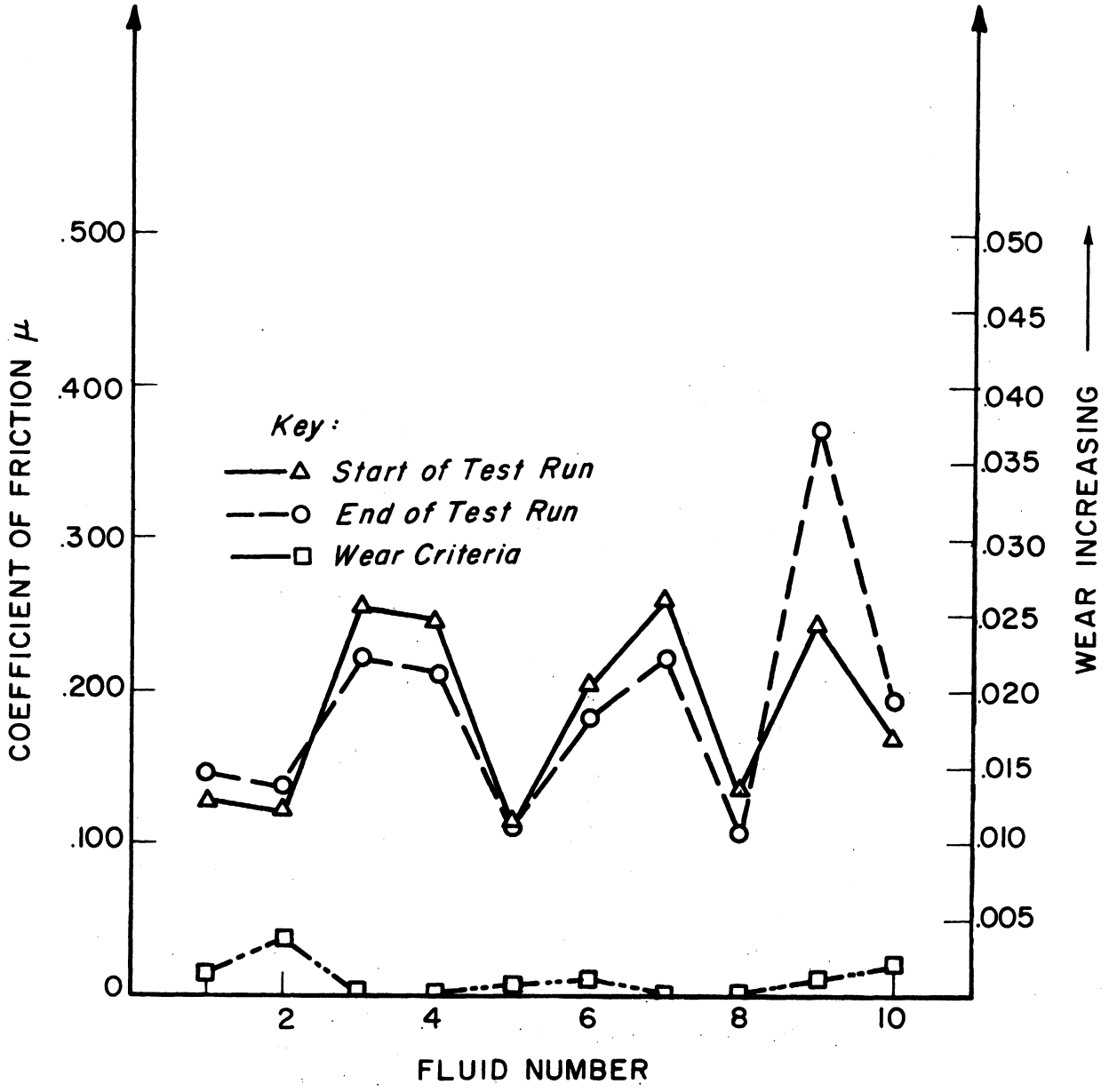

Fig. 6.14. 1018 steel specimen coefficient of friction and wear measurement vs. fluid number at minimum normal load—20 lb.

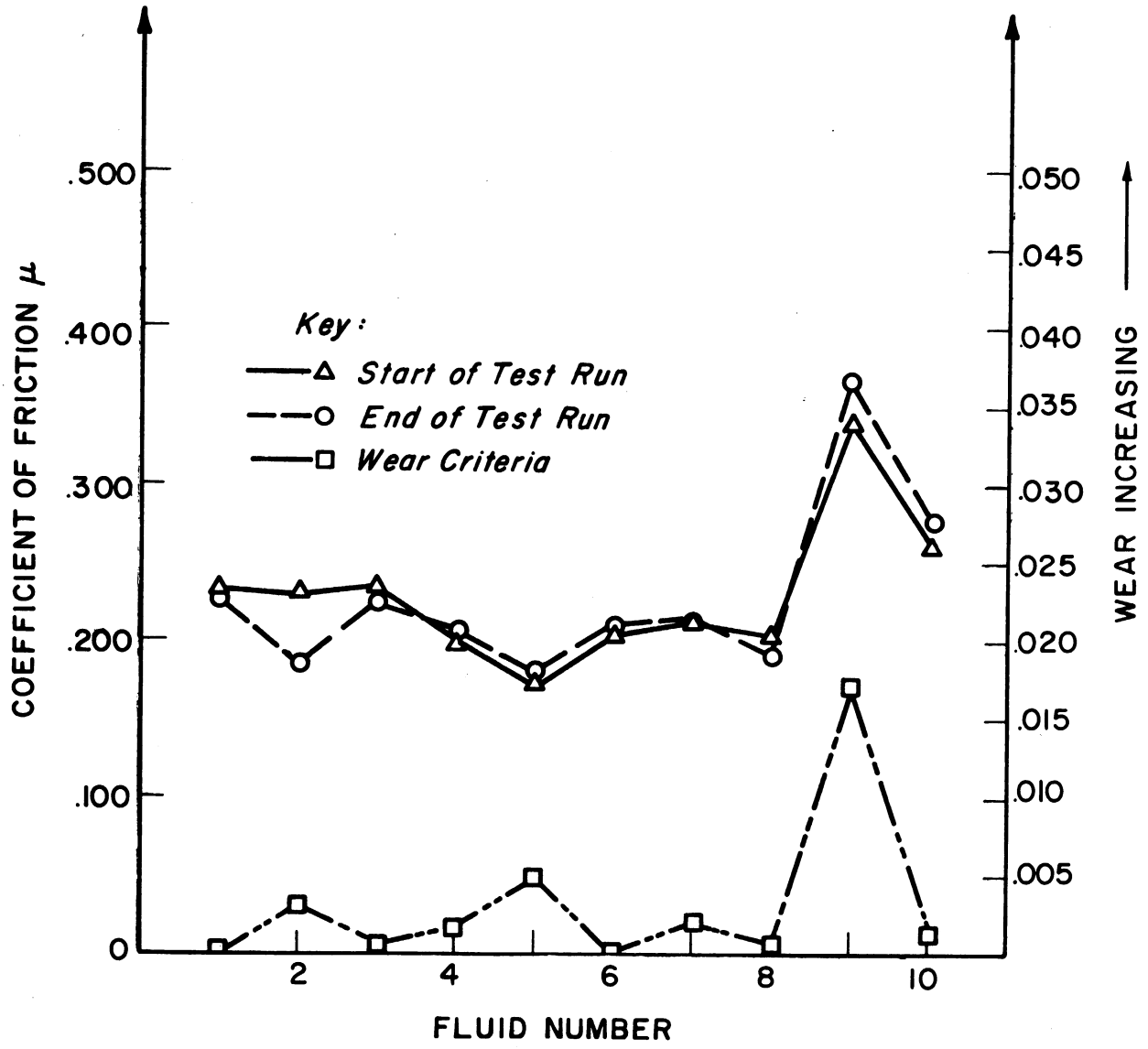

Fig. 6.15. Stainless steel specimen coefficient of friction and wear measurement vs. fluid number at maximum normal load—40 lb.

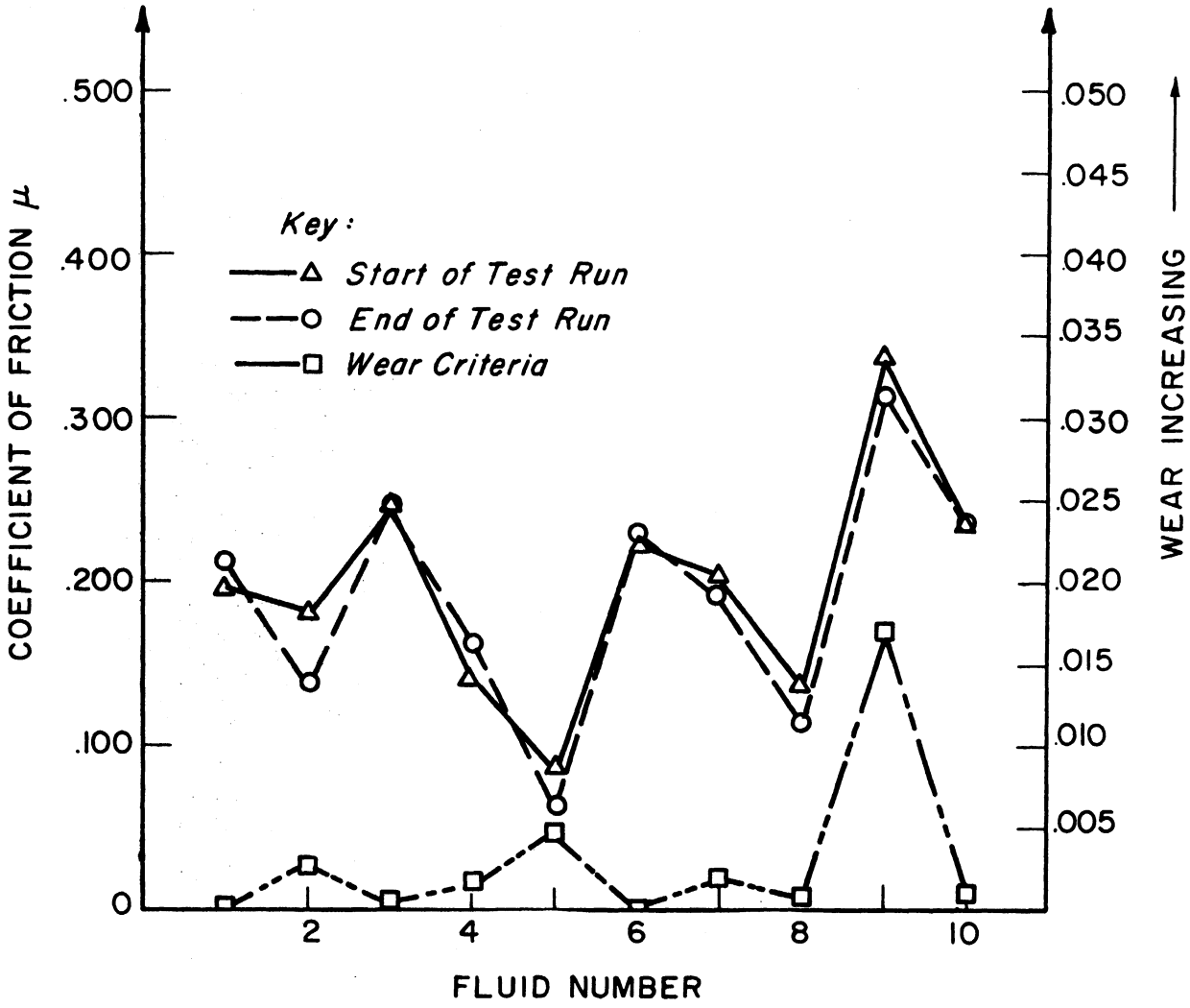

Fig. 6.16. Stainless steel specimen coefficient of friction and wear measurement vs. fluid number at minimum normal load—20 lb.

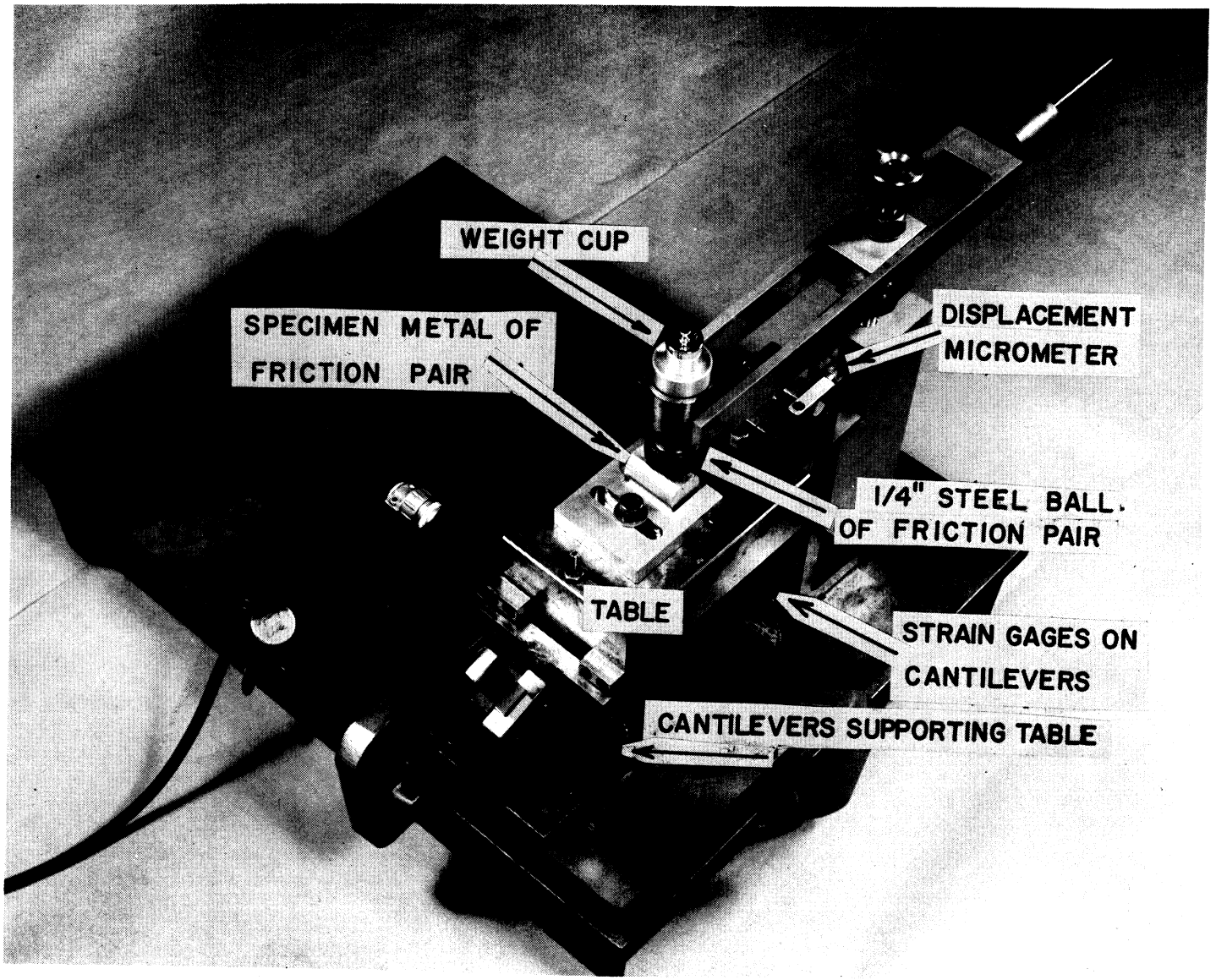

Fig. 6.17. Constant-energy apparatus.

SECTION VII

CONCLUSIONS

Numerous conclusions can be drawn from the data presented in this report. Other important conclusions must be reserved until the chemical nature of the cutting fluids is correlated with the cutting data. Some of the more important findings with regard to the nature of metal cutting and the role of lubrication in metal cutting are as follows:

1. Significant lubrication and friction reduction is possible both in the chip-tool interface (Zone-A) and between the cutting tool and the workpiece (Zone-B).

2. The first necessary functional capability of any cutting fluid is to prevent the formation of a built-up edge.

3. After the formation of a built-up edge has been prevented, the cutting force and energy requirements may increase unless the cutting fluid is capable of substantial boundary lubrication in the chip-tool interface.

4. Lubrication in the chip-tool interface is aided by roughness irregularities of the tool surface. This is a more important factor for tools having small rake angles than for those with larger rake angles.

5. In the absence of a built-up edge, considerable frictional rubbing can occur between the cutting tool and the freshly cut machine surface. Thus, lubrication in Zone-B can become a prime necessity. The need for lubrication in this zone increases with decrease in relief angle and with decrease in the modulus of elasticity of the work material. In some metal-cutting operations, the prevention of seizure or welding appears to be more important than a lower coefficient of friction. High film strength in a lubricant may be a determinant in operations where very thin cuts must be taken.

SECTION VIII

RECOMMENDATIONS FOR FUTURE STUDY

It seems probable that further analysis of the role of the chemistry of cutting fluids will indicate that chemical reaction products will be necessary for the prevention of the formation of a built-up edge with metals which have this tendency. Therefore, a workable basis for the design of cutting fluids might proceed substantially as follows:

1. Classify all metals into two categories—one category to include those like magnesium, which show no significant tendency toward the formation of a built-up edge; the second to include all metals which do exhibit such a tendency to a significant degree.

2. Develop chemicals which will react with each work material of the second category so as to develop low-shear-strength reaction products capable of inhibiting seizure and thereby preventing the formation of built-up edges.

3. Classify all machining operations into one of three categories. The first category would include all operations in which the relief or clearance angles must be small and wherein lubrication in Zone-B is a dominant consideration. The second category would include the opposite extreme in which prevention of the formation of a built-up edge is mandatory to the achievement of the desired size control and surface finish and in which lubrication in Zone-B is of little consequence. The third category, which might be a relatively broad one, would include those operations which for various reasons required some compromise between the extremes represented by the first two categories.

One could then specify the best extreme-pressure lubricant for each metal being cut by an operation in Category 1, in which lubrication in Zone-B is the dominant consideration. Whenever possible, the extreme-pressure properties for this lubrication would be achieved through high film strength. For machining operations of Category 2, in which lubrication in Zone-B is of little consequence, the cutting fluids would be of two types. One would be designed to prevent the formation of a built-up edge and secondarily to achieve as much lubrication in Zone-A as was possible. For interrupted cuts, high film strength, as well as chemical activity, might be beneficial. On the other hand, for continuous cuts, the mobility of the cutting fluid into the chip-tool interface would be more important than high film strength. The compromise cutting fluids which would be blended with the third category of operations would obviously depend upon the nature of the compromise.

It is recommended, therefore, that the approach outlined here be used in further work to test the feasibility of developing better cutting fluids. Broaching provides a quick and critical test of both extremes required of a fluid. The finishing teeth and burnishing elements on a broach provide a severe test for a fluid intended for an effective job of lubrication in Zone-B. The roughing teeth, on the other hand, provide a good test of the ability of the cutting fluid to prevent the formation of the built-up edge. The broaching results presented in this report for carbon steel are a good example of the latter case while the former was demonstrated by the results obtained for the broaching of magnesium.

The ability of the cutting fluid to lubricate in Zone-A beyond prevention of the built-up edge can best be evaluated by an interrupted cut like milling. A new and more sensitive type of milling dynamometer has been designed and partially built which will greatly speed up this type of evaluation.

Finally, the question of compromise with regard to the film strength of the lubricant involves surface finish, residual stresses and size control as well as the probable relationship to chatter. Size control and residual stresses can best be studied with a reaming operation. Surface finish, on the other hand, is more critical in broaching which also lends itself well to the determination of the residual stresses. The orthogonal turning test also lends itself to very rapid determination of film strength and frictional characteristics. However, it does not provide any information on the surface finish, residual stresses, size control, and chatter vibrations. No consistent techniques have as yet been developed for a competent analysis of the chatter problem. Some information on this problem would doubtless be obtained from the tests specified; however, no specific tests on the chatter problem are recommended at this time. In summary, then, it is recommended that future studies be confined to broaching, reaming, turning, and simulated milling with the new dynamometer.

It is recommended that attention be given to the development of improved cutting fluids. The results of this study have pointed most prominently to a need for a good fluid for broaching steel. Of the fluids used in this investigation, only trichlorethylene, which was designated as Fluid No. 9, even approached satisfactory performance in the broaching of both the low-carbon and medium-carbon steels. Only the trichlorethylene did a reasonably effective job of minimizing the built-up edge in broaching. A similar need exists in connection with copper and, to a lesser degree, brass. It is recommended also that the possibilities of developing good and suitable water-base compounds for the lower strength materials, such as aluminum and magnesium, be considered.

APPENDIX A

COMPOSITION AND PROPERTIES OF WORK MATERIALS

1. Aluminum—2011-T3—Solution Heat-Treated and Cold-Drawn

   5.5% copper
   94.5% aluminum

2. Brass—ASTM B-16—Cold-Drawn Free-Cutting Yellow Brass

   61.5% copper
   35.5% zinc
   3.0% lead

3. Copper—ASTM B-133—Cold-Drawn Electrolytic Pitch Copper

   99.92% copper
   0.04% oxygen

4. Magnesium—AZ-31C—Cold-Drawn

   3.0% aluminum
   1.0% zinc
   0.3% manganese
   95.0% magnesium

5. Steel—AISI 1042—Cold-Drawn Medium Carbon Steel

   98.7% iron
   0.42% carbon
   0.75% manganese
   0.04% phosphorus max
   0.05% sulfur max

6. Steel—AISI 1018—Cold-Drawn Low-Carbon Steel

   0.18% carbon
   0.75% manganese
   99.00% iron

7. Stainless Steel—18-8 Type 304 Stainless (Universal Cyclops)

18.-20.% chromium
8.-11.% nickel
0.08 % carbon max
2.% manganese max
67.-72.% iron

TABLE A.1

MECHANICAL PROPERTIES OF METALS USED*

Material	Modulus of Elasticity, psi	Tensile Strength, psi	Breaking Strength, psi	Elongation, %	Reduction in Area, %	BHN, 3000 kg	Meyer Exponent, "n"	Meyer Hardness, 500 kg	Poisson's Ratio
2011S-T3 Aluminum (Solution heat treated and cold drawn)	10×10^6	52,300	43.000	22	47	112	2.12	110	.31
Brass (ASTM B-16)	14×10^6	54,500	51,250	33	46-1/2	126	2.07	120	.33
Copper (ASTM B-133)	17×10^6	40,000	24,200	21	63	95	2.28	87	.33
Magnesium (AZ-31C)	6.5×10^6	39,000	35,000	17	36	104	1.93	58	.35
1042 Steel	30×10^6	118,000	101,500	12-1/2	36	228	1.97	248	.30
1018 Steel	30×10^6	78,300	54,500	21	61	163	1.99	178	.30
Stainless Steel (Universal Cyclops 18-8, type 304)	29×10^6	88,400	55,500	62-1/2	79	170	2.24	145	.30

*Average result of three specimens. All gave approximately same values.

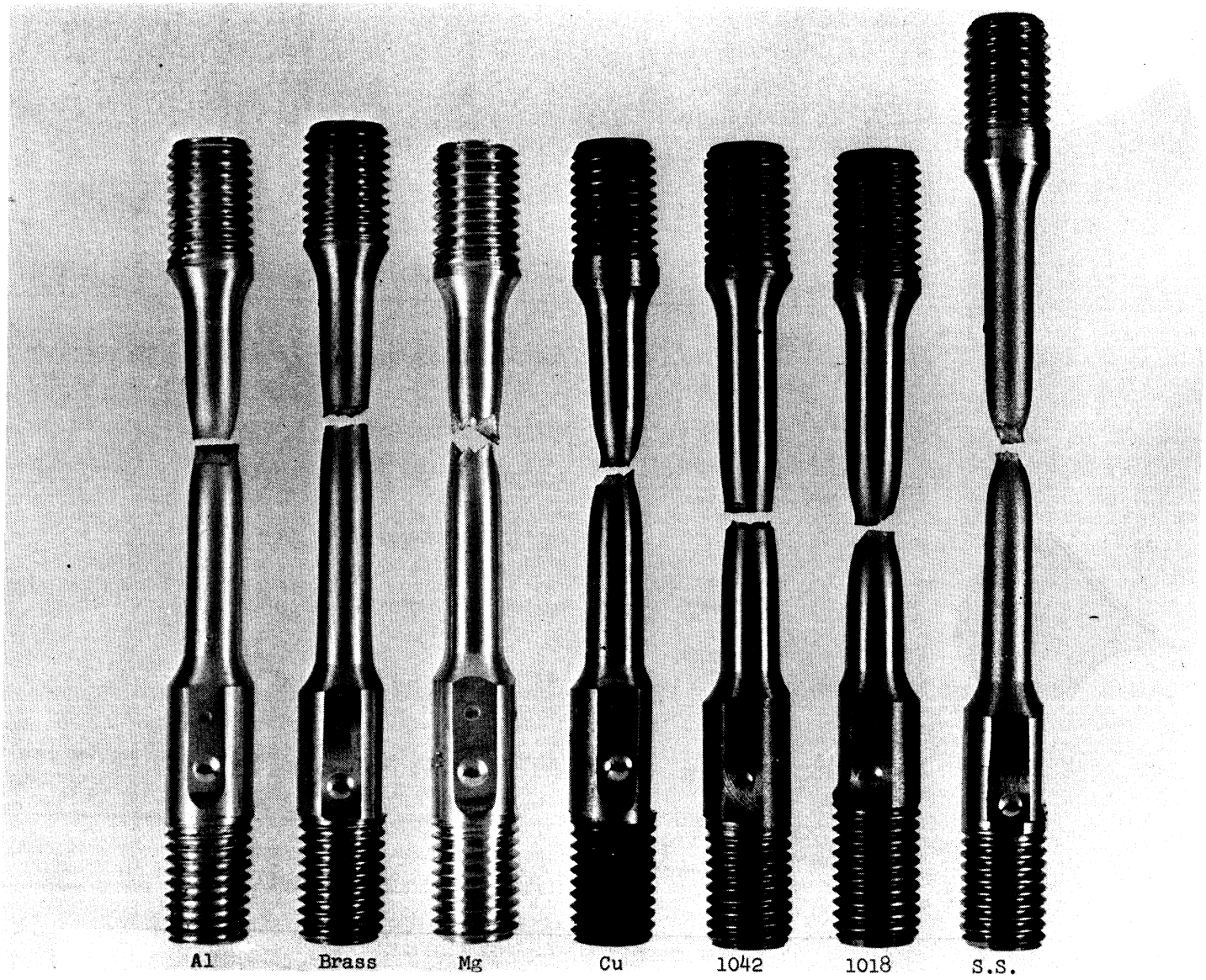

Fig. A.1. Tensile test specimens after failure.

APPENDIX B

CUTTING FLUIDS STUDIED

The seven oils, Nos. 1, 2, 3, 4, 5, 7, and 8 were supplied by the Sun Oil Company. Stuart's Thread Kut 99, Oil No. 6, was procured by the Department of Mechanical Engineering.

The fluids studied were:

1. Sunicut 100
2. 98G + 2.5% Chlorafin 40 (8 + additive)
3. Sunicut 100 + 2.5% Chlorafin 40 (1 + additive of 2)
4. 98G + 11% Sulchlor 99 (8 + additive)
5. Sunicut 21 type 91G + 11% Sulfurized Lard
6. Stuart's Thread Kut 99
7. 98G + 2.5% Ortholeum 162 (8 + additive)
8. 98G
9. Trichlorethylene
10. White Oil (Refined light mineral oil)

91G and 98G are Sun Oil nomenclature for base stock naphthenic lubricating oils.

APPENDIX C

LABORATORY APPARATUS AND TEST PROCEDURES

PRESTRESS APPARATUS

The investigations to determine the influence of known stresses on the forces generated in machining particular specimens were carried out on the fixture shown in Fig. 5.1. The fixture is made so that a beam-type specimen can be prestressed to a known tensile or compressive stress in its outermost surface and that surface can then be machined, the normal and cutting forces being measured by a suitable dynamometer during machining.

The tests were made by mounting the fixture on the table of a planer and adjusting the fixture to prestress the specimen to a stress level of 0 psi, 40,000-psi tension, or 40,000-psi compression. A two-component dynamometer mounted on the crossrail carried the cutting tool, a 1/2-inch square high-speed steel tool bit. The table was driven at a velocity of 14 feet per minute, carrying the workpiece into the tool so that an orthogonal or two-dimensional cut was made.

The specimens machined were made of annealed 1020 steel finish-ground to a thickness of 0.208 inch. The width of the beam was about 1.7 inches prior to machining, 12 inches long, and with a hardness of 111 Bhn. The cuts were made either dry or by applying fluid continuously by hand from a pump-type oil can to the surface being machined. Suitable records of the normal and cutting forces were recorded from the dynamometer during machining. The depth of cut for each pass of the tool was determined by suitable measurements after each cut was completed. After preliminary testing it was decided that a tool geometry of 30° back rake and 6° relief would be used throughout. Initial tests with a 0° back rake resulted in such a poor surface finish that measurements for depth of cut were not reliable. In some instances four very light clean-up cuts of 0.001 to 0.0015 inch were taken prior to each monitored cut.

Tests were made under dry conditions at 0 stress, 40,000-psi tension and 40,000-psi compression, with depths of cut ranging from about 0.001 inch to 0.009 inch. Similar tests were made using Fluids Nos. 6 and 10. In addition, all cutting fluids were evaluated under the same cutting conditions of 0 stress, 14 fpm, at a constant depth of cut of about 0.006 inch. The force measurements of these tests are presented in Section V, both in tabular and in graphical form.

FRICTION-WEAR MACHINE

Figure 6.1 is a general view of the friction-wear machine, a modified vertical drill press. Figure C.1 is a schematic diagram of the machine. A constant member of a friction pair is mounted on the spindle and rotated. A fixed specimen of the metal being studied is mounted on a carrier which moves radially and perpendicularly to the spindle. Figure C.1 shows the relation of the friction pair. The specimen carrier and the loading mechanism are mounted on a square housing which is mounted on ball bearings so that the entire assembly is free to rotate about the centerline of the spindle. The normal load between the friction pair is provided by dead-weights mounted on a table face which slides along two one-inch-diameter horizontal rods.

When the table is in its innermost position, the dead-weight loading mechanism is counterbalanced and the normal load between the specimens is zero. The table is connected by a split nut to a lead screw rotated by a small synchronous motor. When a test is being conducted, the load can be increased linearly with time as the table travels outward from the balance point. The table will engage a preset limit switch which selectively either stops the table and holds the normal load at that value or reverses the synchronous motor causing the load to be reduced at the same rate it had increased. The normal load can be made to oscillate between any preselected values of high and low load including a load of zero.

Both the normal load and the torque or friction reaction are indicated continuously by the use of resistance-wire strain gages mounted on cantilever beams. A carrier-amplifier-recorder provides a continuous time chart of these quantities. The load cell for the normal load lies between the specimen carrier and the dead-weight loading system. A similar load cell is used to constrain the stationary specimen against rotation about the centerline of the drill press spindle.

The following analysis, based on the geometric relations shown in Fig. C.2, is applicable to the fixed-type specimens used in the tests.

(a) Rubbing Area = $A = \pi D h$

where:

$$h = \frac{D}{2} [\cos 2\alpha - \cos \beta 2]$$

therefore:

$$A = \frac{\pi D^2}{2} [\cos 2\alpha - \cos 2\beta] \qquad (1)$$

(b) Mean Radius of Contact in Rubbing Area = r_1

$$r_1 = \frac{D}{2} \sin \frac{2\alpha + 2\beta}{2} = \frac{D}{2} \sin (\alpha + \beta) \qquad (2)$$

(c) Average Radius of Contact in Rubbing Area = r_2

$$A = 2\pi r_2 \frac{D}{2} (2\beta - 2\alpha) = \frac{\pi D^2}{2} (\cos 2\alpha - \cos 2\beta)$$

Therefore:

$$r_2 = \frac{D}{2} \frac{(\cos 2\alpha - \cos 2\beta)}{(2\beta - 2\alpha)} \qquad (3)$$

where:

$(2\beta - 2\alpha)$ is expressed in radians.

(d) Normal Load = N = f(P) (based on Eq. (2))

$$N = 2\pi r_1 P \cos \left(\frac{2\alpha + 2\beta}{2}\right) j$$

where:

P = pounds load per inch of mean length of contact annulus.

Therefore:

$$P = \frac{N}{2\pi r_1 \cos (\alpha + \beta)} = \frac{N}{2\pi \frac{D}{2} \sin(\alpha + \beta)\cos(\alpha + \beta)}$$

$$P = \frac{2N}{\pi D \sin 2(\alpha + \beta)} \qquad (4)$$

(e) Normal Load = N = f(P) (based on Eq. (3))

$$N = 2\pi r_2 P \cos \left(\frac{2\alpha + 2\beta}{2}\right) = 2\pi r_2 P \cos (\alpha + \beta)$$

Therefore:

$$P = \frac{N(2\beta - 2\alpha)}{\pi D \sin(\beta - \alpha) \sin 2 (\alpha + \beta)} \qquad (5)$$

(f) Average Pressure in Rubbing Zone = p (using Eqs. (2) and (4))

$$p = P/a;$$

where:

$$a = \frac{A}{2\pi r} = \frac{\pi D^2}{4\pi r}[\cos 2\alpha - \beta \cos 2]$$

$$p = \frac{2N/\pi D[\sin 2(\alpha + \beta)]}{D^2[\cos 2\alpha - \cos 2\beta]/2D \sin(\alpha + \beta)}$$

Therefore:

$$p = \frac{2N}{\pi D^2[\cos 2\alpha - \cos 2\beta]\cos(\alpha + \beta)} \qquad (6)$$

(g) Average Pressure in Rubbing Zone = p (using Eqs. (3) and (5))

$$p = \frac{N(2\alpha - 2\beta)/\pi D \sin(\beta - \alpha)\sin 2(\alpha + \beta)}{D^2[\cos 2\alpha - \cos 2\beta]/2D(\cos 2\alpha - \cos 2\beta)/(2\beta - 2\alpha)}$$

Therefore:

$$p = \frac{2N}{\pi D^2 \sin(\beta - \alpha)\sin 2(\alpha + \beta)} \qquad (7)$$

NOTE: Equations (6) and (7) are identitites.

(h) Coefficient of Friction—μ

Assume the average friction radius = R = $\frac{D}{2}\cos 2\alpha$

Therefore: friction torque = $\mu pAR = T$

where:

μ = coefficient of friction
p = average pressure in the contact area
A = contact area
R = average radius

Therefore:

$$pA = \frac{N}{\cos(\alpha + \beta)}$$

Therefore:

$$T = \frac{\mu \times N}{\cos(\alpha + \beta)} \times \frac{D}{2} \cos 2\alpha = \frac{\mu ND \cos 2\alpha}{2 \cos(\alpha + \beta)}$$

and

$$\mu = \frac{2 \cos(\alpha + \beta) T}{ND \cos 2\alpha} \qquad (8)$$

NOTE: The exact equation for average friction radius (R) is very complex and the increased accuracy of the results does not justify the additional time required to use it in making calculations.

If it is assumed that angles α and β are nearly equal, because of the limited contact and relatively light load applied to the pair, then the terms $\cos(\alpha + \beta)$ and $\cos 2\alpha$ are equal and drop out, which leaves the final relationship,

$$\mu = 2T/ND.$$

If the coefficient of friction is constant during a test run, the record of the torque reaction would be a constant times the normal load trace. Figure 6.2 is a typical recording trace of torque reaction and normal load versus time. Data points were taken at the beginning of each run at maximum load of 40 pounds and minimum load of 20 pounds. They were then multiplied by the constants developed below to find the values of μ for the data points

$$\mu = 2T/ND$$

D = 1.182 inches
N = 40 pounds maximum
N = 20 pounds minimum
T = trace mm x 0.1 lbs-in/mm at 2X

When N = 40 pounds,

$$\mu = \frac{2(0.1T)}{(40)(1.182)}$$ where T is in mm from trace

$$\mu = 4.23 \times 10^{-3} T$$

When N = 20 pounds,

$$\mu = \frac{2(0.1T)}{(20)(1.182)} \qquad \text{where T is in mm from trace}$$

$$\mu = 8.46 \times 10^{-3} T$$

Procedure

The geometry of the friction pair in this series of tests provided a counterbore on the contact face of the stationary member. Figure C.2 is a sketch of the specimens in the paired condition. After counterboring, the inner edge, which would contact the rotating spherical segment, was seated on a Brinell Hardness Tester using a rotating member loaded to 500 kg. The diameter of the counterbore was unaffected by the seating operation. The width of the formed seat was measured accurately using a toolmaker's microscope.

The friction pair were ultrasonically cleaned and assembled in the friction-wear machine. From a no-load static condition, the thrust load was increased to 40 pounds in 108 seconds while the spindle speed was 740 rpm. The thrust load was then cycled between 20 and 40 pounds in sequence for 10 cycles, which totaled about 22 minutes. The load was reduced to zero again in 108 seconds. The specimens were then ultrasonically cleaned and the chordal distance of the wear area measured, again by a toolmaker's microscope. An average of the maximum and minimum observed wear was recorded as the measured length.

Tables C.1 and C.2 list the values of maximum and minimum torque measured at the beginning and at the end of 10 cycles, when the normal load was varied from 40 to 20 pounds.

The above process was repeated for each of the seven metals in each of the ten fluids, with appropriate measurements taken at the end of each test.

Typical torque curves for each of the seven metals tested with all of the fluids are given in Figs. C.3 through C.9.

CONSTANT-ENERGY APPARATUS

Figure 6.17 shows the constant-energy apparatus used to study the static-dynamic friction characteristics of fluid and metal combinations. It is a rectangular table mounted on four flexible vertical columns at each corner. The columns have electrical resistance wire-type strain gages mounted to monitor the motion of the table. One member of a friction pair is mounted on

the table. The other member is a standard hardened steel ball mounted on the end of the horizontal counterbalanced beam, which can be statically loaded directly over the ball. The loaded ball is brought into contact with the specimen whose surface may be either dry or lubricated with a fluid under investigation.

The table is displaced horizontally and the static-dynamic characteristics of the metal pair and the fluid are determined from records of the motion of the table as it finally returns to rest in the neutral position.

The actual static-dynamic tests were conducted using a cylindrical specimen of the metal to be tested with a flat which had been dry polished to a uniform surface condition by applying the specimen with a figure-eight motion to Minnesota Mining Type E-F silicon carbide wet-dry paper. After the specimen had been ultrasonically cleaned, it was mounted on the table with the prepared flat uppermost and horizontal. The counterbalanced weight cup was loaded with selected weights and the ball brought gently into contact with the flat, on which a drop of the fluid being evaluated had been placed. The table was manually displaced a measured amount—0.020 inch—and released. A tape record of the static and dynamic friction forces and table displacement was made during the period of table motion. The weight was then changed and the entire procedure repeated.

After one fluid had been evaluated for various loads, the friction pair were ultrasonically cleaned, replaced on the table so that a new area would be exposed to the ball, and the tests repeated with a different fluid. This procedure was followed until all seven metals had been tested with all ten fluids at loads from zero up to 150 grams.

One of the principal advantages of using such an arrangement of a plane and a sphere is that Hertzian equations can be applied to predict the stresses and minimum elastic contact areas in the early stages of test before significant wear has taken place. If a test begins with the application of a maximum normal load, the most severe pressures are encountered in the early stages, making it possible to predict and control the upper limits of pressure and shear stress as they are related to the flow properties of the metals under test. Timoshenko[4] gives the following equations for the plane sphere combination:

$$\text{Maximum pressure,} \quad q_o = \frac{3N}{2\pi a^2} \tag{9}$$

$$\text{Maximum shear,} \quad T_o = 0.31\, q_o \tag{10}$$

$$\text{Radius of contact area,} \quad a = [3\pi N(K_1 + K_2)R/4]^{1/3} \tag{11}$$

where:

N = normal load
R = radius of sphere

$$K_1 = (1 - V_1^2)/\pi E_1 \qquad (12)$$

$$K_2 = (1 - V_2^2)/\pi E_2 \qquad (13)$$

V_1, V_2 = Poisson's ratio for the test materials
E_1, E_2 = Modulus of elasticity of the test materials.

Equations (9), (10), and (11) were used in planning the typical experiments which were carried out. The steel sphere used throughout had a radius of .250 inch so that R was a constant.

Tabulated in Table C.3 are values of the maximum and minimum pressures in psi developed at maximum normal loads of 150 grams and minimum normal loads of 1 gram, respectively, for each of the metals tested, using physical properties listed earlier.

The various fluids were evaluated by comparing the log-decrement of the response curve of the displaced table as it was released and returned to rest. A typical response curve for a damped system is shown in Fig. C.10. A series of such curves can be evaluated by comparing the log-decrement of each curve if the system is heavily damped, so that there is an appreciable difference between succeeding cycles. In this instance, however, and particularly at lighter loads, the difference in cycles was not enough to measure accurately so an arbitrary number of cycles was selected as a basis for comparison.

The log-decrement for such curves can be expressed as follows:

$$\delta = \ln \frac{Xn}{Xn + 1}$$

where

δ is the log-decrement
Xn = amplitude of a cycle
$Xn+1$ = amplitude of succeeding cycle

Therefore:

$$e^{\delta} = \frac{Xn}{Xn + 1}$$

$$e^{\delta} = \frac{X_1}{X_2} = \frac{X_2}{X_3} = \frac{X_3}{X_4} \cdots = \frac{Xn}{Xn + 1},$$

where

X_1 is the amplitude of first cycle

if n = 4, n-1 = 3

$$e^{\delta} \cdot e^{\delta} \cdot e^{\delta} = \left(\frac{X_1}{X_2}\right)\left(\frac{X_2}{X_3}\right)\left(\frac{X_3}{X_4}\right) = \frac{X_1}{Xn}$$

Therefore:

$$e^{3\delta} = \frac{X_1}{Xn}$$

Therefore:

$$e^{(n-1)\delta} = \ln \frac{X_1}{Xn}$$

Therefore:

$$\delta = \frac{\ln \frac{X_1}{Xn}}{n-1} .$$

This form of the log-decrement permits the use of any number of cycles needed to read the difference in amplitude. The log-decrement will vary according to the number of cycles at which the amplitude is read, decreasing as the amplitude of the cycle, Sn, decreases. It was decided that the amplitude would be read at the point where Xn was 20% of the amplitude of the first cycle, X_1, or where 80% damp-out had occurred. A plot of the number of cycles to 80% damp-out versus the load would be a function of the log-decrement of the response curves and could be used as a basis for comparing the fluids (see Fig. C.11).

The results of the load versus number of cycles to 80% damp-out are contained on Figs. C.12 through C.18 for the metals and fluids tested. In all cases the two extremes of the series of tests are plotted, i.e., the system which damped most readily, and the system (fluid) which prolonged motion and therefore reduced friction the most. Where the spread between the curves was sufficient intermediate curves were also plotted. The values are given in accompanying tables. Typical response curves of all the metals and fluids at 150 kg loads are given in Figs. C.19 through C.25.

TABLE C.1

FRICTION-WEAR RESULTS

(Maximum torque in mm (2X) at 40 lb normal load
at beginning of test and after 10 cycles.)

Fluid No.	Aluminum	Brass	Magnesium	Copper	1042 Steel	1018 Steel	Stainless Steel
1	24-11	52-40	46-39	58-26	46-39	48-47	55-54
2	39-36	43-40	33-33	39-28	54-50	44-45	54-44
3	40-31	45-35	41-31	47-23	58-55	58-52	55-53
4	26-29	47-42	38-24	43-28	56-52	56-52	47-48
5	29-27	44-39	43-40	38-27	45-43	34-35	40-42
6	33-17	43-39	33-18	38-37	48-41	47-43	48-50
7	38-25	39-38	35-22	39-40	47-42	55-50	50-50
8	39-23	41-30	38-30	40-29	44-43	43-41	48-45
9	55-57	60-73	160-160	90-100	65-80	78-80	80-86
10	33-38	43.5-43	45-10.5	37-33	55-55	50-50	61.5-65

TABLE C.2

FRICTION-WEAR RESULTS

(Minimum torque in mm (2X) at 20 lb normal load
at beginning of test and after 10 cycles.)

Fluid No.	Aluminum	Brass	Magnesium	Copper	1042 Steel	1018 Steel	Stainless Steel
1	7.5-2	23.5-15.5	15-10	27-12	20-13	21-17.5	23-25
2	19-17.5	21.5-17.5	11-11	14.5-8	25-18	20-16	21-16
3	21-11.5	21-10	19-12	26-14	27-26	30-26	29-29
4	6-6.5	23.5-10	14.5-7	13.5-7	26-22	29-25	16.5-19
5	12.5-11.5	19-15	17-13	10.5-5	20-16	13-13	10-7.5
6	13.5-4	23-16.5	8.5-2	13.5-12	22.5-17.5	24-21.5	26.5-27
7	15.5-10	20-22	17-12	17-16	23.5-17.5	31-26	24-22.5
8	16-7	16-7	11.5-9	13.5-7	17.5-14	16-12.5	16-13.5
9	27-27	28-35	70-60	44-48	26-29	29-44	40-37
10	10-15	16.5-16	5-5	16-14.5	23.5-27	20-22.5	28-28

TABLE C.3

MAXIMUM AND MINIMUM PRESSURES DEVELOPED FOR METALS TESTED

Metal	Maximum Pressure at 150 gm N—psi	Minimum Pressure at 1 gm N—psi
Aluminum	42,200	7,950
Brass	48,800	9,170
Copper	53,400	10,000
Magnesium	33,500	6,300
1042 Steel	65,400	12,300
1018 Steel	65,400	12,300
Stainless Steel	65,400	12,300

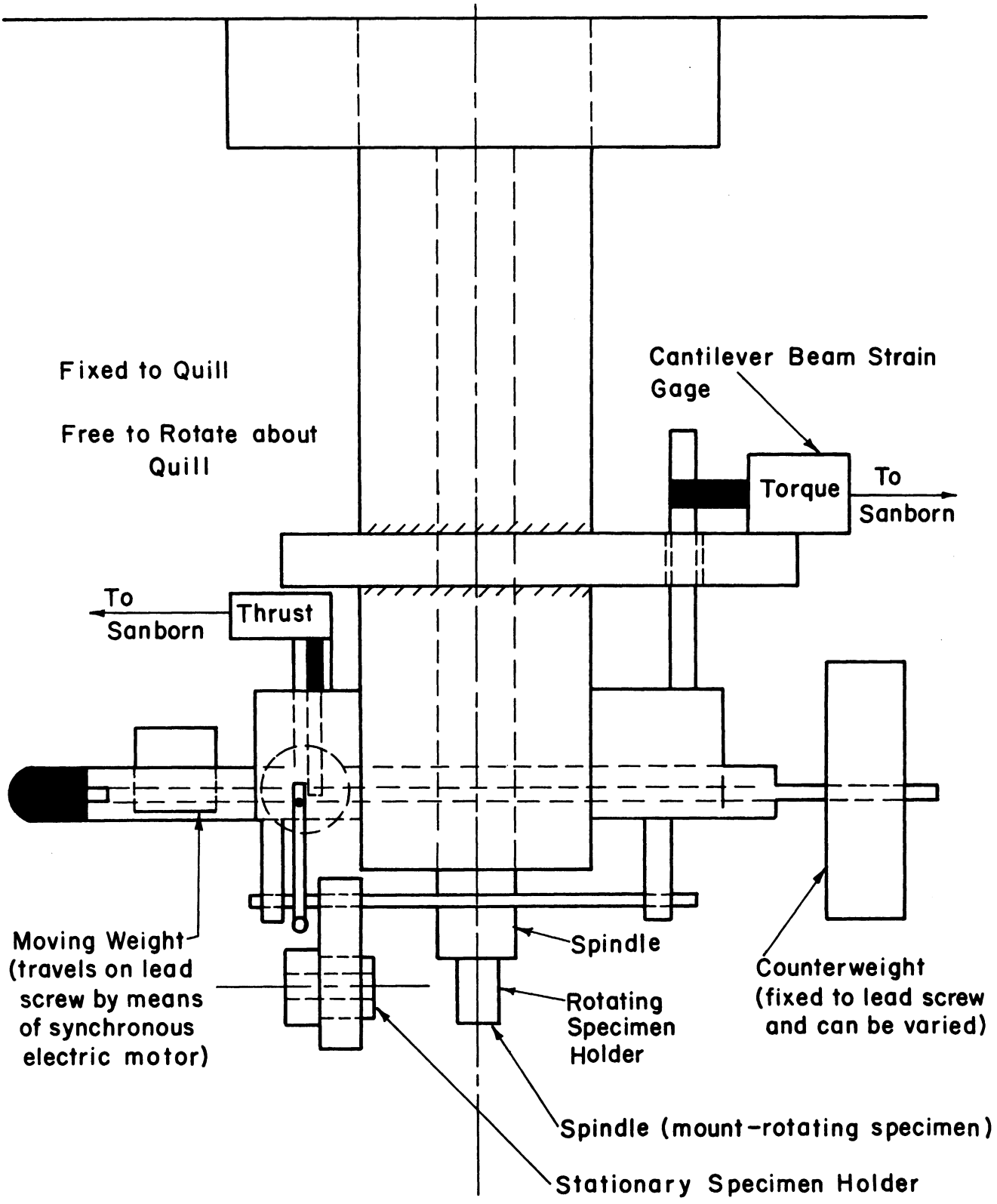

Fig. C.1. Friction-wear machine.

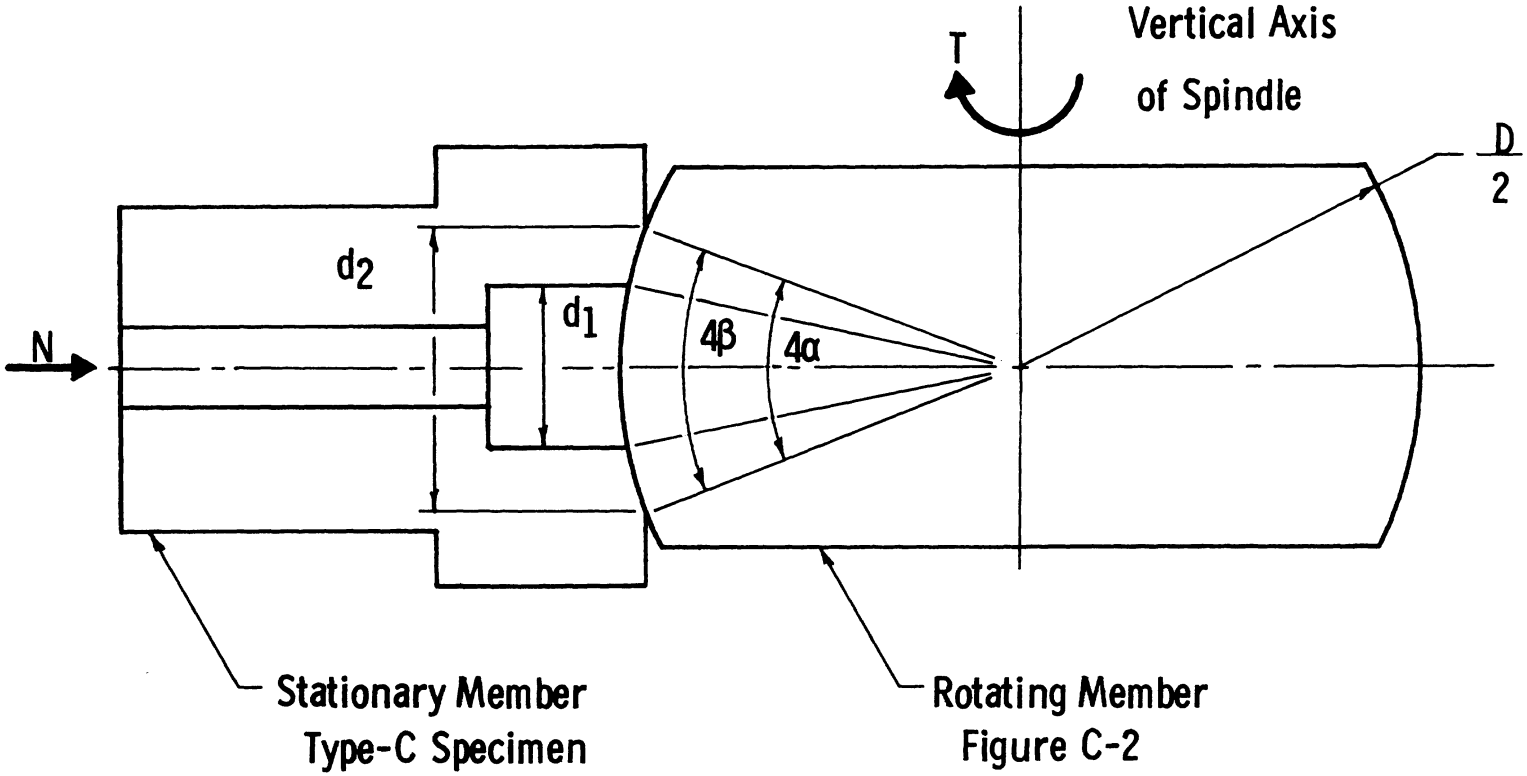

D = diameter, in inches, of rotating sphere
d_1 = diameter, in inches, of counterbore
d_2 = diameter, in inches, of outer contact circle of stationary member with rotating member
4α = inner contact angle of rotating member
4β = outer contact angle of rotating member
T = reaction torque due to friction between pair
N = normal load applied to pair through stationary member.

Fig. C.2. Geometric relations in friction pair.

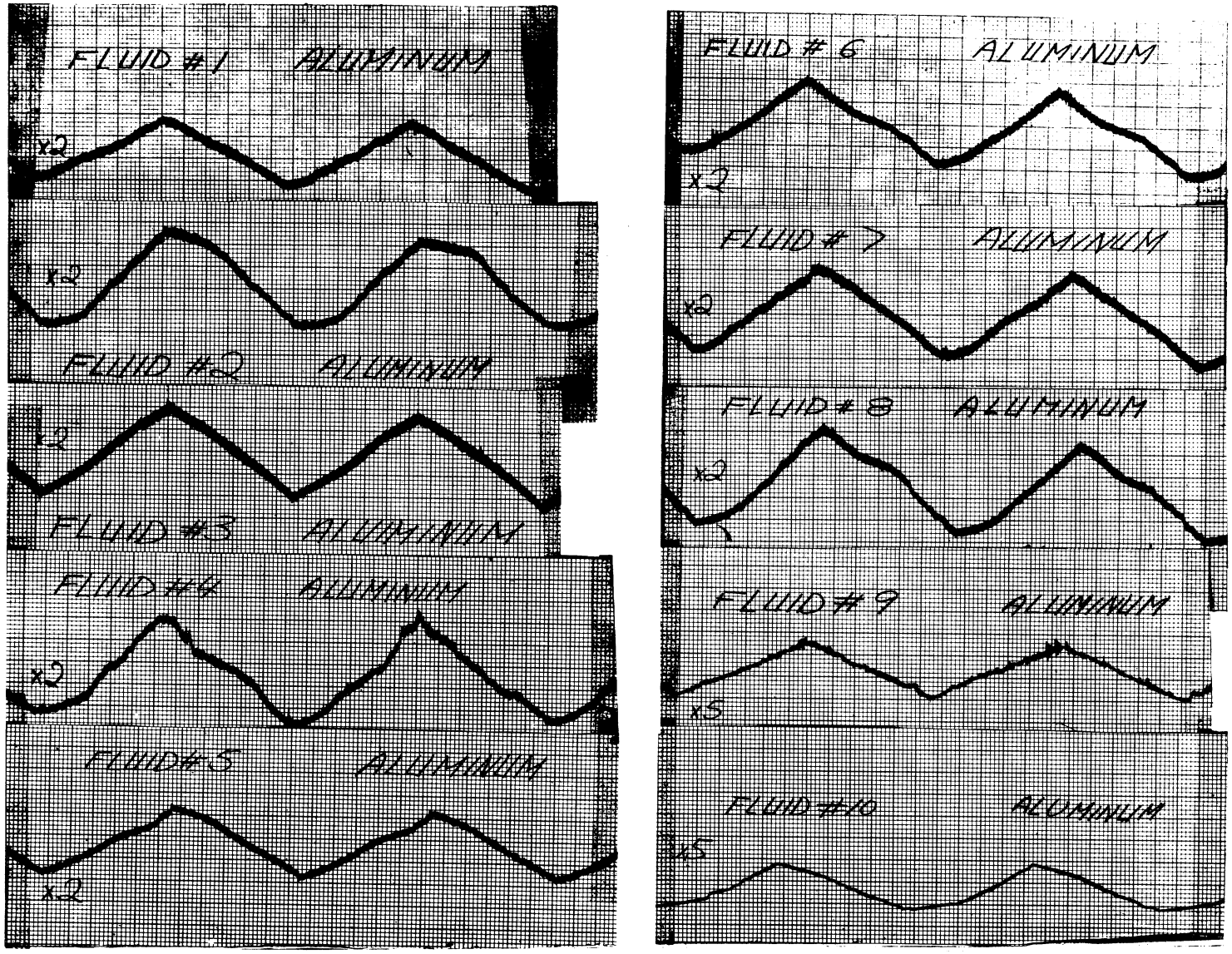

Fig. C.3. Aluminum friction-wear typical torques.

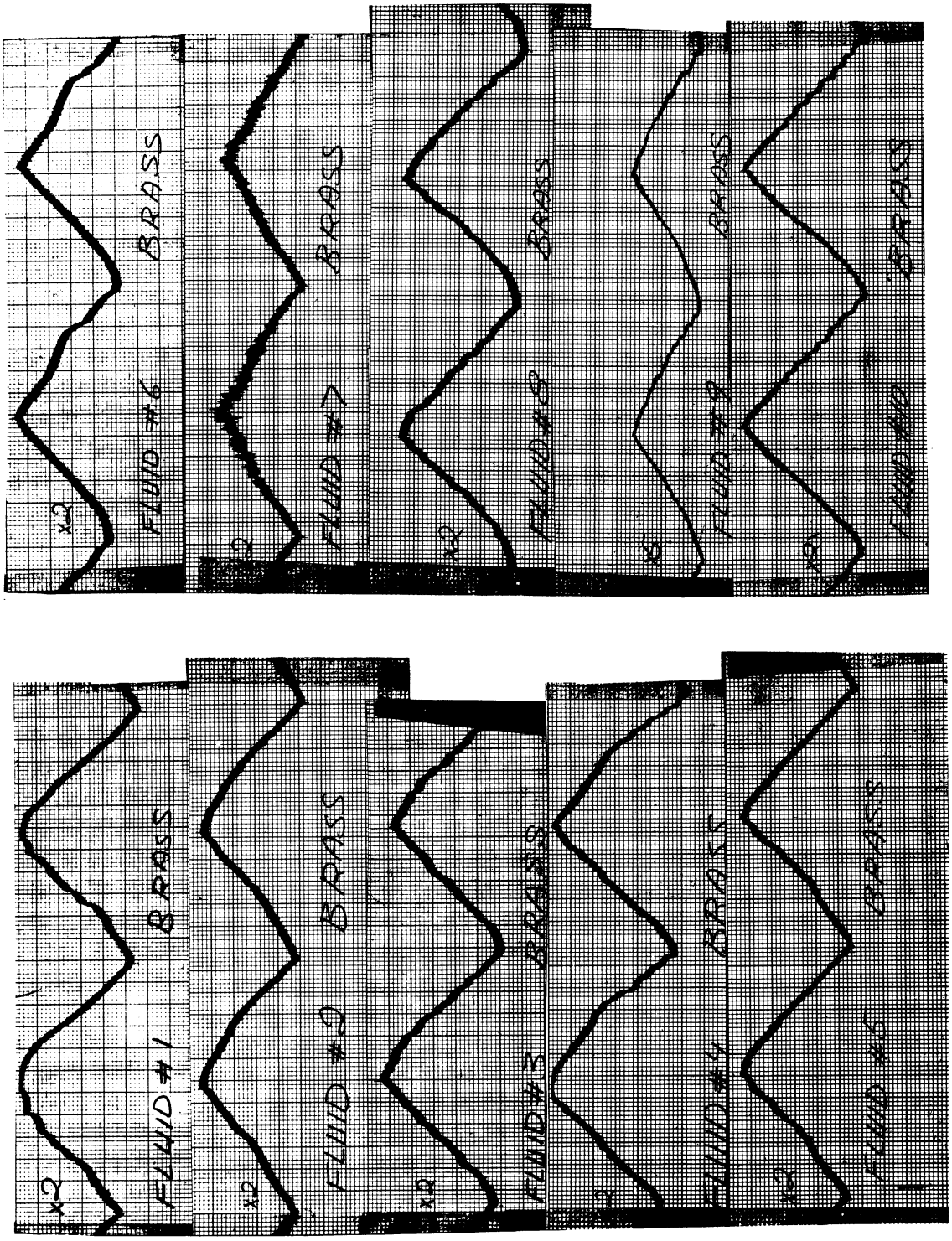

Fig. C.4. Brass friction-wear typical torques.

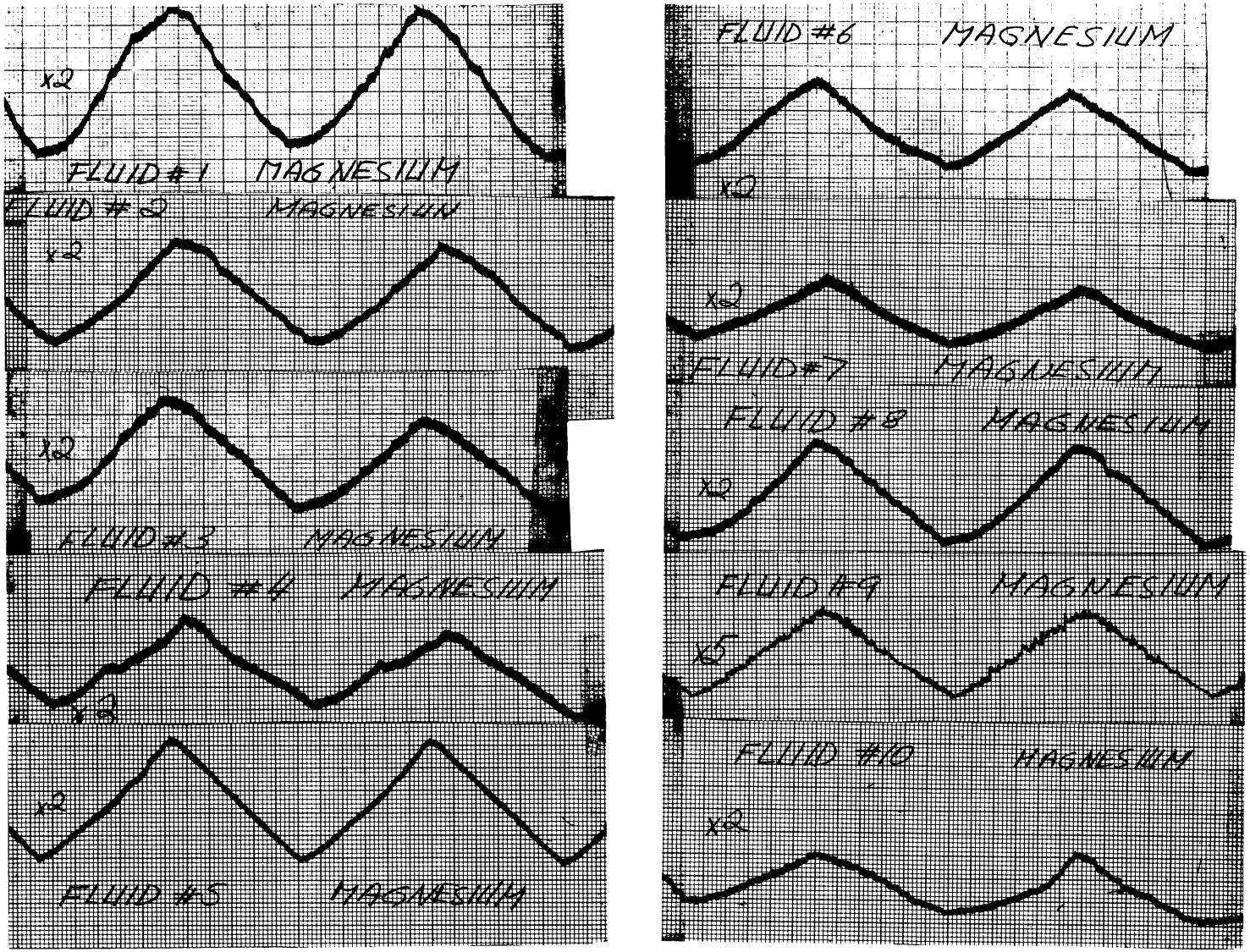

Fig. C.5. Magnesium friction-wear typical torques.

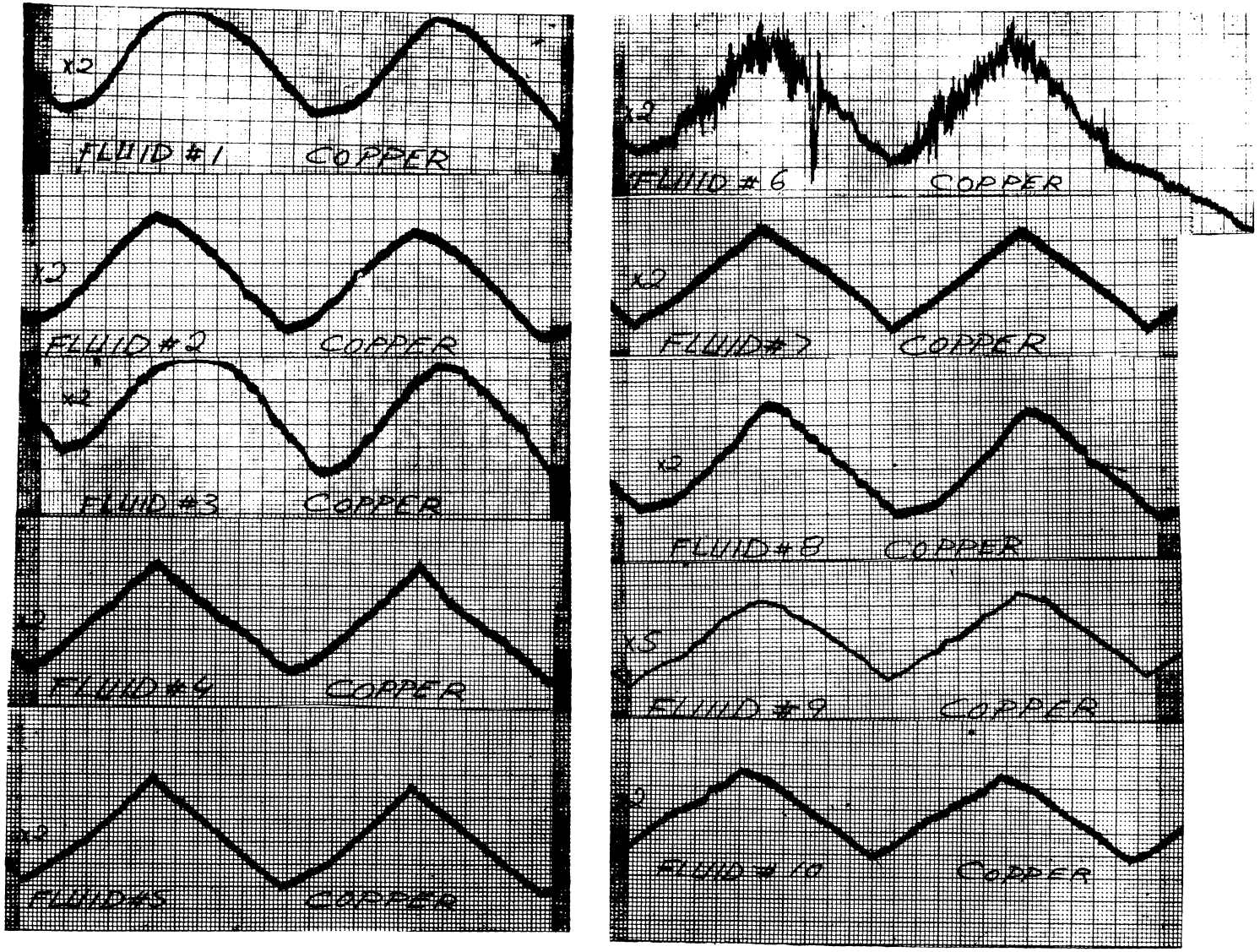

Fig. C.6. Copper friction-wear typical torques.

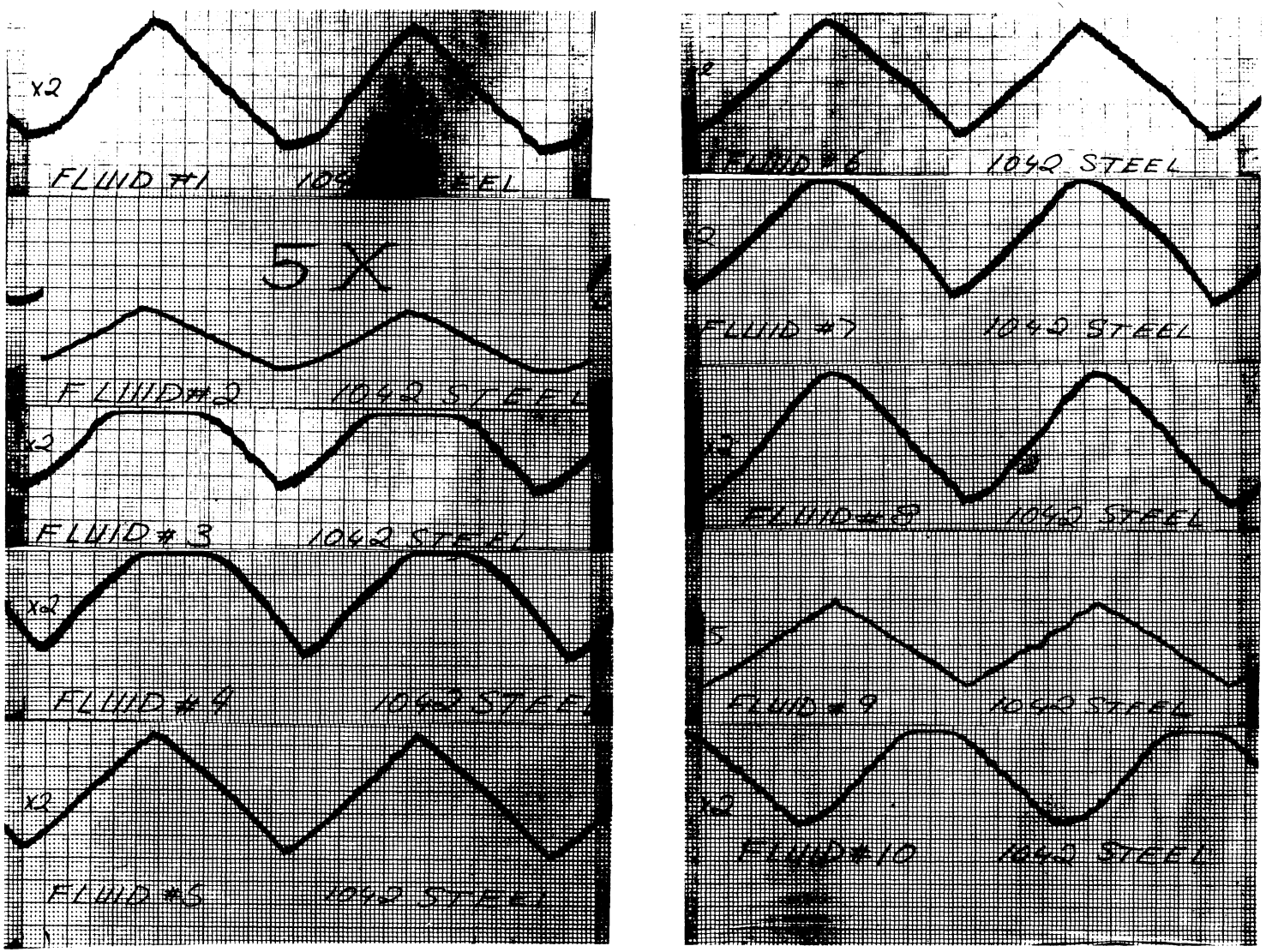

Fig. C.7. 1042 steel friction-wear typical torques.

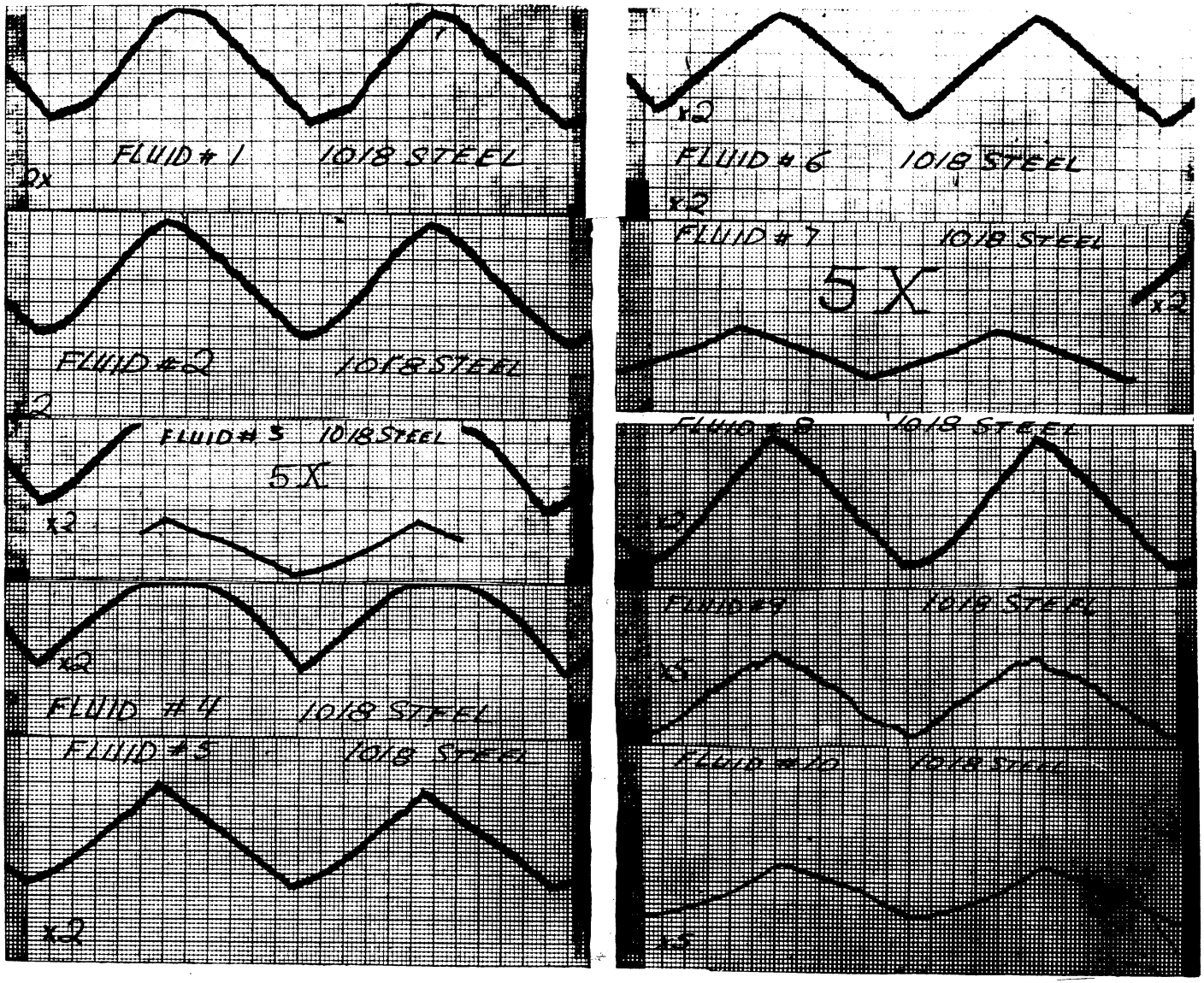

Fig. C.8. 1018 steel friction-wear typical torques.

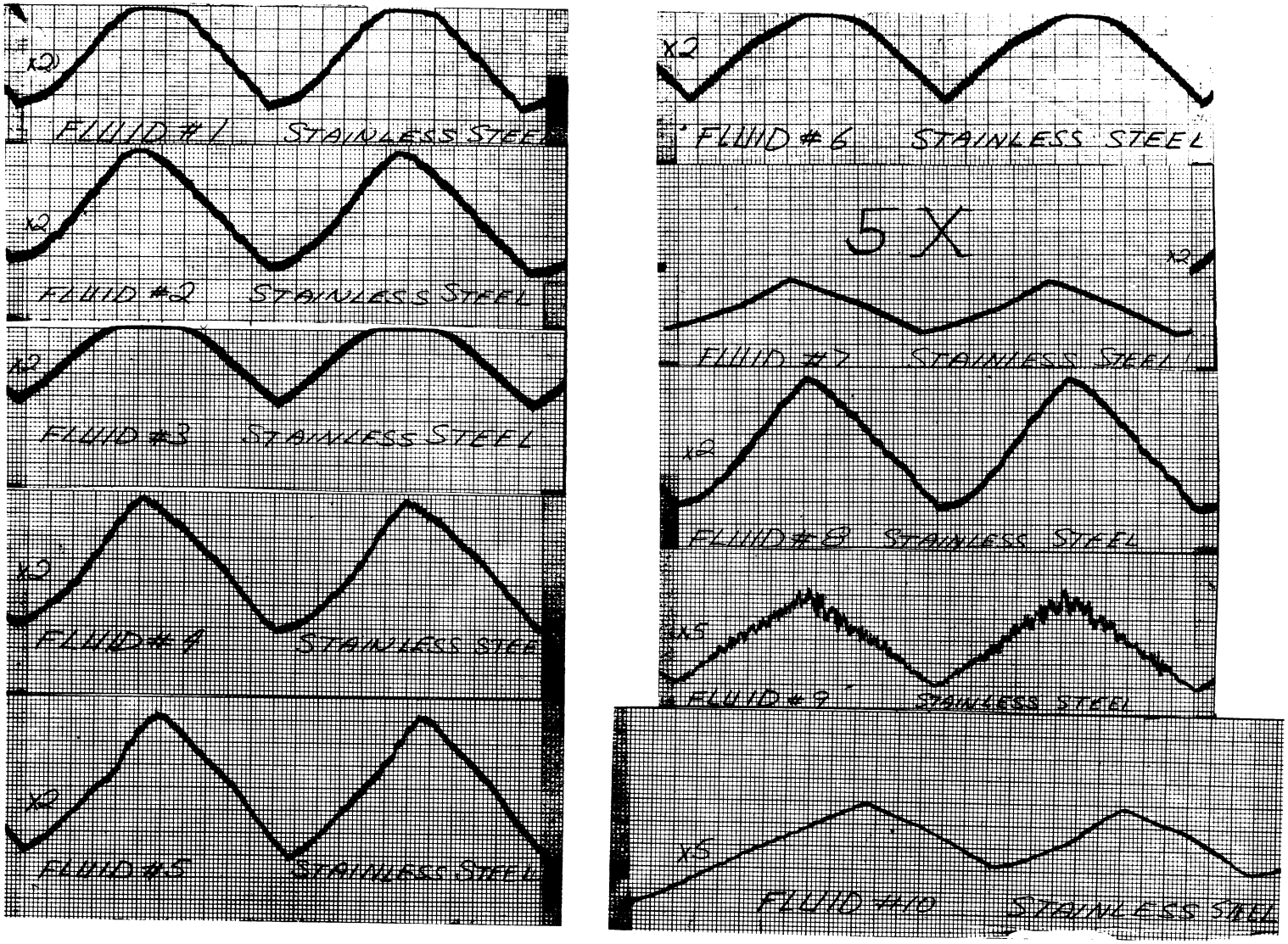

Fig. C.9. Stainless steel friction-wear typical torques.

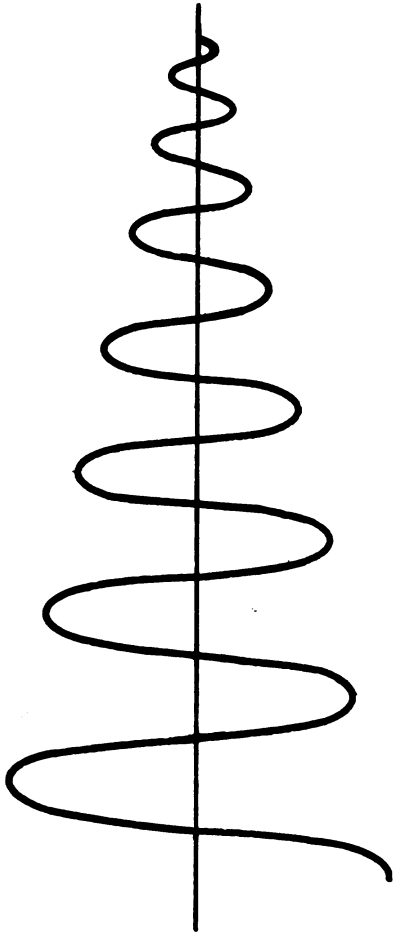

Fig. C.10. Typical response curve for a damped system.

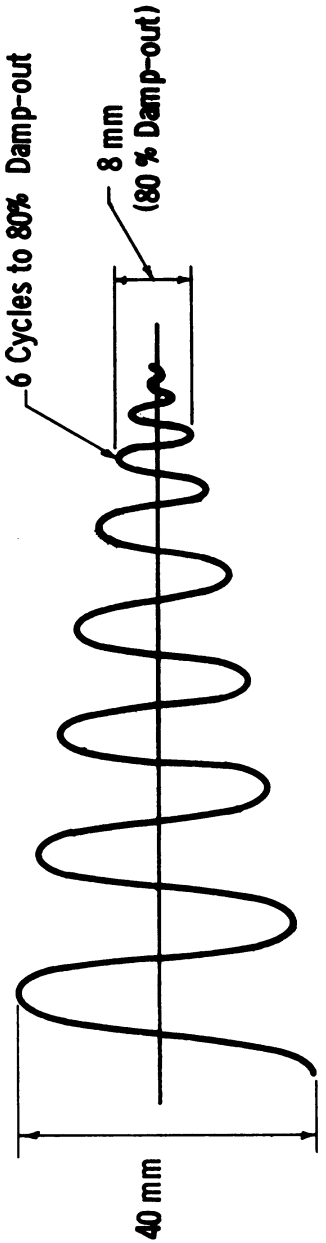

Fig. C.11. Typical analysis of response curve.

STATIC-DYNAMIC TEST
PROJECT 04100

Frequency of Oscillations = 12.35cps
No. of cycles to 80% Damp-out

FLUID

LOAD (gm.)	Dry	1	2	3	4	5	6	7	8	9	10
150	12	15.5	13.5	14	14.5	16	15	12.5	12.5	11	15.5
100	16.5	19.5	18	19	19.5	22	19.5	17.5	17		
50	25.5	31	27.5	29	30	34	30	30	27	23.5	31.5
30											
20	42.5	45.5	44	43	45	48.5	45	46	43.5		
10											
5											
3	64.5	62.5	65.5	65	69.5	68.5	64	68.5	63.5	70	74
2											
1											
Arm Down	73.5	70	71	74	72.5	71.5	73.5	69.5			
Arm Up	71.5	71	75	76	76.5	76.5	75.5	75	73	83.5	

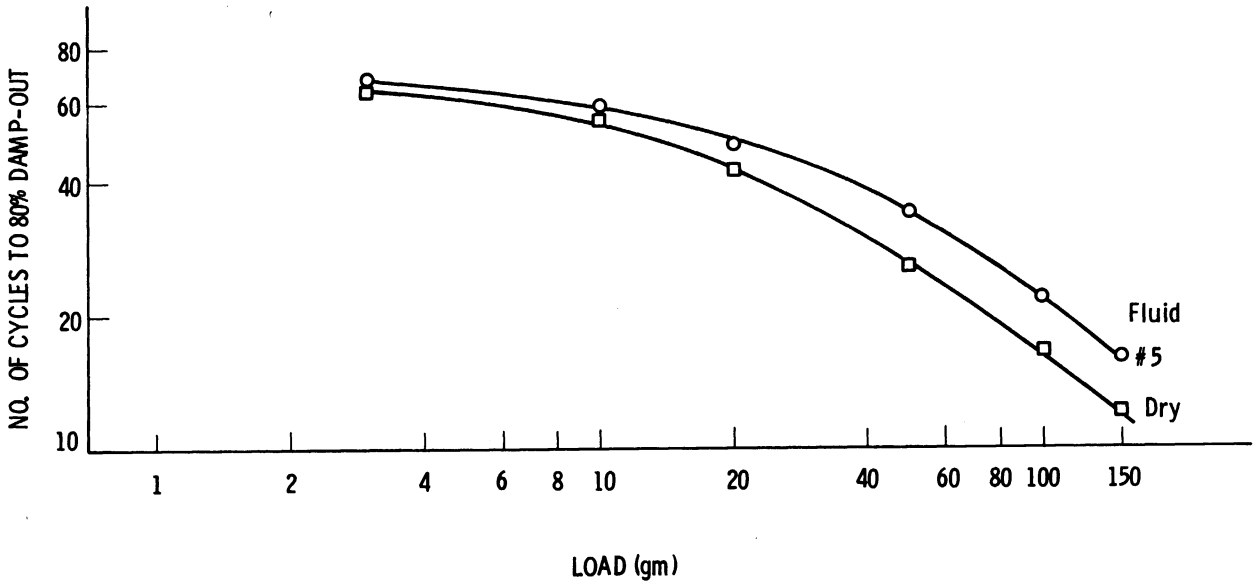

Fig. C.12. Static-dynamic test for aluminum.

STATIC-DYNAMIC TEST
PROJECT 04100

Frequency of Oscillations = 12.35cps
No. of cycles to 80% Damp-out

FLUID

LOAD (gm.)	Dry	1	2	3	4	5	6	7	8	9	10
150	10	11.5	11.5	14.5	14	17.5	17	14	10.5	10	16.5
100	11	15	16	20	20	23.5	22.5	19.5	17.5		
50	18.5	24	29.5	31	32.5	36	33.5	29.5	29.5	25	33
30	24.5	33									
20	32.5	39.5	46.5	46.5	49.5	52.5	49	47	47.5		
10	45.5	54	54	57	59.5	61	59.5	60	60.5		
5	57.5	62									
3	66.5	64.5	69	68.5	74	71	74	72.5	71	80	74.5
2	69.5	66.5									
1	70.5	70									
Arm Down	73	72	77	75	76.5	78	79.5	81.5	77.5		
Arm Up	75.5	72	77	83.5	77	79.5	82	82	79.5	83.5	

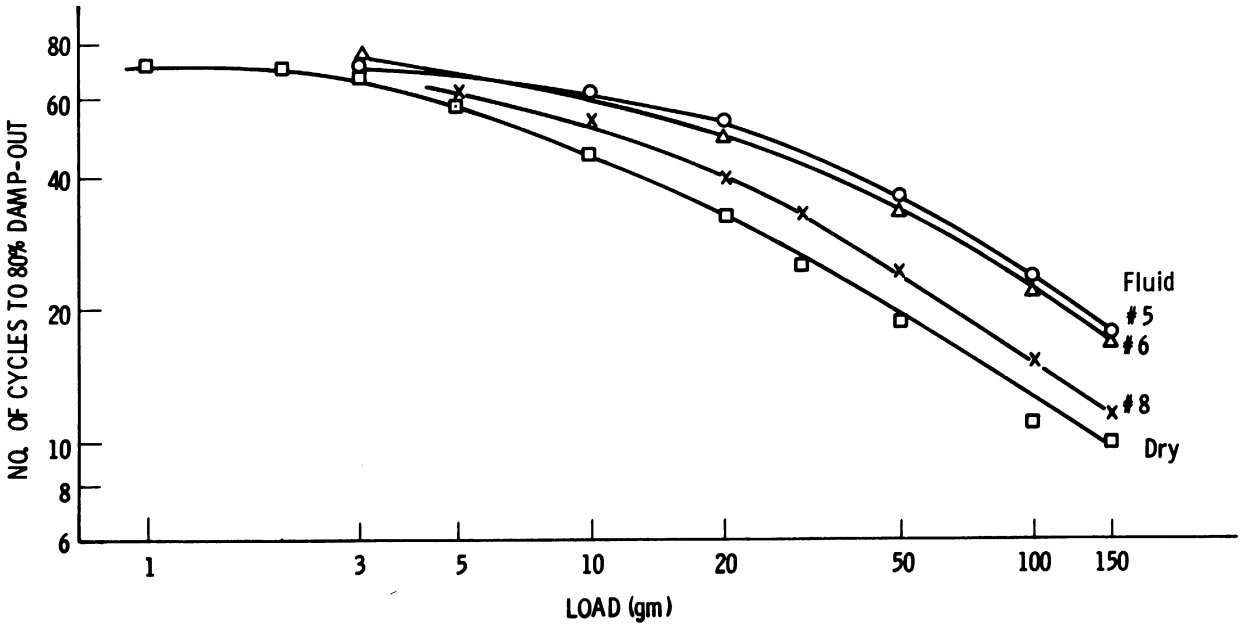

Fig. C.13. Static-dynamic test for brass.

STATIC-DYNAMIC TEST
PROJECT 04100

Frequency of Oscillations = 12.35cps
No. of cycles to 80% Damp-out

FLUID

LOAD (gm.)	Dry	1	2	3	4	5	6	7	8	9	10
150		16	15.5	15.5	16.5	17.5	16.	16.5	13	10.5	17
100	9	21	20	20.5	22	22.5	21	21	17.5		
50	15	31	31	31	34	36	29	31	26.5	24	35
30	23.5	38.5	29.5	38	43	44.5	37	39	33.5		
20	44.5	43.5	46	44	50	52	43	47	38.5		
10	60.5	52.5	56.5	52.5	59	61	54.5	54.5	51	54.5	
5	52.5	57.5	63	57	69	66	65	65.5	61		
3	65.5		63.5	61.5	69	69.5	68	68.5	64	74	74.5
2	66.5		65.5	63.5	68.5		71.5	72	69		
1	72.5		68.5	64.5	71	70.5	73.5	72.5	70		
Arm Down			72	67.5	73	73	74.5	73	73	81	
Arm Up	74		74.5	71	75.5	75	80	77	79	83.5	

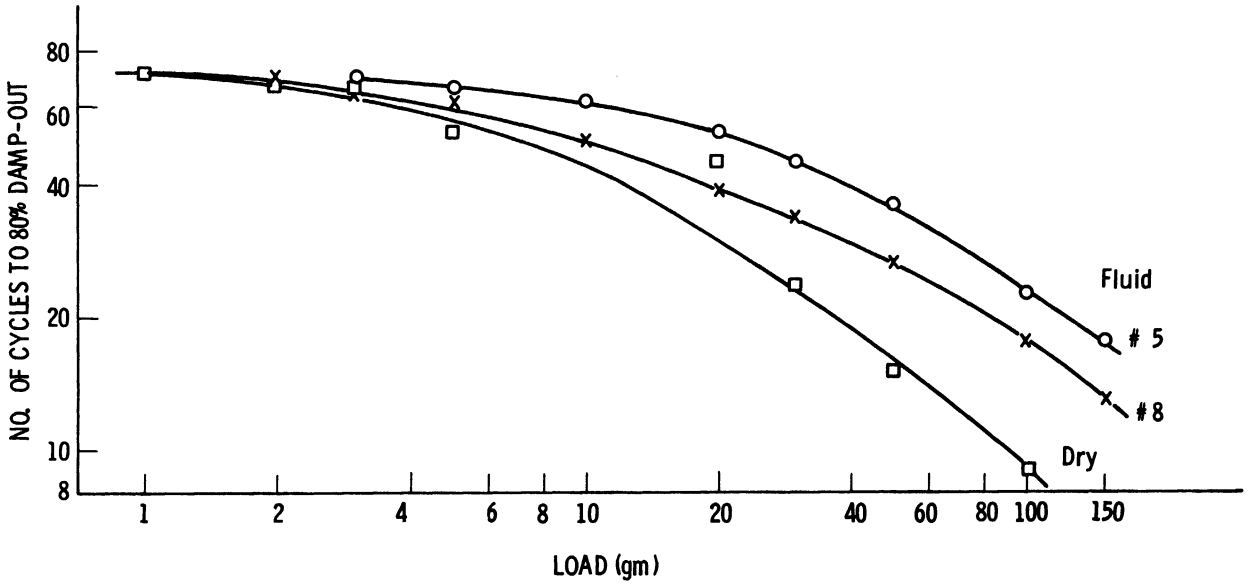

Fig. C.14. Static-dynamic test for copper.

STATIC-DYNAMIC TEST
PROJECT 04100

Frequency of Oscillations = 12.35cps
No. of cycles to 80% Damp-out

FLUID

LOAD (gm.)	Dry	1	2	3	4	5	6	7	8	9	10
150	13.0	15.0	12.9	14.5	13.0	14.5	15.7	12	12.3	7	10.5
100	18.0	19.0	16.2	19.2	19.7	17.3	19.9	15.1	15.5		
50	29.5	29.0	24.4	29.8	32.0	28.6	29.8	26.6	24.6	17.5	22.5
30											
20	43.0	43.0	37.6	44.3	40.8	46.7	44.3	40.8	46.0		
10	51.0	53.0	51.4	55.6	54.8	57.6	62.0	55.8	56.3		
5											
3	61.5	65.7	62.7	64.2	68.6	67.9	65.2	65.6	68.2	70.5	76.0
2											
1											
Arm Down	72.5	72.5	69.5	71.0	72.2	71.2	71.6	73.3	73.2		
Arm Up	75.0	74.0	69.6	73.4	73.0	86.0	76.5	98.4	81.1	83.5	

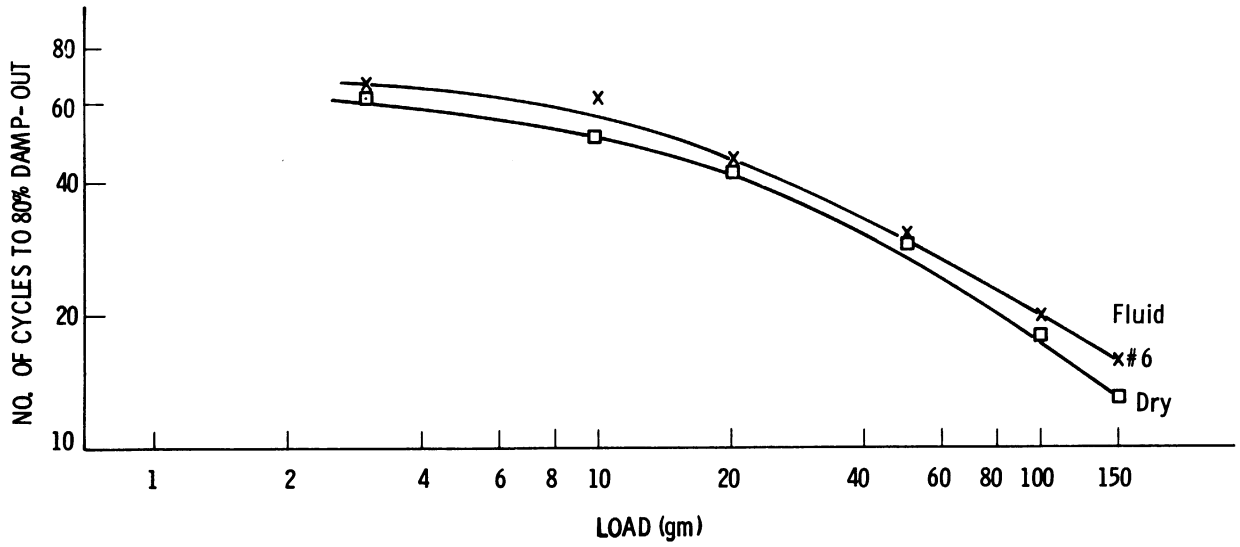

Fig. C.15. Static-dynamic test for magnesium.

STATIC-DYNAMIC TEST
PROJECT 04100

Frequency of Oscillations = 12.35cps
No. of cycles to 80% Damp-out

FLUID

LOAD (gm.)	Dry	1	2	3	4	5	6	7	8	9	10
150	6	13.5	15.6	16.0	17.0	17.0	13.9	15.5	14.5	10.5	17.0
100	7	18	21.7	21.0	22.4	23.8	18.8	20.5	20.0		
50	13	29	32.6	32.5	35.0	35.6	29.5	35.0	30.5	25.5	35
30											
20	24	47	49.3	50.0	50.5	51.0	38.2	49.5	45.5		
10	34.5	54.5	63.2	61.0	60.5	59.3	56.4	62.5	58.0		
5											
3	52	68	73.5	74.0	71.0	69.4	68.2	72.5	68.5	79	80
2											
1											
Arm Down	70.5	72	75.0	75.0	71.5	70.4	70.0	75.0	73.5		
Arm Up	72	73.5	75.7	72.0	75.0	72.2	69.3	78.0	76.0	83.5	

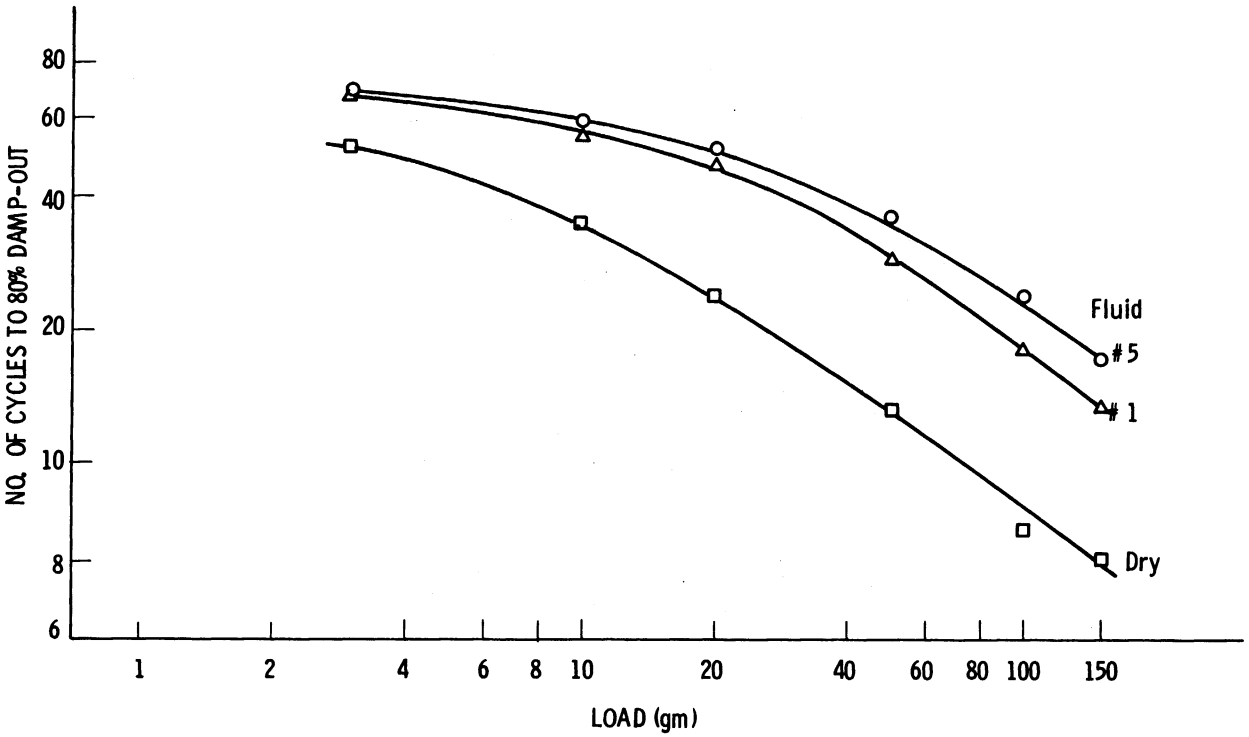

Fig. C.16. Static-dynamic test for 1042 steel.

STATIC-DYNAMIC TEST
PROJECT 04100

Frequency of Oscillations = 12.35cps
No. of cycles to 80% Damp-out

FLUID

LOAD (gm.)	Dry	1	2	3	4	5	6	7	8	9	10
150	15.5	16.5	15	16	16.5	18	13.5	17.5	13.5	10	16
100	22	22.5	21	21	22.5	23.5	18	22	18.5		
50	33.5	33	33	32.5	35	35.5	28	33	31	22.5	33
30											
20	49	48	48	49	52	52	41.5	49	48		
10	58	57	60.5	57.5	60.5	62	53	57.5	59.5		
5											
3	66	66.5	71.5	68.5	70.5	69.5	63	66.5	69	67.5	72
2											
1											
Arm Down	72	70.5	70.5	69.5	72.5	71	69.5	68.5	67		
Arm Up	70.5	69	68	71	73	73	68.5	70.5	73.5	83.5	

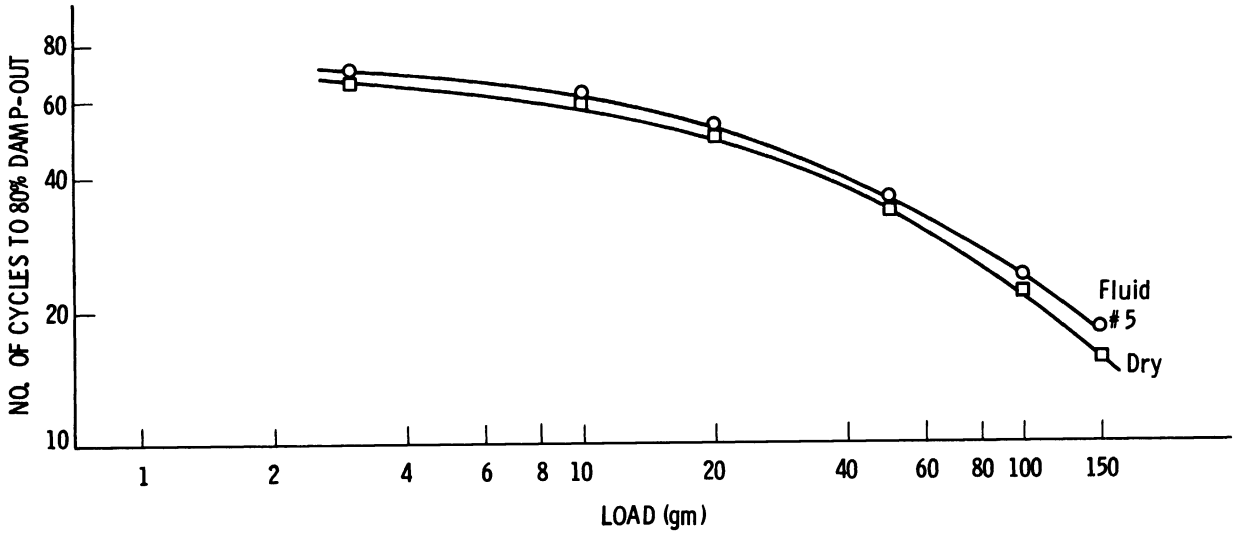

Fig. C.17. Static-dynamic test for 1018 steel.

STATIC-DYNAMIC TEST
PROJECT 04100

Frequency of Oscillations = 12.35cps
No. of cycles to 80% Damp-out

FLUID

LOAD (gm.)	Dry	1	2	3	4	5	6	7	8	9	10
150	11.5	16.0	17.5	17.5	18.5	14.5	15.5	18.0	9.0	10.5	16.5
100	16.0	22.0	22.0	22.0	24.5	20.5	21.4	24.0	18.5		
50	29.0	33.5	38.5	35.0	34.5	35.2	33.0	36.5	35.5	25.0	30.0
30											
20	46.5	45.0	54.5	54.5	56.0	55.8	52.0	54.0	53.0		
10	58.0		66.5	68.0	67.0	68.5	66.5	64.5	62.0		
5											
3	66.0	70.5	78.0	87.0	80.5	84.0	82.0	77.0	74.5	71.0	76.5
2											
1											
Arm Down	77.5	77.5	83.5	87.0	87.5	86.0	85.5	86.0	74.5		
Arm Up	74.5	80.0	85.0	87.5	83.0	85.5	87.0	86.0	79.2	83.5	

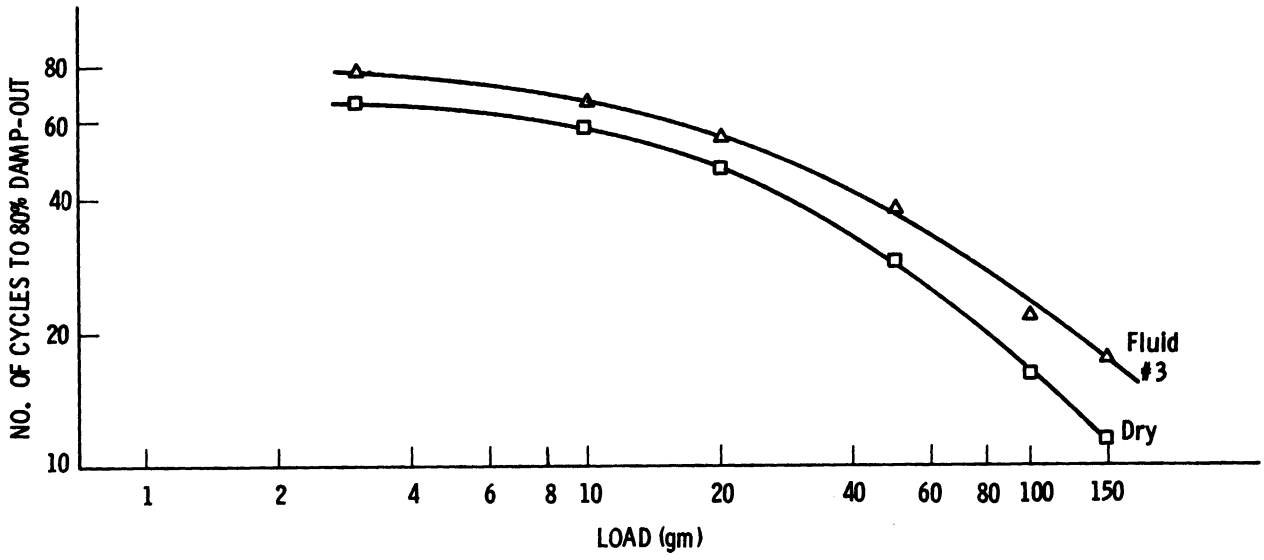

Fig. C.18. Static-dynamic test for stainless steel.

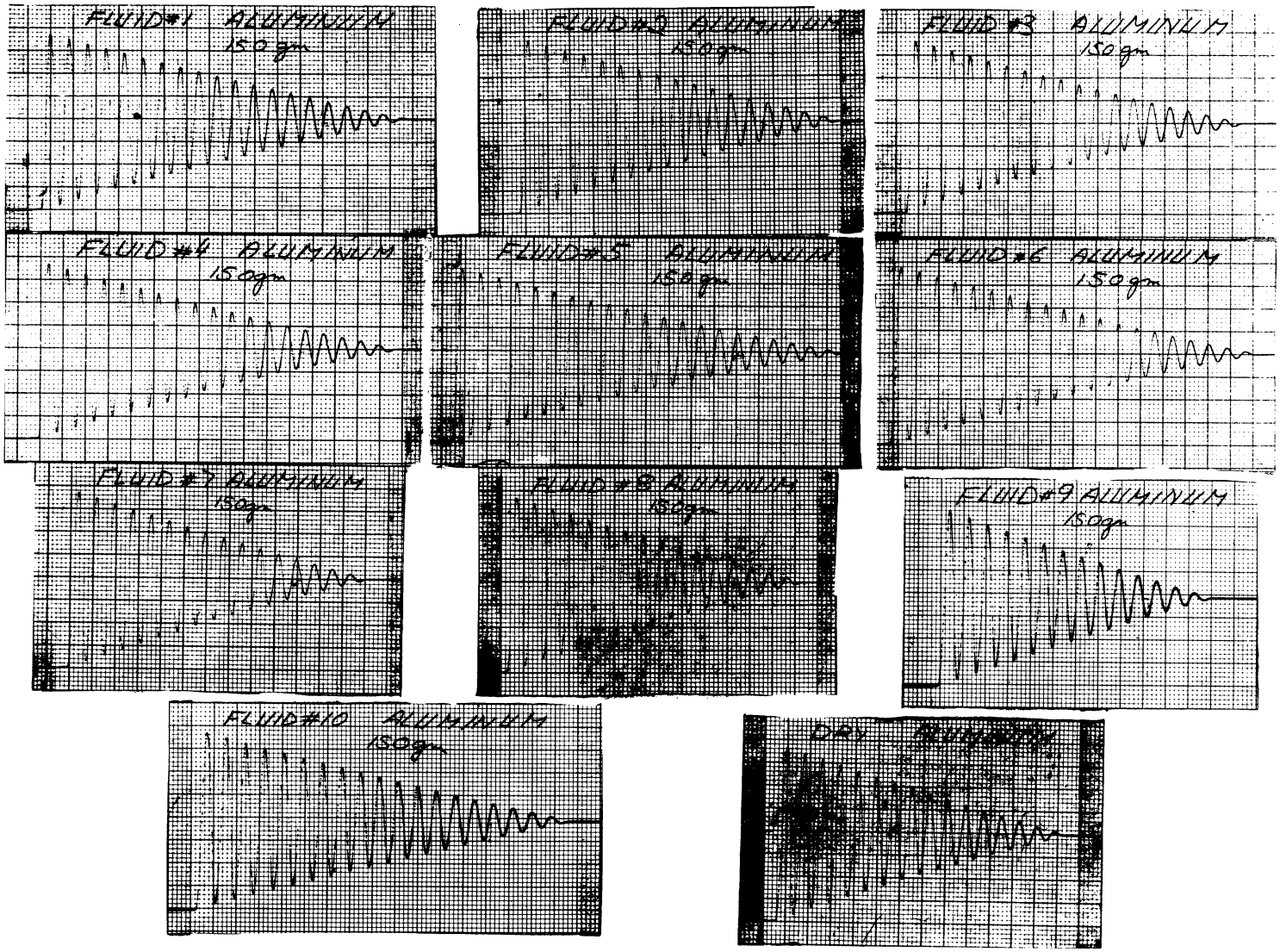

Fig. C.19. Aluminum static-dynamic tests response curves, 150 gm load.

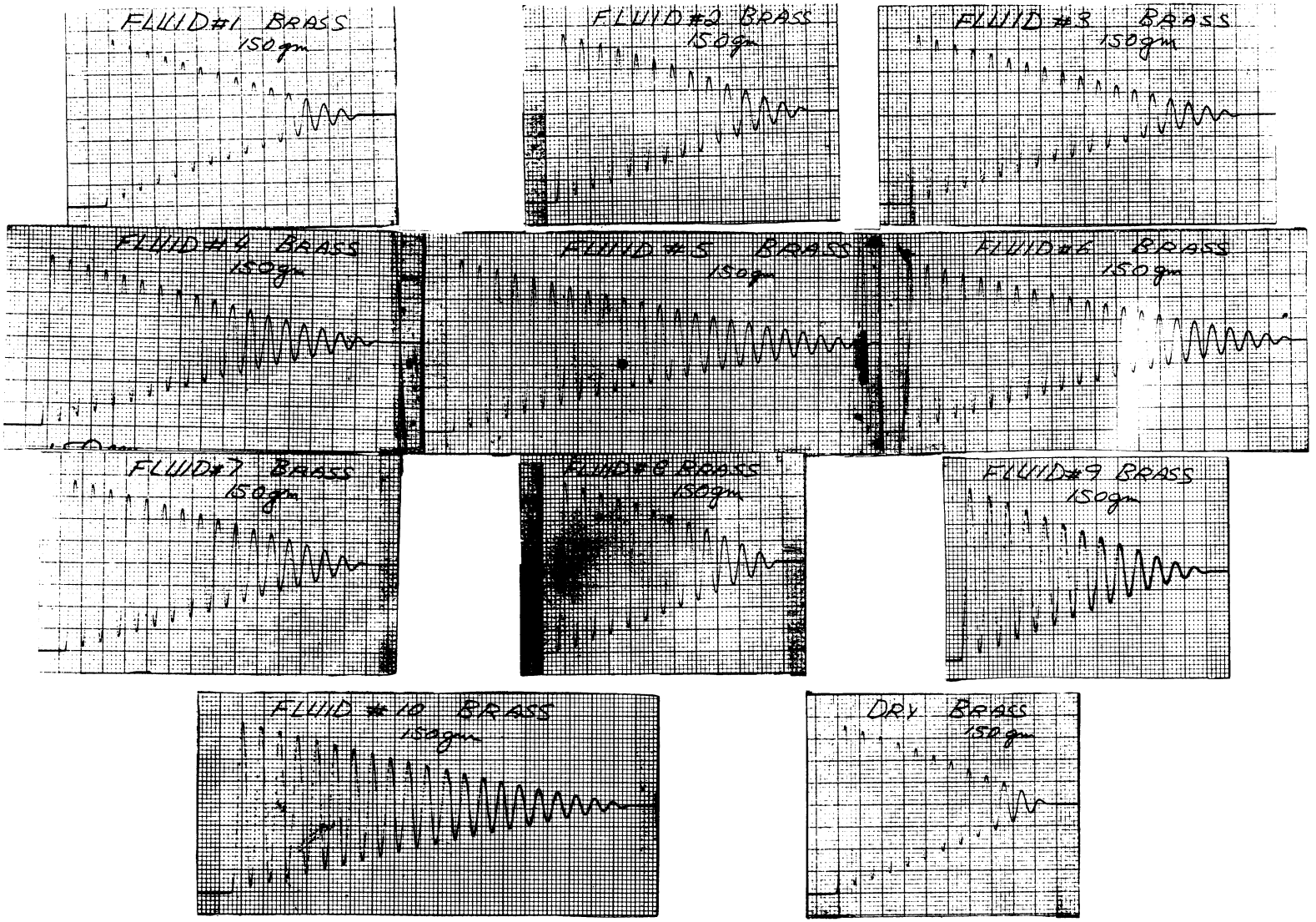

Fig. C.20. Brass static-dynamic tests response curves, 150 gm load.

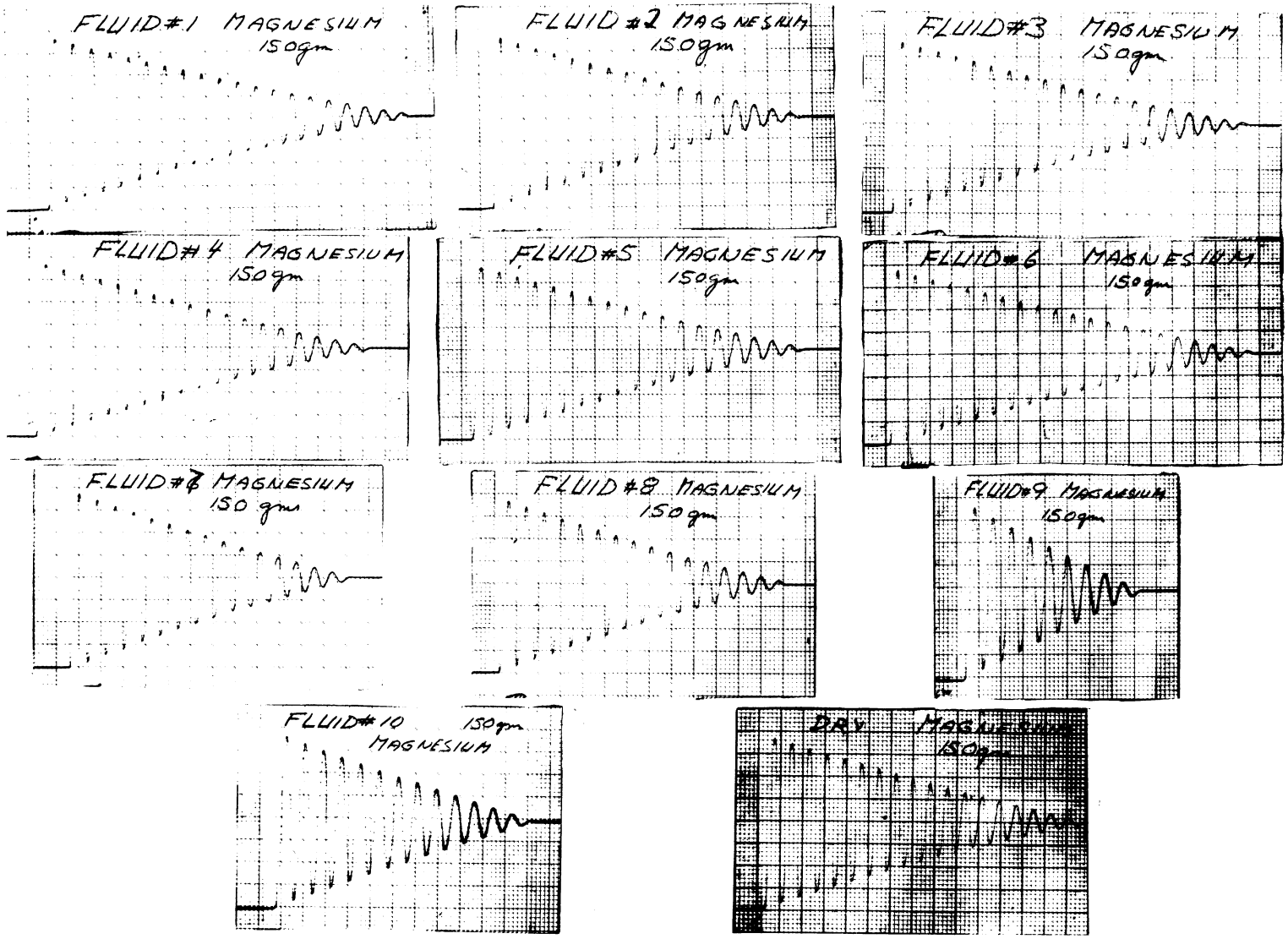

Fig. C.21. Magnesium static-dynamic tests response curves, 150 gm load.

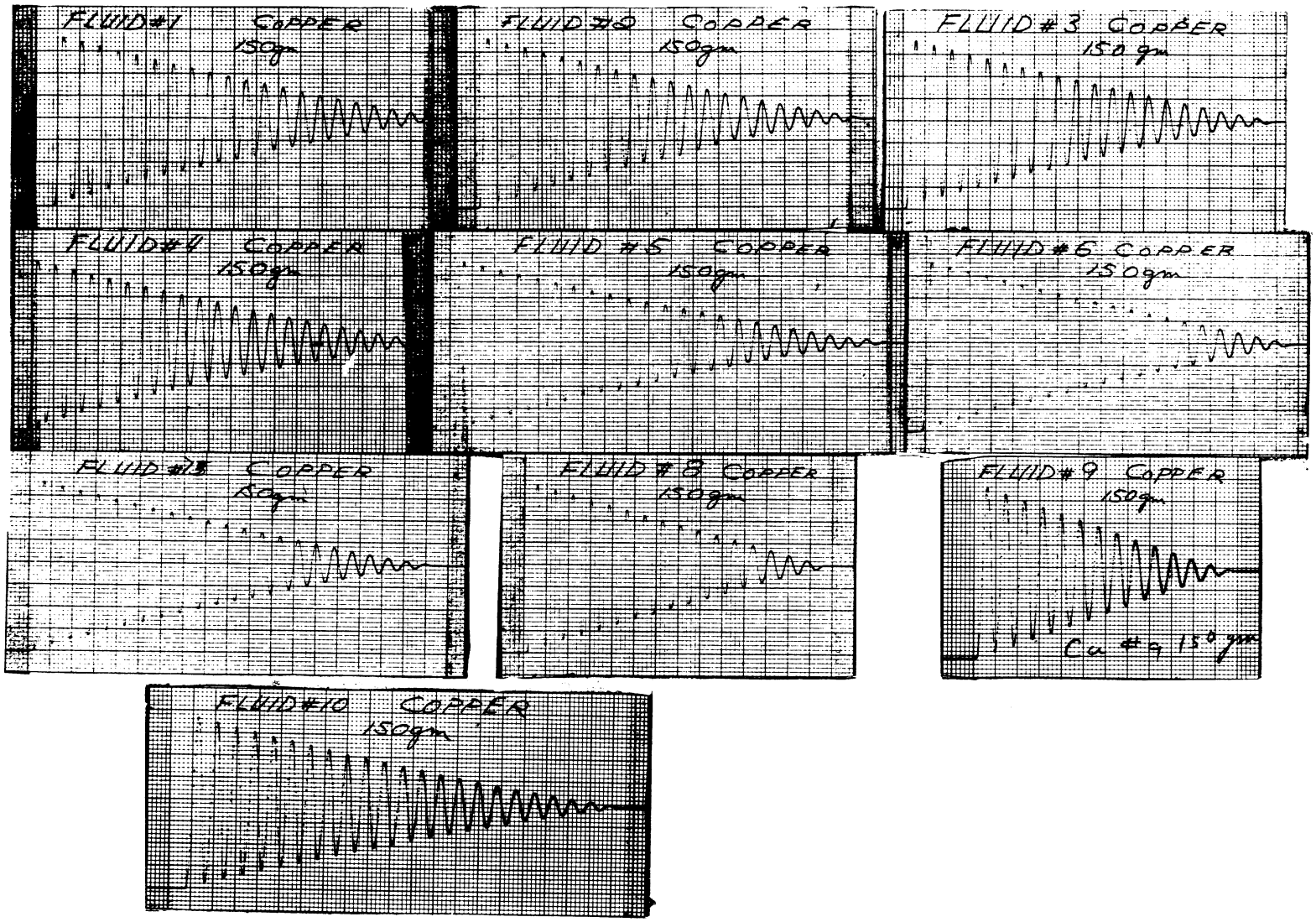

Fig. C.22. Copper static-dynamic tests response curves, 150 gm load.

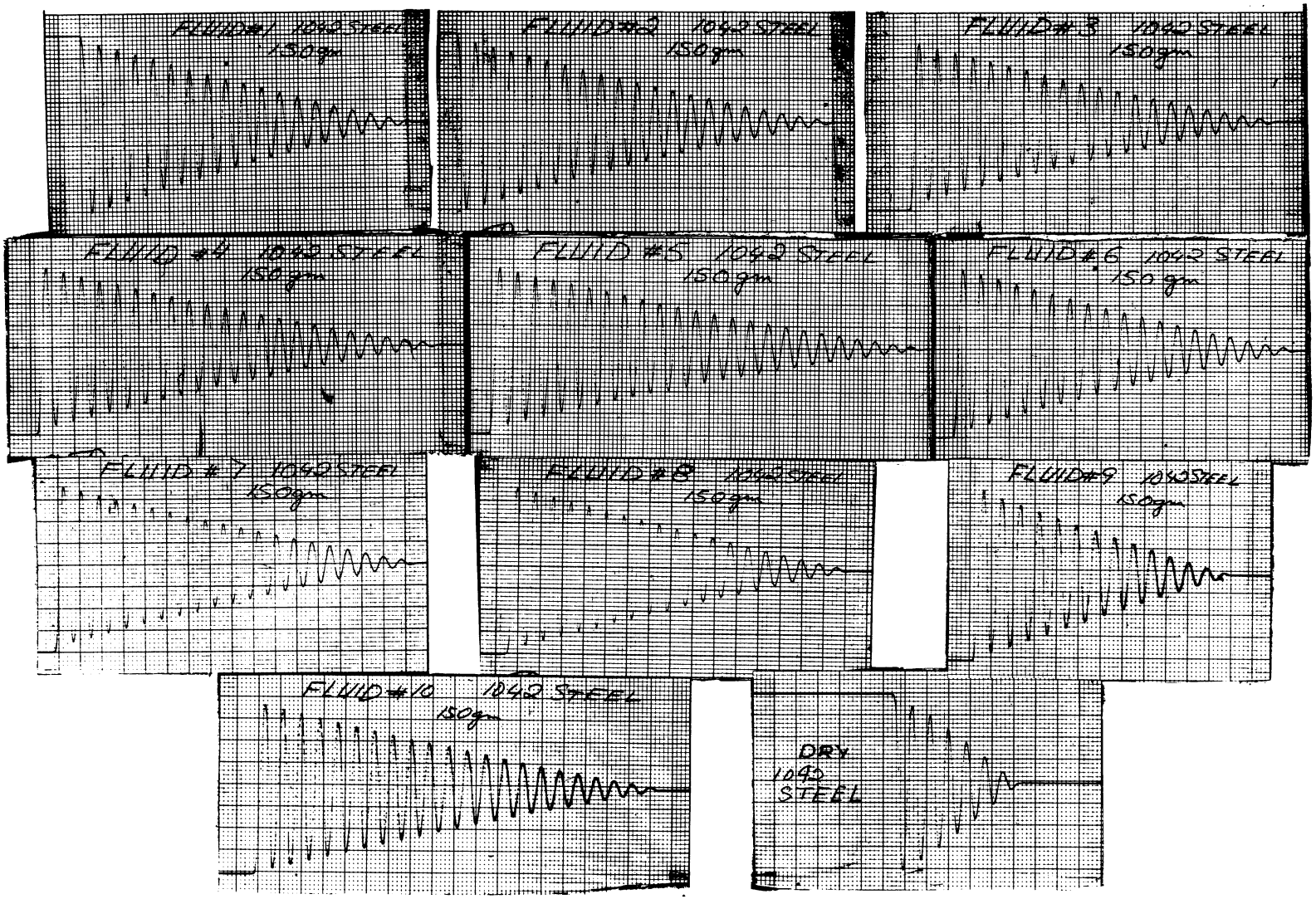

Fig. C.23. 1042 steel static-dynamic tests response curves, 150 gm load.

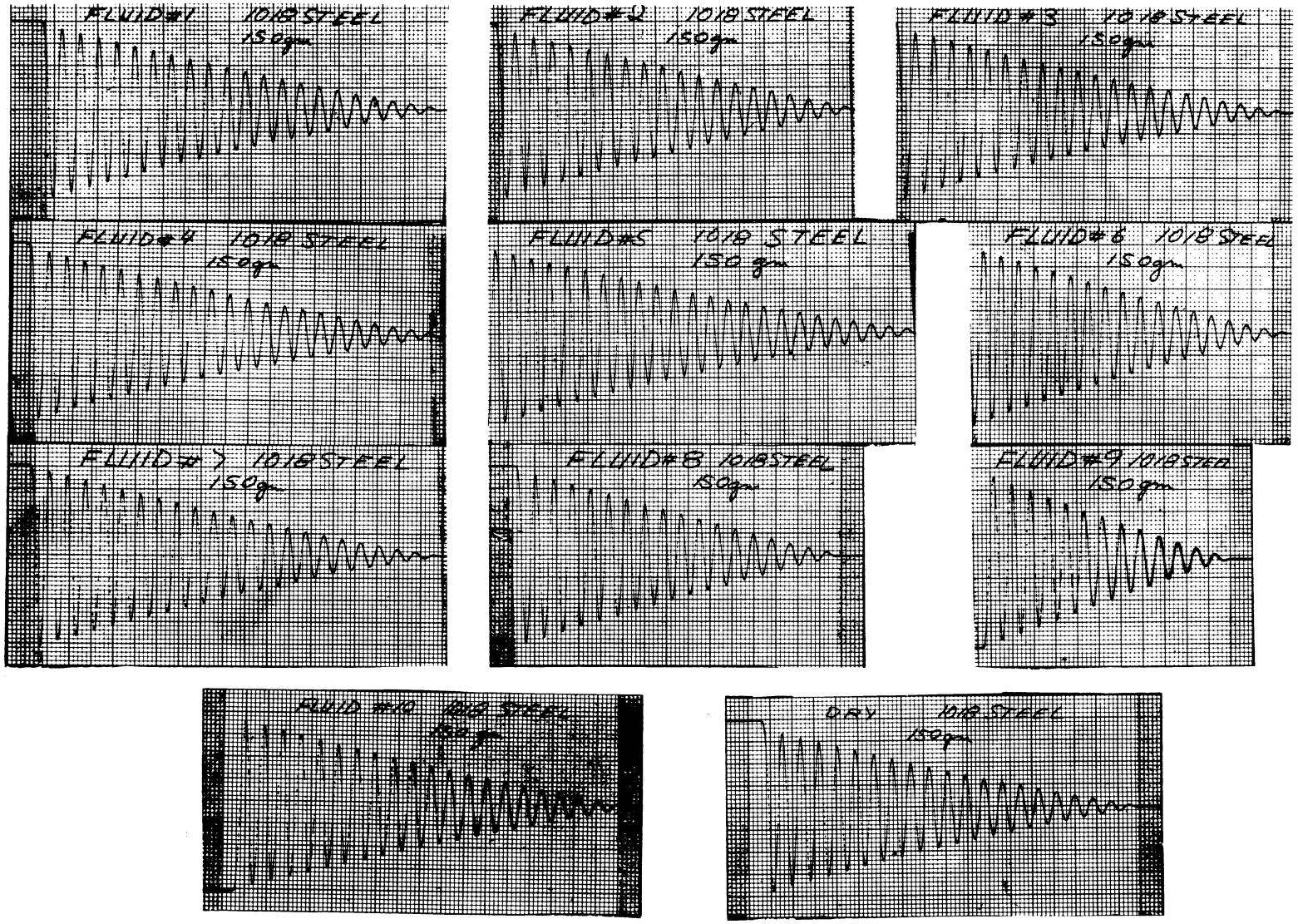

Fig. C.24. 1018 steel static-dynamic tests response curves, 150 gm load.

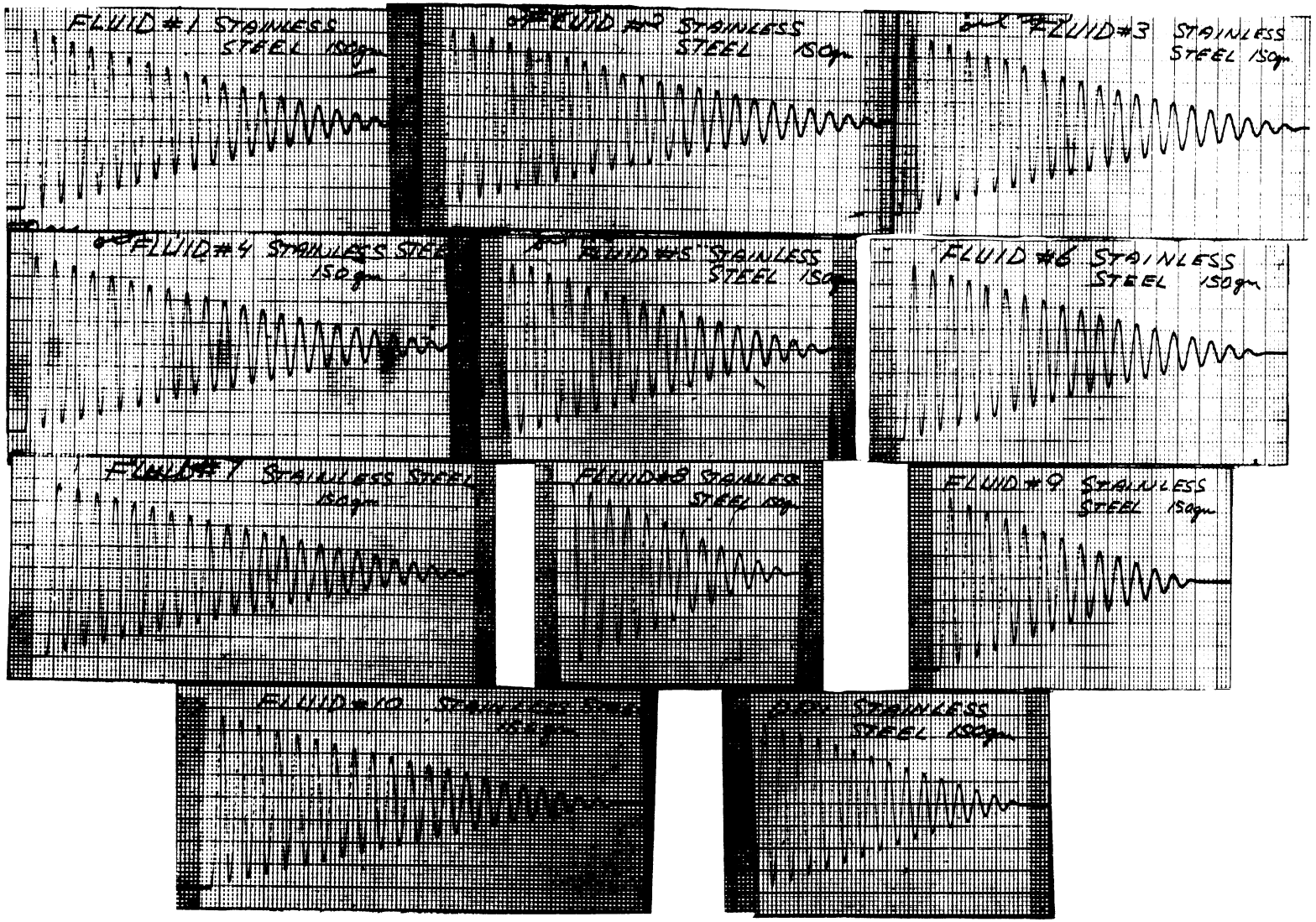

Fig. C.25. Stainless steel static-dynamic tests response curves, 150 gm load.

APPENDIX D

MILLING CUTTER

Figure D.1 shows the general design of the single-tooth milling cutter used in the pendulum dynamometer studies. The flat, when used, was ground on the cutting edge parallel to the top surface of the body of the tool. Surface finish on the ground flats was provided by a grinding motion parallel to the cutting edge. Measurements of the surface finish were made perpendicular to the cutting edge and to the direction of grinding. Conventional grinding provided a surface finish of 30 μin., while the use of a diamond wheel resulted in a surface finish of 3 μin.

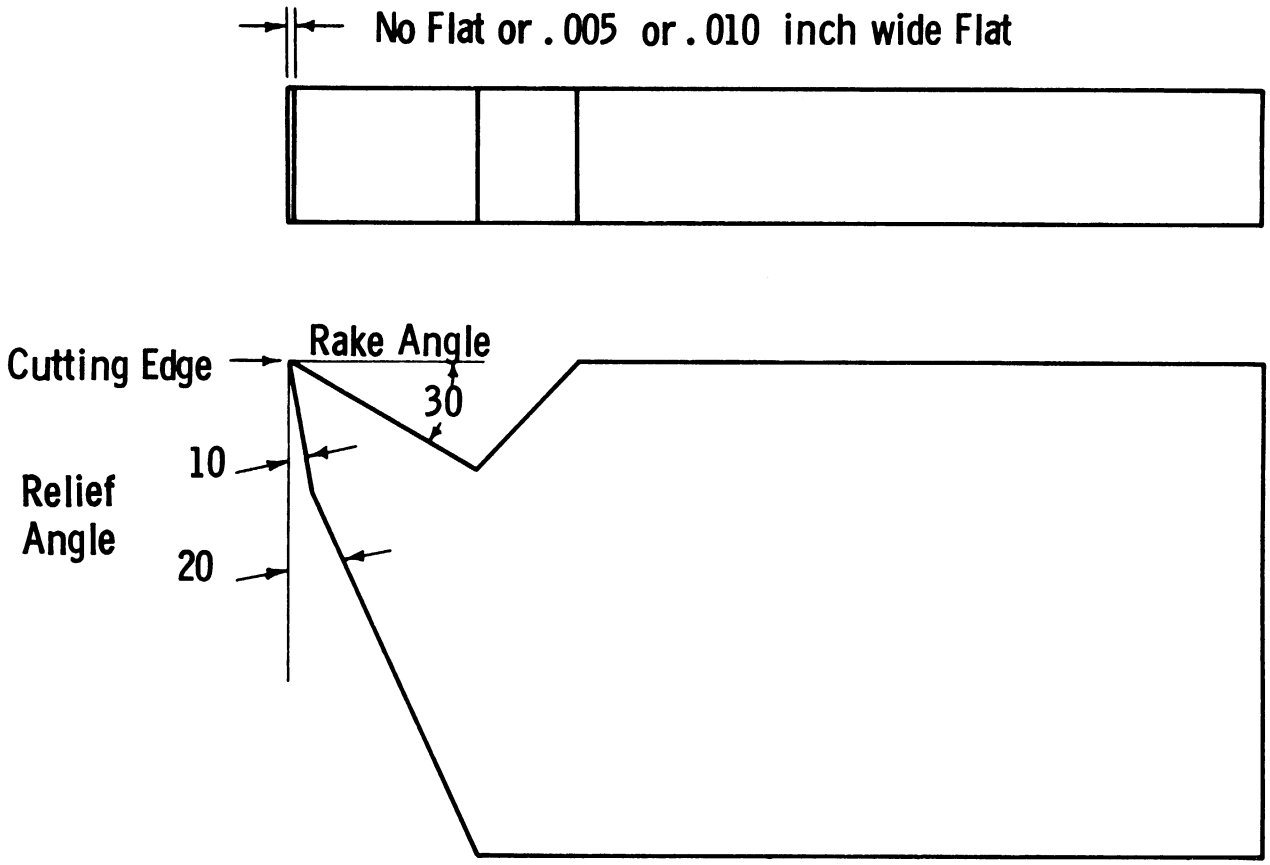

Fig. D.1. Cutter for milling studies with pendulum dynamometer.
Cutter Type: M2-High speed steel.

REFERENCES

1. "Basic Mechanics of the Metal Cutting Process," by M. E. Merchant, Journal of Applied Mechanics, Vol. 66, 1944, A168 to A175.

2. "The Effect of Tool-Chip Contact Area in Metal Machining," ASME, Vol. 80, 1958, pp. 1089-1096.

3. "Crater Wear of Cutting Tools," by K. J. Trigger and B. T. Chao, ASTE Paper No. 24T38. Presented at 24th Annual Meeting of American Society of Tool Engineers, Chicago, Ill., March 19, 1956.

4. Theory of Elasticity, by S. Timoshenko, McGraw-Hill Book Co., 1934, pp. 339-352.